DISCOVERING THE MOLECULAR MECHANISMS UNDERLYING SCHIZOPHRENIA

Doctoral Thesis
Paula Unzueta Larrinaga
2024

Universidad del País Vasco
Euskal Herriko Unibertsitatea

This Doctoral Thesis has been carried out thanks to the financial support of several entities and subsidized projects: Spanish Ministry of Science and Innovation (PID2019-106404RB-I00), Spanish Ministry of Health (PNSD 2019I021) and Basque Government (2019111082, ITIT1211-19 and IT1512/22).

This Doctoral Thesis has resulted in the publication of the following scientific articles:

1. **Unzueta-Larrinaga, P.**, Barrena-Barbadillo, R., Ibarra-Lecue, I., Horrillo, I., Villate, A., Recio, M., Meana, J. J., Diez-Alarcia, R., Mentxaka, O., Segarra, R., Etxebarria, N., Callado, L. F. & Urigüen, L. (2023). Isolation and Differentiation of Neurons and Glial Cells from Olfactory Epithelium in Living Subjects. Molecular neurobiology, 60(8), 4472–4487.
2. Villate A.; Olivares M.; Usobiaga A.; **Unzueta-Larrinaga P**.; Barrena-Barbadillo R.; Callado L.F.; Etxebarria N. & Urigüen L. Differential Serum Metabolomics Profile in Patients with Schizophrenia, Cannabis Use Disorder and Dual diagnosis. Under review in Schizophrenia Bulletin.
3. **Unzueta-Larrinaga, P.**; Olabarrieta E.; Barrena-Barbadillo R.; Diez-Alarcia R.; Rivero G.; Callado L.F. & Urigüen L. Discovering the molecular mechanisms underlying cannabis-induced increased risk of schizophrenia in a double hit rodent model. In preparation.
4. **Unzueta-Larrinaga, P.**; Olabarrieta E.; Barrena-Barbadillo R.; Diez-Alarcia R.; Horrillo I.; Recio M.; Mentxaka O.; Segarra R.; Callado L.F.; Urigüen L. Transcriptomic fingerprint of neurons and glial cells isolated and differentiated from olfactory neuroepithelium of subjects with schizophrenia. In preparation.

ABBREVIATION LIST

ºC - Degrees Celsius of temperature
4E-BP - Eukaryotic translation initiation factor 4E-binding protein
5-HT - 5-hydroxytryptamine / Serotonin
5-HT2AR - Serotonin 2A receptor
5-HT1A - Serotonin 1A receptor
5-HT2C - Serotonin 2C receptor
ACH - Acetylcholine
Akt - Protein kinase B
ANOVA - Analysis of Variance
AP – Antipsychotic
BBB - Blood-Brain Barrier
BCA - Bicinchoninic acid
BCP - Bromochloropropane
BDNF - Brain-Derived Neurotrophic Factor
BMI - Body Mass Index
BSA - Bovine Serum Albumin
bFGF - Basic Fibroblast Growth Factor
Ca^{+2} - Voltage-Gated Calcium
CACNA1C - Calcium Voltage-Gated Channel Subunit α 1 C
CACNA1I - Calcium Voltage-Gated Channel Subunit α 1 I
CACNB2 - Calcium Voltage-Gated Channel Auxiliary Subunit β 2
CB1R - Cannabinoid Receptor 1
CD - Cluster of Differentiation
CNS - Central Nervous System
CNVs - Copy Number Variations
COX-2 - Cyclooxygenase-2
CSF - Cerebrospinal Fluid
DA - Dopamine
DRD2 - Dopamine Receptor D2
DAPI - 4',6-diamidino-2-phenylindole dihydrochloride
dB - Decibels
DI - Discrimination Index
DMEM - Dulbecco's Modified Eagle Medium
DNA - Deoxyribonucleic Acid
DR - Delayed-responders
DLPFC - Dorsolateral Prefrontal Cortex
dsRNA - Double-stranded Ribonucleic Acid
DSM - Diagnostic and Statistical Manual of Mental Disorders

EGF - Epidermal Growth Factor
ELISA - Enzyme-Linked ImmunoSorbent Assay
EpCAM - Epithelial Cell Adhesion Molecule
EPS - Extrapyramidal Symptoms
ERK - Extracellular Signal-Regulated Kinase
FACS - Fluorescence-Activated Cell Sorting
FC - Fold Change
FDR - False Discovery Rate
FEP - First episode of psychosis
GABA - γ-aminobutyric acid
GAD - Glutamate decarboxylase enzyme
GAPDH - Glyceraldehyde 3-Phosphate Dehydrogenase
GD - Gestational Day
GFAP - Glial Fibrillary Acidic Protein
GLU - Glutamate
GPCR - G Protein-Coupled Receptor
GRIA1 - Glutamate Ionotropic Receptor AMPA Type Subunit 1
GRIN2A - Glutamate Ionotropic Receptor NMDA Type Subunit 2A
CSF - Cerebrospinal Fluid
GWAS - Genome-Wide Association Study
HBSS - Hank's Balanced Salt Solution
HPLC - High-performance liquid chromatography
i.p. - Intraperitoneally
ICD - International Classification of Diseases
IDO - Indoleamine 2,3-Dioxygenase
IFN - Interferon
IFN-γ - Interferon-γ
IL - Interleukin
IL-6 - Interleukin-6
IL-12 - Interleukin-12
iN - Induced Neuronal
iPS - Induced Pluripotent Stem
Kyn - Kynurenine
Kyn/Trp - Kynurenine/Tryptophan ratio
KP - Kynurenine Pathway
LPS - Lipopolysaccharide
LSD - Lysergic Acid Diethylamide
MACS - Magnetic Activated Cell Sorting
MAP2 - Microtubule-Associated Protein 2
MAP1B - Microtubule-Associated Protein 1B

MAPK - Mitogen-Activated Protein Kinase
MHC - Major Histocompatibility Complex
mGluR2 - Metabotropic Glutamate Receptor 2
mGluR3 - Metabotropic Glutamate Receptor 3
MIA - Maternal Immune Activation
mTOR - Mechanistic/Mammalian Target of Rapamycin
mTORC1 - mTOR Complex 1
mTORC2 - mTOR Complex 2
mRNA - Messenger Ribonucleic Acid
NA – Noradrenaline
NeuN - Neuronal Nuclei
NF-κB - Nuclear Factor-Kappa B
NMDA - N-Methyl-D-Aspartate
NMDAR - N-Methyl-D-Aspartate Receptor
NORT - Novel Object Recognition Test
NRGN - Neurogranin
NSCs - Neural Stem Cells
OR - Odds ratio
p70S6K - p70 Ribosomal Protein S6 Kinase
PCP - Phencyclidine
PCR - Polymerase Chain Reaction
PDK1 - Phosphoinositide-Dependent Protein Kinase 1
PFA - Paraformaldehyde
PFC - Prefrontal Cortex
PGE_2 - Prostaglandin E2
PH - Pleckstrin Homology
PIP3 - Phosphatidylinositol-3,4,5-Trisphosphate
PI3K - Phosphoinositide 3-Kinase
PND - Postnatal Day
Poly(I:C) – Polyinosinic:Polycytidylic Acid
PPI - Prepulse Inhibition
PR - Poor-responders
PVDF - PolyVinylidene Difluoride
PSA-NCAM - PolySialic Acid-Neural Cell Adhesion Molecule
qPCR - Quantitative Polymerase Chain Reaction
RNA - Ribonucleic Acid
RIN - RNA Integrity Number
rpS6 or S6 - Ribosomal Protein S6
RT - Room Temperature
S6K - Kinase S6

SDS-PAGE - Sodium Dodecyl-Sulfate Polyacrylamide Gel Electrophoresis
sIL-2R - Soluble IL-2 Receptor
SNPs - Single Nucleotide Polymorphisms
SNVs - Single Nucleotide Variants
Sox2 - SRY-Box Transcription Factor 2
SRR - Serine Racemase
STD - Standard
SZ - Schizophrenia subjects
TBS - Tris-buffered saline
TCF4 - Transcription Factor 4
TDO - Tryptophan 2,3-Dioxygenase
TGF-β - Transforming Growth Factor-β
THC - Δ^9-Tetrahydrocannabinol
TLRs - Toll-Like Receptors
TLR3 - Toll-Like Receptor 3
TNF-α - Tumor Necrosis Factor α
Trp – Tryptophan
VTA - ventral tegmental area
WB - Western Blotting

INDEX

Introduction

1. INTRODUCTION

1.1. Schizophrenia

1.1.1. General aspects

Schizophrenia is a chronic, disabling illness that affects about 0.32% of the world's population (Institute for Health Metrics and Evaluation (IHME), 2020). It typically begins in adolescence and worsens over time, reducing life expectancy by approximately 14.5 years (Hjorthøj et al., 2017). Due to its early onset, chronic nature, and associated deficits, schizophrenia ranks among the top ten causes of disability worldwide (Marder & Cannon, 2019). In addition, it is estimated to be the seventh most costly disease in terms of care and loss of productivity (GBD 2017 Disease and Injury Incidence and Prevalence Collaborators et al., 2018). This entails an estimated annual cost of around 3.5 billion dollars in countries such as Spain and up to 102 billion dollars, according to the most pessimistic studies, in countries such as the United States (Chong et al., 2016) taking into account direct costs (treatments, damages, accidents, etc.) and indirect costs (loss of human capital). Additionally, in 2022 the most commonly used atypical antipsychotics in Spain (risperidone and olanzapine) were among the top 8 drugs that generated the highest expenditure, with an economic cost of around 347 million euros (Ministerio de Sanidad, 2022). This explains why research on this disease is a priority objective of global health systems.

The symptoms of schizophrenia include a distortion of thinking, perceptions, emotions, language, self-awareness, and behavior. Clinically, these symptoms are categorized into positive symptoms (such as delusions, hallucinations, and disorganized behavior), negative symptoms (including social withdrawal, apathy, and abulia), and cognitive deficits (involving problems with selective attention, working memory, and learning) (Winship et al., 2019). While negative symptoms remain relatively stable and primarily contribute to functional impairment, positive symptoms tend to be abrupt and transient, often requiring temporary

hospitalization. It is worth noting that positive symptoms respond usually to treatment, whereas current pharmacological approaches are largely ineffective against negative and cognitive symptoms. This discrepancy is a major factor in why schizophrenia reduces life expectancy by 10 to 25 years compared to the general population, with suicide and antipsychotic-related morbidities being the main causes of premature mortality (Hasan et al., 2020).

The course of schizophrenia usually begins with an acute psychotic episode, which in most cases leads to chronification and relapses. The onset of schizophrenia is gradual and subtle, typically over a period of approximately five years. It begins with the manifestation of negative symptoms, followed rapidly by cognitive and social deterioration. This initial phase, known as the prodromal period, may exhibit early indicators like social withdrawal, unconventional thoughts, suspicion, changes in social circles, academic failure, altered sleep patterns, and irritability. However, these manifestations, although prevalent and indicative of an individual's deteriorating mental health, are non-specific and not diagnostic. Subsequently, this phase is followed by the appearance of psychotic symptoms. This debut of positive symptoms is known as first episode of psychosis (FEP) (Figure 1).

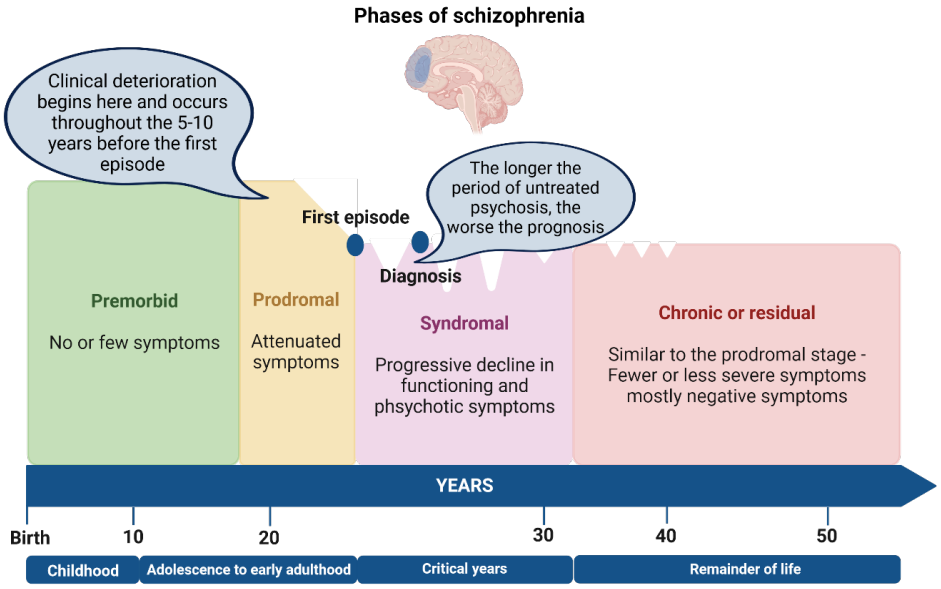

Figure 1: Disease progression in schizophrenia develops through distinct stages. Initiated by the first episode of psychosis, the syndromic stage marks the beginning and extends into the progressive stage. Following the onset of the first psychotic episode, a gradual deterioration of functioning ultimately finish with the long-lasting and chronic effects of the illness. Adapted from Lieberman & First, 2018 using BioRender.com.

1.1.2. Etiology and pathogenesis

Several hypotheses regarding etiopathogenesis of schizophrenia have been suggested, but none has been consistently confirmed. This is the reason why, what causes schizophrenia and how it develops are questions that have occupied the minds of every psychiatric researcher for over a century.

Thus, schizophrenia is a complex condition influenced by a combination of genetic, biological, and environmental factors. Although the precise role of individual genes remains elusive, genomic research has identified specific risk loci linked to the development of schizophrenia. Genetic factors are estimated to contribute to roughly 80% of the risk associated with this disorder (Hilker et al., 2018; Ľupták et al., 2021).

Among the identified genes, certain studies have highlighted those responsible for synaptic proteins, calcium channels, and receptors related to glutamate and dopamine. Moreover, there is growing evidence of a connection between

schizophrenia and variations within the major histocompatibility complex (MHC), a component of acquired immunity (Purcell et al., 2009; Shi et al., 2009; Stefansson et al., 2009). This suggests that immune responses and inflammatory processes might also be involved in the disease's development. For instance, MHC I has been found to influence synapse formation, dendritic growth, and neuroplasticity (Luvsannyam et al., 2022).

However, despite these genetic associations, the task of identifying specific molecular or structural variations responsible for schizophrenia remains a significant challenge. Thus, this complexity underscores the need to explore novel models for identifying interactions that contribute to brain disorders associated with the disease.

Traditionally, it has been believed that schizophrenia affects both sexes in a similar way. However, recent studies suggest notable sex differences, particularly concerning disease onset, progression, and symptomatology (Gogos et al., 2019; Sun et al., 2016). Numerous investigations have highlighted that men have higher prevalence (Jongsma et al., 2019), earlier onset (typically around 18-25 years of age) (Häfner, 2003), more pronounced negative symptoms accompanied by cognitive deficits (Li et al., 2016; Ochoa et al., 2012), and less response to treatment (Haddad et al., 2020).

In contrast, women typically experience a later onset of the disease (after the age of 40-50) (Howard et al., 2000), occurring approximately four years later than in men. Interestingly, some women exhibit a unique second surge of disease onset around the ages of 45 to 49, which is thought to be related to the decline in ovarian hormones during menopause (Häfner, 2003; Sun et al., 2016). Additionally, women often display more affective symptoms, which can frequently result in a higher prevalence of depressive symptomatology (Li, et al., 2016; Ochoa et al., 2012).

Despite numerous studies outlining these well-defined differences in the onset and clinical presentation of schizophrenia between men and women, a

comprehensive understanding of these variations has been lacking. Some studies have linked these differences to the influence of sex hormones and their molecular mechanisms (da Silva & Ravindran, 2015), while others attribute them to comorbidities and behavioral factors like substance abuse, which is more prevalent in men, and has not been consistently controlled for in all studies (Riecher-Rössler et al., 2018).

1.1.2.1. Genetics

Throughout history, schizophrenia has been perceived as one of the neuropsychiatric disorders with the highest genetic component, mainly due to its hereditary nature.

The emergence of this idea dates back to the beginning of 20th century, when twin studies began to gain prominence. These studies revealed that genetics plays a significant etiological role in schizophrenia and established the basis for the search for genetic risk factors. More recent research, including studies in African populations (Gulsuner et al., 2020) and investigations involving monozygotic and dizygotic twins, as well as adopted offspring of mothers affected by schizophrenia, further confirmed the familial nature of this disorder (Jauhar et al., 2022).

In the search for a candidate gene causing schizophrenia, numerous genome-wide association studies (GWAS) have been predominantly employed, revealing disease associations involving single nucleotide polymorphisms (SNPs) and copy number variations (CNVs) across a multitude of genes (Birnbaum & Weinberger, 2017; Caldeira et al., 2019). It just so happens that the small sample size is possibly the factor that most hinders advances in schizophrenia genetics, as a certain threshold of cases and controls is required to reach adequate power to detect small effect variants (Sullivan et al., 2018). In the initial studies of schizophrenia GWAS consortia, the first major findings implicated the MHC region, transcription factor 4 (TCF4) and neurogranin (NRGN) pointing to aberrant brain development and impaired cognitive functioning as potentially

relevant core pathophysiological processes in the context of schizophrenia (Shi et al., 2009; Stefansson et al., 2009).

Recent studies have made significant progress in unraveling the genetic underpinnings of schizophrenia. One study, involving 40,000 cases, identified about 145 significant risk loci, adding 50 new loci to previous research (Pardiñas et al., 2018). In addition, the latest and largest of these GWAS, conducted by the Psychiatric Genomics Consortium, which included a massive cohort of 76,755 patients with schizophrenia and 243,649 controls (Trubetskoy et al., 2022) uncovered common schizophrenia-associated variants at 287 distinct loci.

Within these new studies, several notable associations emerged that shed light on key hypotheses regarding the etiology and treatment of schizophrenia. Among the most prominent findings was the involvement of genes such as *DRD2* (the main target of 1st generation antipsychotic drugs), as well as genes such as metabotropic glutamate receptor 3 (*mGluR3*), glutamate ionotropic receptor NMDA Type Subunit 2A (*GRIN2A*), serine racemase (*SRR*) and glutamate ionotropic receptor AMPA Type Subunit 1 (*GRIA1*), all of which play roles in glutamatergic neurotransmission and synaptic plasticity (Schizophrenia Working Group of the Psychiatric Genomics Consortium, 2014). Moreover, a further focusing on glutamatergic neurotransmission revealed some evidence of polymorphisms in schizophrenia-related genes such as *mGluR2* and *mGluR3*, supporting the glutamatergic hypothesis of schizophrenia (Muguruza et al., 2016).

Furthermore, associations were observed in genes encoding voltage-gated calcium (Ca^{+2}) channel subunits, specifically *CACNA1C*, *CACNB2*, and *CACNA1I*, which extended prior findings implicating these proteins in schizophrenia (Hamshere et al., 2013; Ripke et al., 2013).

Collectively, these advances from GWAS represent significant progress in the understanding of the underlying processes contributing to schizophrenia. As larger sample sizes are employed along with additional analytical and

methodological approaches, the understanding of this complex disorder is expected to deepen.

Finally, regarding CNV studies in schizophrenia, a study of 1,433 patients with schizophrenia reported 66 initial "de novo" CNVs and identified three significant deletions (Stefansson et al., 2008). While no single gene or variant has been identified as sufficient to cause schizophrenia, some rare CNVs and single nucleotide variants (SNVs) with substantial effects have been implicated in the disease's pathogenesis. Moreover, other studies have shown that individuals with schizophrenia exhibit a higher prevalence of rare structural variants, such as deletions and/or duplications of one or more genes, when compared to controls (Singh et al., 2022; Walsh et al., 2008).

1.1.2.2. Neurotransmission systems

In recent years, there has been a growing recognition of the intricate web of polygenic and environmental factors that play a role in the development of schizophrenia. In this evolution of knowledge, researchers have focused significant attention on exploring hypotheses centered on neurotransmitter systems.

Researchers have explored various neurotransmitter systems within the context of schizophrenia (Figure 2), and while dopaminergic dysfunction has received most of the attention (Luvsannyam et al., 2022), there is growing recognition of the potential roles played by serotonin and glutamate in the manifestation of the disease's symptoms. Importantly, these three neurotransmitters and the pathways they operate in are interconnected, hinting at the possibility that multiple pathways may contribute to psychotic symptoms (Stahl, 2018).

As we unravel the complex interplay of genetics and environmental influences in schizophrenia, the study of neurotransmitter systems remains a focal point, offering valuable insights into the condition's pathogenesis.

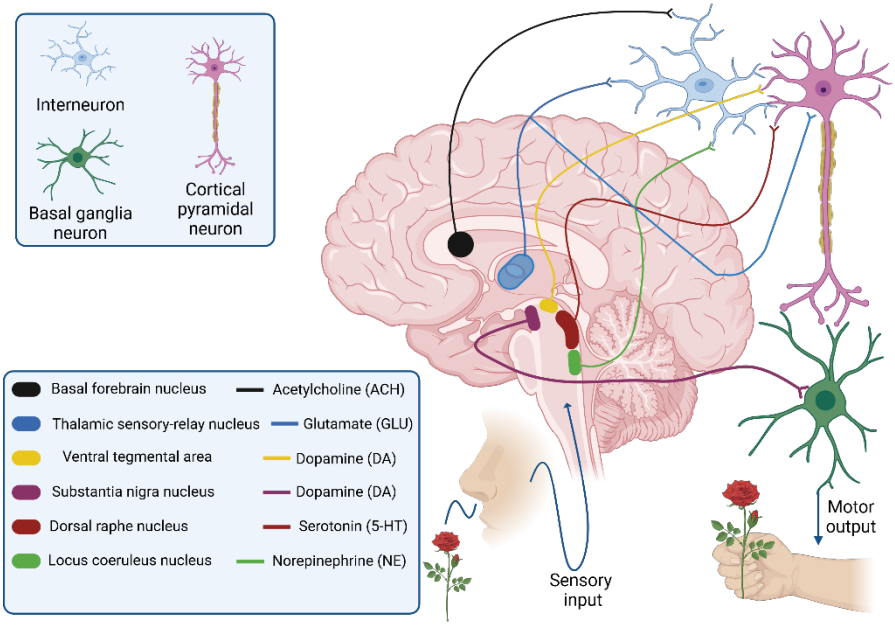

Figure 2: Neuronal circuits and neurotransmitter systems involved in the etiopathogenesis of schizophrenia. Explanation of the different circuits that have been implicated in schizophrenia such as dopamine (DA), serotonin (5-HT), glutamate (GLU), ɣ-aminobutyric acid (GABA), acetylcholine (ACH) and norepinephrine (NE). Adapted from Freedman, 2003 using BioRender.com.

Dopaminergic hypothesis

The dopaminergic system was the initial neurotransmitter system to be identified as potentially disrupted in schizophrenia. This hypothesis proposes that schizophrenia is related to an overactivity of the dopaminergic system in the mesolimbic pathway, which runs from the ventral tegmental area (VTA) to the striatum. This overactivity is thought to underlie the appearance of positive symptoms. In contrast, a dopaminergic hypoactivity in the mesocortical pathway, affecting the prefrontal region, is thought to be responsible for negative symptoms (Ľupták et al., 2021; Stahl, 2018).

Understanding these concepts holds significant implications for the treatment of schizophrenia. The main antipsychotics used to treat the disease, work by blocking dopamine receptors D2 (DRD2). While this effectively alleviates positive symptoms, it can exacerbate negative and cognitive symptoms (De Bartolomeis et al., 2013). Additionally, blocking DRD2 in the nigrostriatal

pathway can lead to unwanted motor side effects (Stahl, 2018). Furthermore, it is important to note that negative and cognitive symptoms do not show improvement with drugs that target dopamine reuptake at the cortical level (Davis et al., 1991; Yamaguchi et al., 2015). Consequently, this hypothesis presents a simplified perspective of the disease and fails to account for all the observations associated with it.

Glutamatergic hypothesis

The glutamatergic hypothesis regarding schizophrenia originates from the notable side effects observed with substances like phencyclidine (PCP) and ketamine, both of which exert clear uncompetitive inhibitory effects on N-methyl-D-aspartate receptors (NMDARs). Administration of NMDAR antagonist can induce psychosis-like states resembling most of the symptoms seen in patients with schizophrenia (Javitt, 2007; Stone et al., 2008).

This hypothesis suggests that dysfunction in NMDAR-mediated neurotransmission may constitute a primary deficiency in the illness. This dysfunction manifests as anomalies in the formation of glutamatergic synapses at various sites. These alterations, lead to heightened glutamatergic signaling within the VTA, ultimately resulting in an excess of dopamine in the striatum via the mesolimbic pathway (Ľupták et al., 2021).

Serotonergic hypothesis

Similar to the dopaminergic theory, the serotonergic theory of schizophrenia also emerged from observations of substance-induced effects. In this case, lysergic acid diethylamide (LSD) drew attention due to its chemical structure resembling serotonin and its ability to induce effects reminiscent of the hallucinations seen in schizophrenia. This led to the proposal that serotonin might play a role in the development of the disease (Woolley & Shaw, 1954).

Building upon this insight, years later, a new class of antipsychotic medication known as clozapine emerged. Notably, clozapine exhibited a higher affinity for 5-HT2 receptors than for DRD2 (Meltzer & Massey, 2011), resulting in greater

effectiveness in the treatment of schizophrenia and the most effective in patients resistant to previous treatment (Davies et al., 2003).

Based on these observations, the serotonergic hypothesis suggests that serotonin exerts an inhibitory influence on dopamine in the cortex, leading to heightened cortical hypodopaminergia. Furthermore, this theory suggests there is an overactivity of serotonergic pathways in the anterior cingulate cortex and dorsolateral prefrontal cortex (DLPFC).

In light of these ideas, it is proposed that the use of atypical antipsychotic medications, which block the serotonin 2A receptor (5-HT2AR), can reverse this inhibitory effect on dopaminergic transmission at the cortical level. This reversal, in turn, can lead to an improvement in the negative symptoms associated with the condition (Baumeister & Hawkins, 2004).

Relevantly, our research group has provided evidence supporting this hypothesis. We demonstrated an increased level of high-affinity 5-HT2AR in the prefrontal cortex (PFC) of individuals with schizophrenia (Muguruza et al., 2013). Furthermore, we found that 5-HT2AR exhibit hyperfunctionality in the PFC of individuals with schizophrenia, with heightened signaling through the Gαi1 protein (García-Bea et al., 2019).

GABAergic hypothesis

There is compelling evidence pointing towards the involvement of specific inhibitory neurons in the cortex and their associated neurotransmitter, γ-aminobutyric acid (GABA), as key players in the pathophysiology of schizophrenia (Lewis et al., 2005). Moreover, GABA and glutamate, both synthesized through similar pathways, exhibit contrasting effects; while glutamate is excitatory and enhances the likelihood of signal transmission, GABA is inhibitory, diminishing the probability of signal transmission (Hampe et al., 2018). As a result, the GABA hypothesis posits that only GABA interneurons, which serve as connectors between neurons, possess defective

NMDARs, differing from the glutamate hypothesis, which suggests a broader distribution of these NMDAR changes (Nakazawa et al., 2012).

This line of thinking is supported by numerous studies that have revealed alterations in both the presynaptic and postsynaptic aspects of GABA neurotransmission. These alterations result in a reduction in the synthesis of GABA mediated by the enzyme glutamic acid decarboxylase (GAD), as well as a decrease in GABA release within brain regions, such as the PFC and nucleus accumbens, in individuals with schizophrenia. These changes could contribute to the disruptions observed in this system within the context of the disease (Huang & Akbarian, 2007). Furthermore, in other brain regions, such as the hippocampus or amygdala, a diminished presence of GABA reuptake proteins has been documented among patients with schizophrenia (Lewis et al., 2008; Steiner et al., 2016).

Endocannabinoid system hypothesis

The cannabinoid hypothesis suggests that increased activation of cannabinoid receptor 1 (CB1R) in GABAergic interneurons in the VTA, amygdala and PFC could lead to a hyperdopaminergic and hypoglutamatergic state (Ľupták et al., 2021).

As mentioned above, cannabis use during adolescence, a period of increased brain vulnerability, increases the risk of developing schizophrenia. Both cannabis extracts and Δ^9-tetrahydrocannabinol (THC), the main psychoactive compound in cannabis, induce transient psychotic states in healthy subjects (Hall & Degenhardt, 2009) and exacerbate symptoms in schizophrenia patients (Foti et al., 2010). Cannabis use disorder occurs in 42% of schizophrenia patients, is strongly associated with more severe symptomatology, and strongly predicts relapse and/or chronicity of psychosis (Kline et al., 2022; Vaissiere et al., 2020). Furthermore, patients with psychosis who regularly use cannabis tend to have worse psychotic symptoms and cognitive dysfunction, as well as a higher

risk of re-hospitalization, as compared to non-users (Moran et al., 2022; Penzel et al., 2022).

Although this relationship has been suggested for some time, the pathways involved are not fully understood. Primarily, the major effects of cannabinoids in the brain are mediated by the activation of CB1R, the most abundant G protein-coupled receptor (GPCR) in the brain. In general, activation of presynaptic CB1R has inhibitory effects on glutamatergic, GABAergic, opioid, dopaminergic and serotonergic neurotransmission, although cannabinoid signaling is extremely complex and diverse (Ibarra-Lecue et al., 2021).

In this regard, some studies have demonstrated the involvement of cannabinoid signaling in the regulation of serotonergic functions, particularly via 5-HT2ARs in the brain. Activation of 5-HT2ARs is thought to indirectly induce the synthesis and release of endocannabinoids, whereas the absence of CB1Rs leads to serotonergic dysregulation in genetically modified mice. In addition, both 5-HT2A and CB1 receptors are expressed in brain structures involved in the regulation of emotions, learning and memory (Ibarra-Lecue et al., 2021).

In addition, chronic administration of THC to mice has been shown to alter 5-HT2AR signalling and confer susceptibility to psychotic states. It is also known that the density of CB1Rs is increased in *postmortem* brain tissue of people with schizophrenia (Urigüen et al., 2009).

1.1.2.3. Immune system alterations in schizophrenia

The immune system is widely recognized as the primary line of defense against invading pathogens. Recently, there has been exponential growth of the interface between immunology and chronic mental illness, including areas such as stress, neuroplasticity, genetics, and cytokines (Miller et al., 2011). In fact, there is a growing body of evidence indicating that immune dysregulation and neuroinflammation play a crucial role in the development of schizophrenia.

The concept of inflammation and immunity being implicated in the pathogenesis of schizophrenia dates back several decades (Menninger, 1919), and it continues to hold significance to this day as nowadays there are numerous epidemiological and genetic studies that establish clear connections between infection and inflammation in relation to schizophrenia (Brown et al., 2010; Karlsson & Dalman, 2020; Khandaker et al., 2015).

As an example, Prostaglandin E2 (PGE_2) plays a somewhat enigmatic role in the realm of schizophrenia, with limited research exploring its implications. Nevertheless, there have been notable reports of heightened PGE_2 levels (Kaiya et al., 1989) within this context. Notably, PGE_2 exerts its influence by stimulating the production of interleukin-6 (IL-6), an immunological marker consistently associated with schizophrenia.

Moreover, this complex interaction extends to the increased expression of cyclooxygenase-2 (COX-2), an enzyme closely intertwined with the effects of PGE_2 in schizophrenia (Das & Khan, 1998). Thus, while research on PGE_2 levels in schizophrenia remains somewhat constrained, the existence of reports indicating elevated PGE_2 levels in plasma of schizophrenia patients (Martinez-Gras et al., 2011) is a worth mentioning aspect of this intricate puzzle.

In the case of cytokines, particularly interleukins (ILs) serve as crucial signaling molecules within the immune system. They are released by various cell types, both immune and non-immune, and exert their proinflammatory or anti-inflammatory effects by binding to specific cytokine receptors on a diverse range of target cells. Changes in cytokine levels in schizophrenia are probably the most studied but controversial area of research in biological psychiatry. Within this context, some of these alterations have been identified as trait markers, including IL-12, interferon-γ (IFN-γ), tumor necrosis factor-α (TNF-α), and soluble IL-2 receptor (sIL-2R). These markers are consistently present in acutely relapsed patients and persist even after antipsychotic treatment. On the other hand, certain cytokines might be better classified as state markers, such as IL-1β, IL-6, and

transforming growth factor-β (TGF-β). State markers tend to manifest during exacerbations of schizophrenia and exhibit a tendency to normalize following antipsychotic treatment (Miller et al., 2011). It is noteworthy that in the context of schizophrenia, a substantial body of research has revealed a heightened prevalence of abnormal cytokine levels. This observation extends not only to patients diagnosed with schizophrenia (Garver et al., 2003; Potvin et al., 2008) but also encompasses their first-degree relatives (Nunes et al., 2006). It is essential to recognize that the nature of cytokine alterations in schizophrenia exhibits variability depending on the clinical status of the individuals involved.

For instance, when examining IL-6, research has shown that elevated IL-6 levels during childhood are associated with an increased risk of developing psychosis and depression in young adulthood (Khandaker et al., 2014; Perry et al., 2021). Similarly, heightened IL-6 levels have been observed in the acute phase of chronic schizophrenia in patients, compared to controls, and these levels tend to decrease with successful antipsychotic treatment (Miller et al., 2011). Furthermore, distinctions can be drawn among subtypes of schizophrenic patients, such as 'delayed-responders' (DR) and 'poor-responders' (PR). Some studies have indicated a significant increase in the cerebrospinal fluid (CSF) levels of the proinflammatory cytokine IL-6 in DR patients with schizophrenia, whereas CSF IL-6 levels in PR schizophrenics and controls were relatively similar (Garver et al., 2003). This research aligns with the idea that schizophrenia displays significant heterogeneity, and it provides evidence suggesting that a central immune process may be occurring specifically in one subtype of schizophrenia (Garver et al., 2003).

Finally, the relationship between the extended duration of the disease, resistance to therapy, and elevated IL-6 levels suggests that different immune processes may be at play in different stages of schizophrenia. Notably, IL-6 serum levels tend to be particularly elevated in patients with an unfavorable course of the disease (Lin et al., 1998) and those with a long history of the illness (Ganguli et al., 1994).

IFNγ, a pro-inflammatory cytokine, is another cytokine implicated in schizophrenia, potentially linked to cognitive function due to its role in the kynurenine pathway (KP). This pathway involves the induction of indoleamine 2,3-dioxygenase (IDO), one of the enzymes responsible for converting tryptophan (Trp) into kynurenine (Kyn) (Campbell et al., 2014), and IFNγ is considered a significant inducer of IDO in the initial steps of the KP (Grohmann et al., 2003).

The status of IFN-γ levels in schizophrenia has provoked considerable discussion (Momtazmanesh et al., 2019). While some research studies have documented diminished levels (Al-Asmari & Khan, 2014; Krause et al., 2013), others have reported heightened levels (Avguštin et al., 2005; Kim et al., 2009; Pedraz-Petrozzi et al., 2020), and certain studies have failed to reveal significant differences (Chiang et al., 2013; Xiong et al., 2014). Consequently, a multitude of investigations, including certain meta-analyses, have identified elevated levels of IFN-γ in chronic schizophrenia patients, whether they are in a state of stability or experiencing acute relapses (Frydecka et al., 2018; Goldsmith et al., 2016; Miller et al., 2011). Conversely, no substantial disruption in IFN-γ levels was found in patients recovering from acute relapses (Borovcanin et al., 2012). Furthermore, decreased IFN-γ levels were documented in patients displaying acute psychotic symptoms who had not been exposed to medications for a minimum of 6 months (Na & Kim, 2008), and in chronic patients. However, specific medication details were not disclosed in these studies (Al-Asmari & Khan, 2014).

One potential explanation for these incongruent findings is the correlation between IFN-γ and body mass index (BMI), a relationship previously established in individuals with psychosis (Frydecka et al., 2018). Given the substantial controversy, it is essential to analyze the changes in IFN-γ levels for each group of patients separately.

Initially, in patients with first-episode, a cluster of studies, including a comprehensive meta-analysis, has disclosed no significant alterations in IFN-γ levels (Borovcanin et al., 2012; De Witte et al., 2014; Lin et al., 2018; Noto et al., 2015). In contrast, another set of studies, encompassing an additional meta-analysis, has reported elevated levels (Ding et al., 2014; Miller et al., 2011).

Research studies have signaled elevated IFN-γ levels among both adult and pediatric patients experiencing their FEP, the majority of whom had previously been prescribed antipsychotic medications (Falcone et al., 2015; Lesh et al., 2018). Nevertheless, Di Nicola et al. reported unaltered IFN-γ levels in adult FEP patients, most of whom were currently on atypical antipsychotics (Di Nicola et al., 2013).

In addition to cytokines, alterations have been observed in other markers and peripheral signaling pathways associated with inflammation in individuals with schizophrenia. The Trp-Kyn metabolic pathway is increasingly gaining attention as a critical regulator of the immune system, with a significant role in the development of various diseases, including psychiatric disorders.

Kyn is produced by degradation of Trp and is a precursor of certain neuroactive metabolites. The breakdown of Trp into Kyn is facilitated by two enzymes, IDO and tryptophan 2, 3-dioxygenase (TDO). This transformation of Trp into Kyn reflects the activity level within the KP. Research conducted on the blood of individuals diagnosed with schizophrenia has reported elevated kynurenine/tryptophan ratio (Kyn/Trp) plasma ratios (Chiappelli et al., 2016; Marx et al., 2021; Okusaga et al., 2016). Furthermore, another study revealed an inverse correlation between increased plasma Kyn/Trp levels and frontal white matter glutamate levels in schizophrenia (Chiappelli et al., 2016). This marks the first instance where plasma Kyn levels can be regarded as an external indicator of brain changes associated with adverse alterations in cortical neurotransmission. This lends support to the notion that KP metabolites can serve

as peripheral markers for brain dysfunction in schizophrenia (Kindler et al., 2020).

Furthermore, as the disease progresses into chronic phases, a neurobiological process of neurodegeneration may unfold as a secondary consequence of inflammation. This process is linked to the involvement of the Trp-Kyn pathway, which, in itself, can trigger additional neurodegenerative effects (Myint et al., 2007).

1.1.2.4. Environmental risk factors

As previously mentioned, the presence of variations in some genes has been associated to a higher risk to suffer schizophrenia. However, this heritable genetic vulnerability is not sufficient for expressing the disease, being the presence of environmental factors prior to the debut of the disease also necessary (Stilo & Murray, 2019). An extensive review on the environmental influence on schizophrenia was carried out some years ago (Van Os et al., 2010), and a recent study has demonstrated the additive interaction between genetic risk for schizophrenia and several environmental exposures (Guloksuz et al., 2019). The environmental factors that have been associated most frequently with schizophrenia are the following:

Urbanicity

Urbanicity can be defined as the influence of living in urban areas at a specific moment and it is complementary to urbanization. In essence, urbanicity denotes the presence of circumstances that are unique to urban environments or significantly more prevalent than in nonurban settings (Vlahov & Galea, 2002).

Several studies have studied the connection between urbanization and the risk of schizophrenia. Some suggest that continuous or recurring exposures to certain factors, more prevalent in urbanized areas, may be responsible for this association. Additionally, there is evidence indicating a relationship between growing up in urban settings and the later development of schizophrenia (Pedersen & Mortensen, 2001).

Explanations for the disparities between urban and rural areas have evolved from factors that affect children around the time of birth to those that have a continuous and recurring impact throughout upbringing. Consequently, urbanicity appears to interact with genetic predisposition (Van Os et al., 2004). While there is no consensus on how to precisely describe urbanicity in research, it has been suggested that the social aspects of urban living may contribute significantly to the associated risk (March et al., 2008).

Migration

The link between migration and the risk of schizophrenia has been extensively documented in the literature (Cantor-Graae & Pedersen, 2013; Close et al., 2016). Numerous studies involving migrant populations have consistently reported higher incidence rates of schizophrenia. Specifically, when examining first-generation immigrants, research indicates a mean relative risk of 2.7, indicating that this group faces an almost threefold increased risk of schizophrenia compared to non-immigrant populations. Moreover, for second-generation immigrants, this risk escalates significantly to a mean relative risk of 4.5 (Cantor-Graae & Selten, 2005).

Interestingly, the degree of risk associated with migration appears to be influenced by the country of origin. In this regard, research on the comprehensive assessment of immigrant cohorts across countries has been limited, as the predominant studies tend to focus only on selected demographic groups that are considered more vulnerable (Cantor-Graae & Selten, 2005). One notable research study conducted in Canada investigates susceptibility to psychotic disorders in a group with diverse geographic origins. Notably, individuals from visible minority groups, such as those with black Caribbean and African backgrounds, tend to face a higher risk of schizophrenia (Kirkbride et al., 2012), whereas immigrants from northern Europe, southern Europe and East Asia had lower risks (Anderson et al., 2015). When these studies were further analyzed based on this factor, it was revealed that migrants originating from countries with predominantly black populations had an almost fivefold higher risk of developing schizophrenia. This

increased risk among this particular group has been suggested to stem from chronic social adversity and discrimination (Morgan et al., 2010).

Maternal immune activation

Accumulating evidence from epidemiologic, clinical, and basic neuroscience research suggests that schizophrenia is primarily a neurodevelopmental disorder. In fact, between the end of the last century and the beginning of the present, several studies have established a connection between schizophrenia and various infections, including influenza (Brown et al., 2004), rubella (Brown et al., 2001), toxoplasmosis (Brown et al., 2005), as well as viruses like herpes simplex (Buka et al., 2001) and cytomegalovirus (Blomström et al., 2012).

The wide range of infections associated with schizophrenia suggests a potential common factor contributing to increased susceptibility (Gilmore & Jarskog, 1997). Consequently, many investigations have sought to link maternal immune activation (MIA) through infections during pregnancy to a heightened risk of schizophrenia in offspring (Choudhury & Lennox, 2021).

As a result, certain studies have focused on the season of birth. Multiple studies have consistently demonstrated that individuals born during the winter or early spring months face a 5-10% higher likelihood of developing schizophrenia, possibly due to the elevated risk of infections during gestation (Davies et al., 2003).

However, what remains unclear in these studies is precisely what stages of gestation make the developing brain more vulnerable to these prenatal aggressions and what is the underlying mechanism inducing these alterations. Some research suggests that the mechanism may be linked to cytokine-associated inflammatory events. These events, coupled with subsequent pathophysiological effects like oxidative stress and temporary deficiencies in macronutrients and micronutrients, play a pivotal role in mediating the adverse consequences of maternal infection on the fetal system (Meyer, 2013; Miller et al., 2013). Another hypothesis suggest that MIA could influence genetically predetermined fetal

brain development, thereby increasing the risk of schizophrenia. It is plausible to extrapolate that a combination of mutations in neurodevelopmental genes and MIA may synergistically heighten the risk of schizophrenia (Handunnetthi et al., 2021).

An alternative hypothesis proposes that MIAs could affect the genetically programmed development of the fetal brain. This influence may manifest through alterations in the transcriptional regulation of genes crucially involved in brain disorders that emerge in adulthood, potentially elevating the risk of schizophrenia later in life (Labouesse et al., 2015). It is plausible to extrapolate that a combination of mutations in neurodevelopmental genes and MIAs may synergistically increase the risk of schizophrenia (Handunnetthi et al., 2021).

Consequently, MIA animal models have emerged as essential tools to establish a causal link between maternal infection during pregnancy and the emergence of schizophrenia-like abnormalities in offspring (Figure 3).

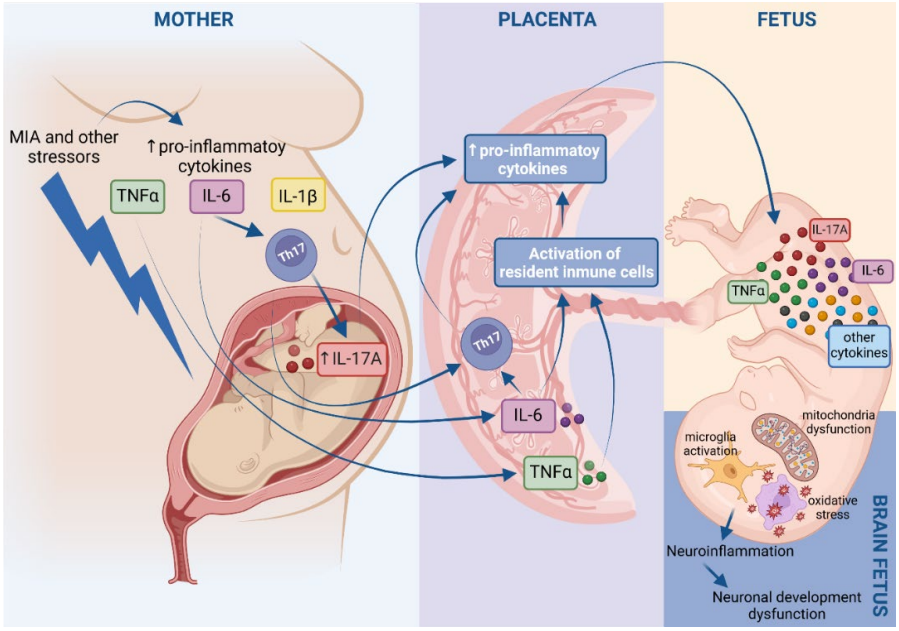

Figure 3: Proposed Mechanism for the Relationship between MIA and Fetal Development. Infections during gestation would produce an activation of the immune system, releasing cytokines such as TNFα, IL-6, or IL-1β. Notably, the heightened IL-6 levels trigger the activation of Th17 lymphocytes, culminating in the release of IL-17A. This cytokine, alongside TNFα and IL-6, can reach the placenta activating resident immune cells. These cells, in turn, release additional proinflammatory cytokines. In addition, Th17 lymphocytes may migrate to the placenta, exacerbating the inflammatory response, affecting placenta function, and causing damage. This inflammatory state could damage the placenta, potentially compromising its integrity and facilitating the passage of cytokines into the fetal circulation. Given the immaturity of the blood-brain barrier (BBB) in the fetus, these cytokines can access the fetal brain. In the brain, there is an activation of microglia causing a cascade of neuroinflammation and heightened oxidative stress. This process may lead to mitochondrial dysfunction, perpetuating a cycle of damage and inducing alterations in neuronal development and synapses. The long-term consequence of this cascade could manifest in disorders such as schizophrenia. Figure adapted from Zawadzka et al., 2021 using BioRender.com.

Childhood trauma and social adversity

Extensive research has delved into the potential risk factors for schizophrenia, with a particular focus on trauma and social adversity experienced during childhood. Childhood adversity includes exposure to abuse, neglect, or family dysfunction (Thomson & Jaque, 2018; Varese et al., 2012). This exposure represents a severe form of stress that can render individuals more susceptible to developing schizophrenia in adulthood. In this sense, refugee children who have experienced traumatic events in their nation of origin, compounded by possible

distress during their journey, face a high susceptibility to profound cognitive and socio-emotional challenges, which may lead to developmental disorders. Consequently, the migration process, particularly for families fleeing as refugees, could rightly be perceived as a form of childhood trauma (Fegert et al., 2018).

Moreover,, a robust connection exists between childhood trauma and the manifestation of schizophrenic symptoms (Morgan et al., 2007; Read et al., 2005). Notably, childhood trauma has a particularly strong association with the most severe forms of positive symptomatology in adulthood, specifically hallucinations (Bentall et al., 2014), as well as affective symptoms (Matheson, et al., 2013).

Cannabis use

Numerous epidemiological studies have shed light on the potential link between cannabis use during early adolescence (Arseneault et al., 2002) and an increased risk of developing psychosis or schizophrenia in later life (Di Forti et al., 2015; Gage, 2019), particularly in individuals who are vulnerable to its effects. This critical period of adolescence appears to amplify the susceptibility to cannabis-related risks. Moreover, it is noteworthy that cannabis consumption is notably more common among individuals diagnosed with schizophrenia compared to the general population. In fact, it stands out as the most frequently used illicit substance among these subjects.

Early development of the disease, increased psychopathology and relapses, failure of antipsychotic treatment, and poor prognosis are some of the consequences that have been attributed to cannabis use in individuals with schizophrenia (Schoeler et al., 2016). These observations underscore the importance of considering the potential adverse impact of cannabis use, especially among those already dealing with schizophrenia. Contrary to these studies, a systematic review of longitudinal studies published in 2004 found no causal relation between cannabis use by young people and psychosocial harm,

but could not exclude the possibility that such a relation exists (Macleod et al., 2004).

Finally, although cannabis abuse is associated with an increased risk of developing a psychotic disorder, most cannabis users do not develop such a disorder, suggesting that other factors are also involved in whether or not the illness develops.

1.1.3. Pharmacological treatment

The limited understanding of the causes of schizophrenia makes the treatment of this disease a significant challenge. Current treatment strategies, which includes antipsychotic medications, are primarily focused towards symptom reduction, aiming to reduce patient suffering while enhancing cognitive and social functioning. However, a common issue is that these treatments tend to be more effective in addressing positive symptoms and preventing relapses (Huhn et al., 2019), often falling short in addressing negative symptomatology (social withdrawal and apathy) and cognitive impairments (Nielsen et al., 2015). Adding to this complexity, approximately 20% of patients exhibit resistance to antipsychotic treatments (Kumar et al., 2016), necessitating the use of polypharmacy. This results in around 70% of individuals with schizophrenia taking at least two medications, and roughly 25% taking up to five or more (Toto et al., 2019). All of this underscores the growing need for a deeper understanding of the condition and more effective therapeutic approaches.

1.1.3.1. Typical antipsychotics

Typical or first-generation antipsychotic medications, like chlorpromazine, haloperidol, fluphenazine, and levorpromazine, represented a significant breakthrough in the treatment of schizophrenia and other mental disorders. These drugs are notably potent antagonists of the DRD2 (Lally & MacCabe, 2015), effectively addressing the positive symptomatology of the disease. However, they exhibit limited efficacy in tackling negative symptoms (Haddad & Correll, 2018) and are associated with considerable side effects, commonly referred to as

extrapyramidal symptoms (EPS). These side effects are primarily a result of DRD2 block in the nigrostriatal dopaminergic pathway and include acute dystonia, akathisia, parkinsonism, and tardive dyskinesia (Divac et al., 2014). Additionally, these medications can lead to hyperprolactinemia due to receptor antagonism in the tuberoinfundibular pathway.

1.1.3.2. Atypical antipsychotics

Over the years, significant progress has been made with the discovery of atypical or second-generation antipsychotic medications like clozapine, risperidone, olanzapine, and quetiapine. These drugs differ from their predecessors by having a lower affinity for DRD2, leading to reduced side effects, particularly in terms of extrapyramidal effects (Lally & MacCabe, 2015). Moreover, they not only antagonize the 5-HT2AR but also exhibit some affinity for other receptors, including serotonergic receptors 5-HT1AR or 5-HT2CR, α1 or α2 adrenergic receptors, and dopaminergic receptors D1 or D3 (Jarskog et al., 2007; Maric et al., 2016).

Currently, atypical antipsychotics are often the treatment of choice, although their superiority in improving overall symptoms, addressing negative symptoms, reducing relapses, or enhancing the quality of life remains uncertain for many of these drugs (Leucht et al., 2013; Zhu et al., 2017). Furthermore, approximately 30-40% of patients are resistant to treatment (Elkis & Buckley, 2016). In such cases, although the effectiveness of these measures has not been conclusively demonstrated empirically (Marder & Cannon, 2019; Samara et al., 2018), patients are frequently prescribed higher doses than recommended or a second antipsychotic (in more than 75% of individuals diagnosed with schizophrenia). Despite initial optimism, there is no clear consensus on the advantages of atypical antipsychotics (with the exception of clozapine) beyond the reduction of EPS in most cases (Jones et al., 2006; Lieberman et al., 2005). Finally, some studies conclude that atypical antipsychotics continue to have notable risks of EPS, particularly akathisia, and that these agents also appear to increase the risk of the

metabolic syndrome, though this effect seems most marked with clozapine and olanzapine (Shirzadi & Ghaemi, 2006). This highlights the urgent need for significant advancements in antipsychotic treatments.

1.2. Akt/mTOR/S6 pathway

1.2.1. General aspects

The Akt/mTOR/S6 pathway (Figure 4) plays a pivotal role in neurodevelopment and neuroplasticity due to its involvement in critical processes such as protein synthesis, cell growth and proliferation (Wullschleger et al., 2006). Both Akt and mechanistic target of rapamycin (mTOR) are serine/threonine kinases with the ability to phosphorylate and regulate numerous biological processes.

Akt stands out as an extraordinarily versatile kinase, deeply involved in a multitude of molecular processes such as cellular growth, apoptosis, and metabolism among others. Akt protein can bind to various targets thanks to its amino-terminal pleckstrin homology (PH) domain, such as phosphatidylinositol-3,4,5-trisphosphate (PIP3) produced by phosphoinositide 3-Kinase (PI3K) or phosphoinositide-dependent protein kinase 1 (PDK1). Several stimuli have been demonstrated to activate PI3K, including α/γ subunits of heterotrimeric G proteins coupled to GPCR. This activation leads to Akt recruitment and activation (Murga et al., 1998). Once localized to the plasma membrane, Akt undergoes a phosphorylation at two sites (Thr308 residue by the PDK1 and Ser473 by the mTOR complex 2 (mTORC2)). Once activated, Akt phosphorylates substrates distributed throughout the cell to regulate multiple cellular functions (Manning & Cantley, 2007).

In particular, in neurons, Akt activation regulates critical processes like neuronal survival, architectural development, and axonal growth. Upon activation, Akt instigates the mTOR complex 1 (mTORC1), composed of mTOR and a set of proteins governing its signaling cascade.

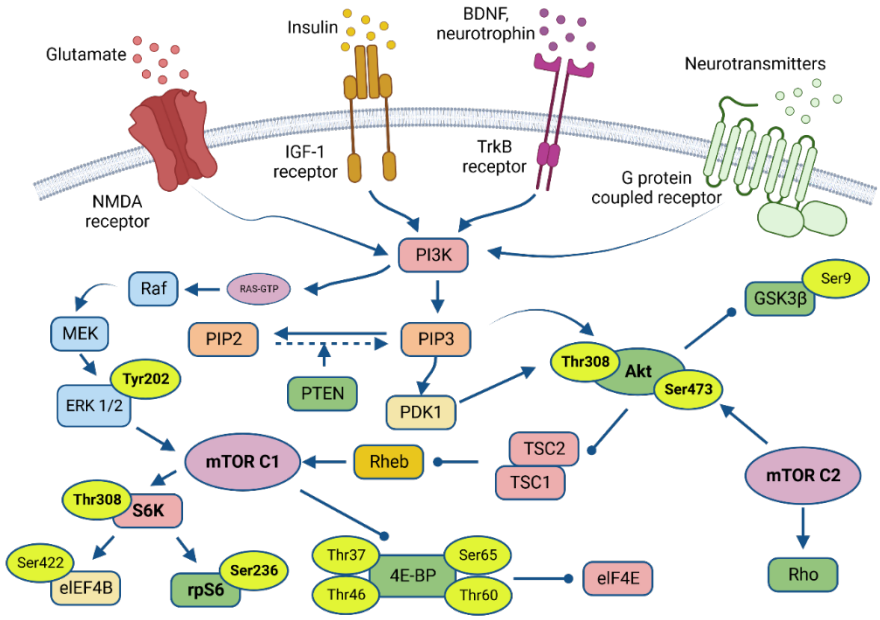

Figure 4: Regulation of the mTOR signaling pathway in the brain. mTORC1 is activated by receptor signaling through the PI3K–Akt pathway. Through its downstream effectors the 4E-BPs and S6K1 and 2, mTORC1 controls neuronal protein synthesis. Adapted from Costa-Mattioli et al., 2013 using BioRender.com.

On the other hand, mTOR is a large, ubiquitously expressed multi-effector serine/threonine kinase that belongs to the PI3K-related kinase family. It interacts with several proteins to form two distinct heteromeric complexes, mTORC1 and mTORC2. Both mTOR complexes consist of numerous proteins that control mTOR signaling, dictate subcellular localization, and regulate substrate specificity; with mTORC1 having six and mTORC2 seven known protein components (Laplante & Sabatini, 2012).

The main function of this complex lies in protein translation and synthesis, apoptosis, autophagy, energy metabolism and cell growth. It oversees two essential components: p70 ribosomal protein S6 kinase (p70S6K) and the eukaryotic translation initiation factor 4E-binding protein (4E-BP). These factors then stimulate downstream substrates, including the ribosomal protein S6 (rpS6 or S6), which plays a critical role in protein synthesis (Ibarra-Lecue et al., 2020). Furthermore, select GPCRs can also activate the RAS-GTP pathway, leading to

the activation of extracellular signal-regulated kinase (ERK) and, subsequently, mTOR activation.

Interestingly, ablation of both phosphorylated (Ser473)-Akt and S6 kinase (S6K), is able to alter 5-HT2A receptors functionality and signaling (Strachan et al., 2010). Furthermore, in the brain, the phosphorylation of rpS6 is induced by various physiological and pharmacological events and has become a widely used marker of neuronal activity (Knight et al., 2012). The exact role of these phosphorylation events remains unknown, although it has been proposed that the phosphorylation of rpS6 is involved in the translational machinery for protein synthesis and in the positive regulation of global protein translation (Ruvinsky & Meyuhas, 2006). Moreover, enhanced rpS6 phosphorylation has been associated with increased levels of proteins in some models of synaptic plasticity as well as in various mouse models of neurological and neurodevelopmental disorders which display an enhanced global protein synthesis (Puighermanal et al., 2017).

All these data collectively suggest that dysfunction in the Akt/mTOR/S6 pathway may contribute to aberrant dendritic reorganization and the loss of dendritic spines in the PFC, ultimately resulting in disruptions in synaptic connectivity.

1.2.2. Akt/mTOR/S6 pathway alterations in schizophrenia

In the context of schizophrenia, there is an emerging notion of reduced activity in the Akt/mTOR/S6 pathway among affected individuals (Chadha et al., 2021; Ibarra-Lecue et al., 2020).

As mentioned, alterations in neurodevelopment may cause susceptibility to environmental factors, increasing the risk of developing schizophrenia. In this context, given the implications of the Akt/mTOR/S6 pathway in brain function and development, it has been suggested that alterations in this intracellular pathway has a relevant role in the etiopathogenesis of the disease (Ibarra-Lecue et al., 2020). However, the molecular mechanisms linking this system to the increased risk of developing schizophrenia are not fully understood.

Akt was the first protein of this cascade to be implicated in schizophrenia (Emamian et al., 2004). In this context, it has been suggested that certain allelic variants in the AKT1 are associated with cognitive impairments, as well as neuroanatomical and functional abnormalities in the PFC (Pietiläinen et al., 2009). Additionally, several case/control and family cohort studies support the hypothesis that AKT1 is a gene involved in schizophrenia (Di Forti et al., 2012; Van Winkel et al., 2011). The association between AKT1 genetic variants and schizophrenia has been confirmed in European, Japanese, Middle Eastern, Chinese, Irish and British populations (Mathur et al., 2010; Schwab et al., 2005; Thiselton et al., 2008). On the other hand, variations in the AKT1 gene have also been associated with the development of schizophrenia in cannabis users (Di Forti et al., 2012; Van Winkel et al., 2011). In this context, a neuroimaging study has shown that healthy subjects carrying an allelic variant of the AKT1 gene present a greater psychotic response after THC administration (Bhattacharyya et al., 2012). Finally, a number of studies provided convergent evidence of a decrease in AKT1 mRNA, protein, and activity levels in the PFC and hippocampus, as well as in peripheral blood of individuals with schizophrenia (Emamian et al., 2004; Thiselton et al., 2008).

In the same line, another element of the Akt/mTOR/S6 pathway that has been implicated in the development of schizophrenia is mTORC1. This complex modulates a large number of cell growth and survival processes, and dysregulation of the functionality of this protein may contribute to an aberrant dendritic organization and a loss of dendritic spines, potentially leading to connectivity issues (Magdalon et al., 2017). So, a dysfunction of mTORC1 has been described in schizophrenia (Chadha & Meador-Woodruff, 2020; Huang et al., 2013), as well as in animal models of the disorder (Amodeo et al., 2019; Goh et al., 2020).

The rpS6 protein, a ribosomal protein involved in protein translation and activated by mTOR (Puighermanal et al., 2017), has also garnered attention in the context of schizophrenia research. Both human studies (Chadha et al., 2021;

Ibarra-Lecue et al., 2020) and animal research (Ibarra-Lecue et al., 2018) have explored its potential relevance to the disorder.

Similarly, the ERK protein, a crucial component of the mitogen-activated protein kinase (MAPK) cascade involved in cell differentiation, has been implicated in the pathophysiology of schizophrenia (McGuire et al., 2017). Animal models have further underscored its involvement in the disease (Hudson et al., 2019; Li et al., 2020).

Lastly, studies in animals have demonstrated that the modulation of signaling within this pathway in the brain cortex can be achieved through certain antipsychotic medications (Liu et al., 2017). However, the long-term effects of these drugs in Akt/mTOR/S6 pathway in individuals with schizophrenia and its potential contribution to the drugs' therapeutic effects remain relatively unexplored.

1.3. The double-hit hypothesis of schizophrenia

Schizophrenia, as already mentioned, is a complex condition resulting from a combination of genetic predisposition and environmental factors. As we have seen so far, there are numerous factors capable of altering neurodevelopment. Following the proposal of the neurodevelopmental hypothesis, the importance of the combination of factors capable of altering neurodevelopment soon became evident. This concept gives rise to the "double-hit hypothesis of schizophrenia", which suggests that genetic susceptibility (first hit) is essential to sensitize an individual to early or late environmental stressors (second hit) (Maynard et al., 2001) (Figure 5). Initially, this hypothesis emerged as a way of unifying the neurodevelopmental hypothesis with a possible genetic origin, although it was soon extended to any combination of the aforementioned factors (Bayer et al., 1999).

In this context, numerous studies support the idea that environmental factors alone appear to have a relatively weak influence on individuals and are unlikely to be the only factor responsible for the development of the disease (Guerrin et

al., 2021; Jauhar et al., 2022; Stilo & Murray, 2010). Additionally, it is well-established that these events must occur during specific developmental windows when individuals are particularly vulnerable due to their neurodevelopmental stage (Winship et al., 2019). Thus, first hit event must occur during fetal neurodevelopment within the mother's pregnancy, while the second hit typically manifests during adolescence or early adulthood. Adolescence is recognized as a notably critical period in the development of the central nervous system (CNS), as previously mentioned. This coordinated sequence of events underscores the intricate nature of schizophrenia's etiology and its temporal relationships within the lifespan.

Regarding genetic factors, it is well-established that issues during pregnancy, such as abnormal fetal growth and development (Cannon et al., 2002), a compromised prenatal environment marked by factors like infection, malnutrition, antibiotic treatment, and psychosocial stress (al-Haddad et al., 2019; Cattane et al., 2020; King et al., 2010), as well as being born in the winter months (Tochigi et al., 2004) can contribute to the emergence of a genetic predisposition, rendering individuals more susceptible to developing schizophrenia in adulthood. On the other hand, later environmental factors encompass experiences like bullying at school and facing discrimination (Varese et al., 2012), early-onset substance abuse (Di Forti et al., 2014; Marconi et al., 2016), immigration-related stressors (Bourque et al., 2011; Cantor-Graae & Pedersen, 2013), socioeconomic influences (Allardyce & Boydell, 2006; Byrne et al., 2004; Paksarian et al., 2015), and social isolation coupled with social defeat (collectively known as social adversities or social trauma) (Stowkowy & Addington, 2012). These environmental elements collectively contribute to the complex landscape of schizophrenia susceptibility and onset. Therefore, prenatal infection, in combination with exposure to drugs such as THC during peripuberty, has been associated with increased risk for neuropsychiatric disorders (Guma et al., 2023).

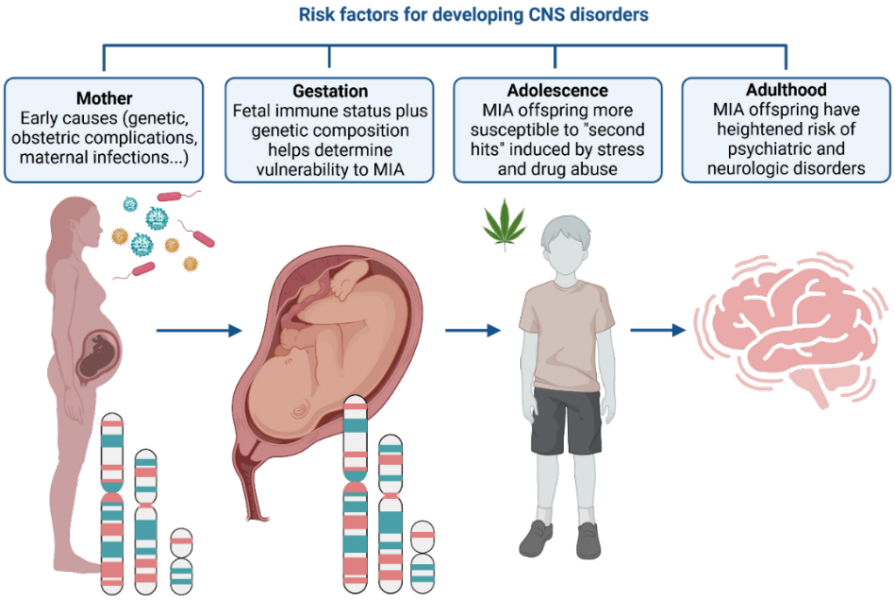

Figure 5: Schematic representation of double-hit hypothesis of schizophrenia. Combination of genetic background and second hits during childhood and adolescence (including stress and drug abuse) associates with the consequences of MIA to increase the likelihood of offspring developing psychiatric disorders as adults. Adapted from Estes & MacAllister, 2016 using BioRender.com.

1.4. Research tools for the study of schizophrenia

Contemporary psychiatry relies on the observation and description of patient behavior for diagnosis. Unfortunately, unlike many medical specialties, psychiatry lacks easily observable markers or changes, such as those revealed through neuroimaging techniques or anatomopathological studies. This underscores the need to identify potential biomarkers, both to distinguish between those affected by a condition and those who are healthy, and to guide personalized treatment approaches.

In recent decades, non-invasive technologies have emerged for studying the structure and function of the human brain. Despite considerable efforts to identify reliable biomarkers based on current disease models, psychiatry still faces significant challenges in this regard. The study of mental disorders, inherent to humans, requires the substrate in which the disorders occur; that is, the nervous tissue (Meana et al., 2014).

Currently, several types of human biospecimens are being used for research, including *postmortem* brain tissue, blood, CSF and genetically engineered cells, such as induced pluripotent stem (iPS) cells and induced neuronal cells. However, these samples are far from providing a useful predictive, diagnostic or prognostic biomarker as the utility of non-neuronal cells for understanding the cellular basis of neurological and neuropsychiatric disorders is limited (Matigian et al., 2008).

1.4.1. Olfactory neuroepithelium

The olfactory neuroepithelium (Figure 6) is an accessible neuronal tissue in adult humans (Féron et al., 1998) capable of demonstrating disease-dependent biological alterations in schizophrenia (McCurdy et al., 2006; Ronnett et al., 2003). Notably, its neuronal progenitor cells present unique characteristics, including self-regeneration abilities and the capacity to generate both neuronal and glial cells, making this tissue the only source of neuronal cell regeneration that can be obtained from a living human being. Therefore, primary cultures derived from biopsies of the olfactory neuroepithelium offer a valuable avenue for studying the neurobiological traits of individuals under different conditions and disease states (Borgmann-Winter et al., 2009).

The cells of the olfactory neuroepithelium are similar to those of the neuroepithelium of the embryonic neural tube (Féron et al., 1998). These precursor cells undergo multiple divisions and subsequently differentiate into mature sensory neurons throughout an individual's life. Thus, the olfactory neuroepithelium contains pluripotent cells capable of *in vitro* proliferation and differentiation into various cell types, including neurons and glia (Matigian et al., 2010). This continuous and robust neurogenesis in the olfactory neuroepithelium is a unique feature of human neural stem cells (Keenan et al., 2010) and has substantial implications, allowing the establishment of new models for studying diseases affecting the central nervous system.

The identification and quantification of cell populations expressing different characteristics define different stages of this process, ranging from stem cells to

progenitor cells and from immature to mature neurons. Neural progenitor cells present in the olfactory neuroepithelium are defined as undifferentiated clonogenic cells with the ability to self-renew, generate neuronal or glial cells, and maintain themselves as neurospheres in cell culture (Idotta et al., 2019; Matigian et al., 2010). Until now, the isolation of such progenitor cells from human and animal models necessitated high-risk surgical methods, including *postmortem* tissue biopsies during autopsies (English et al., 2015). This approach is inherently limiting, as it only permits the study of advanced disease stages, making it unsuitable for early diagnosis, treatment, or prognosis. For all these reasons, it was necessary to improve the methodology for obtaining and maintaining neuronal lines to allow the study of biomarkers, thus achieving a better understanding of brain disorders (Jiménez-Vaca et al., 2018).

On the other hand, these neural progenitor cells from the olfactory neuroepithelium in adult humans can form neurospheres under appropriate *in vitro* culture conditions (Jiménez-Vaca et al., 2018). When cultured in a defined medium containing epidermal growth factor (EGF) and basic fibroblast growth factor (bFGF), these isolated neural progenitor cells, possessing high mitotic capacity, can grow as spherical aggregates referred to as neurospheres. This inherent capacity of neural stem cells (Keenan et al., 2010) makes these structures derived from the olfactory mucosa particularly intriguing for establishing new models to study CNS diseases. Importantly, as they do not necessitate genetic reprogramming, they offer a valuable tool for comprehending disease etiology, enhancing diagnosis, monitoring treatment, and facilitating the development of novel drugs (English et al., 2015; Matigian et al., 2010).

The accessibility and availability of these olfactory neuroepithelium-derived cells provide a unique opportunity to correlate clinical characteristics of living subjects with cellular and molecular functions involved in neuronal processes. These include neuronal maturation and survival, odor detection, signal transduction, and calcium homeostasis. The straightforward process of obtaining neurospheres holds great promise for improving our understanding of disease causation,

diagnosis, treatment monitoring, and the development of innovative therapeutics (Álvarez et al., 2023; Barrera-Conde et al., 2021; Delgado-Sequera et al., 2021; Guinart et al., 2020) .

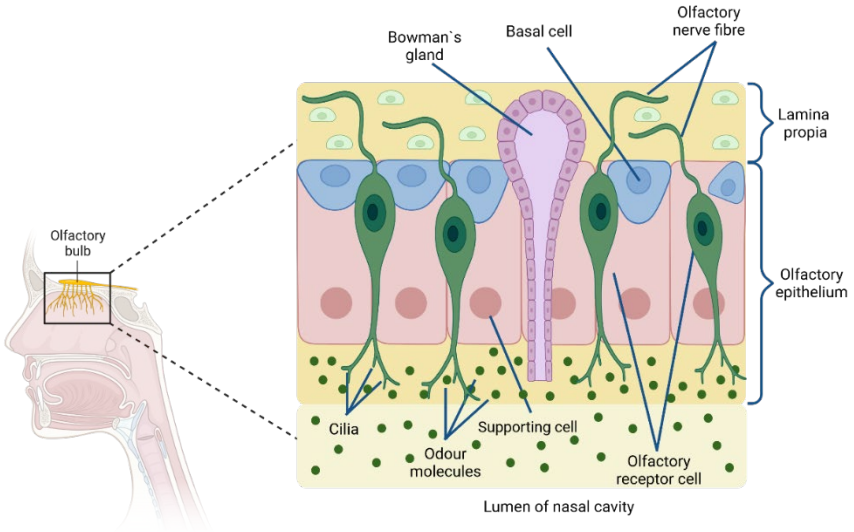

Figure 6: Schematic representation of the olfactory neuroepithelium. The olfactory neuroepithelium is located within the nasal cavity and contains olfactory sensory neurons, sustentacular cells, glandular cells or basal cells. The information is transmitted from the receptors to the olfactory bulb in the brain. Adapted from Gómez-Virgilio et al., 2021 using BioRender.com.

1.4.2. Animal models

Modeling human neuropsychiatric disorders in animals is extremely challenging given the subjective nature of many key symptoms, the lack of biomarkers and objective diagnostic tests, and the relatively early state of the relevant neurobiology and genetics. Nonetheless, the progress in understanding pathophysiology and treatment development would benefit greatly from improved animal models (Nestler & Hyman, 2010). To date, certain animal models have managed to approximate some disease characteristics, including abnormal social behavior, motivation, working memory, emotion, and executive functions. However, some specific symptoms unique to these disorders in humans (hallucinations and delusions) make it challenging to extract meaningful results from these animal models (Winship et al., 2019).

To be considered a useful and effective animal model, it must meet three primary validity criteria (Figure 7). All animal models for schizophrenia must demonstrate appropriate face validity (similarity of symptoms), construct validity (replication of theoretical neurobiological rationale and pathology), and predictive validity (showing the expected pharmacological response to known antipsychotic treatments and potential new adjunct therapies) for the clinical disorder being modeled (Jones et al., 2011).

Face validity takes into account the importance of the chosen species and strain. It asks whether the chosen animal species and strain are appropriate and relevant to the human disorder. In essence, it assesses whether the model looks like it should represent the human condition on the surface. Construct validity evaluates how well the animal model replicates the underlying processes that give rise to the disease. This includes factors like genetics, environmental influences, and drug exposure. It seeks to determine whether the model reproduces the theoretical basis and pathology of the human disorder. Finally, predictive validity assesses the model's ability to predict both the onset of symptoms and the effectiveness of therapeutic interventions. It questions whether the model responds to treatments in a manner consistent with the clinical disorder it aims to mimic. In summary, these validity criteria serve as essential benchmarks for evaluating the effectiveness of animal models in replicating and studying neuropsychiatric disorders. They ensure that the models chosen for research are not only relevant and accurate representations but also capable of providing insights into the disorder's underlying mechanisms and potential treatment strategies.

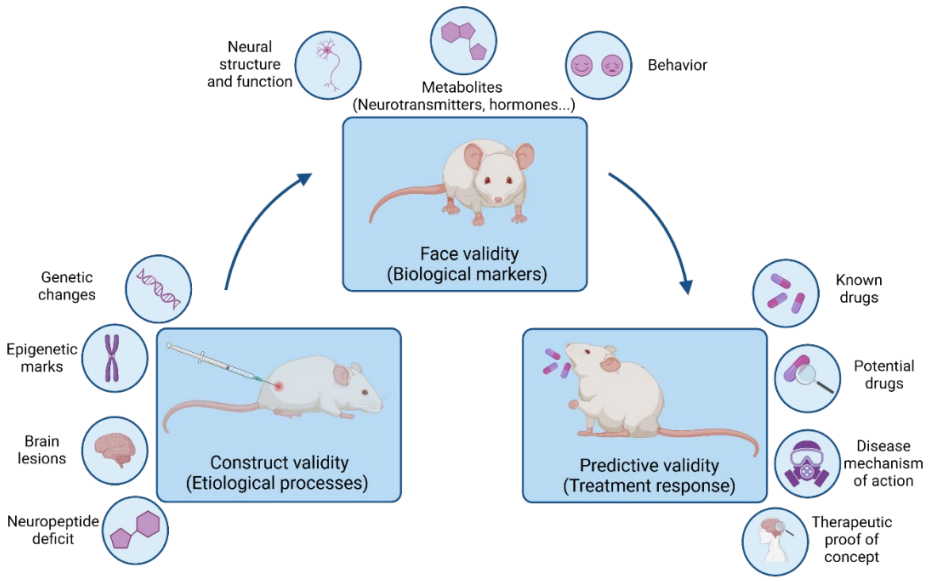

***Figure 7: Scheme of the three types of validators that animal models of schizophrenia should meet. Adapted from Mabunga et al., 2015* using BioRender.com.**

Regarding schizophrenia, animal models used to study the disease typically fall into three categories: drug-induced models, genetic models, and developmental models. Drug-induced models employ substances that increase dopaminergic tone, such as amphetamines or non-competitive NMDA antagonists like ketamine. Genetic models involve the modification of genes identified in GWAS as genetic models of schizophrenia (Winship et al., 2019). Lastly, developmental models are based on environmental manipulations during prenatal, perinatal, or early postnatal stages. Similar to humans, symptoms in animal developmental models emerge during adolescence-like period (Winship et al., 2019).

One class of these animal models utilizes immune-activating agents that primarily stimulate the mother's innate immune system, such as the synthetic double-stranded RNA analogue polyinosinic:polycytidylic acid (Poly(I:C)), which simulates viral immune responses, or the bacterial endotoxin lipopolysaccharide (LPS) to evoke bacterial responses (Solek et al., 2018). Rodents exposed to MIA during gestation exhibit some neurochemical and behavioral similarities to individuals with schizophrenia. Moreover, this type of

model has been used in combination with subsequent environmental alterations, such as stress or cannabis administration, to mimic the double-hit mouse model, where neurodevelopment is disrupted during its two most vulnerable stages: prenatal and adolescence (Winship et al., 2019).

As mentioned earlier, current single-hit animal models have certain limitations and discrepancies regarding their construct and face validity. This has led to the preference for using double-hit neurodevelopmental models in the study of schizophrenia because they have been shown to have more effects than single-hit exposure on certain features of the disease, and may therefore be suitable as a model for studying the molecular basis of schizophrenia, demonstrating that the accumulation of risk factors has effects on neurodevelopment (Guma et al., 2023). These double-hit models are considered ideal for replicating the heterogeneity of the disease by introducing environmental modifications during two crucial phases of neurodevelopment (Winship et al., 2019). These double-hit models typically involve various combinations of prenatal and postnatal risk factors. They usually begin with an initial adverse event during gestation, such as genetic predisposition or prenatal insult, followed by a second insult during adolescence. This approach may offer valuable insights into comprehending the progression of the disease.

In this context, there are several environmental factors that can serve as risk factors associated with schizophrenia. These include maternal infection/immune activation, social/physical stress, and the administration of various drugs like NMDAR antagonists, corticosterone, cannabis, or methamphetamine (Guerrin et al., 2021).

The Poly(I:C) + THC double-hit mouse model of schizophrenia

One of the frequently used double-hit models in this context is the Poly(I:C)/THC model as it has been well demonstrated that in addition to infections and activation of the maternal immune system, the use of cannabinoids represents another crucial factor in the development of schizophrenia. In this model, mice

are exposed to prenatal MIA and adolescent exposure to chronic THC (Guma et al., 2023).

Poly(I:C), a synthetic double-stranded RNA (dsRNA) analog, shares a molecular pattern found in the replication of viruses commonly associated with MIA (Lester & Li, 2014). The mammalian immune system can detect dsRNA molecules through the Toll-like-Receptor 3 (TLR3), an innate immune receptor. When dsRNA binds to this receptor, it initiates a pro-inflammatory signaling cascade, activating the nuclear factor kappa B (NF-κB) and interferon (IFN) (β, α, etc.). These factors promote the expression of pro-inflammatory cytokines that induce systemic changes throughout the body including changes in neurons and glia.

The expression pattern of these TLRs in different tissue may also influence their impact on fetal neurodevelopment. For instance, while TLR3 is expressed in various tissues, placental expression of TLR3 is one of the highest among all human tissue types (Nishimura & Naito, 2005). This places TLR3 in closer proximity to the maternal-fetal interface, suggesting that the effects of activating different TLRs may result in phenotypes driven by distinct underlying mechanisms (Haddad et al., 2020).

Creating MIA animal models using Poly(I:C) involves several critical factors that demand careful consideration. These include the timing of administration during gestation, the choice of animal strain, the route of administration, and the dosage. These variables can significantly impact the outcomes of Poly(I:C) MIA experiments (Kentner et al., 2019; Meyer et al., 2009; Mueller et al., 2019). Regarding route of administration, dose and gestational timing, previous studies have shown that intraperitoneal administration of doses above 5 mg/kg administered on gestational day (GD) 9.5 produce behavioral and neurochemical changes in mice offspring similar to some symptoms observed in schizophrenia, along with sensorimotor changes (Guma et al., 2021; MacDowell et al., 2021; Meyer et al., 2008; Prades et al., 2017). Numerous epidemiological studies consistently highlight the strongest associations between offspring risk and

maternal infections occurring during the first and second trimesters of pregnancy. Consequently, in the majority of rodent studies involving Poly(I:C) MIA model, the immune challenge is typically administered at the developmental equivalent timing in rodents. This timing is of paramount importance due to the dynamic variations in maternal immune responses throughout pregnancy and the evolving vulnerability of the developing fetus during gestation. Considering the heightened susceptibility of the nervous system during the initial and middle stages of gestation, early administration during gestation becomes more relevant and suitable for modeling schizophrenia (Reisinger et al., 2015).

Despite the large number of preclinical studies that have utilized the Poly(I:C) MIA model to investigate neurodevelopmental disorders, interpretation is not straightforward due to the variability in MIA parameters and experimental conditions between studies. This variability has been previously acknowledged (Meyer et al., 2009) and is receiving increasing attention in more recent research (Careaga et al., 2018; Mueller et al., 2018). Despite these challenges, the viral MIA model has demonstrated substantial face, construct, and predictive validity in a considerable body of literature.

In the context of double-hit models involving THC, it is important to highlight that THC is the main cannabinoid found in *Cannabis sativa*, and responsible for its psychoactive effects. This has led to a growing interest in using THC to mimic the second hit in these models.

Chronic THC exposure during adolescence has been found to trigger the overactivation of a pro-hallucinogenic signaling pathway mediated by 5-HT2A receptors, regulated by the Akt/mTOR pathway (Ibarra-Lecue et al., 2018). Moreover, it has been shown that exposure to THC during adolescence can ameliorate disruptions in dopaminergic activity in the VTA induced by MIA (Lecca et al., 2019). However, it is important to note that in other studies, despite recognizing behavioral alterations caused by these separate impacts, no significant positive or negative synergistic effects were observed (Stollenwerk &

Hillard, 2021). In some cases, the observed differences were subtle, and this could be attributed to the lower dosages employed in these latter studies (Guma et al., 2023).

In this case, it is also necessary to take into account the time of administration, with the postnatal days (PND) of administration coinciding with puberty in mice (Guma et al., 2023). This is crucial because during adolescence, the brain is still undergoing critical developmental processes such as neuronal maturation, myelination, synaptic pruning, dendritic plasticity, and volumetric growth (Malone et al., 2010). Furthermore, heavy cannabis use during adolescence has been associated with subtle alterations in brain circuits. These changes include cortical thinning in the temporal and frontal regions (Jacobus et al., 2014) and reduced volumes of the orbitofrontal gyri (Filbey et al., 2014). Moreover, an early onset of consumption is also linked to early disease development and increased psychopathology (Arseneault et al., 2002).

Finally, given the conflicting outcomes from these studies, it is imperative to continue research in this direction. This pursuit serves a dual purpose: firstly, to establish a reproducible model encompassing both impacts effectively, and secondly, to delve deeper into the mechanisms that underlie the heightened risk of schizophrenia attributed to these two factors.

Hypothesis and Objectives

2. HYPOTHESIS AND OBJECTIVES

Hypothesis:

Study I: The neural progenitors present in the olfactory neuroepithelium of subjects with schizophrenia give rise to neurospheres, neurons and glial cells that exhibit a specific fingerprint characterized by neurodevelopmental alterations and an aberrant signaling of the Akt/mTOR/S6 pathway.

Study II: The double-hit rodent model based on MIA together with a chronic exposure to THC during the adolescence displays a specific schizophrenia-like phenotype characterized by cognitive, neurodevelopmental alterations, and an aberrant signaling of the Akt/mTOR/S6 pathway.

General objective:

Study I: Evaluation of the developmental and transcriptional characteristics, as well as the status of the Akt/mTOR/S6 signaling pathway of neural cells derived from olfactory neuroepithelium of controls and subjects with schizophrenia in order to develop trait, state and prognostic biomarkers and thus generate the knowledge base for personalized medicine in schizophrenia.

Study II: Evaluation of phenotypical, molecular and transcriptional characteristics, as well as the status of the Akt/mTOR/S6 signaling pathway of a double-hit rodent model of schizophrenia.

Specific objectives:

Study I:

- **Objective 1:** Development of a non-invasive, easy, reproducible and reliable method for the isolation, culture and characterization of neurospheres, neurons and glial cells from the olfactory neuroepithelium in living subjects.

- **Objective 2:** Isolation and culture of neurospheres, neurons and glial cells derived from the olfactory neuroepithelium of subjects with schizophrenia and their matched controls.
- **Objective 3:** Evaluation of the developmental and transcriptional characteristics of neurospheres, neurons and glial cells derived from the olfactory neuroepithelium of subjects with schizophrenia and their matched controls.
- **Objective 4:** Evaluation of the status and the functionality of the proteins of the Akt/mTOR/S6 signaling pathway in neurons and glial cells derived from the olfactory neuroepithelium of subjects with schizophrenia and their matched controls.

Study II:

- **Objective 1:** Establishment of a double-hit rodent model of schizophrenia based on: (1) MIA together with (2) chronic exposure to THC during the adolescence.
- **Objective 2:** Phenotypical evaluation of the double-hit rodent model of schizophrenia.
- **Objective 3:** Evaluation of the transcriptomic profile of the brain cortex in the double-hit rodent model of schizophrenia.
- **Objective 4:** Evaluation of the status and the functionality of the proteins of the Akt/mTOR/S6 signaling pathway in the brain cortex of the double-hit rodent model of schizophrenia.

Subjects, Materials and Methods

3. SUBJECTS, MATERIALS AND METHODS

3.1. Subjects

3.1.1. Human samples

The olfactory neuroepithelium was obtained by nasal exfoliation conducted by qualified nurses at the Department of Psychiatry of the Hospital Universitario de Cruces (Barakaldo, Spain) or at the Faculty of Medicine and Nursery of the University of the Basque Country (UPV/EHU) (Leioa, Spain). Prior to the extraction of samples, all participants provided written consent. The entire procedure was approved by the corresponding Human Research Ethics Committee (University Cruces Hospital, code CEIC CEI E22/27).

A total sample size of 20 subjects (10 cases and 10 controls) was used in this Doctoral Thesis. Subjects who met inclusion criteria for schizophrenia based on a Structured Clinical Interview (DSM-V, or ICD-10) were included into the study as cases. For controls, inclusion criteria were age 18-60 and no neurological or psychiatric diagnoses. Controls were recruited regarding sex and age matching criteria with cases. Exclusion criteria for all subjects included, meeting criteria for any severe mental disorder different from schizophrenia, history of severe congenital, medical, or neurological illnesses, current medical conditions affecting the nasal region (such as rhinitis or bleeding).

General information regarding the demographic characteristics of the experimental groups can be found in Table 1 and Table 2.

Table 1: **Demographic characteristics of case subjects.** Gender, age, psychiatric diagnosis, antipsychotic (AP) treatment and other relevant treatments prescribed.

Cases					
Case	**Gender**	**Age (years)**	**Psychiatric diagnosis**	**AP prescribed**	**Other treatments prescribed**
EPI001	Male	28	Schizophrenia	Paliperidone im, clozapine	-
EPI002	Male	32	Schizophrenia	Aripiprazole im, olanzapine	Escitalopram
EPI003	Female	21	Schizophrenia	Paliperidone	-
EPI004	Female	30	Schizophrenia	Olanzapine im	-
EPI005	Male	32	Schizophrenia	Aripiprazole im	-
EPI006	Male	38	Schizophrenia	Aripiprazole im	-
EPI007	Female	23	Schizophrenia	Aripiprazole im, quetiapine	-
EPI008	Female	39	Schizophrenia	Aripiprazole	Lithium
EPI009	Female	42	Schizophrenia	Quetiapine	-
EPI010	Male	25	Schizophrenia	Risperidone im	Sertraline

Table 2: **Demographic characteristics of control subjects.** Gender, age, and its matched case subject.

Controls			
Control	**Matched case**	**Gender**	**Age (years)**
Control 1	EPI001	Male	27
Control 2	EPI002	Male	31
Control 3	EPI003	Female	23
Control 4	EPI004	Female	31
Control 5	EPI005	Male	34
Control 6	EPI006	Male	40
Control 7	EPI007	Female	24
Control 8	EPI008	Female	34
Control 9	EPI009	Female	45
Control 10	EPI010	Male	23

3.1.2. Animals

Wild-type male and female CD-1 mice (Charles Rivers, Wilmington, MA, USA) were used for all the experiments described in this Doctoral Thesis. Animals were maintained at the animal facilities of the UPV/EHU and housed (4-6 animals per cage) under controlled temperature (23 ± 1ºC), on a normal 12 hours (h) light/dark cycle (lights on between 8 am – 8 pm), with free access to food and water.

Animal care and all procedures involving mice were performed in accordance with the European Directive for the Protection of Vertebrate Animals used for experimental and Other Scientific Purposes (European Union Directive 2010/63/EU) and were approved by the Ethic Committee for Animal Welfare of the UPV/EHU (CEBA M20/2022/072).

3.1.2.1. Double-hit mouse model: MIA and THC chronic administration

The double-hit mouse model generated for this study consisted on a first hit or priming event, which relied on inducing MIA by Poly(I:C) administration during gestation followed by a second event, THC administration, occurring during the peripubertal phase of the resulting offspring.

For the breeding procedure, two females and one male were housed per cage and the presence/absence of vaginal plugs was checked every morning. When a vaginal plug was detected (GD 0.5), pregnant females were separated from the males and grouped together. Depending on the treatment assigned (either saline or Poly(I:C)), the pregnant females were then housed separately in cages, with a maximum of two females per cage. The weight of each pregnant female was closely monitored from this point onward.

Poly(I:C) was dissolved in saline solution (0.9% NaCl) and then heated in a bath at 50ºC for a few minutes (min). For proper re-hybridization, the Poly(I:C) was cooled completely and then aliquoted. To verify that the dissolution was successfully carried out, the concentration of three randomly selected aliquots

was quantified with the NanoDrop® RD-1000 spectrophotometer (Thermo Fisher Scientific, IL, USA).

Pregnant dams were randomly assigned to receive a single dose of either the saline solution (NaCl 0.9%; volume 5 ml/kg; n= 13) or Poly(I:C) (7.5 mg/kg; volume 5 ml/kg; n= 17) on GD 9.5, equivalent to the first-to-second trimester of human gestation. The timing and dosage of Poly(I:C) were chosen based on preliminary findings (Haddad et al., 2020; MacDowell et al., 2021; Perez-Palomar et al., 2023; Reisinger et al., 2015).

After weaning, at PND21, pups born of saline or Poly(I:C) treated dams, were housed in groups of 4-6 animals until the end of experimental procedures. This housing arrangement was based on two factors: whether the offspring came from a mother that received Poly(I:C) or one receiving saline, and the specific chronic treatment scheduled to receive, either THC or a control vehicle. Thus, the resulting groups were as follows: (1) offspring from mothers treated with saline and vehicle (control group), (2) offspring from mothers treated with saline and undergoing a chronic THC treatment (THC group), (3) offspring from mothers treated with Poly(I:C) and vehicle (Poly(I:C) group) and (4) offspring of Poly(I:C) treated mothers exposed to a chronic THC administration (Poly(I:C)/THC group, representing the double-hit paradigm). This information is summarized in Figure 8.

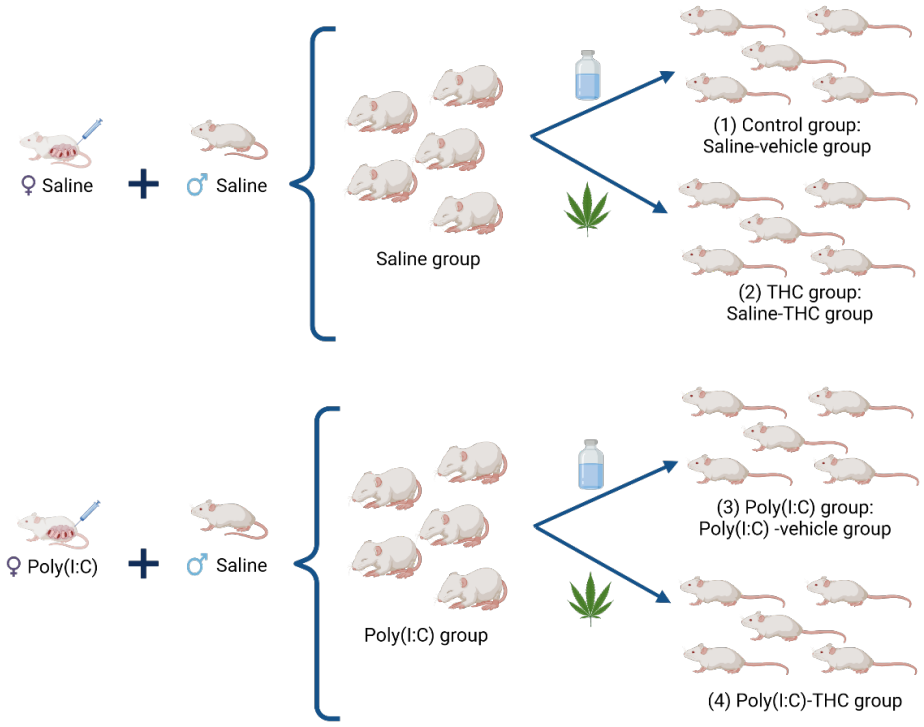

Figure 8: **Schematic representation of experimental groups.** Experimental groups generated along the project and the pharmacological treatments proposed for each group. Created with BioRender.com.

For chronic treatment, mice received intraperitoneal administration of either saline solution (NaCl 0.9%; volume 5 ml/kg i.p.) or THC (10 mg/kg i.p.) (Puighermanal et al., 2013) daily for 30 days beginning from PND21 (Ibarra-Lecue et al., 2018). Drugs were dissolved in a mixture of ethanol, cremophor and saline (0.9% NaCl) at a ratio of 1:1:18. Following this period, a 5-day interval was established to allow for a washout period (Ibarra-Lecue et al., 2018) before conducting subsequent behavioral assessments and eventually proceeding with the euthanasia of the animals. After euthanize, brains were removed and cortex dissected and stored at -80ºC until assays (Figure 9A and 9B).

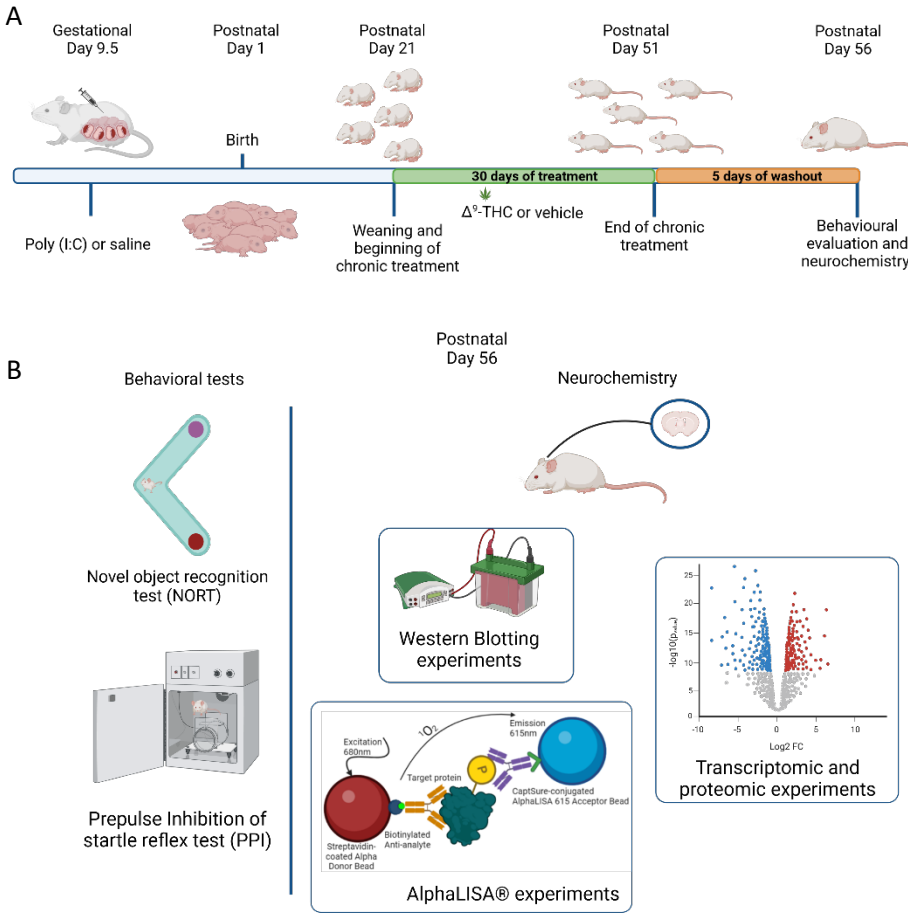

Figure 9: **Schematic representation of the double-hit mouse model, behavioral tests and neurochemical assays.** Developmental protocol and pharmacological treatments to generate the double-hit mouse model proposed in this work (A). Behavioral tests and neurochemical assays evaluation after double-hit mouse model generation (B). Created with BioRender.com.

3.2. Materials

- **Agilent technologies, Inc (Waldbronn, Germany):** Agilent RNA 6000 Nano Kit, RNA 6000 Nano Ladder.
- **Bio-Rad Laboratories (Hercules, CA, USA):** Ammonium persulfate (APS), Bradford Protein Assay, 2x Laemmli buffer, N-N-N-N'-tetramethylenediamine (TEMED) and molecular weight marker for sodium dodecylsulfate polyacrylamide gel electrophoresis (SDS-PAGE).
- **Carlo Erba Reagents (Barcelona, Spain):** Methanol.

- **Cayman Chemical (Ann Arbor, Michigan, USA):** Prostaglandin E 2 ELISA Kit – Monoclonal
- **Gibco-BRL (New York, USA):** Dulbecco's Modified Eagle Medium/Ham F-12 (DMEM/F12), Fetal Bovine Serum (FBS), 2% glutamine and 1% streptomycin-penicillin, Recombinant Human EGF.
- **Invitrogen (Barcelona, Spain):** BCA Protein Assay Kit, RiboPure™ RNA Purification Kit, Human IFNγ ELISA Kit, Human IL-6 ELISA kit.
- **National diagnostics (Atlanta, GA, USA):** Acrylamide 30% - bisacrylamide 0.8%.
- **Miltenyi Biotec (Germany):** Anti-PSA-NCAM MicroBeads, MS Separation columns.
- **Panreac Química S.A.U. (Barcelona, Spain):** 4′, 6′-diamidino-2-phenylindole dihydrochloride (DAPI), Glacial acetic acid and HCl (37%).
- **Perkin Elmer (Whaltham, Massachusetts, EEUU):** Alpha SureFire Ultra Lysis Buffer (5X), 1/2 Area OptiPlate-96, AlphaLISA® SureFire® Ultra™ Multiplex assay kits, Alpha SureFire® Ultra™ Multiplex kits.
- **Quimivita (Barcelona, Spain):** Ethanol.
- **Sigma-Aldrich (Saint Louis, Missouri, USA):** 1-Bromo-3-chloropropane (BCP), Bovine serum albumin (BSA), glycine, β-mercaptoethanol, sorbitan monolaurate (Tween 20), Protease Inhibitor Cocktail, Phosphatase Inhibitor Cocktail, Tris (2-Amino-2-(hydroxymethyl)-1,3-propanediol) hydrochloride (Tris HCl), dimethyl sulfoxide (DMSO), Pellet pestles, 4% paraformaldehyde (PFA), polyoxyl 35 hydrogenated castor oil (Cremophor®), Basic fibroblast growth factor (bFGF), Sodium chloride (NaCl), potassium chloride (KCl), disodium phosphate (Na_2HPO_4), monopotassium phosphate (KH_2PO_4), magnesium chloride ($MgCl_2$), calcium chloride dihydrate ($CaCl_2$-$2H_2O$), magnesium chloride hexahydrate ($MgCl_2$-$6H_2O$), sodium bicarbonate ($NaHCO_3$), Immobilon®-FL PVDF (0.45 micron filter),

Polyriboinosinic-polyribocytidylic acid sodium salt (Poly(I:C)), Ethylene diamine tetra-acetic acid (EDTA), Octyl sodium sulfate, Sodium dihydrogen phosphate monohydrate (H_2NaPO_4).

- **StemCell Technologies (Vancouver, Canada):** NeuroCult™ NS-A Proliferation Medium, NeuroCult™ NS-A Differentiation, 0.5% trypsin-EDTA.
- **THCPharm (Frankfurt, Germany)**: (6aR,10aR)-6,6,9-Trimethyl-3-pentyl-6a,7,8,10a-tetrahydro-6H-benzo[c]chromen-1-ol (Δ^9-THC).
- **Thermo Fisher Scientific (Waltham, Massachusetts, USA)**: Pierce™ ECL western blotting substrate, EasYFlasks Nunc 25-cm^2, EasYFlasks Nunc 75-cm^2, EasYFlasks Nunc 175-cm^2, Nunc™ 15 ml and 50 ml sterile polypropylene conical centrifuge tubes, azida, Triton X100, Perchloric acid ($HCLO_4$).
- Water was purified by a Milli-Q Gradient system (Burlintong, Milford, MA, USA).

3.3. Methods

3.3.1. Nasal exfoliation

The olfactory neuroepithelium was obtained via nasal exfoliation from 10 subjects with schizophrenia and 10 healthy donors. A sterile swab (2.4 cm long and 3 mm in diameter) was gently moved in circular motions within the nasal cavity. Each donor underwent this process using four separate swabs to exfoliate the middle and upper areas of both nasal cavities. Once exfoliated, each swab was placed in tubes with 250 µl of supplemented DMEM medium (a mixture of Dulbecco's Modified Eagle Medium/Ham F-12, supplemented with 10% fetal bovine serum, 2% glutamine, and 1% streptomycin-penicillin), while keeping the samples on ice. Four samples were obtained from each individual, two from both the middle and upper sections of each nostril. The sample from the upper part of the right nostril was combined with the sample from the middle part of the left nostril and placed in the same tube. This process was replicated for the other two

samples. One of the combined samples was used to culture adherent cells, and the other for neurospheres culture (Figure 10).

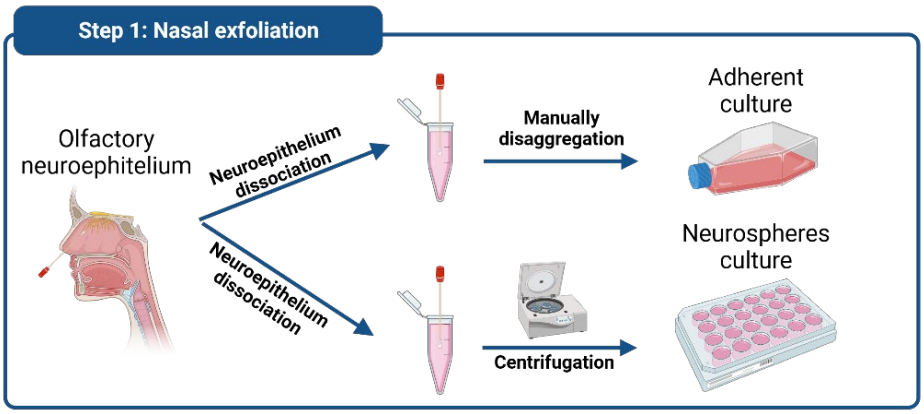

Figure 10: **Schematic representation of the obtention of cells from olfactory neuroepithelium and different samples obtained.** Created with BioRender.com.

3.3.2. Culture of Neurospheres from olfactory neuroepithelium

The samples obtained through nasal exfoliation underwent a manual disintegration process followed by a centrifugation (500xg for 5 min, at room temperature (RT)). After centrifugation, supernatant was removed and the pellet was resuspended in 500 µl of NeuroCult™ NS-A Proliferation Medium enhanced with 20 ng/ml Human Recombinant EGF, 10 ng/ml Human Recombinant bFGF, and 2 µg/ml Heparin Solution (supplemented NeuroCult™ NS-A Proliferation Medium).

This mixture was then placed in a 25-cm^2 flask or 24 well plates (depending on the subsequent-test s) with 4 ml or 200 µl/well of the supplemented medium respectively. Cells were cultivated at 37ºC with 5% CO_2 and monitored using a standard bright-light microscope (Primovert KMAT, Zeiss, Germany). For the correct growth and proliferation of the neurospheres, 500/1,000 µl of supplemented NeuroCult™ NS-A Proliferation Medium was added every two days throughout the growth process. This renews the nutrients in the medium and prevents the acidification of the medium, preventing the neurospheres from dying.

When neurospheres reached around 100-150 µm in diameter, they were subjected to passages to evaluate their ability to regenerate and multiply and to obtain a larger number of cells for further experiments. This usually happened 7-14 days after initial seeding, although in certain instances, this could extend to 21 days. Normally in the case of the controls, 5 passages were made and in the case of the subjects, 2/3 passages since as further discussed later, in this case the neurospheres were smaller and divided less as passages were made.

At the same time, another flask containing neurospheres was maintained without undergoing any passage. Supplement of the proliferation medium without growing factors was provided every two days to renew nutrients until spontaneous adhesion to the flask surface occurred. Upon adhesion, the neurospheres-culture medium was replaced with a differentiation medium (NeuroCult™ NS-A Differentiation) to encourage cell differentiation. This would result in a pure culture of cells of neuronal lineage. After 30 days in the differentiation medium, the mix of cells were completely differentiated and ready for experiments (Figure 11). Obtaining differentiated cells from neurospheres was extremely complicated and the number of cells obtained was very low. For this reason, subsequent experiments were performed with adherent cells and neurospheres, but not with neuronal lineage from neurospheres.

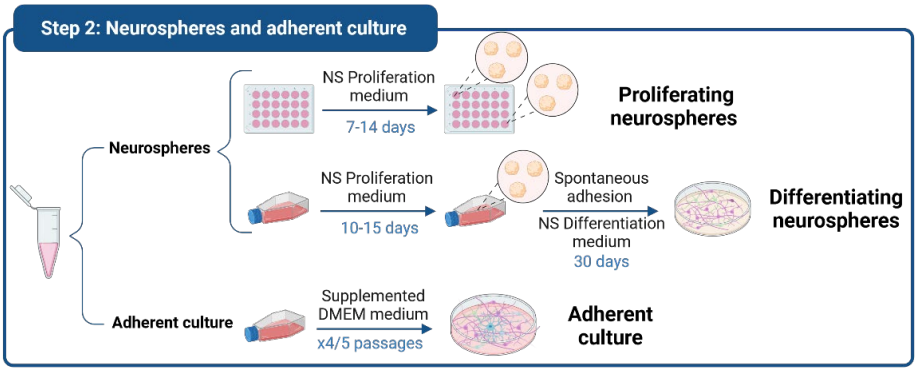

Figure 11: **Schematic representation of the workflow for the culture of proliferating and differentiating neurospheres and adherent culture.** Created with BioRender.com.

3.3.2.1. Measurement of growth and size of neurospheres

To evaluate the regeneration and multiplication capacity of the neurospheres, a series of passages were carried out, studying in each of them both the size and the number of generated neurospheres. For this purpose, after centrifugation and resuspension of the pellet, 100 cells (Fluidlab R-300, Anvajo, Germany) were seeded per well with proliferation medium. In the following days, the number of neurospheres formed per 100 seeded cells was determined and their diameters were measured. In the case of controls, the neurospheres reached passage 5, while in the case of the subjects, only passage 2/3 was reached, since the neurospheres lost their proliferative capacity and died before reaching passage 5.

3.3.3. Adherent culture of cells from olfactory neuroepithelium

In order to culture adherent cells, the samples were manually disaggregated, placed in a 25-cm^2 flask, and cultured at 37ºC with 5% CO_2 using supplemented DMEM medium. In this case, a total change of medium was carried out every two days until confluence was reached with the aim of renew nutrients and prevent cell death due to lack of nutrients. Once the cells reached confluence, passages were carried out to promote cell growth. For this, the cells were washed twice with sterile and tempered phosphate buffered saline (PBS 1X). They were then detached using 0.5% trypsin-EDTA, neutralized with supplemented DMEM medium, subjected to centrifugation at 1000×g RT for 5 min, and the resulting pellet was resuspended in supplemented DMEM medium. Finally, the cells were distributed over a larger surface to create a reserve of cells. Through this method, cells at various maturation stages were generated.

3.3.3.1. Magnetic Activated Cell Sorting (MACS) of adherent culture

For the isolation and purification of neuron- or glia-enriched cultures, anti-PSA-NCAM micro beads were used for the positive selection of PSA-NCAM+ cells from the adherent cell cultures. Anti-PSA-NCAM micro beads recognize polysialic acid (PSA), which is linked to the extracellular domain of the neural cell adhesion molecule (NCAM, CD56) (Rougon & Marshak, 1986). Once

culture reached confluence at passage 5 (approximately 4/5 days after seeding, although it depends on the cells in the culture), cells were washed twice with sterile and tempered PBS 1X, detached with 0.5% trypsin-EDTA, neutralize with supplemented DMEM medium, and centrifuged at 300×g for 10 min RT. The supernatant was removed and the pellet was resuspended in 60 µl of buffer (0.5% Bovine Serum Albumin (BSA) in PBS 1X) per 10^7 total cells (Fluidlab R-300, Anvajo, Germany) well mixed and incubated for 10 min RT at 4ºC. The cells were then incubated with 20 µl of anti- PSA-NCAM MicroBeads/10^7 cells for 15 min RT at 4ºC in a rotatory mixer. Finally, cells were washed by adding 1 ml of buffer/10^7 cells, centrifuged at 300×g RT for 10 min and the pellet resuspended in 500 µl of buffer/10^8 cells.

After magnetic labeling, cells were passed through MACS column (Miltenyi Biotec, Germany) placed in a strong permanent magnet. The ferromagnetic spheres in the column amplify the magnetic field by 10,000-fold, thus inducing a high gradient. Unlabeled cells (PSA-NCAM-) passed through the column while magnetically labeled cells (PSA-NCAM+) were retained within it. After removal of the column from the magnetic field, the retained fraction was eluted. Both fractions, labeled (PSA-NCAM+, neuron-enriched fraction) and non-labeled (PSA-NCAM-, glia-enriched fraction), were completely recovered. The glia-enriched culture was then seeded in NeuroCult™ NS-A Differentiation medium with medium changes every 2 days for approximately 30 days. The neuron-enriched culture, however, was first seeded in supplemented DMEM medium to allow cell growth and after 7 days, medium was changed to NeuroCult™ NS-A Differentiation with medium changes every 2 days until 30 days (Figure 12).

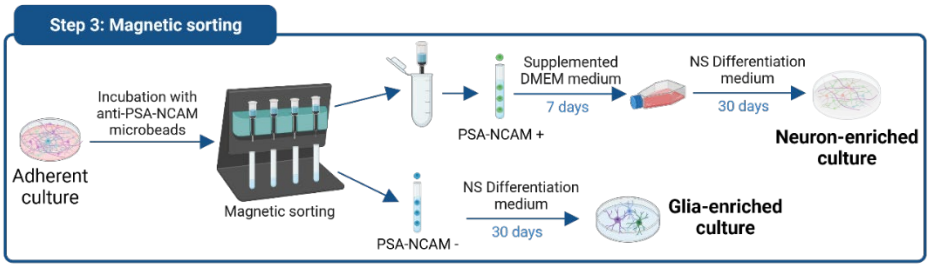

Figure 12: Schematic representation of the workflow for the magnetic selection of cells from adherent cells for obtaining neuron- and glia-enriched cultures. Created with BioRender.com

3.3.4. Immunofluorescence

To determine the different cells present in the cultures, an immunofluorescence characterization was carried out. This characterization was done with cells obtained from 8 controls and in the passage 5, which is the one that was going to be used in all the following experiments. The preparation of the cells was the same in all cell types except in the case for the proliferating neurospheres cultures. In this case, a previous precipitation of the floating cells on a slide was required.

For the immunofluorescence, cells underwent two rounds of washing using sterile and temperature-regulated PBS 1X, after which they were fixed using 4% paraformaldehyde (PFA) in PBS 1X, with gentle shaking for 20 min at 4ºC. Following the fixation, another round of washing with PBS 1X occurred, succeeded by two washes of 5 min and 90 rpm with solution A (PBS with 1% BSA and 0.02% azide) at RT. This was followed by a quick wash using solution B (PBS with 0.5% Triton X100) at RT, with 5 min of agitation at 90 rpm to permeabilize the membrane, and concluded with two more washes using solution A (at RT and 5 min of agitation at 90 rpm). After the washing steps, cells were incubated for 1 h at RT with agitation at 90 rpm, using a blocking solution (PBS with 2% BSA and 0.02% azide). Subsequently, the cells were incubated overnight at 4ºC with primary antibodies, appropriately diluted in a solution containing PBS with 0.5% BSA and 0.1% azide. Further details regarding the

conditions of primary and secondary antibodies for immunofluorescence experiments are described in Table 3.

Table 3: **Details of the antibodies used and their dilutions for immunofluorescence experiments in cell cultures.**

Antibody type	Target	Host	Company	Reference	Dilution
Primary	βIII-Tubulin	rabbit	StemCell	60052	1:1,000
Primary	Epithelial Cell Adhesion Molecule (EpCAM)	mouse	ThermoFisher	11-5791-82	1:500
Primary	Glial Fibrillary Acidic Protein (GFAP)	rabbit	DAKO	Z0334	1:4,000
Primary	Microtubule-Associated Protein 1B (MAP1B)	rabbit	ThermoFisher	PA5-82798	1:500
Primary	Microtubule-Associated Protein 2 (MAP2)	mouse	ThermoFisher	13-1500	1:500
Primary	Musashi-1	rat	Thermofisher	14989682	1:500
Primary	Nestin	mouse	Merck	MAB5326	1:500
Primary	Neuronal-Nuclei (NeuN)	mouse	Merck	MAB377	1:500
Primary	Polysialylated-Neural Cell Adhesion Molecule (PSA-NCAM)	mouse	Miltenyi	130-117-394	1:1,000
Primary	SRY-Box Transcription Factor 2 (Sox2)	rabbit	ThermoFisher	PA1094	1:1,000
Secondary	Alexa Fluor™ 594	goat anti-rabbit	Invitrogen	A-11037	1:1,000
Secondary	Alexa Fluor™ 488	goat anti-rat	Invitrogen	A-11006	1:1000
Secondary	Alexa Fluor™ 488	donkey anti-mouse	Invitrogen	A-21202	1:1,000
Secondary	Alexa Fluor™ 594	donkey anti-mouse	Invitrogen	A-21203	1:1,000

The following day, the primary antibodies were removed and the cells were washed three times with solution A (at RT, for 5 min, with agitation at 90 rpm). Subsequently, the cells were exposed to secondary antibodies for 90 min at RT, with agitation at 90 rpm and in the absence of light. After the removal of secondary antibodies, the cells were washed three times again with solution A (at RT, for 5 min, with agitation at 90 rpm). The nuclei were stained using 4',6-diamidino-2-phenylindole dihydrochloride (DAPI) at a dilution of 1/5,000 for 15 min at RT with agitation at 90 rpm. Finally, the cells were washed for the last two times with cold PBS 1X for 5 min at RT and 90 rpm and kept in PBS 1X until they were analyzed under the microscope.

Images were acquired using a Nikon Eclipse 80I microscope and processed using ImageJ software.

3.3.5. Fluorescence-Activated Cell Sorting (FACS)

Once the presence of different cell types in the cultures was determined, the proportion of glial vs. neuronal cells was studied by performing a Flow Cytometry assay. Sample preparation started with two washes using sterile and warmed PBS 1X. Next, 0.5% trypsin-EDTA was used to detach the cells from the flask, and the cells were placed in an incubator at 37ºC for 2 min. Once the cells had fully detached, the trypsin was neutralized by pipetting the differentiation medium both up and down across the flask's surface, facilitating the detachment of numerous cells. After confirming the successful detachment of cells, the cell mixture was collected in a falcon tube. A centrifugation process at 500×g for 10 min was then conducted, leading to the removal of the supernatant and the resuspension of the resultant pellet within 600 µl of a blocking solution (PBS with 2% BSA and 0.02% azide). This mixture was agitated for a duration of 1 h at 4ºC. Primary antibodies were added into the blocking solution (PBS with 2% BSA and 0.02% azide) (Table 3) and left to incubate overnight with agitation at 4ºC. On the subsequent day, the cell mixture underwent another centrifugation step at 500×g for 10 min, resulting in the discarding of the supernatant and the resuspension of the pellet within 600 µl of sterile (cold) PBS 1X. Another centrifugation was done at 500×g for 10 min, with the supernatant once again being discarded, and the pellet resuspended within 600 µl of a secondary antibody dilution in the blocking solution (PBS with 2% BSA and 0.02% azide) (Table 3). Following a 90 min incubation with agitation at 4ºC, the cells underwent two rounds of washing and centrifugation at 500×g for 10 min each. Finally, the resultant pellets were resuspended twice – first in 600 µl of PBS 1X, and subsequently in 600 µl of HBSS solution (Hank's Balanced Salt Solution), the necessary solution for sample analysis in the cytometer.

Once all this process was carried out, the samples were filtered through a sterile sieve with a pore diameter of 50 µm (BD Filcon, sterile, cup-type, ref: 340629)

to avoid clumps in the sample line. Finally, cell samples were analyzed and sorted in a BD FACSJazz Cell sorter equipped with two independently aligned B488 and Y/G561 lasers. System pressure was 27 psi.

3.3.6. Enzyme-Linked ImmunoSorbent Assay (ELISA)

To study which compounds the cells released into the medium and to see if there were differences between the different cultures, culture medium was collected from each cell type culture on passage 5 and a series of compounds were quantified by enzyme-linked immunosorbent assay (ELISA) and HPLC techniques. Commercial ELISA kits were used for the identification and quantification of IFNγ, IL-6, and PGE_2 in culture medium samples. However, the quantification of Trp and Kyn was performed by HPLC with electrochemical detection.

In the case of ELISA kits, protein content in the culture medium was measured by the Bradfors's method, and sample preparation was carried out according to the manufacturer's instructions. No dilution was performed and the absorption peak was at 450 nm.

On the other hand, in the case of HPLC each sample was initially diluted at a 1:5 ratio in 0.1 M $HClO_4$ and 100 µl EDTA. Following this, centrifugation at 18,000×g for 15 min was used to filter the samples using Costar® Spin-X® Centrifuge Tubes (0.22 µm Pore CA Membrane, Corning). The concentrations of Trp and Kyn were determined by comparing them to reference standards that were prepared and injected on the same day. The mobile phase composition consisted of 150 mM H_2NaPO_4, 0.2 mM EDTA, 4.3 mM octyl sodium sulfate (pH 6.3), and 8% (vol/vol) methanol. This mobile phase was filtered and delivered at a flow rate of 0.2 ml/min using a Hewlett-Packard model 1200 pump. Separation occurred at 30ºC on a Zorbax Eclipse Plus column (3.5 µm C18, 2.1×150 mm, Agilent Technologies, Spain). Trp and Kyn were detected amperometrically by a Hewlett-Packard model 1049 A detector at an oxidizing potential of +950 mV.

3.3.7. Gene expression analysis

RNA extraction and purification

RNA extraction and purification from neuron- and glia-enriched cultures, and mouse cortex (50 mg) was carried out with the Commercial Ambion RiboPure™ kit (Invitrogen), following commercial specifications.

Samples were disrupted by using 1 ml of TRIzol®. This step is essential to achieve effective homogenization of the sample and cell lysis. Once the mixture attained a homogeneous consistency, the resultant solution was incubated at RT for 5 min. Then 100 µl of bromochloropropane (BCP) were added. After that, the tubes underwent vortexing, followed by an incubation period of 2 to 3 min at RT. Subsequently, they were subjected to centrifugation at 12,000×g for 15 min at 4ºC. Following centrifugation, the mixture underwent separation into distinct phases: a lower, red organic phase; an intermediate phase; and an upper, colorless aqueous phase containing the RNA (Figure 13).

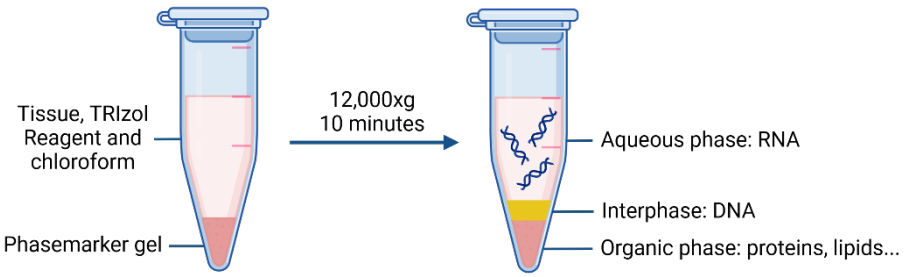

Figure 13: **Tissue homogenization with TRIzol® Reagent, before and after centrifugation.** Created with BioRender.com

Afterwards, 400 µl of the aqueous phase were transferred to a separate tube and mixed with 400 µl of 70% ethanol. This mixture was then vortexed. Subsequently, 700 µl of this mixture were transferred to a filter cartridge-collection tube assembly and centrifuged at 12,000×g for 30 seconds at RT. This step allowed the binding of RNA to the filter cartridge. The filter was subsequently rinsed three times using two different washing solutions and the RNA was eluted using 100 µl of RNAse-free water into a Recovery Tube.

The final RNA samples were stored at a temperature of -80ºC until experiments were done. The process of RNA extraction and purification is outlined in Figure 14.

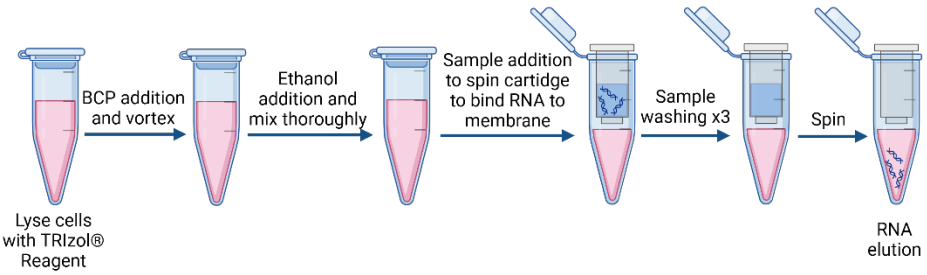

Figure 14: ***RNA extraction and purification process, step by step.*** *Created with BioRender.com*

RNA quality and concentration determination

The total RNA concentration was measured using a Nanodrop® RD-1000 spectrophotometer (Thermo Fisher Scientific, IL, USA). Additionally, the 260/280 and 260/230 ratios of absorbance were assessed using the same Nanodrop® RD-1000 instrument. 260/280 ratio is employed to gauge the purity of RNA, with a value of 2 indicating purity. The 260/230 ratio is used as a supplementary measure of nucleic acid purity, with an anticipated value between 2 and 2.2. All RNA samples in these experiments exhibited enough concentration to perform next experiments, as well as higher ratios of purity.

Furthermore, the assessment of RNA Integrity Number (RIN) was conducted using the 2100 Bioanalyzer by Agilent Technologies. The Agilent Expert software assigned a score ranging from 0 to 10 to each trace, based on the ribosomal RNA peaks and the presence of RNA degradation products. This score was determined by evaluating the signal between the 5S and 18S bands, between the 18S and 28S bands, and following the 28S band. The RIN number served as an indicator of RNA quality, with a RIN score of 10 being the highest achievable. Only samples with a RIN score ≥ 8 were considered valid. The RIN values for all RNA samples were assessed using Agilent 2100 Bioanalyzer, employing Agilent

RNA nano chips and Agilent RNA6000 Nano Kit (Fleige & Pfaffl, 2006; Trabzuni et al., 2011). All RNA samples in these experiments exhibited RIN values higher than 8.

Libraries preparation and sequencing

The massive RNA sequencing was performed by the Genomics Unit of the Madrid Science Park. Libraries were prepared using the NEBNext® Poly(A) mRNA Magnetic Isolation Module and NEBNext® UltraTM II Directional RNA Library Prep for Illumina® kits (New England Biolabs), starting with 91 ng of total RNA. The instructions from "Chapter 1: Protocol for use with NEBNext® Poly(A) mRNA Magnetic Isolation Module" were followed. A 13-cycle PCR was used to amplify the libraries mentioned in the protocol.

After quantifying the libraries, an equimolar mixture was prepared, purified using AMpure XP beads (Beckman Coulter), and quantified via qPCR using a reference library from the Genomics Unit and the KAPA SYBR® FAST qPCR kit for the LightCycler® 480 equipment.

The equimolar mixture was sequenced on the Illumina® NovaSeqTM 6000 using the NovaSeqTM Reagent 1.5 kit (100 cycles) in a single-read 1x100 run.

Post-sequencing, the TopHat program within the G-PRO suite (Biotechvana) was employed to map and locate different sequences against the reference genome, yielding a correct mapping read percentage of 93 to 95%. Subsequently, a differential expression analysis was conducted using the CuffDiff program, which analyzes the RNA expression of each gene normalized by its size and the global RNA expression of each sample. It compares between groups, applying false discovery rate (FDR) correction and obtaining Fold Change (FC) values.

3.3.8. Sample preparation for AlphaLISA® and Western Blotting experiments

3.3.8.1. Total homogenate of neuron- and glia-enriched culture cells

For AlphaLISA® and Western Blotting (WB) experiments neuron-enriched (PSA-NCAM+) and glia-enriched (PSA-NCAM-) cell cultures in passage 4/5 were used. Cultures were maintained for 30 days in NeuroCult™ NS-A differentiation medium, and then washed twice with sterile and warmed PBS 1X and detached from the flask using 0.5% trypsin-EDTA. When the cells were fully detached, the trypsin was neutralized with differentiation medium and the cell mixture was collected in a falcon tube. A centrifugation was carried out at 4,000 rpm for 22 min at RT, leading to the removal of the supernatant. The resulting pellet was diluted in 500 µl of homogenization buffer and stored at -80ºC until the experiments were conducted.

For AlphaLISA® experiments, after protein measurement each sample was loaded in the well in their original concentration. Results were interpreted in relation to the protein concentration.

For the WB experiments, cell pellets were resuspended in 600 µl of homogenation buffer (50 mM Tris-HCl, 150 mM NaCl, 5 µl/ml Protease Inhibitor Cocktail, 5 µl/ml Phosphatase Inhibitor Cocktail, pH 7.4) using a syringe (Sterican needle 0.50 x 25 mm. 25 G x 1"). Inmediately after, 60 µl of a buffer containing detergents (BDC buffer) (50 mM Tris-HCl, 150 mM NaCl, 10% Igepal, 5% sodium deoxycholate, 1% SDS, 250 mM CHAPS, pH 7.4) was added (1:10 ratio). Samples were kept on ice for 30 min and were then centrifuged at 14,000 rpm, 4ºC for 10 min, keeping supernatants and discarding pellets. Protein content was determined using DC-method (BioRad), using bovine serum albumin as a standard. 6x concentrated commercial Laemmli buffer and homogenation buffer were added to 0.69 µg/µl or 0.35 µg/µl protein aliquots and samples were stored at -80ºC until the experiments were conducted.

3.3.8.2. Total homogenates of mice brain cortex

For AlphaLISA® experiments, mouse cortex samples (150-200 mg) were thawed at 4ºC and homogenized in 1.2 ml of commercial homogenization buffer supplemented with protease and phosphatase inhibitors using a motorized homogenizer for small samples. Three pulses of ten seconds each were applied to achieve homogenization of the majority of the sample. To remove solid debris that might have resisted homogenization, the homogenate was centrifuged for 2 min at 230×g and 4ºC, following which 1 ml of the supernatant was collected.

After protein measurement, the samples were diluted in homogenization buffer to a final concentration of 4 µg/µl, 0.25 µg/µl and 0.12 µg/µl and aliquoted at -80ºC until the experiment was conducted. Finally, an external control sample (pool) at same concentrations was also prepared and stored in aliquots of 100 µl at -80ºC.

For the WB experiments, the sample preparation was the same as that used for AlphaLISA® technique. The samples used were the ones diluted in homogenization buffer to a final concentration 4 µg protein/µl. Then, 2x concentrated commercial Laemmli buffer and β-mercaptoethanol were added to each sample, vortexed and kept at -80ºC until WB experiments. Before each day of experiment, all samples were heated at 95ºC for 5 min.

3.3.8.3. Determination of protein content

The protein concentration in the homogenates was determined using the bicinchoninic acid (BCA) colorimetric method, following the manufacturer's specifications. The assays were performed in triplicate in 96-well microplates, with the samples previously diluted 1:10. The absolute protein concentration was estimated by interpolation on a standard curve of bovine serum albumin (BSA), loaded in triplicate on the same plates within a concentration range of 0.05 – 2 µg/µl. The absorbance of the reactions was measured at 562 nm using a CLARIOstar PLUS multimodal reader.

3.3.9. AlphaLISA® technique

The AlphaLISA® technique is a sandwich method used for protein measurement, including their phosphorylated forms, which streamlines procedures such as WB. This approach comprises four fundamental elements: two antibodies (one biotinylated and the other attached to a proprietary CaptSure™ tag), acceptor beads (coated with the CaptSure™ conjugate), and donor beads.

The process was carried out according to the specifications of the commercial company and was the same for cells and mouse cortex. First, 10 µl of the previously homogenized samples (mice cortex or cells) were added to the plate. To determine the concentration of protein required for each kit, the technique was set-up by testing different concentrations and incubation times. In both cases, the incubation conditions were the same but, in the case of mouse cortex, an optimal protein concentration was defined for each kit (Table 4), whereas in the case of cells, each sample was added to its initial concentration and then the signal was corrected for protein amount.

***Table 4*: Summary table of the specific conditions employed for AlphaLISA® experiments in mice.**

Kit	Protein mouse cortex (µg)	Signal/Noise ratio	Temperature (ºC)	Agitation	First incubation (h)	Second incubation (h)
ALSU-TAKT-B-HV	1.2 µg	5.22	25ºC	Yes	1 hour	1 hour
ALSU-PAKT-C-HV	1.2 µg	10.09	25ºC	Yes	1 hour	1 hour
ALSU-TMTOR-B-HV	2.0 µg	43.54	25ºC	Yes	1 hour	1 hour
ALSU-PMTOR-C-HV	2.0 µg	95.47	25ºC	Yes	1 hour	1 hour
MPSU-PTERK-M-HV	0.62 µg	2.79/4.15	25ºC	Yes	2 hour	1 hour
MPSU-PTRPS6-B-HV	1.2 µg	2.64/2.54	25ºC	Yes	2 hour	1 hour
TBSU-PS6R-A-HV	1.2 µg	8.28	25ºC	Yes	2 hour	1 hour

Then, the commercial solutions containing the antibodies were added along with the acceptor beads coated with the CaptSure™ conjugate, which was responsible for detecting one of the antibodies, and left to incubate for 1-2 h (Table 4). This incubation allowed the antibodies to specifically interact with the total proteins and/or the phosphorylated forms. After incubation, the solution containing the

donor beads was added and incubated with the homogenate and other components for 1 h in dark conditions at 22-25ºC.

AlphaLISA® SureFire® Ultra™ assay kit

In the AlphaLISA® SureFire® Ultra™ assay (Figure 15), donor beads are coated with streptavidin to capture one of the antibodies, which is biotinylated. Acceptor beads are coated with a proprietary CaptSure™ agent that immobilizes the other antibody, labeled with a CaptSure™ tag. In the presence of target protein, the two antibodies bring the donor and acceptor beads close together, generating signal emission from the acceptor beads. The amount of light emission is directly proportional to the amount of protein present in the sample. In this case, the recorded emission was at 615 nm, which corresponded to the europio present in the beads.

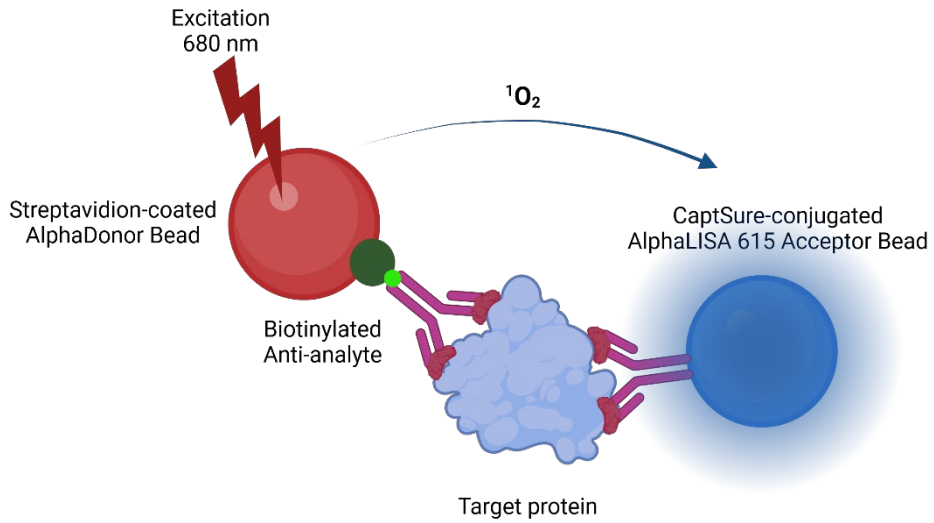

Figure 15: **AlphaLISA® simple assay kits.** The biotinylated antibody, attached to the donor bead, recognizes a protein's epitope, while the second antibody can recognize another epitope of the protein or specifically the epitope containing phosphorylation. Typically, it is this second antibody that, thanks to the Captsure™ label, would bind to the acceptor bead containing europium that emits at 615 nm. Created with BioRender.com.

AlphaLISA® SureFire® Ultra™ Multiplex assay kit

In the case AlphaLISA® SureFire® Ultra™ Multiplex assay kits (Figure 16), both phosphorylated and total levels of endogenous proteins can be simultaneously determined. The 615 nm (Europio) signal corresponds to the phosphorylated form, and the 545 nm (Terbio) signal corresponds to the total form. These kits have been formulated to provide superior signal: background assay windows and to perform without interference in the presence of extraneous antibodies, making it amenable to the study of therapeutic and blocking antibodies. These kits contain two acceptor beads, which will emit at two different peaks. In this assay, the Alpha 615 Acceptor bead is coated with the CaptSure™ antibody, which binds the CaptSure™-tagged anti-phospho target antibody. The Alpha 545 Acceptor bead is coated with the CaptSure2™ agent, which binds the CaptSure2 tagged anti-total target protein antibody. The Alpha Donor bead binds the biotinylated anti-total target protein antibody. This multiplex kit technology makes it possible to determine the amount of total and phosphorylated protein in a single experiment. In this case, it is necessary to calculate the interference between europium and terbium emissions (cross-talk).

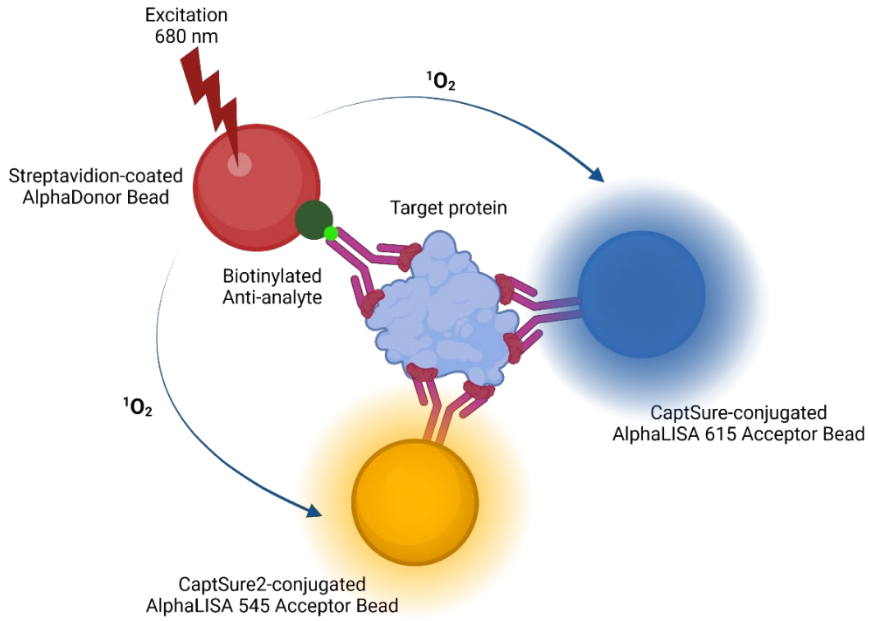

Figure 16: **AlphaLISA® Multiplex kits.** The biotinylated antibody, attached to a donor bead, recognizes a protein's epitope. A second antibody, attached to a Captsure™ label, recognizes another epitope of the protein, and a third antibody, also attached to a Captsure™ label, specifically recognizes the epitope containing phosphorylation. The antibody bound to the total protein is attached to an acceptor bead that will emit at 545 nm, while the antibody recognizing phosphorylation is attached to an acceptor bead that will emit at 615 nm. Created with BioRender.com

Quantification of the luminescence intensity signal

Once the incubation time finished, a CLARIOstar PLUS multimodal reader, compatible with AlphaLISA® technology, was used to detect the emission at 615 and 545 nm using the preset settings.

CLARIOstar PLUS multimodal reader provides a measurement of photoluminescence in counts ("Alphacounts"). After obtaining all the results, the triplicates of each value were analyzed, calculating their average, standard deviation, and coefficient of variation (CV). Values from triplicates with CV > 5% were excluded.

To obtain the relative amount of protein, the mean of the counts obtained for each protein and mouse was divided by the mean count value obtained for the pool, taken as a reference value. Thus, relative or pool-corrected values were obtained.

In addition, the phosphorylated/total protein ratio was calculated by dividing the value obtained for the phosphorylated protein, once corrected for pool, by the total protein amount, also corrected for pool. These data were subjected to statistical analysis.

3.3.10. Western Blotting

Gel electrophoresis

The technique of electrophoresis in polyacrylamide gels under denaturing conditions (SDS-PAGE) was used to sort proteins based on their size. These polyacrylamide gels had two parts: the upper stacking gel containing 5% polyacrylamide, and the lower running gel containing 12% polyacrylamide in the case of mice brain cortex and 10% polyacrylamide in the case of cells obtained from olfactory neuroepithelium (neuron- and glia-enriched cells).

The same amount of protein was loaded in all experiments (20 μg of protein in each well in the case of mice brain cortex and 36 μg of protein in each well in the case of neuron- and glia-enriched cells). Apart from the samples of interest, in all the experiments, a molecular weight marker and an inter-experimental control sample (pool) was loaded in each gel.

After loading, electrical current of 80 V was set up in the first stage of electrophoresis for 30 min. This allowed all the proteins to concentrate in the stacking gel. Afterwards, 120 V current was applied for around 120 min to separate proteins by their size along the running gel (this step concluded when the blue front exits the running gel). Electrophoresis was stopped when samples reached the end of the gel, and then transferred to polyvinylidene fluoride or polyvinylidene difluoride (PVDF) membranes.

Transference into PVDF membranes

Prior to transfer, the PVDF membranes were activated. For this purpose, they were immersed in methanol (1 min) and then in milliQ water (1 min). After finishing the activation, they were kept in transfer buffer until they were used.

Then, proteins were transferred into PVDF membranes using an electric field.

The polyacrylamide gels (previously washed quickly with transfer buffer) and these membranes (previously activated) were placed in direct contact, surrounded by extra thick blot filter paper (previously wetted with transfer buffer) to maintain contact and keep them under pressure. The transfer process was conducted in semi-dry conditions during 20 min at 15 V.

Blocking and immunodetection

Membranes were incubated at RT and agitation for 1 h with a blocking solution to minimize non-specific signals. This blocking solution varied depending upon the type of antibody used. Following this, the membranes were incubated overnight at 4ºC with continuous agitation and the respective primary antibody (diluted in 5% skim milk, 0.1% Tween 20 in TBST or in 5% BSA, 0.1% Tween 20 in TBST) (Table 5).

After washing the membranes, they were again incubated (1 h at RT) with corresponding horseradish peroxidase-conjugated secondary antibodies (Table 5). Membrane immunodensity signal was then respectively detected in an Amersham Imager 680 (Cytiva Life Sciences, Malborough, Massachusetts, USA) following addition of ECL WB substrate (Thermo Fisher Scientific).

Table 5: **Details of the antibodies used and their dilutions for WB experiments in mice.**

Antibody type	Clonality	Target	Host	Company	Reference	Dilution
Primary	Polyclonal	Akt	Rabbit	Cell Signaling	9272	1:1,000
Primary	Monoclonal (clone D9E)	Phospho(Ser^{473})-Akt	Rabbit	Cell Signaling	4060	1:1,000
Primary	Monoclonal (clone 54D2)	rpS6	Mouse	Cell Signaling	2317	1:500
Primary	Monoclonal (clone D57.2.2E)	Phospho($Ser^{235/236}$)-rpS6	Rabbit	Cell Signaling	4858	1:500
Primary	Monoclonal (clone C-9)	ERK 1/2	Mouse	Santa Cruz	Sc-514302	1:500
Primary	Monoclonal (clone E-4)	Phospho($Tyr^{202/204}$)-Erk 1/2	Mouse	Santa Cruz	Sc-7383	1:500
Primary	Polyclonal	β-actin	Rabbit	Abcam	Ab8227	1:200,000
Primary	Monoclonal (clone AC-15)	β-actin	Mouse	Sigma Aldrich	A1978	1:200,000
Primary	Monoclonal (clone 7F9)	Vinculin	Mouse	Santa Cruz	Sc-73614	1:500
Primary	Monoclonal (clone G-9)	GAPDH	Mouse	Santa Cruz	Sc-365062	1:500
Secondary	Polyclonal	Rabbit IgG (H+L)	Goat	Jackson InmunoResearch	111-035-144	1:5,000
Secondary	Polyclonal	Mouse IgG (H+L)	Goat	Jackson InmunoResearch	115-035-146	1:5,000

Quantification of the immunoreactive signal

Signal quantification was performed using the software Image Studio Lite 5.2 (LI-COR Biosciences, Nebraska, USA). For the WB experiments, the values were normalized by β-actin in the case of mice and by the mean of Vinculin, β-actin and GAPDH in the case of neuron- and glia-enriched cultures and they were also adjusted against the value of the inter-experimental reference sample (pool). All samples were assessed in a minimum of three replicated experiments. Normalized values were then calculated in percent change to the pool in each gel. The mean across the experimental replicates obtained in at least three different gels was taken as the final estimate.

3.3.11. Measurement of temperature and weight in pregnant dams

To ensure the validation of the accurate immune response triggered by Poly(I:C), the weight and temperature were measured for CD-1 pregnant dams treated with saline solution or Poly(I:C) (Kentner et al., 2019). Both body weight (Redfern et al., 2017) and temperature (Cunningham et al., 2007; Mueller et al., 2019) have

been established as indicators of a exposure to immunogens, such as Poly(I:C), as part of the broader inflammatory sickness response.

The process of measuring the weight and temperature was initiated 48 h prior to the administration of either Poly(I:C) or saline and was continued for a duration of 48 h following the administration of Poly(I:C) or saline to monitor the recovery period. On the day of administration (GD 9.5), the body weight and temperature were measured just before the administration of the saline/Poly(I:C) at the starting point (+ 0 h), as well as at time intervals of 3, 6, 24 (GD 10.5), and 48 h (GD 11.5) after the administration. To facilitate this process, a thermocouple probe (RET-3 Rectal Probe for Mice, Bioseb, Montpellier, France) connected to a digital thermometer (BioSeb 8851 K.J.T. Type; Bioseb, Montpellier, France) was gently inserted into the rectum at a maximum depth of 9 mm. A consistent temperature reading was obtained within 10 seconds of insertion (Mueller et al., 2019).

3.3.12. Behavioral tests

3.3.12.1. Novel object recognition test (NORT)

The NORT was used to evaluate the cognition-related behavior. All the experiments were carried out in the same room with the same experimental conditions. Before each session, mice were allowed to acclimate to the room and get used to the experimental conditions for at least 1 h.

During the test, mice were placed within an L-shaped maze composed of two identical perpendicular arms set at 90° angles, 25 cm in length, 20 cm in height, and 5 cm in width, as detailed in a previous description (da Cruz et al., 2020) (Figure 17). The lighting intensity inside the maze remained constant at 40 lux.

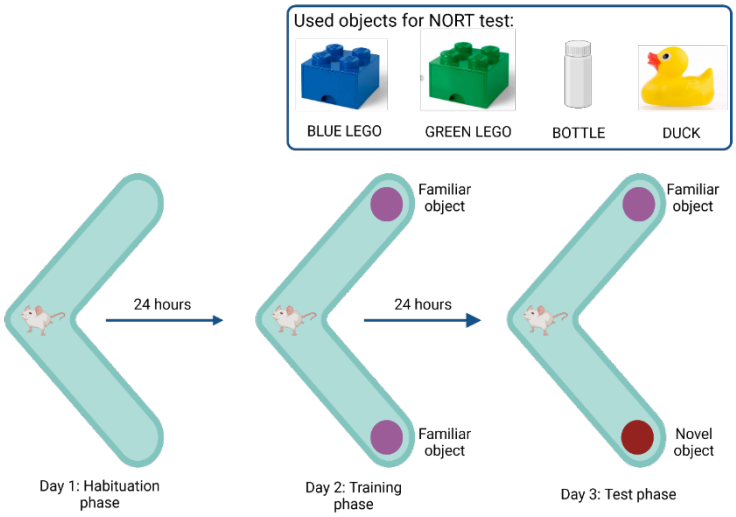

Figure 17: **Schematic representation of the L-shaped maze used in NORT experiments.** Created with BioRender.com

The NORT procedure included three days of tests, each lasting 9 min. On the first day, mice got used to the maze and the test area for 9 min without any objects present. Then, on the second day, there was a training session. Two identical objects (familiar objects) were placed in the maze, and mice were allowed to explore the objects freely for 9 min. The time (seconds) spent exploring each object was recorded. On the third day, the test day, one of the objects was changed to a new object (novel object). Again, the exploration time for each object was recorded.

Every trial was recorded with a ceiling camera above the place where mice were tested. Recorded videos were analyzed by an investigator blinded to the experimental animal identity by means of the software Behavior Scoring Panel© 2008 by A. DUBREUCQ Version 3.0 beta.

All objects underwent a prior testing to ensure an unbiased preference. The chosen objects were distinct from one another in terms of color, shape, and texture. This deliberate distinction facilitates the discrimination between objects during the test phase.

It was established that the animals are exploring an object when they face the object with their nose within 2 cm, and/or if mice are sniffing or biting the object. On the contrary, simply climbing over or leaning on an object was not considered an exploratory behavior. To prevent the accumulation of olfactory cues, mazes and objects were cleaned with a solution of 75% ethanol between each trial.

The discrimination index (DI), which measures cognitive impairment, was established as the relationship between novel and familiar exploration times: (Time devoted to the novel object - Time devoted to the familiar object) / (Total exploration time).

3.3.12.2. Prepulse Inhibition of Startle Reflex test (PPI)

Before each trial, the equipment was calibrated, and the animals were introduced into the experimental setting for 1 h, allowing them to acclimatize to the experimental conditions.

PPI was carried out in a startle chamber (PanLab, Barcelona, Spain). Every session began with a 10 min acclimatization period. This time allowed the animal to become familiar with the holder and the startle box, helping it stay calm and minimizing stress during the test. Throughout this acclimatization period, a constant background of 60 dB white noise was played. Subsequently, five startle pulse-alone trials were conducted to establish a more consistent response from the animals. These initial pulses were excluded from the subsequent analysis. These initial five trials consisted on pulse-alone trials in which 120 dB of white noise was presented independently for a duration of 20 milliseconds (ms).

Following that, mice were exposed to a pseudo-randomized sequence involving various scenarios: first, ten pulse-alone trials characterized by a brief burst of white noise (120 dB, 40 ms); then, ten prepulse-alone trials were conducted for each prepulse intensity (10 ms at 77, 82, or 87 dB). Additionally, ten prepulse-pulse trials for each prepulse intensity were performed, where the prepulse and pulse were separated by a 60 ms interval; and finally, ten trials were executed without any stimulus, in which only the background noise was presented. To

allow variability, the intervals between these trials varied, specifically 10, 12, 15, 20, and 25 seconds (Ibarra-Lecue et al., 2018; Unzueta-Larrinaga & Urigüen, 2023).

The eight trials were presented in a randomized order within each block, with the intertrial interval (ITI) varying randomly between 10 and 30 seconds. This variability aimed to reduce the likelihood of habituation over successive trials.

For every trial, the highest level of the startle response (maximum amplitude of the startle reaction) was recorded. The average startle response within each subgroup of trials was then utilized for analysis. Notably, trials without any stimulus (no-stimulus trials) and those involving only the prepulse (prepulse-alone trials) did not trigger any significant startle response. Thus, their data were excluded from the analysis. The entire testing session lasted approximately 30 to 33 min.

To prevent the accumulation of olfactory cues, boxes and holders were cleaned with a solution of 75% ethanol between each session.

PPI was calculated as follow: % PPI = 100—[(startle response to prepulse-pulse trial/startle response to pulse-alone trial) × 100].

3.4. Data and statistical analysis

Data were analyzed using the Graphpad Prism™ Software version 10 (GraphPad Software, San Diego, California, USA) and InVivoStat free software. All the results are expressed as means ± standard error of the mean (SEM). In all statistical analysis, a p-value < 0.05 was considered as statistically significant. Before the statistical analysis of each experiment, all samples from the control and experimental groups were submitted to Grubbs's outlier test (GraphPad Software) to identify potential outliers. If an outlier was identified, it was removed from further analysis.

Different statistical analysis were performed for the suitable interpretation of the results as explained below.

3.4.1. Levels of PGE_2, IL-6, Kyn/Trp and IFNγ in the medium of neuron- or glia-enriched cultures

Statistical analyses consisted on a paired t-test for each subject comparing the levels of the different molecules in neuron or glial cultures.

3.4.2. Evaluation of size and growth of neurospheres

A two-way repeated measures ANOVA analysis followed by Bonferroni's multiple comparisons test was performed in the comparison between schizophrenia subjects and controls. The variables assessed were time and size or number of neurospheres formed depending on the study.

3.4.3. Transcriptomic analysis of mice and cell samples

For this purpose, the fold change and q value obtained were taken into account. The fold change is the degree of change in expression (value 1 would represent no change; values less than 1 indicate repression and greater than 1, overexpression of the gene). The q-value is an adjusted p-value, which takes into account the false discovery rate (FDR). The application of an FDR becomes necessary when we are measuring thousands of variables (e.g., gene expression levels) from a small sample (e.g., a couple of individuals). In this case, a q-value of 0.05 was set which implied assuming that 5% of the tests that turned out to be statistically significant were false positives.

3.4.4. AlphaLISA® and WB experiments of cells samples

Comparison between cases and controls within each of the groups (neuron- and glia-enriched culture) was made by means of two-tailed unpaired t-test.

3.4.5. AlphaLISA® and WB experiments of mice samples

The levels of total protein and its phosphorylated forms were subjected to a three-way ANOVA test. The factors considered in this analysis were sex (male and female mice), MIA treatment (Poly(I:C) or saline), and cannabis exposure treatment (THC or vehicle).

3.4.6. Temperature and weight monitoring

Temperature and weight data obtained from monitoring experiments was analyzed using two-way repeated measures ANOVA followed by Bonferroni's multiple comparison, in order to see the contribution of time and saline or Poly(I:C) administration to temperature or weight changes. The variables assessed were time and treatment.

3.4.7. Pregnancy outcome

Comparisons between litters of Poly(I:C) and saline pregnant dams were done by two-tailed unpaired t-test.

3.4.8. Behavioral tests of the double-hit mouse model

Three-way ANOVAs followed by Bonferroni's multiple comparisons test were used to analyze the experiments involving the behavior of the double-hit animal model (NORT and PPI). Results were analyzed by three-way ANOVAs considering the factors "sex" (male or female mice), "MIA" (saline or Poly(I:C) treatment) and "THC" (presence or absence of THC chronic treatment in the adolescence period).

In NORT, before the assessment of outlier testing, mice exploring less than 10 seconds in total (total exploration time) were removed from the analysis, considering they were not performing the recognition of the objects properly.

In the PPI test, mice that did not increase in response with increasing dB were removed from the saline/vehicle group, considering that since it was the control group, they were not performing the test properly.

Results

4. RESULTS

4.1. Study I: Cell cultures from olfactory neuroepithelium

The samples extracted from the olfactory neuroepithelium served for the establishment of different cell culture types. As previously described, the growth conditions for each culture were meticulously adapted according to the specific cell type inherent to each culture. This approach yielded four distinct types of cell cultures: (1) neurospheres, (2) differentiated neurospheres, and an adherent culture subsequently subdivided into (3) neuron-enriched and (4) glia-enriched cultures.

To ascertain the characteristics of these cell cultures, a comprehensive assessment was conducted utilizing both bright-field microscopy and immunofluorescence. Notably, in the case of neuron- and glia-enriched cultures, an additional characterization was applied through FACS.

Post-characterization, a series of comparative studies were initiated, comparing cultures derived from control subjects with those obtained from subjects diagnosed with schizophrenia. The primary objective of these studies was to unveil potential alterations linked to schizophrenia within the intricate mechanisms underlying the survival and development of neural progenitor cells.

4.1.1. Characterization of proliferating neurospheres

4.1.1.1. Bright-field visual characterization of proliferating neurospheres

To validate the presence and functionality of neural stem cells (NSCs) in nasal exfoliate samples, our initial objective was to establish a neurosphere culture and assess the proliferative and differentiating capacities of these cells. When subjected to a specialized proliferation medium, NSCs aggregated to form compact structures (Figure 18A). Notably, these neurospheres demonstrated a distinctive ability to undergo division without initiating differentiation, as could be observed in the bright-field microscopy images (Figure 18B).

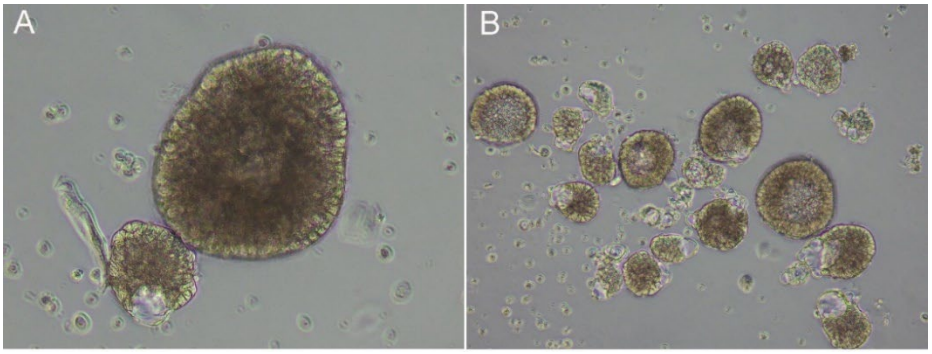

Figure 18: **Proliferating neurospheres.** Bright-field visual characterization of (A) growing neurospheres (20X) and (B) proliferating neurospheres (10X).

Following the disassembly of neurospheres, through a combination of centrifugation and manual pipetting, and subsequent cultures in new flasks, the single cells reassembled. This process led to the emergence of new neurospheres, which showed a sustained and unlimited proliferation capacity. The successful regeneration of neurospheres post-disaggregation underscores the robustness and regenerative potential of the NSCs present in the nasal exfoliate, confirming their viability for further investigation and experimentation.

4.1.1.2. Characterization of proliferating neurospheres by immunofluorescence

Immuno-characterization (method explained in 3.3.4) of the spheres revealed the presence of specific neural markers such as Sox2 (Figure 19A and 19E), Musashi-1 (Figure 19B), and Nestin (Figure 19F) as well as their co-localization (Figure 19D and 19H). The presence of these neural markers strongly validates, under the given experimental conditions, the capacity of these cells derived from the olfactory neuroepithelium to generate neurospheres comprising neural progenitor cells. These results demonstrate the neurogenic potential of the sampled cells and reinforces the suitability of the neurosphere culture for subsequent investigations into neural stem cell behavior and functionality.

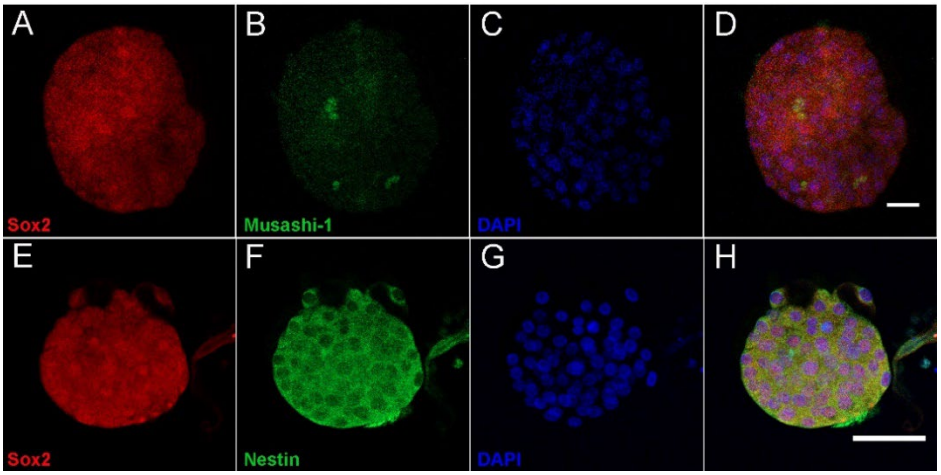

Figure 19: **Characterization of proliferating neurospheres by immunofluorescence.** Immunostaining of neural markers Nestin, Sox2 and Musashi-1. Double labelling of (A) Sox2 (red), (B) Musashi-1 (green) and (D) merged image for Sox2 and Musashi-1. Double labelling of (E) Sox2 (red), (F) Nestin (green) and (H) merged image for Sox2 and Nestin. (C, G) DAPI was used to stain the nuclei (blue). Bar = 20µm.

4.1.2. Characterization of cells differentiated from neurospheres

4.1.2.1. Bright-field visual characterization of cells differentiated from neurospheres

Following the adhesion of neurospheres to the flask, a spectrum of cells at diverse stages of differentiation became evident. Notably, a subset of these cells exhibited distinct neuronal characteristics, marked by the presence of projections establishing connections with neighboring cells (Figure 20A and 20B). In certain instances, these differentiating cells displayed the development of synaptic terminals, further indicating the progression towards a neuronal phenotype (Figure 20C). This observed differentiation underscores the dynamic nature of the neurosphere-derived cells and provides valuable insights into their potential to undergo specialized neural development under controlled experimental conditions.

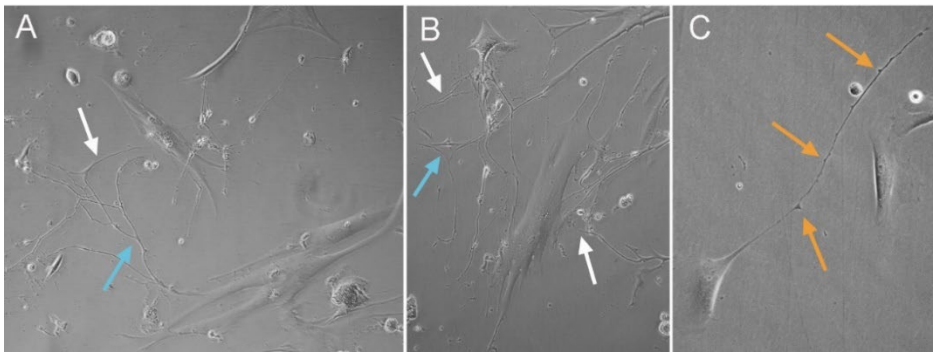

Figure 20: **Bright-field visual characterization of differentiated neurospheres culture.** (A, B) Cell with neuronal shape and long prolongation (white arrow) connecting with another similar cell (blue arrow) (C) and dendritic spines (orange arrow).

4.1.2.2. Characterization of cells differentiated from neurospheres by immunofluorescence

Immunofluorescence assays (method explained in 3.3.4) demonstrated the presence of specific neural markers such as βIII-Tubulin (Figure 21A and 21C), Nestin (Figure 21A), GFAP (Figure 21B), and MAP2 (Figure 21C), in the cells grown from neurospheres differentiation.

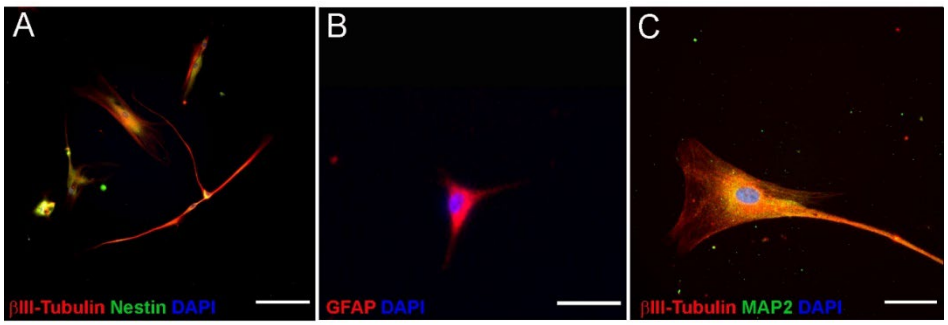

Figure 21: **Characterization of differentiating cells from neurospheres by immunofluorescence.** Double immunostaining of (A) βIII-Tubulin and Nestin, (B) GFAP, and (C) double staining of βIII-Tubulin and MAP2. Nuclei were stained with DAPI. (A, B) Bar = 200 µm and (C) 50 µm.

Despite their potential to give rise to cells exhibiting both neuronal and glial characteristics, the yield of cells derived from neurospheres remained notably limited. Furthermore, once these cultures of differentiated cells originating from neurospheres reached full cellular capacity, the ability to propagate the culture

was hindered, leading to cell death. This phenomenon is attributed to the fact that fully developed neurons and glial cells do not engage in cellular division.

As emphasized earlier, the primary objective of this research was to obtain neuronal and glial cells for the investigation of potential cellular and molecular hallmarks associated with schizophrenia. The limited yield of cells obtained from neurospheres raised concerns about the practical utility of these cultures for research purposes. To address this limitation, a strategic decision was made to cultivate adherent cultures from the olfactory neuroepithelium and subsequently differentiate the cells in this culture into neurons and glial cells. This approach aims to enhance the yield of neural cells for robust and meaningful investigations into the cellular and molecular underpinnings of schizophrenia.

4.1.3. Characterization of adherent cells

Under the provided experimental conditions, olfactory neuroepithelium cells can be directed into a mixed culture predominantly composed of cells predisposed for neural differentiation.

4.1.3.1. Bright-field visual characterization of adherent cultures

Once cells from the olfactory neuroepithelium are seeded, the progressive growth of the culture can easily be observed with the bright-field microscope. Figure 22A represents the cell culture at day 2, Figure 22B at day 4 and Figure 22C at day 6 after seeding, with cells beginning to approach confluence. Passage is performed once the culture reaches its critical point.

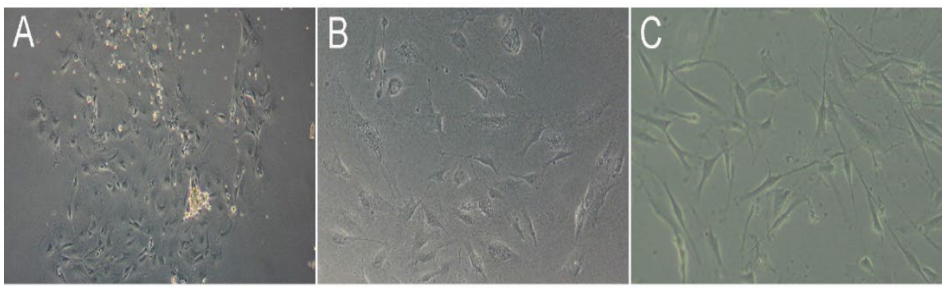

Figure 22: **Bright-field visual characterization of adherent cells from olfactory neuroepithelium.** Cells growing at different days after seeding (A) passage 0, (B) passage 2 and (C) passage 4, (10X).

In the initial passages, a diverse array of cell morphologies was observed, directly mirroring the heterogeneous composition of the culture. Consequently, the coexistence of cells at various stages of maturation became evident. As the passages advanced, this cellular heterogeneity gradually diminished, giving way to a dynamic shift in cell morphology that reflected an ongoing maturation process. The progression of cell morphology was characterized by a transformation from an initial heterogeneous and indistinguishable state to a subsequent stage marked by elongation and heightened morphological clarity. This transformation is indicative of the neural cell differentiation process. The observed evolution in cell morphology not only highlights the maturation dynamics within the culture but also underscores the successful transition toward a more homogenously differentiated neural cell population over successive passages.

4.1.3.2. Characterization of adherent cultures by immunofluorescence

The expression of neural markers was evaluated with immunofluorescence (method explained in 3.3.4) using specific antibodies against the neuronal proteins βIII-Tubulin (Figure 23A) and MAP2 (Figure 23C), as well as glial protein GFAP (Figure 23B). Results show the presence of these neural markers, which underscores the maturation trajectory of the culture, culminating in the development of a more specialized population predominantly composed of neural and glial cells.

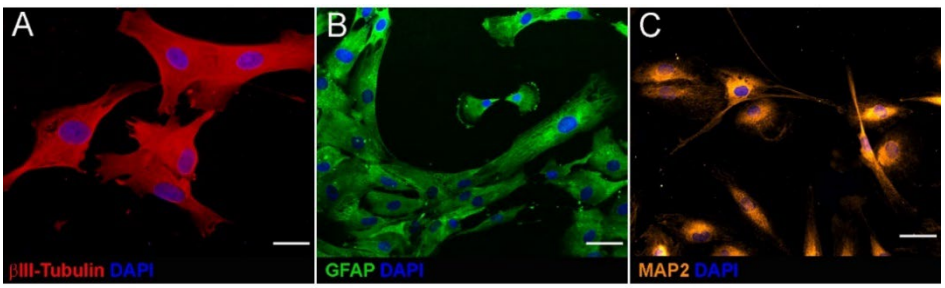

Figure 23: **Characterization of adherent cells by immunofluorescence.** Immunostaining of (A) βIII-Tubulin, (B) GFAP and (C) MAP2. DAPI was used to stain the nuclei. Bar = 50 µm.

4.1.4. Characterization of neuron- and glia-enriched culture

To attain a more specific culture, a strategic decision was made to selectively harvest only those cells within the adherent culture that were undergoing differentiation into neurons. This involved careful selection of these cells and reseeding them in a new plate. Facilitating this targeted selection process, as previously elucidated, was the use of PSA-NCAM as a neuronal surface marker. Specifically, cells expressing PSA-NCAM were chosen for its role in indicating the differentiation into neurons, ensuring a more precise isolation of the desired cell population for subsequent experimentation and culture refinement. This approach aims to enhance the specificity of the culture, focusing on the neural differentiation pathway and facilitating a more controlled and specialized experimental environment.

4.1.4.1. Bright-field visual characterization of neuron- and glia-enriched culture

Bright field microscopy images of PSA-NCAM+ cells positively identified at 10X magnification, unveiling their distinctive neuronal morphology characterized by elongated extensions that establish connections with neighboring cells (Figure 24A and Figure 24B). Subsequently, a differentiated cell, portraying the characteristic shape of a neuron at 10X magnification, is depicted (Figure 24C). Advancing to a higher magnification of 20X, Figure 24D shows an elongation emanating from a neuron, providing a detailed view of the intricate neuronal morphology. Further exploration reveals the terminal end of a neuron's extension forming a synaptic button-like connection with another cell, highlighting the intricate cellular interactions (Figure 24E).

In contrast, Figures 24F and 24G show cells that do not express PSA-NCAM (enriched in glial cells) under bright-field microscopy at 10X magnification, emphasizing an alternative growth pattern characterized by larger cellular aggregates and less elongated cells. This detailed analysis using bright-field microscopy allows for a clear distinction between the neuronal and glial components within the culture, providing valuable insights into the specific

cellular compositions fostered by the presence or absence of PSA-NCAM.

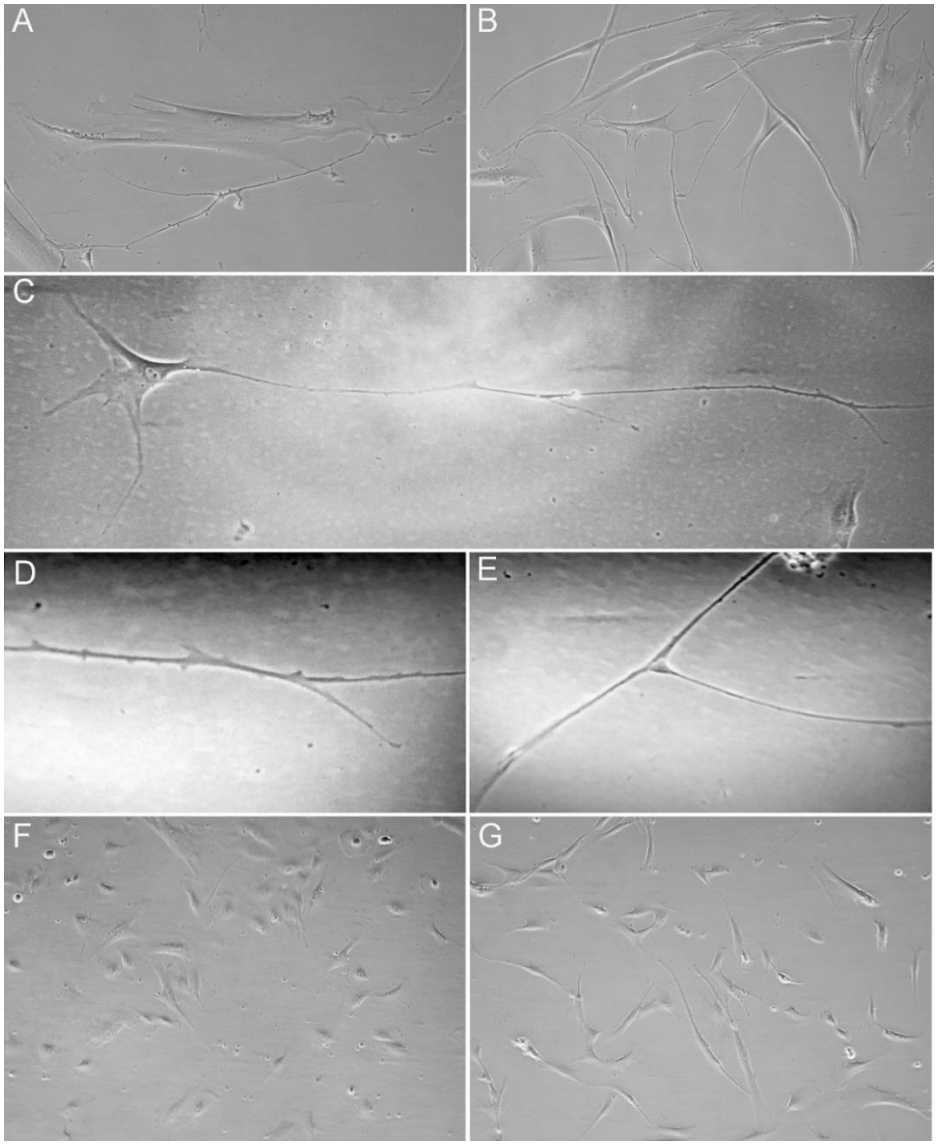

Figure 24: **Bright-field visual characterization of the neuron- or glia-enriched cultures.** Bright-field image of PSA-NCAM positive cells (neuron-enriched fraction) (10X) showing (A, B) neuronal shape and long prolongations connecting with other cells. (C) Differentiated cell with a characteristic neuron shape (10X). (D) A prolongation of a neuron (20X) and (E) end of a prolongation of a neuron in a synaptic button-like connection between two different cells (20X). (F, G) Bright-field image of glia-enriched fraction cell culture (10X) showing a different growth pattern, with larger aggregates and less elongated cells.

4.1.4.2. Characterization of neuron- and glia-enriched cultures by immunofluorescence

First, and in order to validate the efficacy of the separation, immediately after the magnetic sorting (method explained in 3.3.3.1) the presence of PSA-NCAM was evaluated in the neuron-enriched cultures, as seen in Figures 25A and 25C. Subsequently, these cultures were allowed to grow for approximately 30 days before additional immunofluoresece analyses (method explained in 3.3.4).

Neuron-enriched cultures abundantly express the specific neuronal proteins MAP1B (Figure 25D), Nestin (Figure 25E), βIII-Tubulin (Figure 25G), NeuN (Figure 25H), and MAP2 (Figure 25K) as demonstrated the immunofluorescence assays. Moreover, co-expression of MAP1B and Nestin (Figure 25F), βIII-Tubulin and NeuN (Figure 25I) and βIII-Tubulin and MAP2 (Figure 25L) was found in the neural-enriched cultures. To ensure the specificity of the culture and discard the presence of epithelial cells within the derived cultures from the olfactory neuroepithelium, EpCAM labeling was employed. EpCAM was not identified in the neuron-enriched cultures (Figure 25M and 25O), confirming the absence of epithelial cells.

These findings collectively support and substantiate the outcomes of the immunofluorescence assessments, reinforcing the neural identity of the enriched cultures.

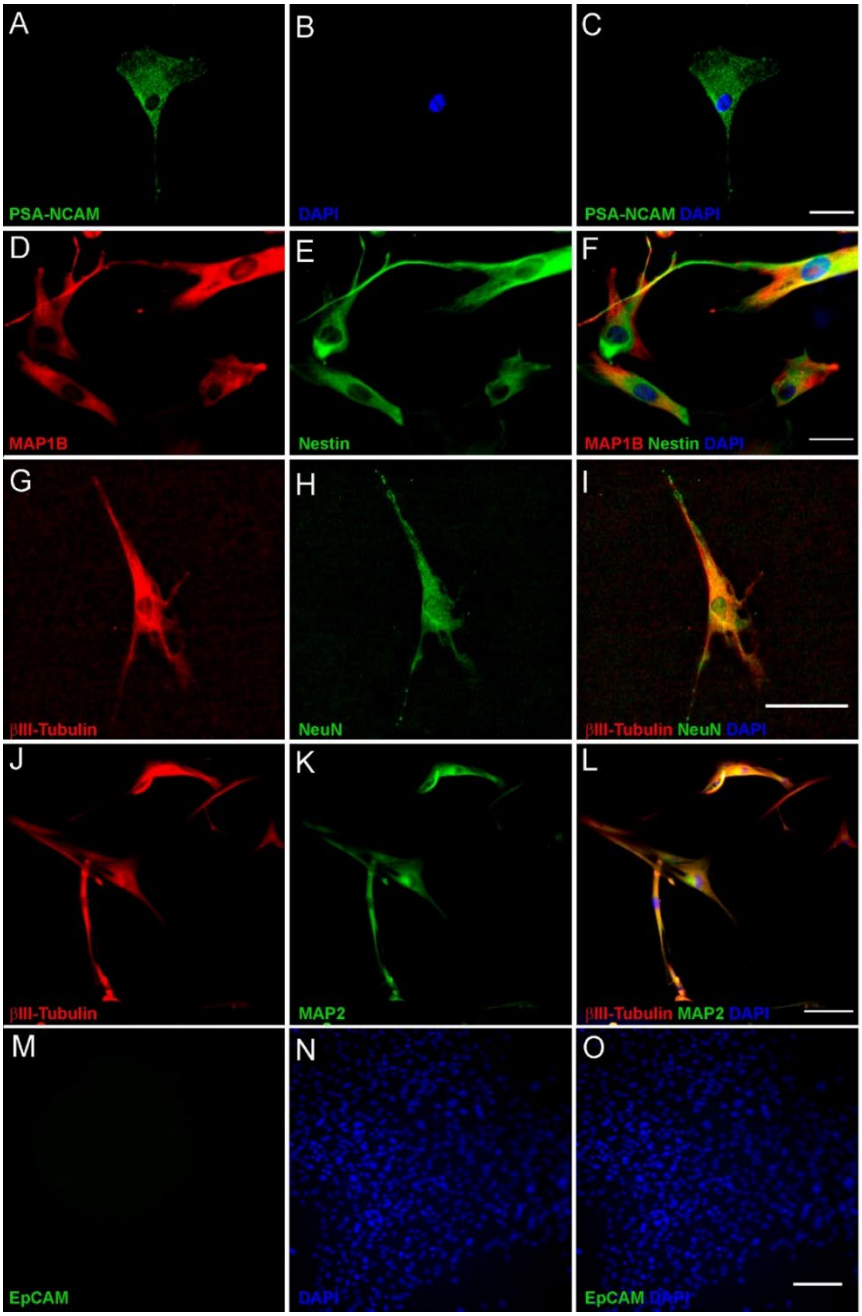

Figure 25: **Characterization of neuron-enriched culture by immunofluorescence.** Immunostaining of (A, C) PSA-NCAM in the neuron-enriched cultures immediately after magnetic sorting. Labelling of (D) MAP1B and (E) Nestin and (F) merged image for MAP1B and Nestin. Labelling of (G) βIII-Tubulin and (H) NeuN and (I) merged image for βIII-Tubulin and NeuN. Labelling of (J) βIII-Tubulin and (K) MAP2 and (L) merged image for βIII-Tubulin and MAP2. (M, O) Labelling of EpCAM. (B, N) DAPI was used to stain the nuclei. Bar = 200µm.

In contrast, in glia-enriched cultures (Figure 26), PSA-NCAM was not detectable after the magnetic separation (Figure 26A). Subsequent immunofluorescence assays in glia-enriched cultures, revealed the presence of distinct glial proteins, with notable expression of GFAP (Figure 26D). Again, to ensure the specificity of the culture and discard the presence of epithelial cells within the derived cultures from the olfactory neuroepithelium, EpCAM labeling was employed. EpCAM protein was not identified in the glia-enriched cultures as seen in Figure 26G and Figure 26I, confirming the absence of epithelial cells. This comprehensive analysis reinforces the fidelity of the glia-enriched cultures and verifies the successful elimination of epithelial cell contaminants, further establishing the purity and specificity of the glial cell population.

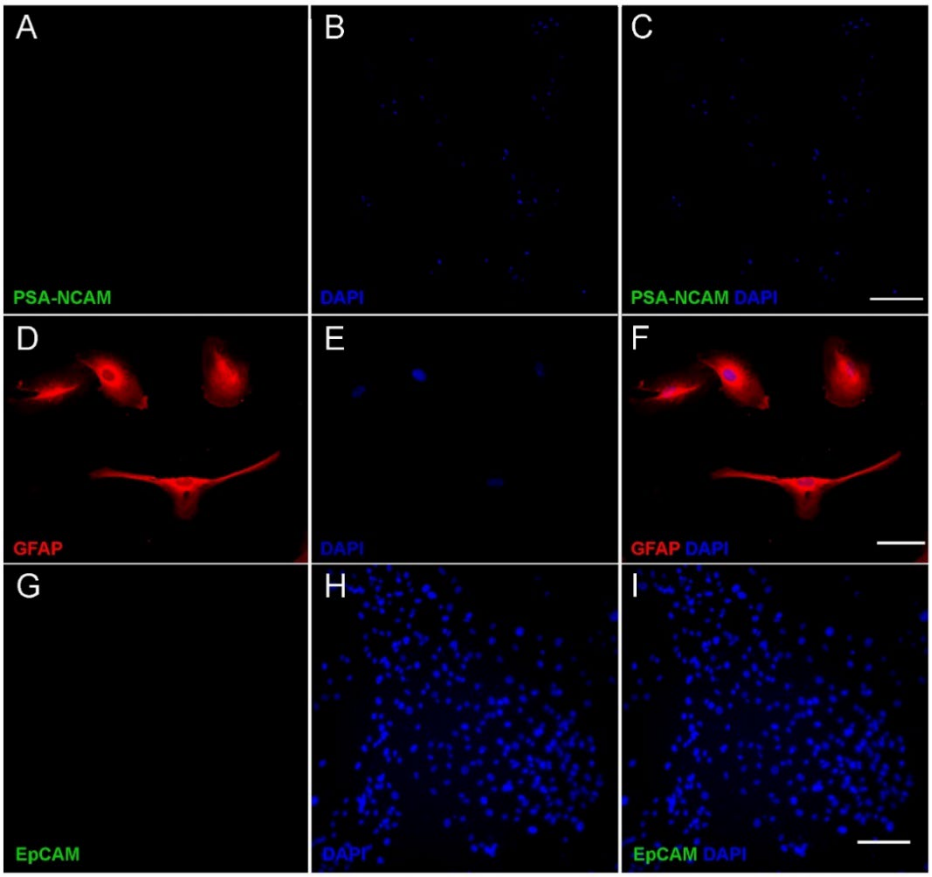

Figure 26: **Characterization of glia-enriched culture by immunofluorescence.** (A, C) Immunostaining of PSA-NCAM. (D, F) Labelling of GFAP and (G, I) EpCAM. DAPI was used to stain the nuclei (B, E, H). Bar = 200µm.

4.1.4.3. Characterization of neuron and glia-enriched cultures by Fluorescence-Activated Cell Sorting (FACS)

To confirm the observed results from bright-field microscopy and immunofluorescence, flow cytometry analysis was employed (method explained in 3.3.5), specifically labeling cells with NeuN and GFAP to assess the percentages of neuronal and glial populations in each culture type. Additionally, EpCAM labeling was used to definitively exclude any presence of epithelial cells. As illustrated in Figure 27, the analysis revealed that up to 46% of cells in the PSA-NCAM positive culture (neuron-enriched cultures) expressed NeuN (Figure 27A). On the contrary, the flow cytometry assessment demonstrated a minimal presence of GFAP positive cells (1.90%) in these cultures.

Conversely, in the glia-enriched cultures, the percentage of cells expressing GFAP was of 48%, leaving only 0.095% NeuN positive cells (Figure 27B). In addition, the presence of cells co-expressing both NeuN and GFAP markers was noted, attributed to the immature nature of the cells (0.7% in neuron-enriched cells and 8.02% in glia-enriched cells). Lastly, a significant percentage of cells approximately 41% in neuron-enriched cultures and approximately 44% in glia-enriched cultures were found to be non-viable after sample processing.

Moreover, the flow cytometry analysis gave a residual value of 0.093% of EpCAM positive cells in neuron-enriched cultures (Figure 27C) and 0.73% in glia-enriched cultures (Figure 27D).

These findings highlight the complexity of cellular identities within the cultures and emphasize the need for careful consideration and interpretation of flow cytometry data in the context of mixed cell populations. Further refinement and optimization of sorting techniques may be necessary to enhance the purity of the isolated cell populations.

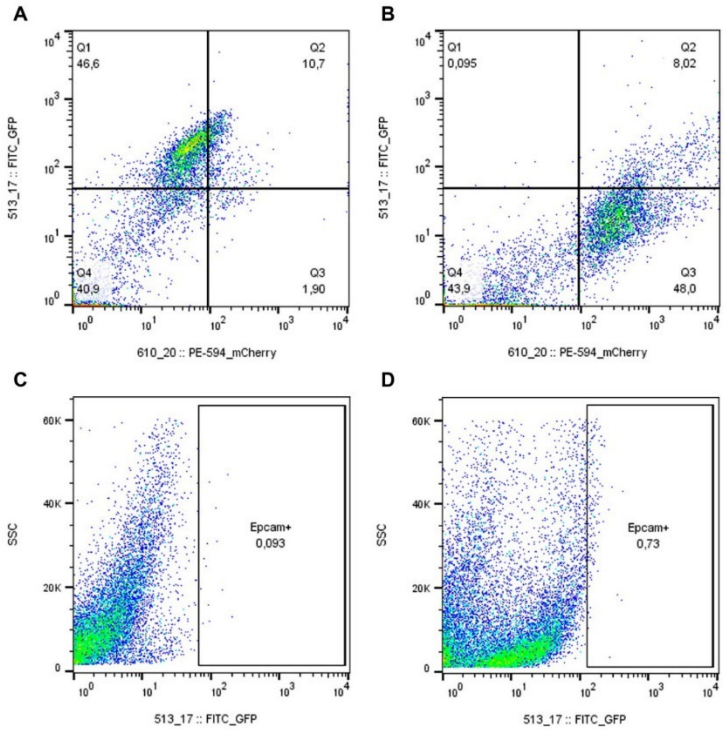

Figure 27: **FACS of neuron- and glia-enriched cultures.** (A) Sorting cells under the described conditions yielded over >46% NeuN and FITC positive cell populations in neuron-enriched cultures and (B) 48% GFAP and mCherry positive cell populations in glia-enriched cultures. FACS plots of negative control for EpCAM in (C) neuron-enriched cultures and in (D) glia-enriched cultures.

4.1.5. Quantification of IFNγ, IL-6, PGE_2, Trp and Kyn in mediums of neuron- and glia-enriched cultures by ELISA

One of the main objectives of this Doctoral Thesis was to establish a biological substrate from patient samples for the identification and measurement of disease-related traits, states, or prognostic biomarkers. Thus, different immunoassays (method explained in 3.3.6) were conducted to determine whether the enriched cultures could generate and release detectable molecules in the culture medium, serving as potential biomarkers. A selection of well characterized molecules previously used in psychiatry research were measured, particularly those linked to the inflammatory component of schizophrenia (including IFNγ, PGE_2, IL-6, and the Kyn/Trp).

As depicted in Figure 28, the cells of both types of cultures demonstrated the capability to produce and release these compounds. Moreover, in glia-enriched cultures, a significant increase was observed in the levels of PGE_2 (Neuron: 5.83 ± 4.65 pg/mg prot; Glia: 14.44 ± 7.27 pg/mg prot; increase: +147.68%, p=0.04) (Figure 28A), and the Kyn/Trp (Neuron: 0.04 ± 0.003; Glia: 0.06 ± 0.01, increase: +40.67%, p=0.03) (Figure 28B) compared to neuron-enriched cultures. On the other hand, in neuron-enriched cultures, a significant increase in IFNγ levels was found (Neuron: 82.55 ± 16.56 pg/mg prot; Glia: 45.20 ± 8.59 pg/mg prot; increase: +82.65%, p=0.03) (Figure 28C) compared to glia-enriched cultures. No significant differences were observed in the IL-6 levels (Figure 28D) between both cultures. These findings underscore the differential production of these molecules in both culture types and suggest that variations in the levels of these mediators could potentially serve as valuable biomarkers for further exploration in the context of psychiatric research.

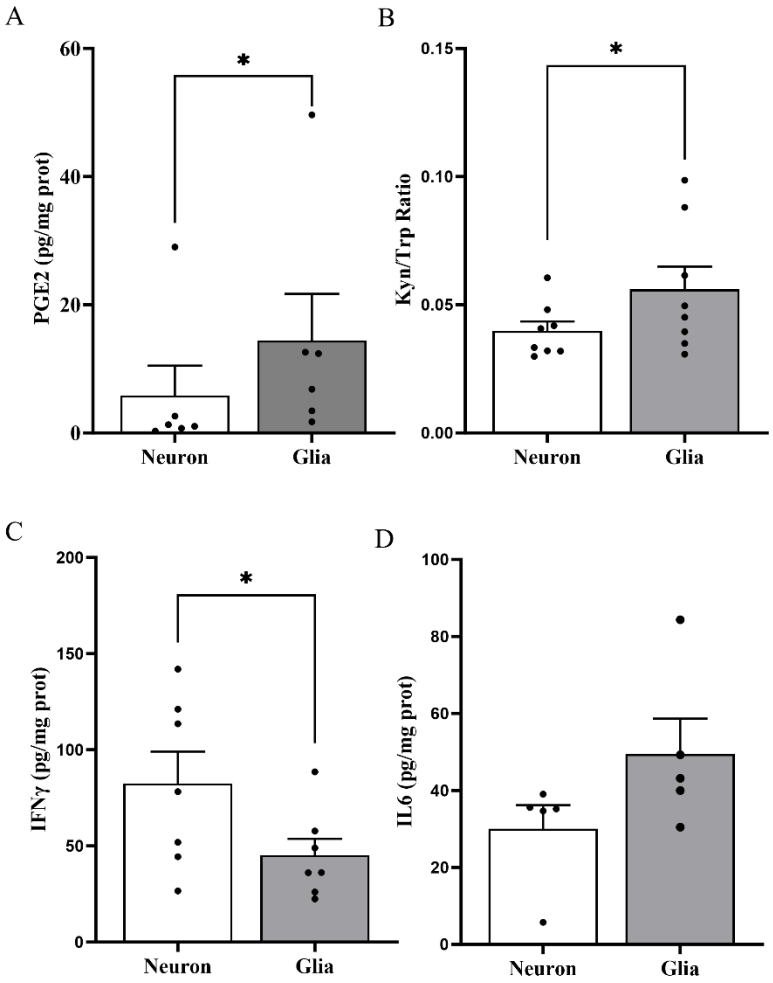

Figure 28: **Levels of PGE_2, IL-6, Kyn/Trp and IFNγ in the mediums of neuron- and glia-enriched cultures.** (A) Levels in pg/mg protein of PGE_2 (n=6), (B) ratio of Kyn/Trp (n=8), (C) levels in pg/mg protein of IFNγ (n=7), and (D) levels in pg/mg protein of IL-6 (n=5) measured by ELISA assay in both neuron-enriched and glia-enriched cultures medium. Bars represent the mean ± SEM and circles individual values. Statistical analyses consisted on a paired T-test for each subject comparing the levels of the different molecules in neuron or glial cultures. Statistically significance was set at *p<0.05.

4.1.6. Evaluation of proliferation and size of neurospheres

In order to study the putative differences between the development of the neurospheres from schizophrenia and control subjects, their proliferating capability as well as the size were evaluated (method explained in 3.3.2.1). A strongly significant decrease was observed in both the proliferative capacity (Figure 29, Table 6) and size (Figure 30, Table 7) of neurospheres derived from

patients with schizophrenia in comparison to those obtained from control individuals. This finding underscores a distinct alteration in the neurosphere dynamics associated with schizophrenia, shedding light on potential differences in neural progenitor cell behavior and proliferation between both groups.

In the evaluation of neurosphere proliferation, statistical analysis showed a significant effect of schizophrenia factor resulting in a decrease (-41.09%, p=0.0008) in number of primary neurospheres (P0) obtained by plating 100 cells/subject of schizophrenia group comparing with their matched controls [F_{SZ} (1, 6) = 12.27, p=0.0128] (C: 70.70 ± 10.38; SZ: 41.65 ± 8.03). Furthermore, a significant effect of the day factor was observed. This indicates that as time progressed, the differences in neurosphere formation became more pronounced between the control group and subjects with schizophrenia. The temporal aspect of this interaction underscores the evolving nature of neurosphere dynamics over time, accentuating the distinction between the two groups and providing valuable insights into the temporal patterns of neurosphere alterations associated with schizophrenia.

Table 6: **Two-way repeated measures ANOVA analysis conducted in order to evaluate the effect of time (days), schizophrenia and its interaction on the growth of neurospheres.**

	Number of neurospheres	**Self-renewal**
Days	**F (4, 24) = 68.66, p<0.0001**	**F (4, 24) = 148.60, p<0.0001**
Schizophrenia	**F (1, 6) = 12.27, p=0.0128**	**F (1, 6) = 135.00, p<0.0001**
Days x Schizophrenia	F (4, 24) = 1.36, p=0.2767	**F (4, 24) = 37.04, p<0.0001**

However, when measuring neurosphere self-renewal capacity, a significant decrease in the number of neurospheres was consistently observed in subjects with schizophrenia. Specifically, a reduction (-68.05%, p<0.0001) in the number of newly-formed neurospheres was evident in schizophrenia group when compared to the control group (C: 69.80 ± 12.96; SZ: 22.30 ± 4.43). Following Bonferroni's post-hoc test, a decline (Day 17: -72.86%, p<0.0001; Day 20: -69.30%, p<0.0001; Day 23: -68.00%, p<0.0001; Day 26: -63.72%, p<0.0001;

Day 30: -69.05%, p<0.0001) in regenerative capacity was consistently observed across all measured days in individuals with schizophrenia when compared to control subjects (Day 17 - C: 35.00 ± 2.85; SZ: 9.50 ± 0.64, Day 20 - C: 53.75 ± 2.95; SZ: 16.50 ± 1.50, Day 23 - C: 68.75 ± 5.12; SZ: 22.00 ± 1.73, Day 26 - C: 79.25 ± 6.14; SZ: 28.75 ± 3.17, Day 30 - C: 112.30 ± 3.56; SZ: 34.75 ± 3.83) These findings highlight a consistent and significant reduction in neurosphere formation in subjects with schizophrenia, particularly noticeable from the first passage onward, providing valuable insights into the ongoing alterations in neural progenitor cell dynamics associated with the disease.

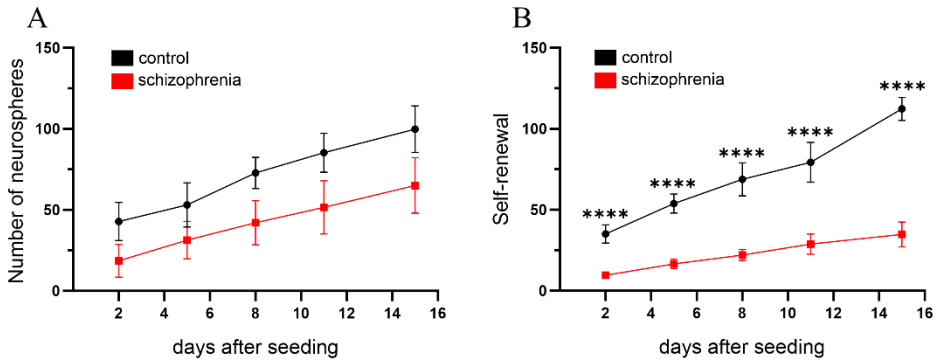

Figure 29: **Number of newly formed neurospheres in schizophrenia and control group over the days per 100 cells seeded.** Comparison between controls (n=4) and subjects with schizophrenia (n=4) in the number of neurospheres formed over the days per 100 cells seeded in the first passage (0-15 days). Bars (mean ± SEM) showing (A) the number of primary neurospheres (P0) obtained by plating 100 cells/subject obtained from the nasal exfoliation from schizophrenia subjects (n=4) and their matched controls (n=4). (B) Neurosphere self-renewal capacity evaluated by the number of newly formed neurospheres (bars represent mean ± SEM) of the first-generation (P1)/plated cells x 100) obtained from the dissected tissue from schizophrenia subjects (n=4) and their matched controls (n=4=). All the significant differences are indicated by asterisks. *p<0.05; **p<0.01, ***p<0.005, ****p<0.001 as assessed by two-way repeated measures ANOVA followed by Bonferroni's multiple comparisons test.

Regarding the size of the neurospheres, a similar pattern of growth was observed. Patients initially had smaller neurospheres, but this size difference was not statistically significant from the outset. As the days went by, the size of patients' neurospheres gradually decreased respect to ones from controls, until statistically significant differences became apparent. After two-way repeated measures ANOVA, the study revealed a significant interaction effect between time and

schizophrenia indicating as mentioned above, that as time progressed, differences in neurospheres size became more pronounced between controls and schizophrenia subjects.

Table 7: **Two-way repeated measures ANOVA analysis conducted in order to evaluate the effect of time, schizophrenia and its interaction on the size of neurospheres.**

Two-way repeated measures ANOVA parameters for size of neurospheres

	Passage 0	**Passage 1**	**Passage 2**
Days	**F (1.358, 8.146) = 126.21, p<0.0001**	**F (1.467, 8.800) = 160.73, p<0.0001**	**F (2.432, 14.59) = 366.32, p<0.0001**
Schizophrenia	F (1, 6) = 5.63, p=0.0553	**F (1, 6) = 10.66, p=0.0172**	**F (1, 6) = 26.41, p=0.0021**
Time x Schizophrenia	**F (4, 24) = 5.47, p=0.0028**	**F (4, 24) = 11.35, p<0.0001**	**F (4, 24) = 49.83, p<0.0001**
	Passage 3	**Passage 4**	**Passage 5**
Days	**F (1.964, 11.79) = 193.71, p<0.0001**	**F (2.224, 13.34) = 175.49, p<0.0001**	**F (1.778, 10.67) = 71.62, p<0.0001**
Schizophrenia	**F (1, 6) = 71.73, p=0.0001**	**F (1, 6) = 82.52, p<0.0001**	**F (1, 6) = 39.56, p=0.0008**
Time x Schizophrenia	**F (4, 24) = 32.31, p<0.0001**	**F (4, 24) = 34.73, p<0.0001**	**F (4, 24) = 14.58, p<0.0001**

Following Bonferroni's post-hoc test, no statistically significant differences were found in neurosphere size in passages 0 and 1. The differences began to exhibit statistical significance at passage 2 where a significant decrease (-45.77%, p=0.0006) in neurospheres size of schizophrenia patients comparing with controls (C: 208.00 ± 8.13; SZ: 112.80 ± 6.57) was observed. At this point, a clear reduction in the size of neurospheres in subjects with schizophrenia compared to the controls was evident.

From this day onwards, the reduction in the size of neurospheres in subjects with schizophrenia became increasingly apparent. In passage 3 and 4, a substantial decrease (Passage 3: -40.04%, p=0.0001; Passage 4: -48.31%, p=0.0001) was observed again in neurospheres size of schizophrenia patients comparing with controls (Passage 3 - C: 112.40 ± 14.54; SZ: 67.40 ± 6.37, Passage 4 - C: 118.20 ± 14.64; SZ: 61.10 ± 5.79). Lastly, in passage 5, the final passage, the reduction (-70.40%, p<0.0001) in the size of neurospheres in subjects with schizophrenia became unmistakable, with significant reduction of neurospheres diameter of schizophrenia patients compared to controls (C: 124.00 ± 14.40; SZ: 36.70 ± 8.04).

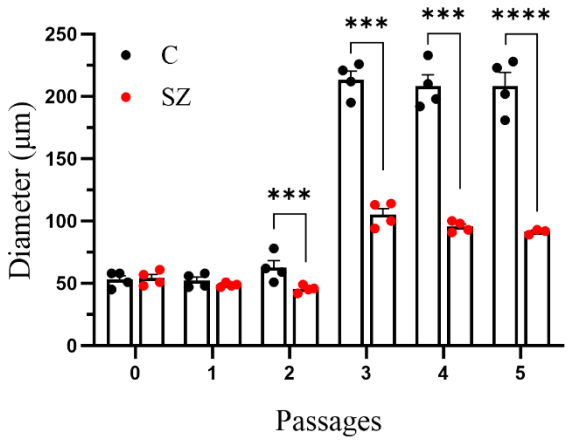

Figure 30: **Size of formed neurospheres over the days in control and schizophrenia groups.** Comparison between controls (n=4) and subjects with schizophrenia (n=4) in the size of neurospheres formed over passages. Graphical representation bars (means ± SEM) showing the diameter of neurospheres (mean ± SEM) at passages P0-P5 obtained from the nasal exfoliation from schizophrenia subjects (n=4) and their matched controls (n=4). ***p<0.001.

4.1.7. Whole transcriptome analysis of neuron- and glia-enriched cultures from subjects with schizophrenia and their controls

Differential expression analysis (method explained in 3.3.7) was conducted to unveil the altered expression of genes in both neuron- and glia-enriched cultures from patients with schizophrenia as compared to healthy controls. The results of this analysis are presented in Table 8 for neuron-enriched cultures and Table 9 for glia-enriched cultures, providing a comprehensive overview of the genes exhibiting differential expression in each cell type. This exploration aims to identify and characterize the specific genes that may contribute to the molecular signatures associated with schizophrenia in distinct neuronal and glial populations.

Table 8: **Representation of the upregulated and downregulated genes in neuron-enriched cultures of schizophrenia subjects vs. controls.** Summary table of the data obtained after massive sequencing of neuron-enriched cultures. Log fold change and q-value for each gene.

A) DOWNREGULATED GENES		
Gene name	**log2_fold_change**	**q_value**
SCG2	-5.1408	0.01886
DPP4	-4.3766	0.01886
L1CAM	-4.3482	0.01886
PLXDC1	-4.0663	0.01886
GALNT15	-3.8314	0.01886
SOWAHD	-3.7248	0.01886
RNF157	-3.5536	0.04424
NPTXR	-3.5488	0.01886
EPGN	-3.4685	0.01886
STC2	-2.4811	0.01886
CACNA1A	-2.4639	0.01886
QPCT	-2.4604	0.03379
ANKRD1	-2.3729	0.03379
H1-2	-2.2611	0.01886
TRIM16L	-2.1637	0.01886
CCND2	-2.1086	0.01886
HMOX1	-2.0897	0.01886
NOTCH3	-2.0691	0.04424
STC1	-2.0420	0.01886
KCNE4	-1.9789	0.01886
BEX1	-1.9731	0.01886
PYGL	-1.8156	0.01886
H2BC21	-1.8127	0.03379
H2AC6	-1.5323	0.01886

B) UPREGULATED GENES		
Gene name	**log2_fold_change**	**q_value**
NUF2	4.5845	0.0442
PTN	4.4312	0.0189
ISLR	3.6949	0.0189
DPT	3.3854	0.0189
MN1	3.2665	0.0189
CEP128	2.9133	0.0189
KRT34	2.7573	0.0189
APOD	2.6964	0.0189
CACNB4	2.4119	0.0189
ITIH5	2.392	0.0189
CRABP2	2.333	0.0189
MEF2C	2.2135	0.0189
RPH3AL	2.1971	0.0442
RCAN2	1.9945	0.0338
TEX41	1.8768	0.0189
LOXL4	1.8709	0.0189
OLFML3	1.8583	0.0189
TWIST2	1.6278	0.0442
AKAP12	1.5468	0.0442
PHGDH	1.4904	0.0189

Table 9: **Representation of the upregulated and downregulated genes in glia-enriched cultures of schizophrenia subjects vs. controls.** Summary table of the data obtained after massive sequencing of glia-enriched cultures. Log fold change and q-value for each gene.

A) DOWNREGULATED GENES		
Gene name	log2_fold_change	q_value
TMC6	-5.5868	0.01849
DYSF	-4.9645	0.04897
MFAP5	-4.2635	0.03161
ANKRD1	-4.1647	0.04139
SIM2	-4.0034	0.01849
EPGN	-3.6651	0.03161
TM4SF20	-3.4291	0.04139
UCHL1	-3.4265	0.01849
PRPS1	-3.3868	0.01849
SEL1L3	-3.3641	0.01849
MAP3K7CL	-3.2786	0.03161
LINC00595	-3.1389	0.01849
STC2	-3.1231	0.01849
DSG2	-3.0881	0.04139
NPTXR	-2.3763	0.04139
H1-2	-2.3316	0.01849
ABI3BP	-2.3222	0.01849
ICAM5	-2.0894	0.04897
PLAAT3	-2.0805	0.04897
PLK2	-2.0664	0.01849
TUFT1	-2.0292	0.04139
SLC7A11	-1.9893	0.04139
TXNRD1	-1.9683	0.04897
MAMDC2	-1.9149	0.01849
H2AC6	-1.9121	0.01849
SNHG5	-1.8499	0.01849
KCNE4	-1.8357	0.03161
ATP10D	-1.7977	0.03161
H2BC21	-1.7769	0.01849
MAP1B	-1.6953	0.01849
SCD5	-1.6711	0.01849
PYGL	-1.5402	0.04139

B) UPREGULATED GENES		
Gene name	log2_fold_change	q_value
CPXM1	3.9971	0.01849
FGF18	3.8224	0.01849
TPD52	3.6897	0.04139
SFRP2	3.5564	0.01849
NPNT	3.2493	0.04897
SEMA6D	2.9172	0.01849
MN1	2.8957	0.01849
PRELP	2.5476	0.01849
CXCL12	2.4258	0.01849
SECTM1	2.3600	0.01849
DCN	2.2602	0.03161
CDKN1C	2.2388	0.04897
MYO1F	2.2303	0.01849
LOXL4	2.1731	0.01849
EPHB6	2.1689	0.01849
AUTS2	2.1179	0.04897
COL5A3	2.0959	0.01849
C1R	2.0803	0.01849
NYNRIN	1.9922	0.03161
FHL1	1.9794	0.01849
VSTM4	1.9169	0.04897
TWIST2	1.8679	0.01849
S1PR3	1.8418	0.03161
PODN	1.7458	0.01849

The volcano plot of neuron-enriched cultures (Figure 31A) reveals a distinct discrimination between patients with schizophrenia and healthy controls based on gene expression levels in neurons. In neurons, 44 differentially expressed genes were identified (Table 8), with 24 genes upregulated (red) and 20 downregulated (blue). Notably, the genes represented in this volcano plot in the context of the gene ontology (GO) (Figure 31B) show diverse connections to various neural physiological aspects, with a prominent association with neurodevelopment. These genes are implicated in influencing the development, function, and communication of neurons, as well as playing roles in metabolic and signaling processes crucial for the functioning of the nervous system. The identification of these differentially expressed genes in neuron-enriched cultures

provides valuable insights into potential molecular mechanisms underlying schizophrenia within the neuronal context.

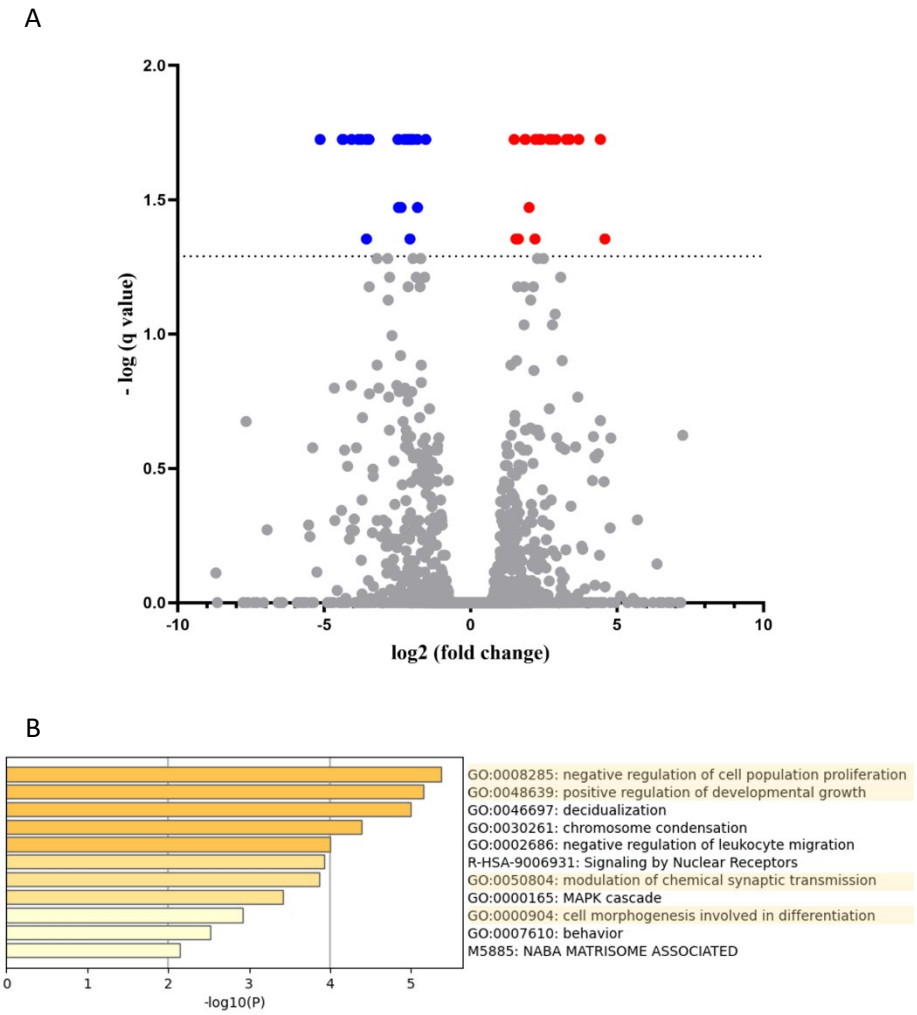

Figure 31: **Differential gene expression in schizophrenia subjects (n=4) vs. controls (n=4) in neuron-enriched culture.** (A) Volcano plot where it is represented the negative of the logarithm in base 10 of the q-value vs. the logarithm in base 2 of FC (fold change; number of times of change). In red or blue, genes differentially expressed up- or down-regulated respectively in patients with schizophrenia vs. controls (adjusted p-value < 0.05;–log (q value) =1.35). (B) Enriched ontologies clusters.

The volcano plot of glia-enriched cultures (Figure 32A) indicates that patients with schizophrenia were discriminated from controls by the gene expression levels in glial cells. In glial cells, 56 differentially expressed genes were found

(Table 9), with 24 genes upregulated (red) and 32 downregulated (blue). Looking at the GO (Figure 32B) these genes are predominantly related to axonogenesis, organization of the extracellular matrix, modulation of synaptic transmission and a negative regulation of cell migration.

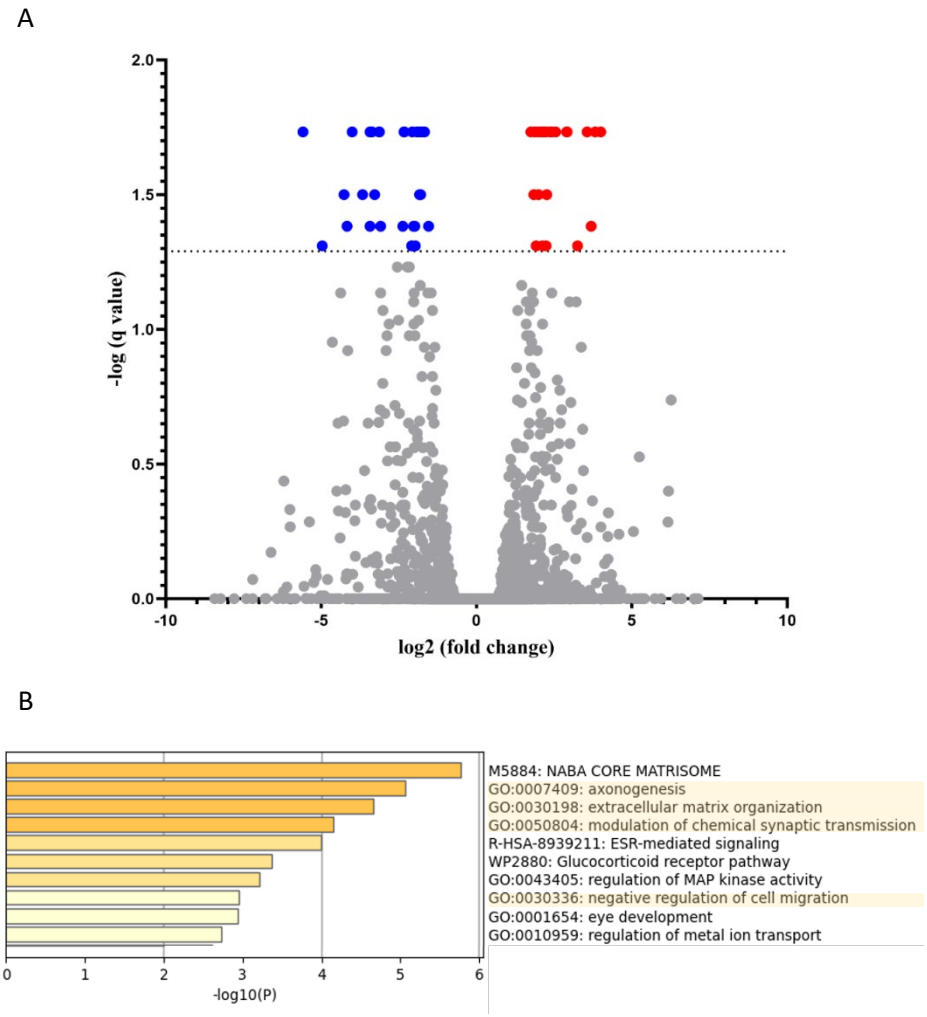

Figure 32: **Differential gene expression in schizophrenia subjects (n=4) vs. controls (n=4) in glia-enriched culture.** Volcano plot where it is represented the negative of the logarithm in base 10 of the unadjusted p-value vs. the logarithm of FC (fold change; number of times of change). In red or blue, genes differentially expressed up- or down-regulated respectively in patients with schizophrenia vs. controls (adjusted p-value < 0.05;–log (q value) =1.35). (B) Enriched ontologies clusters.

4.1.8. Akt/mTOR/S6 pathway quantification in neuron- and glia-enriched cultures

As it has been previously explained, the Akt/mTOR/S6 pathway plays a pivotal role in neurodevelopment and neuroplasticity. Additionally, there is an emerging notion of an altered activity of the Akt/mTOR/S6 pathway in the brain of subjects with schizophrenia. In order to elucidate the status of this signaling pathway in neuron- and glia-enriched cultures from subjects with schizophrenia and their matched controls, the quantification of total proteins and the phosphorylated forms was carried out with different experimental approaches, AlphaLISA® assays (method explained in 3.3.9) and Western Blotting experiments (method explained in 3.3.10).

4.1.8.1. Detection of total proteins and phosphorylated forms by AlphaLISA® assays

4.1.8.1.1. Total Akt protein and phosho(Thr450)-Akt

No significant differences were observed in the Akt protein levels in either the neuron- or glia-enriched cultures between control subjects and schizophrenia patients (Figure 33A). In the same way, no significant differences were found in the levels of the phosphorylated form phospho(Thr450)-Akt in either the neuron- or glia-enriched cultures between control and schizophrenia subjects (Figure 33B). Consequently, no differences were found in the ratio phospho(Thr450)-Akt / Akt between both groups (Figure 33C).

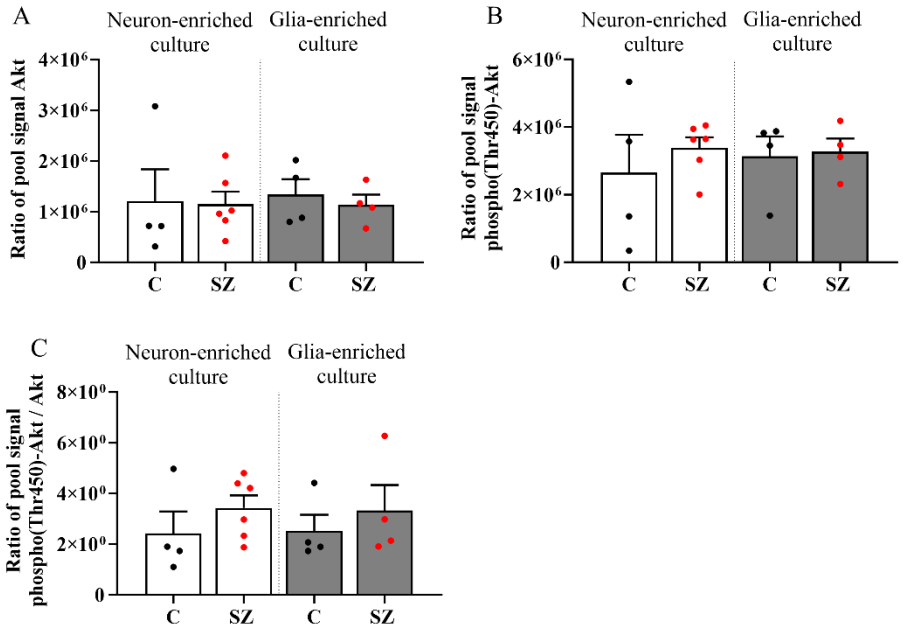

Figure 33: **Relative levels of (A) Akt protein, (B) phospho (Thr450)-Akt and (C) ratio phospho(Thr450)-Akt / Akt in neuron- and glia-enriched cultures in schizophrenia subjects (SZ) and control (C) groups.** Bars represent the mean ± SEM (n=4-6 subjects per group) of the relative levels of total protein and phosphorylated form calculated from the "Alpha counts" signal values and normalized by the value obtained for the sample pool. The results were analyzed by two-tailed unpaired t-test analyzing the difference between schizophrenia and control group both in neuron- or glia-enriched culture.

4.1.8.1.2. Total ERK 1/2 protein and phospho(Tyr202/204)-ERK 1/2

No significant differences were observed in the ERK 1/2 (Figure 34A) or in the phosphorylated form phospho(Tyr202/204)-ERK 1/2 (Figure 34B) protein levels in either the neuron- or glia-enriched cultures between control and schizophrenia subjects. In the same way, no significant differences were found in the ratio phospho(Tyr202/204)-ERK 1/2 / ERK 1/2 between both groups (Figure 34C).

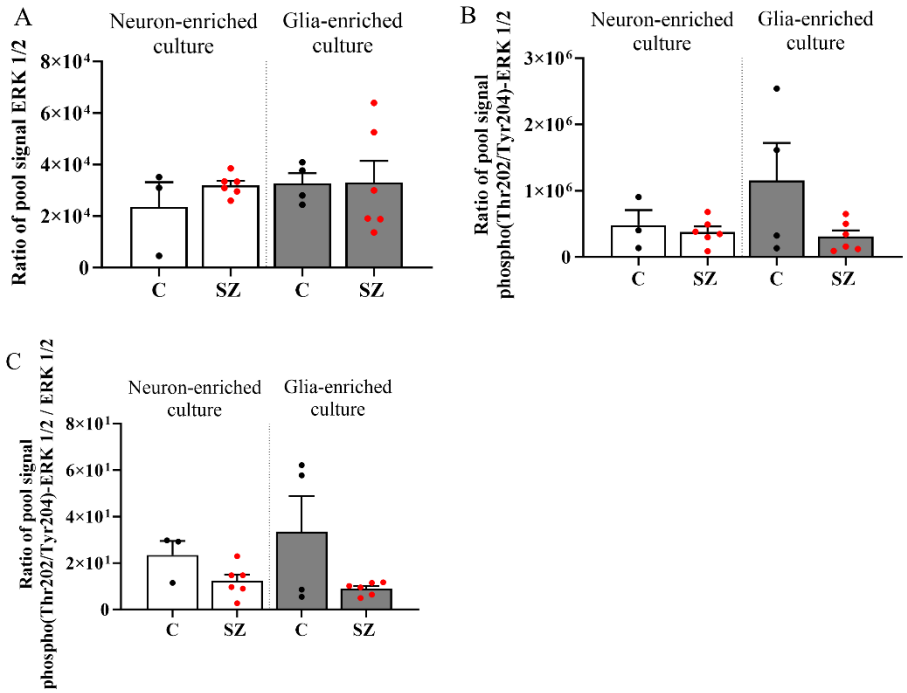

Figure 34: **Relative levels of (A) ERK 1/2 (B) phospho(Tyr202/204)-ERK 1/2 and (C) ratio phospho(Tyr202/204)-ERK 1/2 / ERK 1/2 in neuron- and glia-enriched cultures in schizophrenia subjects (SZ) and control (C) groups.** Bars represent the mean ± SEM (n=3-6 subjects per group) of the relative levels of total protein and phosphorylated form calculated from the "Alpha counts" signal values and normalized by the value obtained for the sample pool. The results were analyzed by two-tailed unpaired t-test analyzing the difference between schizophrenia and control group both in neuron- or glia-enriched culture.

4.1.8.1.3. Total mTOR protein and phospho(Ser2448)-mTOR

No significant differences were found in the mTOR protein levels in either the neuron- or glia-enriched cultures between control and schizophrenia subjects (Figure 35A). In the same way, no significant differences were found in the levels of the phosphorylated form phospho(Ser2448)-mTOR in either the neuron- or glia-enriched cultures between control and schizophrenia subjects (Figure 35B). Consequently, no differences were found in the ratio phospho(Ser2448)-mTOR / mTOR between both groups (Figure 35C).

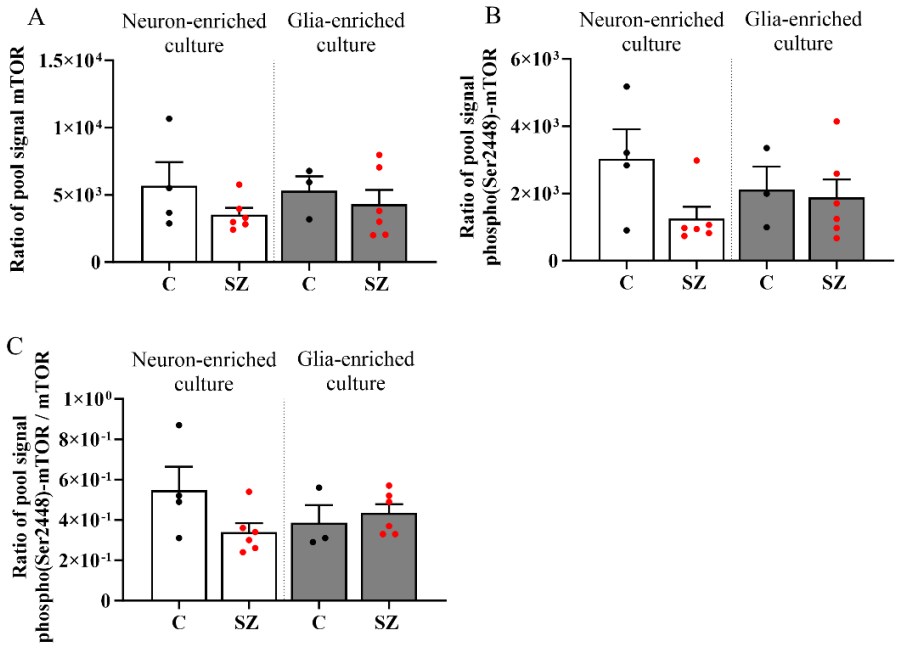

Figure 35: **Relative levels of (A) mTOR protein, (B) phospho(Ser2448)-mTOR and (C) ratio phospho(Ser2448)-mTOR / mTOR in neuron- and glia-enriched cultures in schizophrenia subjects (SZ) and control (C) groups.** Bars represent the mean ± SEM (n=3-6 subjects per group) of the relative levels of total protein and phosphorylated form calculated from the "Alpha counts" signal values and normalized by the value obtained for the sample pool. The results were analyzed by two-tailed unpaired t-test analyzing the difference between schizophrenia and control group both in neuron- or glia-enriched culture.

4.1.8.1.4. Total p70S6K protein and phospho(Thr389)-p70S6K

A significant decrease (-82.37%, $p<0.05$) was found in total p70S6K protein levels in neuron-enriched cultures of subjects with schizophrenia compared with controls (C: 6131 ± 2995; SZ: 1081 ± 115. 9). On the contrary, no differences were observed in glia-enriched cultures (Figure 36A). Moreover, a significant decrease (-64.75%, $p=0.0187$) was observed in the phosphorylated form phospho(Thr389)-p70S6K in neuron-enriched culture of subjects with schizophrenia (C: 339 ± 101.5; SZ: 119.5 ± 15.39), but not in glia-enriched cultures (Figure 36B). Finally, a significant increase (+100%, $p=0.0386$) was observed in the phospho(Thr389)-p70S6K / p70S6K glia-enriched cultures (C: 0.055 ± 0.019; SZ: 0.11 ± 0.013). Conversely, in neuron-enriched culture, an increase was also observed, but it did not reach statistical significance (Figure 36C).

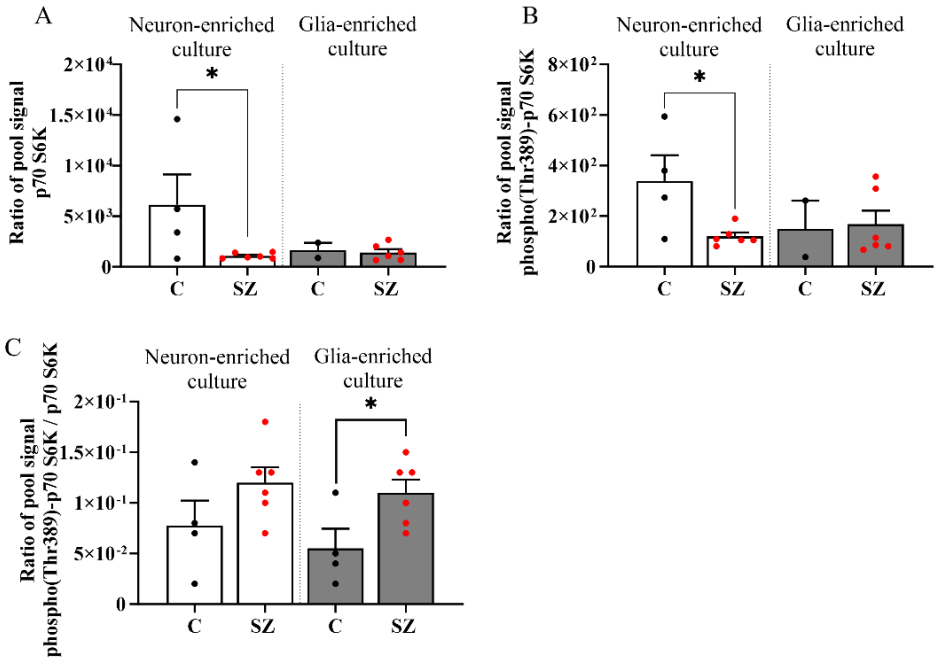

Figure 36: **Relative levels of (A) p70S6K protein, (B) phospho(Thr389)-p70S6K and (C) ratio phospho(Thr389)-p70S6K / p70S6K in neuron- and glia-enriched cultures in schizophrenia subjects (SZ) and control (C) groups.** Bars represent the mean ± SEM (n=3-6 subjects per group) of the relative levels of total protein and phosphorylated form calculated from the "Alpha counts" signal values and normalized by the value obtained for the sample pool. The results were analyzed by two-tailed unpaired t-test analyzing the difference between schizophrenia and control group both in neuron- or glia-enriched culture. *p<0.05.

4.1.8.1.5. Total rpS6 protein and phospho(Ser235/236)-rpS6

A significant increase (+715.16%, p=0.0484) was observed in the rpS6 protein levels in neuron-enriched cultures from subjects with schizophrenia when compared with controls (C: 4122 ± 3267; SZ: 33601 ± 9923) (Figure 37A). However, these differences were not observed in glia-enriched cultures.

In contrast, no significant differences were found in the phosphorylated form phospho(Ser235/236)-rpS6 in either the neuron- or glia-enriched cultures of subjects with schizophrenia compared with their controls (Figure 37B). However, a striking and significant decrease (-94.16, p=0.0067) was observed in the ratio phospho(Ser235/236)-rpS6 / rpS6 in neuron-enriched cultures from subjects with schizophrenia compared to their controls (C: 4.51 ± 1.472; SZ: 0.2633 ± 0.08954) (Figure 37C).

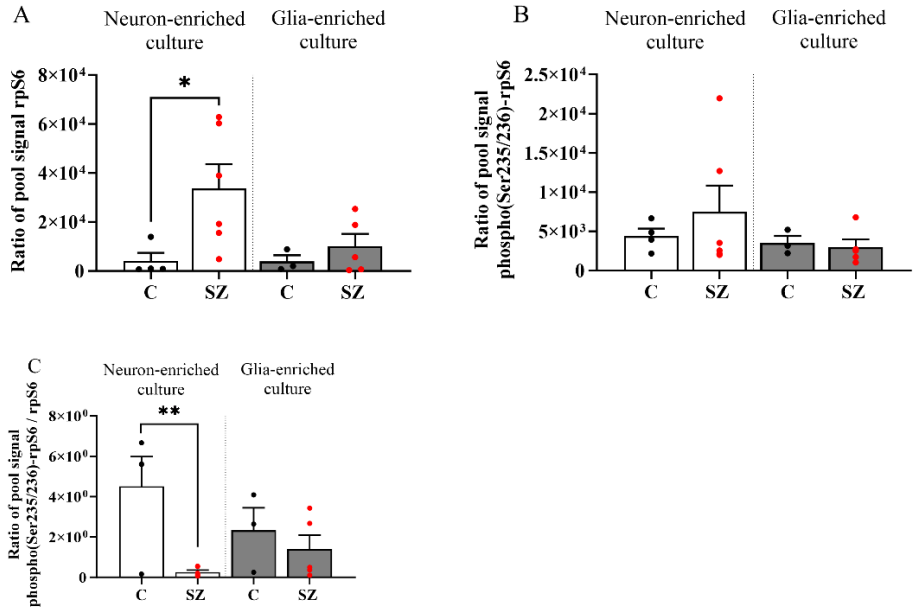

Figure 37: **Relative levels of (A) rpS6 protein, (B) phospho(Ser235/236)-rpS6 and (C) ratio phospho(Ser235/236)-rpS6 / rpS6 in neuron- and glia-enriched cultures in schizophrenia subjects (SZ) and controls (C).** The values shown are the mean ± SEM (n=3-6 subjects per group) of the relative levels of protein and phosphorylated form calculated from the "Alpha counts" signal values and normalized by the value obtained for the sample pool. The results were analyzed by two-tailed unpaired t-test analyzing the difference between schizophrenia and control group both in neuron- or glia-enriched culture. Significance was set at *p<0.05, **p<0.01.

4.1.8.2. Detection of total proteins and phosphorylated forms by Western Blotting

4.1.8.2.1. Housekeeping standardization

Choosing of proper loading control is a crucial issue for the reproducibility of WB experiments. However, recent research has questioned the validity of classical housekeeping proteins, and different factors (i.e. SDS and temperature) has been described to impact results of Ponceau S staining, used as total protein loading control. Moreover, number of assays with the current kind of samples is scarce in the literature. For all these questions, we finally decided to use the mean immunostaining level of three of these housekeepings as normalization factor.

Vinculin, β-actin and GAPDH were chosen between some of the most usual and because their different molecular weights expand through a wide range of protein sizes (117 kDa, 42 kDa and 37 kDa, respectively).

The values obtained for the quantification of vinculin, GAPDH and β-actin protein of neuron- and glia-enriched cultures are displayed in Figure 38 (A and B respectively).

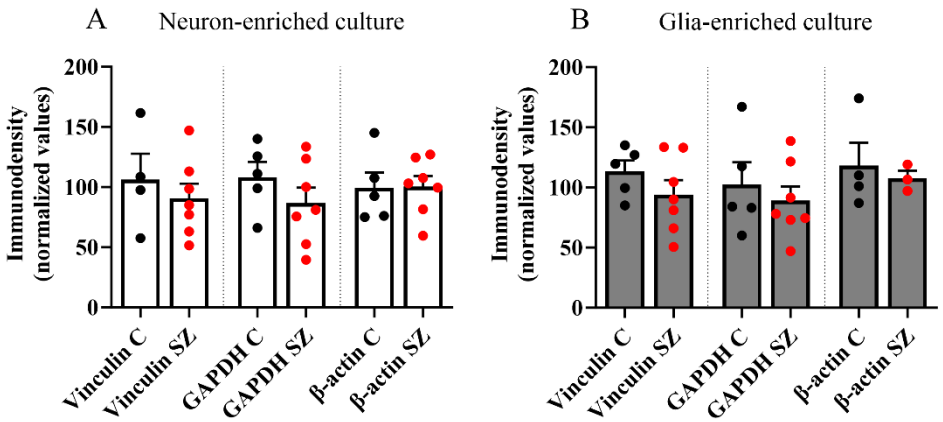

Figure 38: **Immunodensity values for (A) vinculin, GAPDH and β-actin of neuron-enriched culture, (B) vinculin, GAPDH and β-actin of glia-enriched culture in schizophrenia subjects (SZ) and control (C) groups.**

4.1.8.2.2. Total Akt protein and phospho(Ser473)-Akt

The results of the two-tailed unpaired t-test for Akt, phospho(Ser473)-Akt, and the phospho(Ser473)-Akt / Akt ratio are represented in Figure 39.

No significant differences were observed in the Akt protein levels in either the neuron- or glia-enriched cultures between control and schizophrenia subjects (Figure 39A). However a significant increase (+157%, p=0.0234) was observed in the levels of the phosphorylated form phospho(Thr450)-Akt in schizophrenia group of neuron-enriched culture compare to control group (C: 49.77 ± 10.66; SZ: 128.0 ± 24.76) (Figure 39B). No differences were found in the ratio phospho(Thr450)-Akt / Akt between both groups (Figure 39C). Representative image of bands obtained are shown in Figure 39D.

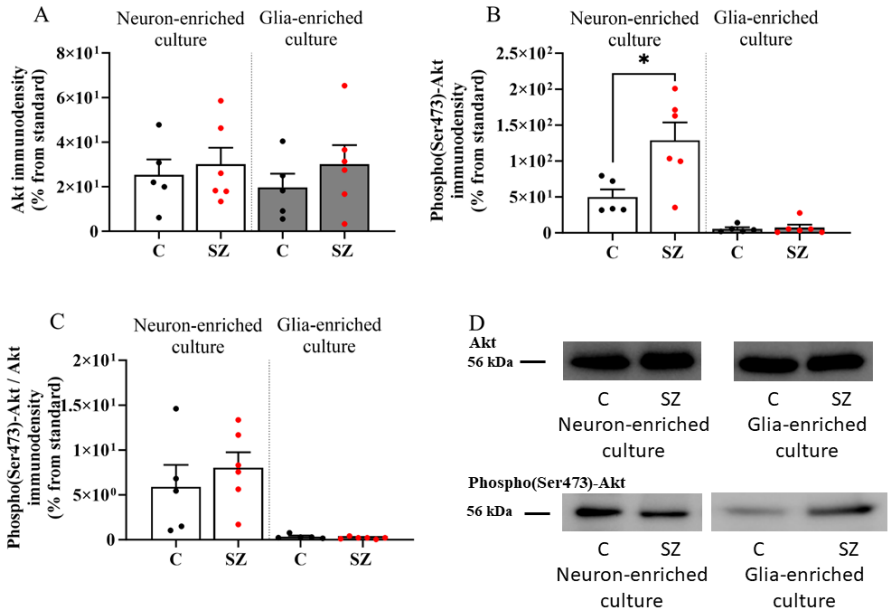

Figure 39: **Immunodensity values for (A) Akt, (B) phospho(Ser473)-Akt and (C) ratio phospho(Ser473)-Akt / Akt in neuron- and glia-enriched cultures in schizophrenia subjects (SZ) and control (C) groups. (D) Representative images of immunoblots.** Immunodensity values were normalized respect to a standard sample (STD) loaded by duplicate into each gel. Bars represent the mean ± SEM (n=5-6 per group) of the individual values depicted in points. The results were analyzed by two-tailed unpaired t-test analyzing the difference between SZ and C group both in neuron- or glia-enriched culture. *p<0.05.

4.1.8.2.3. Total ERK 1/2 protein and phospho(Tyr 202/204)-ERK 1/2

The results of the two-tailed unpaired t-test for ERK 1/2, phospho(Tyr202/204)-ERK 1/2, and the phospho(Tyr202/204)-ERK 1/2 / ERK 1/2 ratio are represented in Figure 40. No significant differences were observed in the ERK 1/2 (Figure 40A) or in the phosphorylated form phospho(Tyr202/204)-ERK 1/2 (Figure 40B) protein levels in either the neuron- or glia-enriched cultures between control and schizophrenia subjects. In the same way, no significant differences were found in the ratio phospho(Tyr202/204)-ERK 1/2 / ERK 1/2 between both groups (Figure 40C). Representative image of bands obtained are shown in Figure 40D.

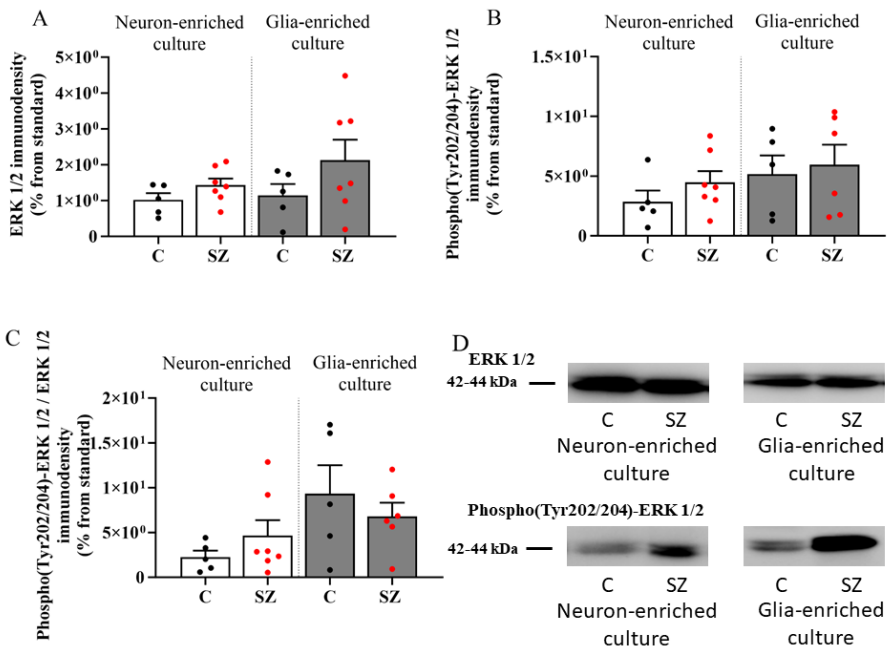

Figure 40: **Immunodensity values for (A) ERK 1/2, (B) phospho(Tyr202/204)-ERK 1/2 and (C) ratio phospho(Tyr202/204)-ERK 1/2 / ERK 1/2 in neuron- and glia-enriched cultures in schizophrenia subjects (SZ) and control (C) groups. (D) Representative images of immunoblots.** Immunodensity values were normalized respect to a standard sample (STD) loaded by duplicate into each gel. Bars represent the mean ± SEM (n=5-7 per group) of the individual values depicted in points. The results were analyzed by two-tailed unpaired t-test analyzing the difference between SZ and C group both in neuron- or glia-enriched culture.

4.1.8.2.4. Total rpS6 protein and phospho(Ser235/236)-rpS6

A significant increase (+132.88%, p=0.0152) was found in total rpS6 protein levels in neuron-enriched cultures of subjects with schizophrenia compared with controls (C: 1.35 ± 0.51; SZ: 3.14 ± 0.35). On the contrary, these differences were not observed in glia-enriched cultures (Figure 41A). Moreover, no significant differences were observed in phospho(Ser235/236)-rpS6 neither in the neuron- or glia-enriched culture of subjects with schizophrenia (Figure 41B). Finally, a significant decrease (-89.33%, p=0.0324) was observed in phospho(Ser235/236)-rpS6 / rpS6 ratio of neuron-enriched cultures (C: 7.43 ± 3.23; SZ: 0.79 ± 0.20). Conversely, in glia-enriched culture, no differences were observed (Figure 41C). Representative image of bands obtained are shown in Figure 41D.

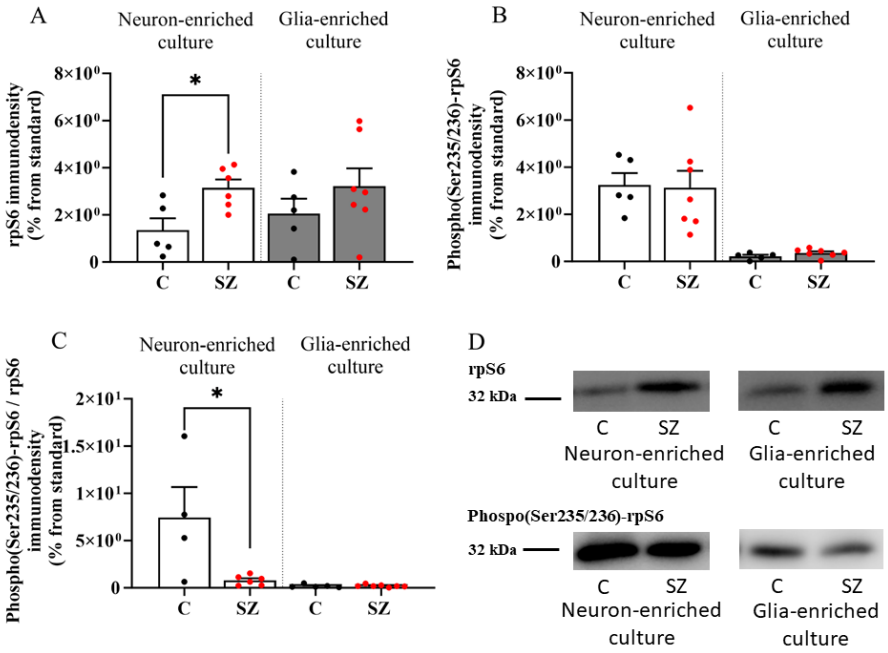

Figure 41: **Immunodensity values for (A) rpS6, (B) phospho(Ser235/236)-rpS6 and (C) ratio phospho(Ser235/236)-rpS6 / rpS6 in neuron- and glia-enriched cultures in schizophrenia subjects (SZ) and control (C) groups. (D) Representative images of immunoblots.** Immunodensity values were normalized respect to a standard sample (STD) loaded by duplicate into each gel. Bars represent the mean ± SEM (n=4-7 per group) of the individual values depicted in points. The results were analyzed by two-tailed unpaired t-test analyzing the difference between SZ and C group both in neuron- or glia-enriched culture.

In summary, the experiments revealed significant differences between controls and individuals with schizophrenia. Firstly, there was a marked reduction in neurospheres self-renewal capacity in schizophrenia patients, evidenced by a notable decrease in both neurospheres number and size compared to controls. Furthermore, variations in gene expression were detected in neuron- and glia-enriched cultures, shedding light on potential molecular mechanisms underlying the disease. Lastly, regarding the study of proteins involved in the Akt/mTOR/S6 pathway, differences were primarily observed in Akt, showing an increase in its phosphorylated form in neuron-enriched cultures of schizophrenia subjects compared to controls. Additionally, a decrease in both total and phosphorylated forms of p70S6K was noted in neuron-enriched cultures of schizophrenia subjects, along with an increase in its ratio in glia-enriched cultures of

schizophrenia subjects compared to controls. Notably, the most pronounced changes were observed in rpS6, with an increase in its total form and a decrease in the ratio in neuron-enriched cultures of schizophrenia subjects compared to controls.

4.2. Study II: Double-hit mouse model combining MIA and THC chronic treatment

4.2.1. Evaluation of the dose-response to Poly(I:C) administration

In order to evaluate the maternal immune response induced by the administration of Poly(I:C), all pregnant dams were monitored for weight and temperature (method explained in 3.3.11).

4.2.1.1. Temperature monitoring

Monitoring of body temperature is represented in Figure 42. The initial body temperature for vehicle treated dams was 38.6 ± 0.5ºC, while for Poly(I:C) treated dams, it was 38.3 ± 0.5ºC. Two-way ANOVA analysis revealed a significant effect of time [F_{Time} (2.596, 33.74) = 9.229, p=0.0002], but not of the Poly(I:C) treatment itself [$F_{Poly(I:C)}$ (1, 13) = 0.08590; p=0.7741]. Moreover, no significant interaction between both time and Poly(I:C) was found [$F_{TimexPoly(I:C)}$ (5, 65) = 0.7377; p=0.5979].

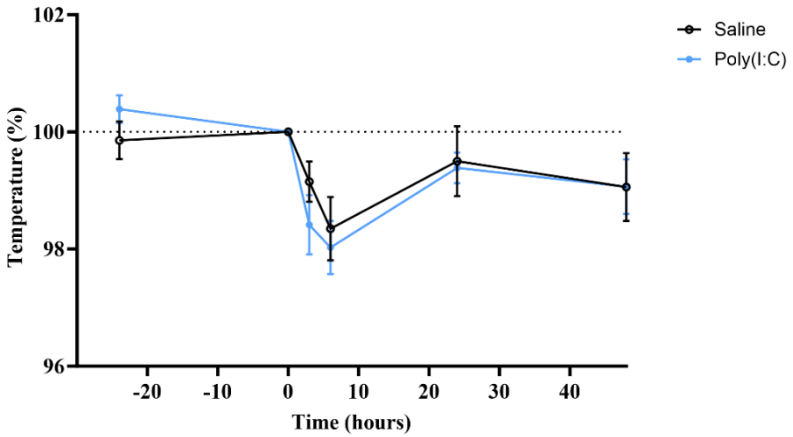

Figure 42: **Measurement of body temperature of pregnant dams exposed to Poly(I:C) or saline.** Body Temperature is expressed as a percentage of the temperature measured at the moment of vehicle/ Poly (I:C) administration (% 0C to 0 h, T0=100%). Control (n= 7) and Poly(I:C) (n= 8) mice are plotted. Results were analyzed by a two-way repeated measures ANOVA followed by Bonferroni's multiple comparison test. Points are representations of the mean ± SEM values.

In the case of saline treated mothers, body temperature decreased over time, reaching a maximum effect 6 h after the administration. However, administration of Poly(I:C) triggered a more pronounced decrease in body temperature 3 and 6 h after administration. Body temperature was recovered 24 h after both Poly(I:C) and saline administration.

4.2.1.2. Weight monitoring

Monitoring of body weight is represented in Figure 43. The initial body weight for saline treated dams was 31.81 ± 2.02 g while for Poly(I:C) treated dams, it was 32.02 ± 2.84 grams. Two-way ANOVA detected a significant effect of the time [F_{Time} (2.60, 31.24) = 46.52, p<0.0001], and of the Poly(I:C) treatment itself [$F_{Poly(I:C)}$ (1, 12)= 14.22, p=0.0027]. Moreover, a significant interaction between both time and Poly(I:C) was found [$F_{TimexPoly(I:C)}$ (5, 60)= 6.09, p=0.0001]. Bonferroni´s post-hoc test showed a significant difference in the % of body weight between saline treated and Poly(I:C) treated dams 3 h (p=0.0011) and 6 h (p=0.0126) after the administration.

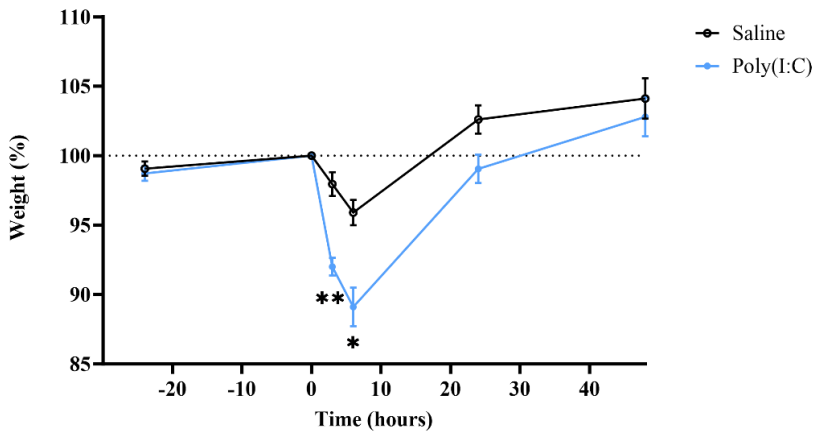

Figure 43: **Measurement of body weight of pregnant dams exposed to Poly(I:C) or saline.** Body weight is expressed as a percentage. Control (n= 7) and Poly(I:C) (n= 7) mice are plotted. Results were analyzed by means of two-way repeated measures ANOVAs followed by Bonferroni's multiple comparison post-hoc test. Points represent mean ± SEM values. *Indicate a significant difference detected by Bonferroni's multiple comparison test in the % of body weight between vehicle treated and Poly(I:C) treated dams at a specific time point. *p<0.05, **p<0.01.

In the case of the weight of pregnant dams treated with saline, a slight decrease in weight was observed at 3 and 6 hours, which may be due to the usual variations in weight during the day. Moreover, this slight decrease was completely recovered 24 hours after saline administration, even with an increase over the initial weight. This is because females in gestation will increase their weight considerably as the pregnancy progresses. In the case of the weight of pregnant dams treated with Poly(I:C), a more pronounced weight loss was observed at 3 hours, which continued until 6 hours after treatment. 24 and 48 hours after Poly(I:C) administration an increase in % of body weight was observed. This is because the effect of the Poly(I:C) administration is transitory and ended 24 h after the Poly(I:C) was administrated. The effect of Poly(I:C) administration on body weight is an indirect measure of the immune response induced by this immunogenic, and Poly(I:C) challenged pregnant dams demonstrate to have a transitory systemic response to this substance.

4.2.1.3. Impact of MIA in pregnancy outcome

To conclude the validation of the effect of Poly(I:C) administration, the number of pups born in each litter (Figure 44). In the case of dams administered with saline, the number of pups born per litter was approximately 11.56 while in the case of dams administered with Poly(I:C) the number of pups born per litter decreased to an average of 5.22 litters. The comparison between Poly(I:C) exposed and saline exposed groups demonstrated a significant decrease (-54.84%, $p<0.0001$) (saline: 11.56 ± 0.41; Poly(I:C): 5.22 ± 1.14). This result highlights a statistically significant difference in pregnancy outcomes between the two groups, suggesting a potential association between Poly(I:C) exposure and altered pregnancy outcomes.

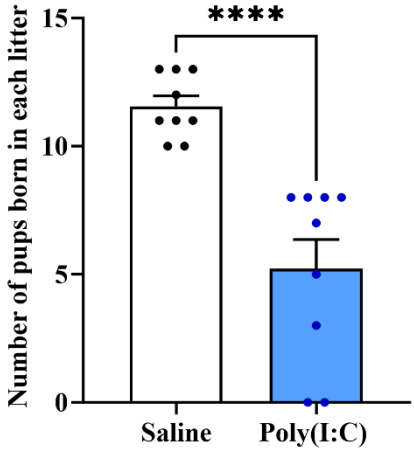

***Figure 44: N*umber of litters of pregnant dams exposed to Poly(I:C) or saline.** Control (n= 9) and Poly(I:C) (n= 9) mice are plotted. Results were analyzed by means of two-tailed unpaired t-test and are represented as mean ± SEM values. ****p<0.0001.

4.2.2. *In vivo* characterization of the double-hit mouse model of MIA and THC chronic treatment

4.2.2.1. Phenotypical evaluation of the double-hit mouse model

4.2.2.1.1. Cognitive evaluation: Novel Object Recognition Test (NORT)

The NORT (method explained in 3.3.12.1) is a widely utilized research tool in studies involving mice and other rodents to assess memory and the ability to recognize novel objects. This test leverages the innate inclination of animals to explore novel objects with greater interest than familiar objects. The primary objective of the NORT is to evaluate short-term memory and recognition abilities in animals, providing valuable insights into their cognitive function and learning capabilities.

In the NORT, the ability of mice to recognize a novel object is interpreted as an indicator of cognitive function and short-term memory. If mice spend more time exploring the novel object compared to the familiar object, it is assumed that they have remembered the familiar object from the training phase and are demonstrating a recognition response.

The Discrimination Index (DI) serves as the main parameter for assessing cognitive impairment in the NORT, where positive DI values indicate good

discrimination between objects. DI was quantified in Poly(I:C) treated male and female mice with or without a chronic treatment with THC during adolescence (Figure 45). Total exploration time was also measured (Figure 46).

The results of the statistical analysis using three-way ANOVA (Table 10) unveiled significant effects of several variables on the observed outcomes separately on from each other. Specifically, Poly(I:C) administration exhibited a statistically significant influence in the DI, [$F_{Poly(I:C)}$ (1, 76) = 10.03, p=0.0022] producing a significant decrease (-48.88%, p=0.0022) in Poly(I:C) group when comparing to saline group (saline: 0.32 ± 0.04; Poly(I:C): 0.17 ± 0.04). Similarly, the variable sex displayed a noteworthy impact [F_{sex} (1, 76) = 4.287, p=0.0418] producing a significant decrease (-37.93%, p=0.0418) in DI of male mice comparing with female mice (male: 0.18 ± 0.04; female: 0.29 ± 0.04). Finally, the variable THC demonstrated a highly significant effect [F_{THC} (1, 76) = 36.90, p<0.0001], explaining a significant decrease (-76.32%, p<0.0001) in THC group comparing with vehicle group (vehicle: 0.38 ± 0.03; THC: 0.09 ± 0.04). These findings provide a comprehensive understanding of the factors influencing cognitive performance in the NORT paradigm.

Table 10: **Results of the three-way ANOVA analysis evaluating the effect of Poly(I:C), sex and THC in discrimination index in NORT.** Three-way ANOVA analysis conducted in order to evaluate the effect of Poly(I:C), sex, THC and their interactions on the NORT discrimination index (DI).

Three-way ANOVA parameters for discrimination index	
Poly(I:C)	**F (1, 76) = 10.03, p=0.0022**
Sex	**F (1, 76) = 4.29, p=0.0418**
THC	**F (1, 76) = 36.90, p<0.0001**
Poly(I:C) x Sex	F (1, 76) = 0.55, p=0.4615
Poly(I:C) x THC	F (1, 76) = 0.55, p=0.4621
Sex x THC	F (1, 76) = 0.14, p=0.7114
Poly(I:C) x Sex x THC	F (1, 76) = 0.34, p=0.5614

However, when assessing interactions between these variables, no significant effects were observed for the interactions Poly(I:C) x sex, Poly(I:C) x THC, sex x THC, and Poly(I:C) x sex x THC. These findings suggest that while individual factors such as Poly(I:C), sex, and THC play a significant role in influencing the observed outcomes, the combination of various factors does not seem to enhance the individual effect of each of them.

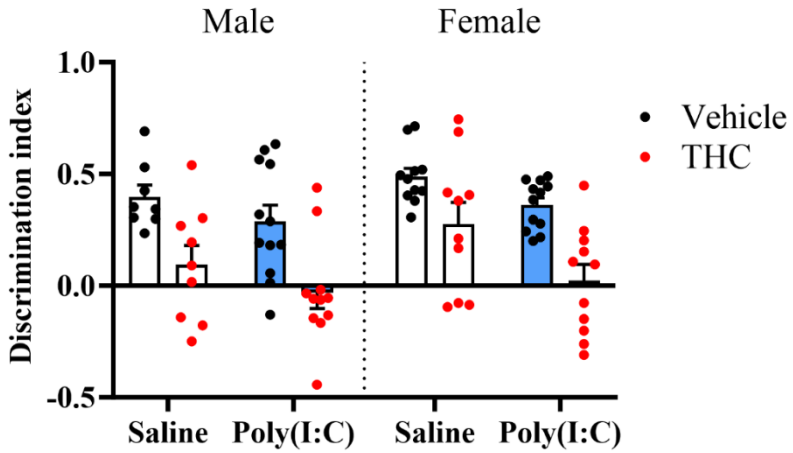

Figure 45: **Graphical representation of the Discrimination Index (DI) in the NORT.** Individual DI values of male and female mice of the four experimental groups (saline/vehicle, saline/THC, Poly(I:C)/vehicle and Poly(I:C)/THC) are plotted. Bars represent mean ± SEM values (n=8-12 subjects per group). Data were analyzed using three-way ANOVA followed by Bonferroni's multiple comparisons test. Results are shown in Table 10.

On the other hand, regarding total exploration time, results of the three-way ANOVA (Table 11), revealed significant influences of certain variables together with their interactions. First, the variable sex showed a remarkable impact [F_{sex} (1, 78) = 30.71, p<0.0001] resulting in a significant decrease (-46.54%, p<0.0001) in the exploration time of males compared to females (male: 38.29 ± 3.39; female: 71.62 ± 5.02). The interaction between Poly(I:C) and THC [$F_{Poly(I:C)xTHC}$ (1, 78) = 4.050, p=0.0476] was also statistically significant although after Bonferroni´s post-hoc test there were no significant differences among groups. Finally, the main effects of Poly(I:C) and THC, as well as the interactions Poly(I:C) x sex, sex x THC, and Poly(I:C) x sex x THC, were not statistically significant.

Table 11: **Results of the three-way ANOVA analysis evaluating the effect of Poly(I:C), sex and THC in total exploration time in NORT.** Three-way ANOVA analysis conducted in order to evaluate the effect of Poly(I:C), sex, THC and their interactions in the NORT total exploration time.

Three-way ANOVA parameters for total exploration time	
Poly(I:C)	F (1, 78) = 0.64, p=0.4251
Sex	**F (1, 78) = 30.71, p<0.0001**
THC	F (1, 78) = 0.21, p=0.6459
Poly(I:C) x Sex	F (1, 78) = 0.01, p=0.9282
Poly(I:C) x THC	**F (1, 78) = 4.05, p=0.0476**
Sex x THC	F (1, 78) = 0.86, p=0.3553
Poly(I:C) x Sex x THC	F (1, 78) = 0.67, p=0.4144

While the variable sex as well as the interaction between Poly(I:C) and THC emerged as influential factors, other factors and interactions did not exhibit discernible impacts. These findings underscore the multifaceted nature of the disease, where sex plays a substantial role, and the interaction between particular components can contribute to varying outcomes.

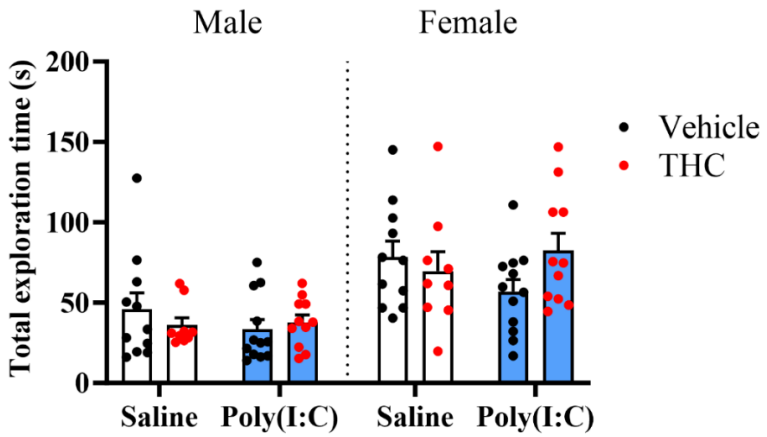

Figure 46: **Graphical representation of the total exploration time in the NORT.** Individual values of male and female mice of the four experimental groups (saline/vehicle, saline/THC, Poly(I:C)/vehicle and Poly(I:C)/THC) are plotted. Bars represent mean ± SEM values (n=9-12 subjects per group). Data were analyzed using three-way ANOVA followed by Bonferroni's multiple comparisons test.

4.2.2.1.2. Sensorimotor gating evaluation: Pre-pulse Inhibition (PPI)

PPI (method explained in 3.3.12.2) is a behavioral test commonly employed in rodent models, including mice, to investigate sensorimotor gating deficits often associated with schizophrenia. PPI measures the reduction in the startle response when a weak non-startling stimulus (pre-pulse) is presented shortly before a strong startling stimulus (pulse). This phenomenon reflects the brain's ability to filter and inhibit irrelevant sensory information, a process impaired in individuals with schizophrenia. The inhibition of the startle response (% PPI) by each pre-pulse intensity was statistically analyzed by three-way ANOVA (Table 12). The % PPI in every pre-pulse-pulse trial was calculated and is represented in Figure 47. Increasing the intensity of the pre-pulse (77-87 dB) is expected to increase PPI, which is consistent with the overall behavior in all experimental groups.

Table 12: **Results of the three-way ANOVA analysis evaluating the effect of Poly(I:C), sex and THC in % PPI response.** Summary of three-way repeated measures ANOVA analysis performed to test the effects of THC, Poly(I:C) and sex as well as the potential interactions in % PPI at 77, 82 and 87 dB.

Three-way ANOVA parameters for prepulse inhibition test			
	77 dB	**82 dB**	**87 dB**
Poly(I:C)	F (1, 61) = 2.68, p=0.1066	**F (1, 61) = 6.09, p=0.0165**	**F (1, 61) = 11.11, p=0.0015**
Sex	F (1, 61) = 2.23, p=0.1403	F (1, 61) = 2.44, p=0.1235	F (1, 61) = 0.28, p=0.5956
THC	F (1, 61) = 0.03, p=0.8718	F (1, 61) = 0.63, p=0.4320	F (1, 61) = 0.30, p=0.5841
Poly(I:C) x Sex	F (1, 61) = 0.02, p=0.9027	F (1, 61) = 0.47, p=0.4955	F (1, 61) = 1.32, p=0.2549
Poly(I:C) x THC	F (1, 61) = 0.31, p=0.5797	F (1, 61) = 0.73, p=0.3976	**F (1, 61) = 5.69, p=0.0202**
Sex x THC	F (1, 61) = 0.41, p=0.5256	F (1, 61) = 0.60, p=0.4102	F (1, 61) = 2.14, p=0.1488
Poly(I:C) x Sex x THC	F (1, 61) = 0.01, p=0.9852	F (1, 61) = 1.00, p=0.3206	F (1, 61) = 3.52, p=0.0653

The results of the three-way ANOVA analysis showed that in 77 dB none of the evaluated variables, including Poly(I:C), sex and THC, as well as their interactions, showed statistically significant effects.

On the other hand, the data of 82 dB indicate that the variable Poly(I:C) had a statistically significant effect producing a significant decrease (-32.48%,

p=0.0165) in Poly(I:C) group comparing with saline group (saline: 42.91 ± 4.67; Poly(I:C): 28.97 ± 4.08) [$F_{Poly(I:C)}$ (1, 61) = 6.085, p=0.0165]. However, none of the other variables or interactions, including sex, THC, and their combinations, showed significant effects on the observed phenomenon. Therefore, while Poly(I:C) demonstrated significance, the other variables and interactions did not exhibit significant effect or interaction.

Finally, results of the three-way ANOVA analysis in 87 dB show that Poly(I:C) induced a significant decrease (-61.52%, p=0.0015) of the total variation [$F_{Poly(I:C)}$ (1, 61) = 11.11, p=0.0015] comparing with saline group (saline: 63.95 ± 4.32; Poly(I:C): 24.61 ± 7.07). Additionally, the interaction Poly(I:C) x THC [$F_{Poly(I:C)xTHC}$ (1, 61) = 5.688, p=0.0202] was found to produce a significant influence regardless of sex when comparing saline/vehicle mice with Poly(I:C)/vehicle mice, indicating a potential link between prenatal immune activation and cannabis exposure in the context of schizophrenia. Bonferroni´s post-hoc test showed a significant decrease (-60.02%, p=0.0042) in % PPI in 87dB between saline/vehicle and Poly(I:C)/vehicle groups (saline/vehicle: 61.55 ± 4.14; Poly(I:C)/vehicle: 24.61 ± 7.07). However, the main effects of sex, THC, and other interactions, including Poly(I:C) x sex, sex x THC, and Poly(I:C) x sex x THC, did not reach statistical significance.

In summary, these findings suggest that prenatal immune activation, represented by Poly(I:C), may play a significant role in the susceptibility to schizophrenia or, at least in cognitive sensorimotor gating. Furthermore, the interaction with "THC" implies that environmental factors, such as cannabis exposure, may interact with prenatal immune activation to influence the development of the disorder.

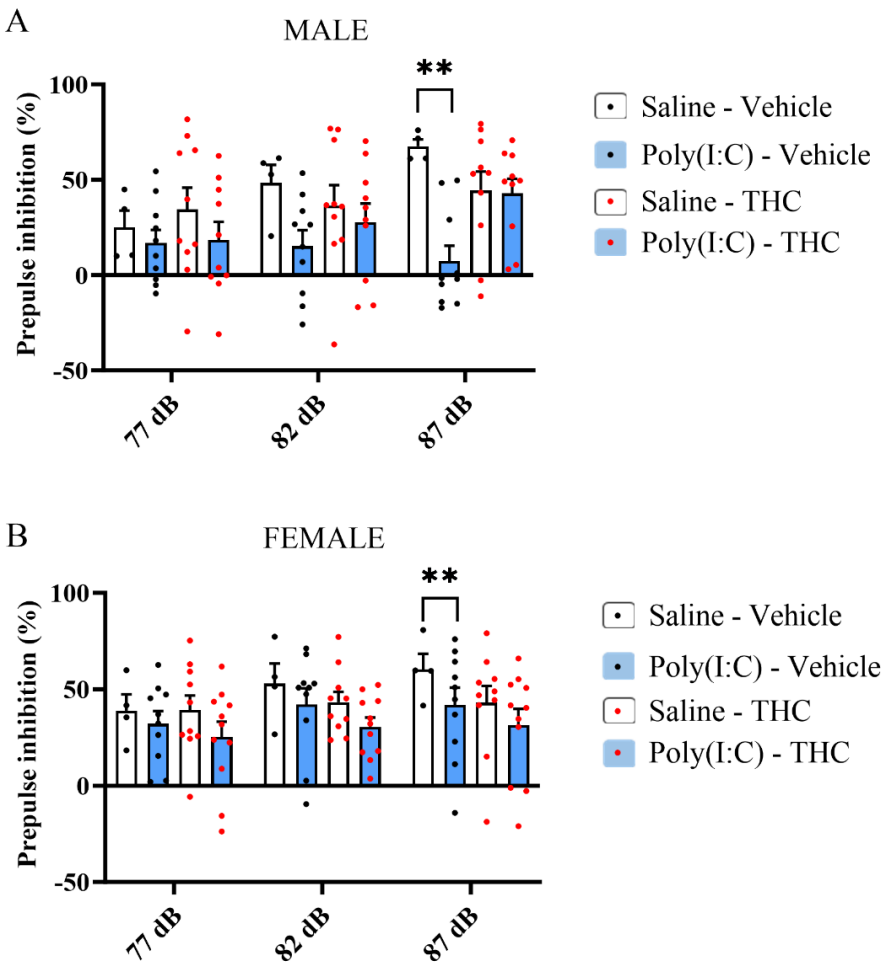

Figure 47: **Graphical representation of the % PPI at 77, 82 and 87dB in males (A) and females (B).** Individual values of male and female mice of the four experimental groups (saline/vehicle, saline/THC, Poly(I:C)/vehicle and Poly(I:C)/THC) are plotted. Bars represent mean ± SEM values (n=4-11 subjects per group for females and n=4-10 subjects per group for males). Data were analyzed using three-way ANOVA followed by Bonferroni's multiple comparisons test. **p<0.01

4.2.3. Whole transcriptomic analysis of double-hit mouse model

Schizophrenia is a complex and multifactorial mental disorder involving a genetic and environmental interplay. While several genes have been identified that may be related to schizophrenia, it is important to note that there is no single "causative" gene for the illness, and genetic predisposition is just one of the contributing factors.

4.2.3.1. Differential gene expression in Poly(I:C)/vehicle vs. saline/vehicle mice.

Differential expression analysis (method explained in 3.3.7) was performed to elucidate the altered expression of genes in the Poly(I:C) treated mice group compared with controls. In males, 227 differentially expressed genes were identified, with 84 genes upregulated and 143 downregulated. In females, 489 differentially expressed genes were found, with 150 genes upregulated and 339 downregulated. The volcano plots indicate that mice which came from a dump treated with Poly(I:C) were discriminated from controls by the gene expression levels in both males (Figure 48A) and females (Figure 48B). In the GO analysis (Figure 48C), it is observed that genes within the Poly(I:C) group, compared to the saline/vehicle group, exhibit alterations closely associated with behavior, signaling by GPCRs, modulation of learning through chemical transmission, and the neuronal system. These findings shed light on the potential regulatory roles of these genes in fundamental neural processes, offering insights into both physiological and pathological conditions of the nervous system.

A

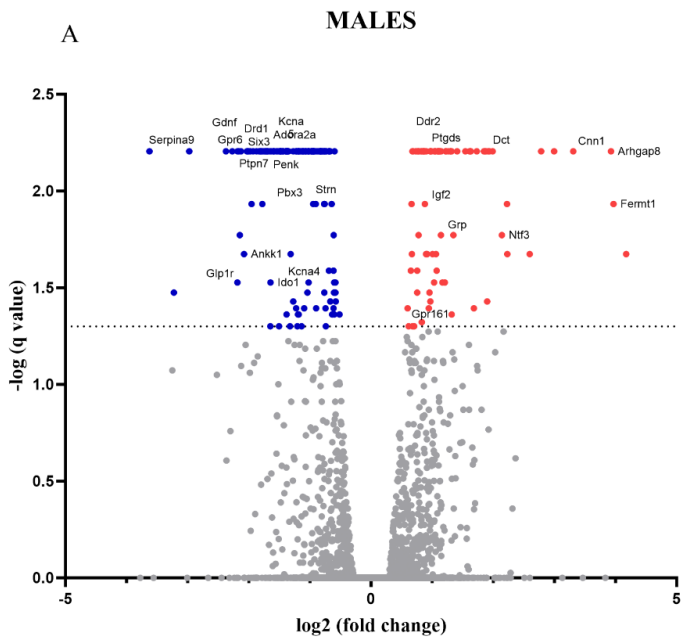

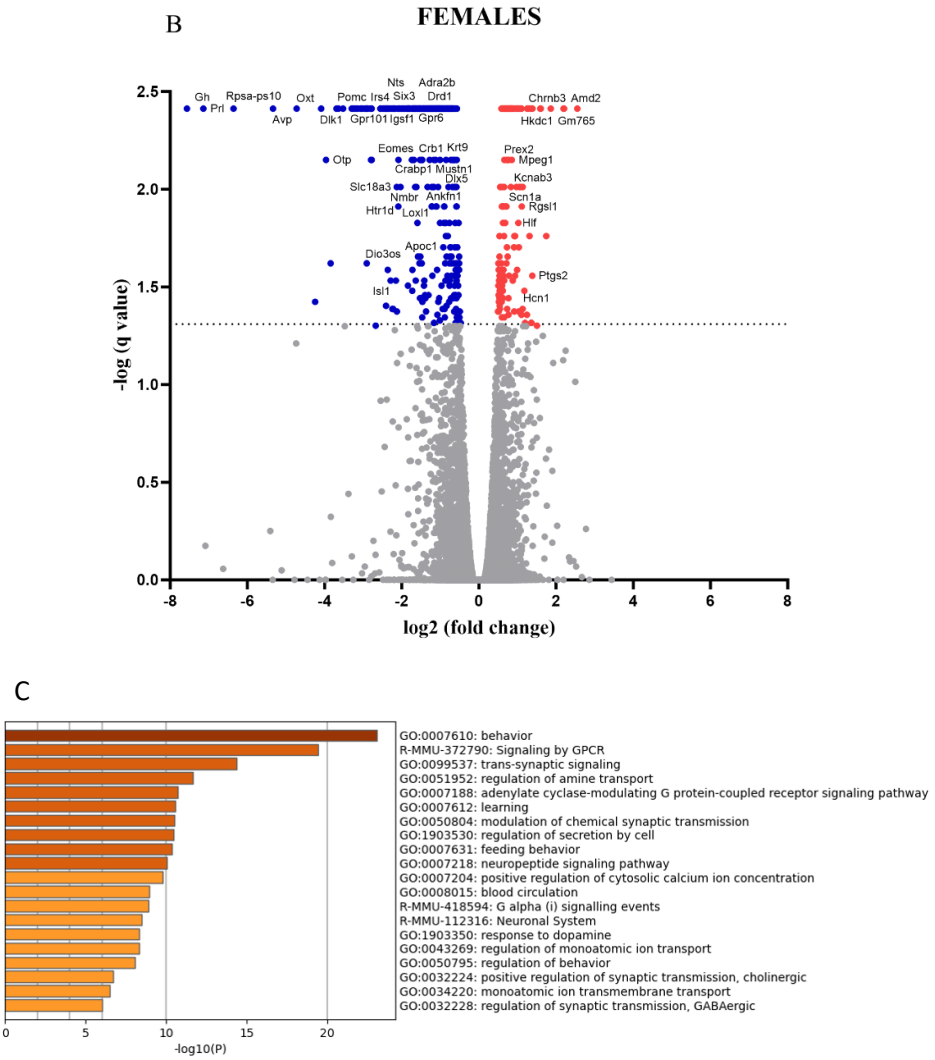

Figure 48: **Effect of Poly(I:C) in differential gene expression of (A) male (n=3) and (B) female (n=3) mice. (C) Enriched ontologies clusters.** Volcano plot where it is represented the negative of the logarithm in base 10 of the q-value vs. the logarithm in base 2 of FC (fold change; number of times of change). In red or blue, genes differentially expressed up- or down-regulated, respectively (adjusted p-value < 0.05;–log (q value)=1.35). The genes named in the volcano plot are the most relevant ones associated with crucial ontologies in schizophrenia. Enriched ontologies where an enrichment analysis is shown on sets of genes of Poly(I:C) group compared saline/vehicle mice group.

These results show differences in the analysis of gene expression responses to Poly(I:C) treatment in mice relative to control groups. Firstly, the most prominent distinction lies in the varying number of genes displaying differential expression

between the two sexes (227 in males compared to 489 in females). This dissimilarity may arise from variations in the response to Poly(I:C) between males and females or differences in the sensitivity of gene detection in both sexes. Another noteworthy difference is the distribution of regulated genes with regard to upregulation and downregulation. In both sexes, more genes are downregulated than upregulated. However, the proportions of upregulated and downregulated genes differ between males and females, possibly reflecting variations in the biological response.

4.2.3.2. Differential gene expression in saline/THC vs. saline/vehicle mice.

Differential expression analysis was performed to elucidate the altered expression of genes in the group of mice treated with chronic THC compared with controls. Among males, we identified 507 genes displaying differential expression, comprising 238 upregulated and 269 downregulated genes. In females, we detected 186 genes with altered expression, including 38 upregulated and 148 downregulated genes. The visual representation in the form of a volcano plot underscores the distinctive gene expression patterns in both male (Figure 49A) and female (Figure 49B) mice treated with chronic THC, effectively distinguishing them from the control group. In the GO analysis, it is evident that genes from the THC group, in comparison to the saline/vehicle group, display alterations associated with behavior, signaling by GPCRs, regulation of neurotransmitter levels, modulation of chemical synaptic transmission, and the neuroanatomical system. These observations suggest a potential influence of THC-related genetic activity on various aspects of neural function.

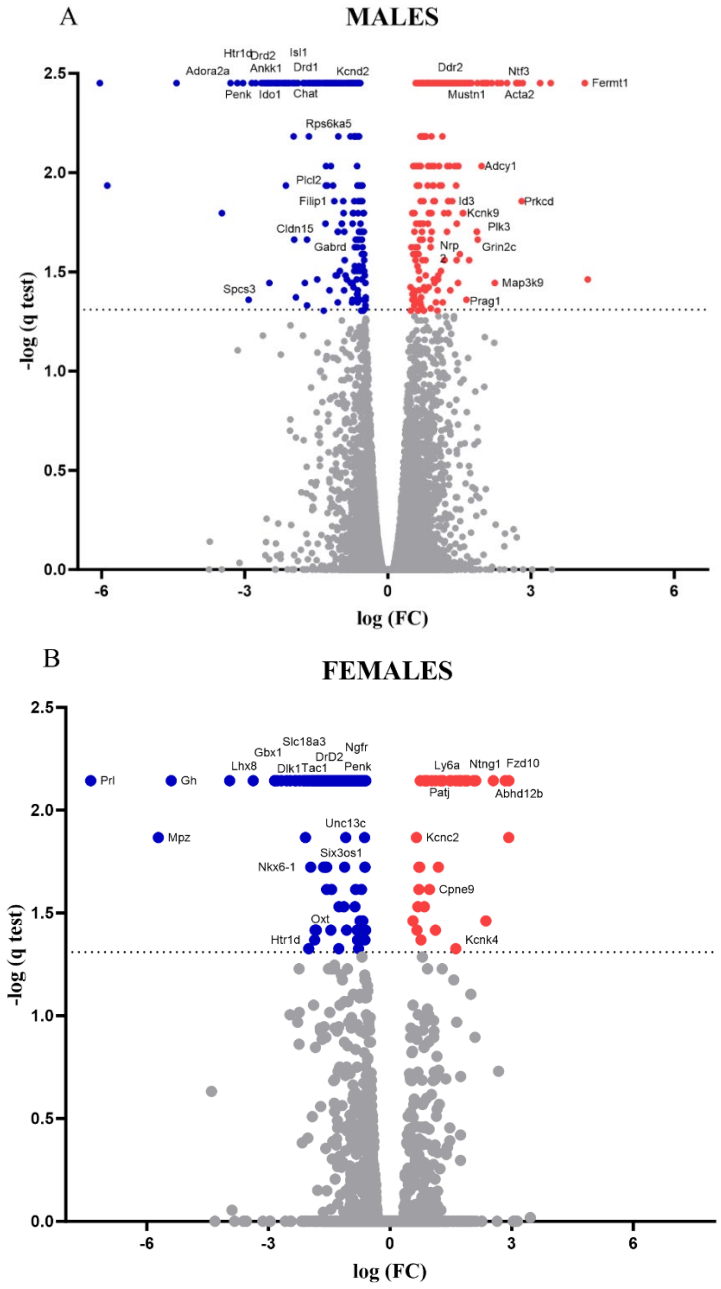
A
MALES
Htr1d
Drd2
Isl1
Adora2a
Ankk1
Drd1
Kcnd2
Ddr2
Ntf3
Fermt1
Penk
Ido1
Chat
Mustn1
Acta2
Rps6ka5
Adcy1
Plcl2
Filip1
Id3
Prkcd
Kcnk9
Cldn15
Plk3
Gabrd
Nrp
Grin2c
Map3k9
Spcs3
Prag1
-log (q test)
log (FC)
B
FEMALES
Slc18a3
Ngfr
Gbx1
DrD2
Lhx8
Dlk1Tac1
Penk
Ly6a
Ntng1
Fzd10
Prl
Gh
Patj
Abhd12b
Unc13c
Mpz
Kcnc2
Six3os1
Nkx6-1
Cpne9
Oxt
Htr1d
Kcnk4
-log (q test)
log (FC)

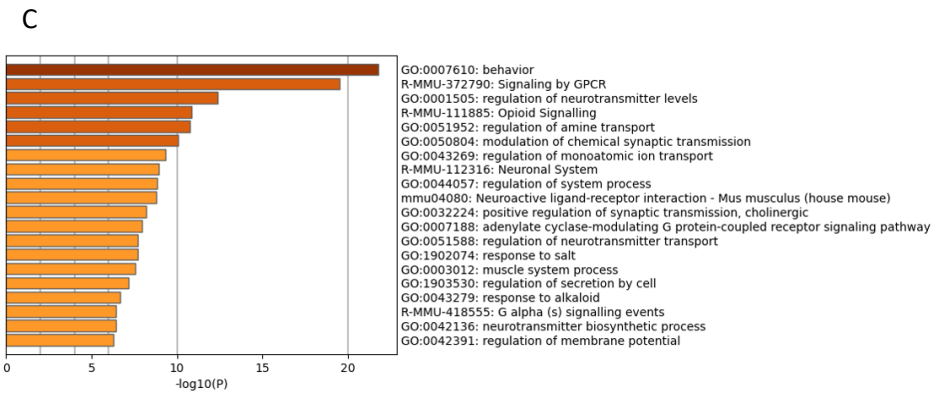

Figure 49: **Effect of THC in differential gene expression of (A) male (n=3) and (B) female (n=3) mice. (C) Enriched ontologies clusters.** Volcano plot where it is represented the negative of the logarithm in base 10 of the q-value vs. the logarithm in base 2 of FC (fold change; number of times of change). In red or blue, genes differentially expressed up- or down-regulated, respectively (adjusted p-value < 0.05;–log (q value)=1.35).The genes named in the volcano plot are the most relevant ones associated with crucial ontologies in schizophrenia. Enriched ontologies where an enrichment analysis is shown on sets of genes of Poly(I:C) group compared saline/vehicle mice group.

These findings reveal variations in the analysis of gene expression responses to THC treatment in mice compared to control groups. Firstly, a notable variance in the number of genes exhibiting differential expression emerges between the two sexes with 507 genes in males compared to 186 in females. This dissimilarity may arise from variations in the response to THC chronic effect between males and females. Another noteworthy difference is the distribution of regulated genes concerning upregulation and downregulation. In both sexes, a greater number of genes are downregulated than upregulated, with a striking difference in females (38 upregulated genes as opposed to 148 downregulated genes). Furthermore, it is evident that when considering the impact of THC in isolation, more genes are altered than when solely examining the Poly(I:C) factor in males. Conversely, in females, a greater number of genes are affected by the Poly(I:C) factor alone as compared to the THC factor alone. This suggests that, in females, the Poly(I:C) factor elicits more pronounced effects than in males, while in males, the THC factor is responsible for the more prominent effects.

4.2.3.3. Differential gene expression in Poly(I:C)/THC vs. Poly(I:C)/vehicle mice.

Differential expression analysis was conducted to unveil gene expression alterations in the double-hit mouse model (Poly(I:C) + THC) in comparison to the Poly(I:C) group. In males, we identified 634 differentially expressed genes, comprising 333 upregulated and 301 downregulated genes. Among females, 238 differentially expressed genes were observed, with 173 genes displaying upregulation and 65 showing downregulation.

Volcano plot exemplifies the discrimination of mice receiving a combination of Poly(I:C) and chronic THC treatment from the Poly(I:C)/vehicle group both in males (Figure 50A) and females (Figure 50B). In scrutinizing the GO data (Figure 50C), differences emerge between the genetic profiles of the Poly(I:C) group and those of the Poly(I:C)/THC group. Notably, alterations associated with behavior, trans-synaptic signaling, neurotransmitter transport, learning or memory processes, neuronal system function, and the intricate development of neuron projections are shown. These observations suggest that exposure to Poly(I:C), along with potential THC influence, may intricately modulate neural functionality and structural maturation.

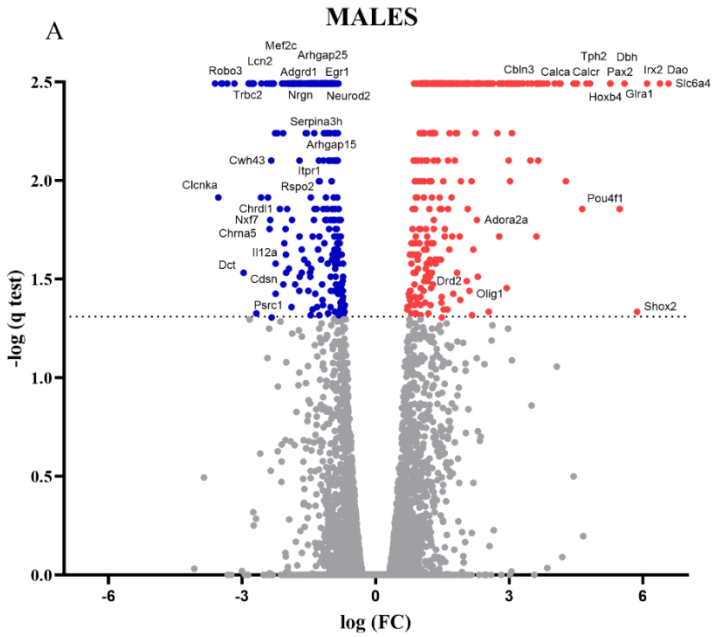

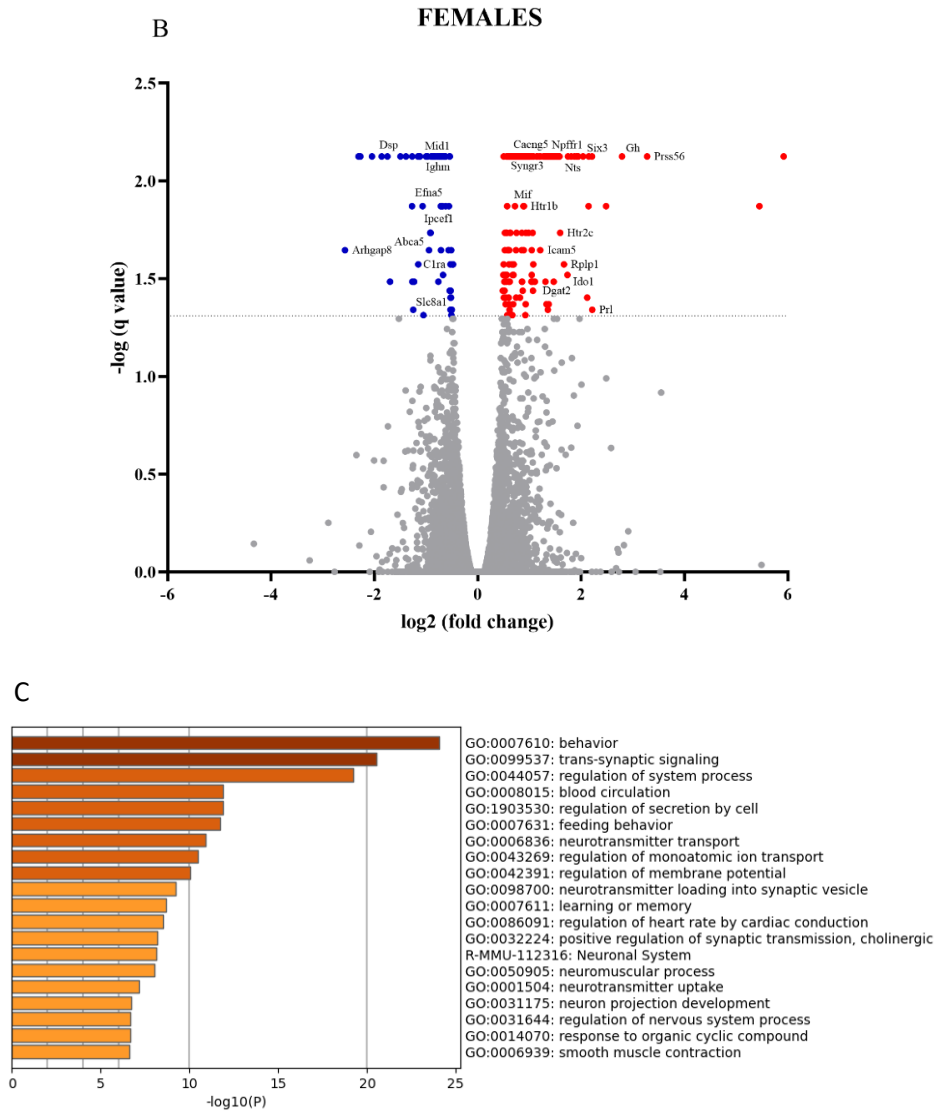

Figure 50: **Effect of Poly(I:C)/THC vs. Poly(I:C)/vehicle in differential gene expression of (A) male (n=3) and (B) female (n=3) mice. (C) Enriched ontologies clusters.** Volcano plot where it is represented the negative of the logarithm in base 10 of the q-value vs. the logarithm in base 2 of FC (fold change; number of times of change). In red or blue, genes differentially expressed up- or down-regulated, respectively (adjusted p-value < 0.05;–log (q value)=1.35). The genes named in the volcano plot are the most relevant ones associated with crucial ontologies in schizophrenia. Enriched ontologies where an enrichment analysis is shown on sets of genes of Poly(I:C) group compared saline/vehicle mice group.

In this case, the study involves a double-hit mouse model, combining Poly(I:C) and THC treatments which differs from the prior examples that singularly investigated either Poly(I:C) or THC treatment. The combination of these two treatments can have unique effects on gene expression compared to individual treatments. Firstly, there is a higher number of differentially expressed genes in males (634 genes) compared to the Poly(I:C) treatment alone (227 genes). This could be due to a synergistic or additive effect of the combined treatments on gene expression. However, in the case of females, this synergistic effect is not as pronounced. Instead, they exhibit a lower number of differentially expressed genes in the double-hit mouse model (238 genes) compared to the Poly(I:C) treatment alone (489 genes). In this case, the synergistic effect of Poly(I:C) plus THC is not observed.

Finally, the balance between upregulated and downregulated genes varies between sexes within the double-hit mouse model. Notably, both males and females show a higher prevalence of upregulated genes, but males, in particular, display a more significant number of upregulated genes. In contrast, females have fewer downregulated genes in the double-hit mouse model. This variation may stem from the unique interactions between Poly(I:C) and THC in females, giving rise to distinct gene expression patterns.

4.2.3.4. Differential gene expression in Poly(I:C)/THC vs. saline/THC mice.

Differential expression analysis was performed to elucidate the altered expression of genes in the double-hit mouse model (Poly(I:C) + THC) compared with THC group. In males, 958 differentially expressed genes were identified, with 522 genes upregulated and 436 downregulated. Among females, 156 differentially expressed genes were found, with 95 genes upregulated and 61 downregulated. Volcano plot exemplifies the discrimination of mice receiving a combination of Poly(I:C) and chronic THC treatment from the saline/THC mice, both in males (Figure 51A) and females (Figure 51B). In the analysis of the GO (Figure 51C), it becomes apparent that genes in the THC group, in contrast to those in the Poly(I:C)/THC group, demonstrate notable changes linked to

behavior, learning and memory functions, the neuronal system, and synaptic transmission, particularly within the dopaminergic pathway. These discoveries highlight the complex relationship between exposure to Poly(I:C), the influence of THC, and the modulation of critical neural functions.

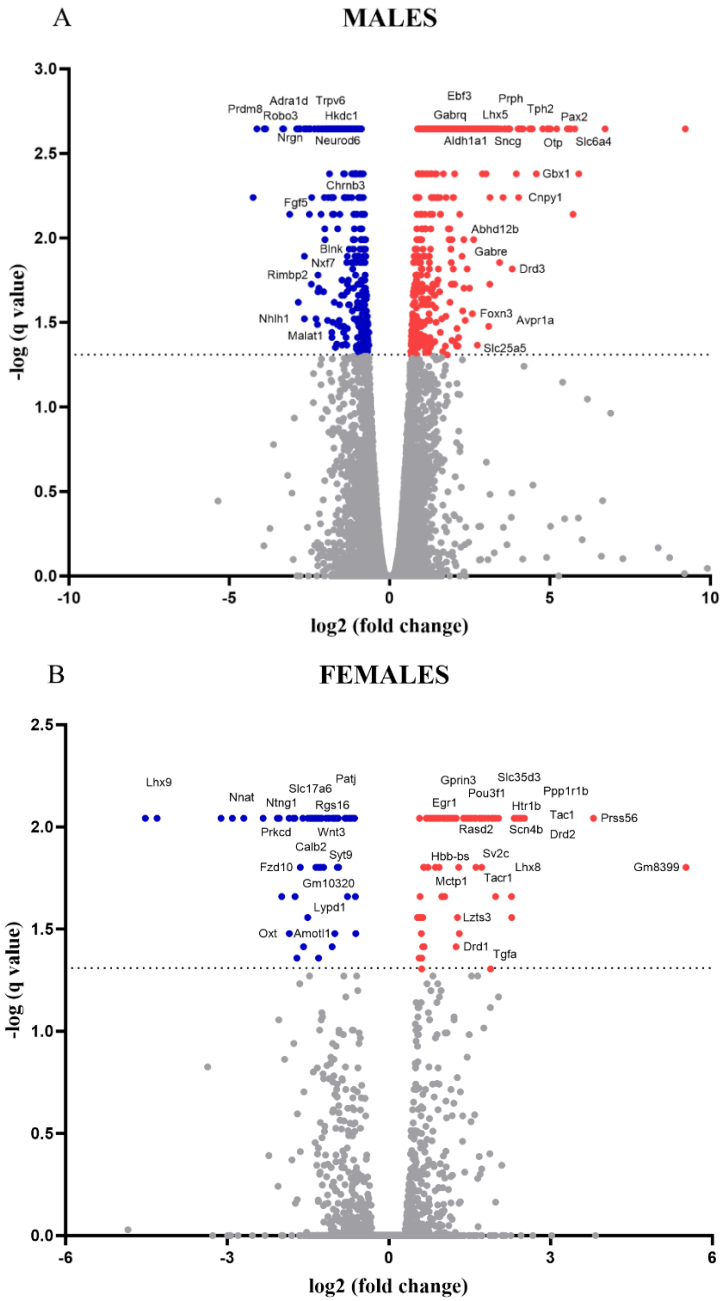

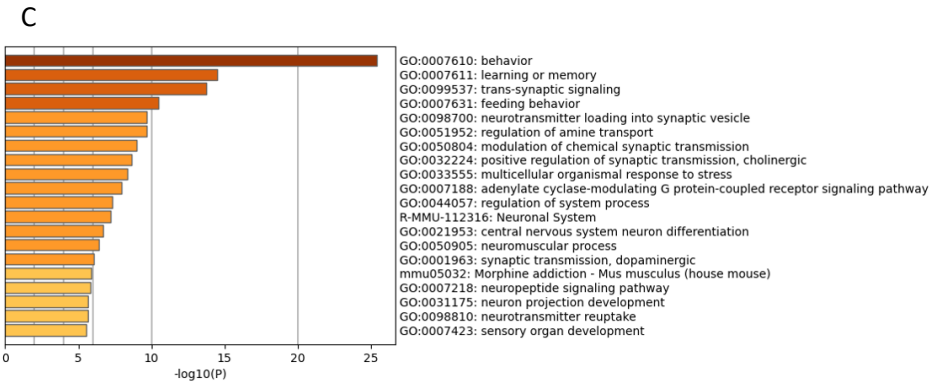

Figure 51: **Effect of Poly(I:C)/THC vs. saline/THC differential in gene expression of (A) male (n=3) and (B) female (n=3) mice. (C) Enriched ontologies clusters.** Volcano plot where it is represented the negative of the logarithm in base 10 of the q-value vs. the logarithm in base 2 of FC (fold change; number of times of change). In red or blue, genes differentially expressed up- or down-regulated, respectively (adjusted p-value < 0.05;–log (q value)=1.35). The genes named in the volcano plot are the most relevant ones associated with crucial ontologies in schizophrenia. Enriched ontologies where an enrichment analysis is shown on sets of genes of Poly(I:C) group compared saline/vehicle mice group.

In this case, the study compares a double-hit model, combining Poly(I:C) and THC treatments with saline/THC group. The combination of these two treatments can have unique effects on gene expression compared to individual treatments. Firstly, there is a higher number of differentially expressed genes in males (958 genes) compared to THC treatment alone (507 genes). This could be due to a synergistic or additive effect of the combined treatments on gene expression. However, in the case of females, this synergistic effect is not as pronounced. Instead, they exhibit a lower number of differentially expressed genes in the double-hit mouse model (156 genes) compared to the THC treatment alone (186 genes). In this case, the synergistic effect of Poly(I:C) plus THC is not observed. Finally, the balance between upregulated and downregulated genes varies between sexes within the double-hit model. Notably, both males and females show a higher prevalence of upregulated genes. In contrast, females have fewer downregulated genes in the double-hit mouse model than in the group of THC only.

4.2.4. *In vitro* assays of double-hit mouse model

4.2.4.1. Akt/mTOR/S6 pathway quantification in the double-hit mouse model mouse

In order to elucidate the status of this signaling pathway in double-hit mouse model mouse, the quantification of total proteins and the phosphorylated forms was carried out with different experimental approaches, AlphaLISA® assays (method explained in 3.3.9) and Western Blotting experiments (method explained in 3.3.10).

4.2.4.1.1. Detection of total proteins and its phosphorylated forms in the cerebral cortex of the double-hit mouse model by AlphaLISA® assays.

4.2.4.1.1.1. Total Akt protein and phosho(Thr450)-Akt

The values obtained in the quantification of total Akt protein, its phosphorylated form (phospho(Thr450)-Akt), and the ratio between phospho(Thr450)-Akt/Akt are shown in Figure 52 (A, B, and C, respectively). Furthermore, the results from the three-way ANOVA analysis are presented in Table 13.

Table 13: **Results of three-way ANOVA analysis to study the effects of Poly(I:C), THC, sex and their interactions on the levels of total Akt, phospho(Thr450)-Akt and the ratio between phospho(Thr450)-Akt/Akt.**

Three-way ANOVA parameters for Akt AlphaLISA® assays			
	Akt	**Phospho(Thr450)-Akt**	**Phospho(Thr450)-Akt/Akt**
Poly(I:C)	F (1. 33) = 0.06, p=0.8034	F (1, 33) = 3.66, p=0.0643	F (1, 33) = 0.32, p=0.5750
Sex	F (1, 33) = 1.82, p=0.1860	F (1, 33) = 1.79, p=0.1897	F (1, 33) = 1.04, p=0.3157
THC	F (1, 33) = 0.37, p=0.5495	F (1, 33) = 1.27, p=0.2669	F (1, 33) = 0.72, p=0.4024
Poly(I:C) x Sex	F (1, 33) = 0.73, p=0.3991	**F (1, 33) = 4.16, p=0.0494**	F (1, 33) = 0.01, p=0.9169
Poly(I:C) x THC	F (1, 33) = 0.25, p=0.6186	F (1, 33) = 0.02, p=0.8756	F (1, 33) = 0.45, p=0.5090
Sex x THC	F (1, 33) = 0.53, p=0.4715	F (1, 33) = 1.30, p=0.2621	F (1, 33) = 0.03, p=0.8626
Poly(I:C) x Sex x THC	F (1, 33) = 0.18, p=0.6713	F (1, 33) = 0.99, p=0.3281	F (1, 33) = 0.26, p=0.6143

Regarding total Akt protein, statistically significant effects of Poly(I:C), THC, or sex were not observed (Figure 52A). For phospho(Thr450)-Akt, significant interaction was observed between Poly(I:C) and sex [$F_{Poly(I:C)xsex}$ (1, 33) = 4.162, p=0.0494]. Further analysis using Bonferroni's post-hoc test revealed a notable decrease (-25.04%, p=0.041) in the Poly(I:C) group compared to the saline group (saline/vehicle/male: 1.21 ± 0.12; Poly(I:C)/vehicle/male: 0.91 ± 0.04), which was significant only in male mice. However, these effects were not observed in females, and THC did not influence any of the phospho(Thr450)-Akt levels (Figure 52B). Finally, in the case of the ratio of protein phospho(Thr450)-Akt/Akt, the statistical analysis did not reveal any significant effects of Poly(I:C), THC, or sex (Figure 52C).

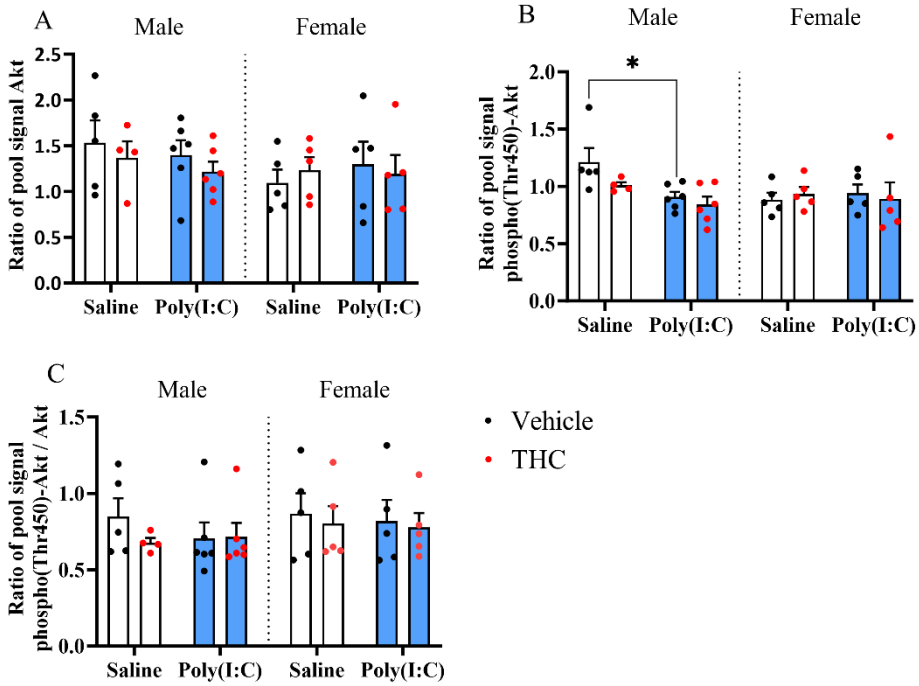

Figure 52: **Relative levels of (A) Akt protein, (B) phospho(Thr450)-Akt, and (C) ratio phospho(Thr450)-Akt / Akt in males and females of the different experimental groups..** The values shown are the mean ± SEM (n=4-6 per group) of the relative levels of protein and phosphorylated form calculated from the "Alpha counts" signal values and normalized by the value obtained for the sample pool. The results were analyzed by three-way ANOVA analyzing the influence of Poly(I:C), THC administration and sex.

4.2.4.1.1.2. Total ERK 1/2 protein and phospho(Tyr202/204)-ERK 1/2

The values obtained for the quantification of total ERK 1/2 protein, its phosphorylated form (phospho(Thr202/Tyr204)-ERK 1/2), and the ratio of phospho(Thr202/Tyr204)-ERK 1/2 / ERK 1/2 are displayed in Figure 53 (A, B, and C, respectively). Additionally, the results from the three-way ANOVA analysis are presented in Table 14.

Table 14: **Results of three-way ANOVA analysis to study the effects of Poly(I:C), THC, sex and their interactions on the levels of total ERK 1/2, phospho(Thr202/Tyr204)-ERK 1/2 and the ratio between phospho(Thr202/Tyr204)-ERK 1/2 / ERK 1/2.**

Three-way ANOVA parameters for ERK 1/2 AlphaLISA® assays			
	ERK 1/2	**Phospho(Thr202/Tyr204)-ERK 1/2**	**Phospho(Thr202/Tyr204)-ERK 1/2 / ERK 1/2**
Poly(I:C)	F (1, 39) = 2.38, p=0.1312	**F (1, 39) = 13.08, p=0.0008**	F (1, 39) = 3.44, p=0.0713
Sex	F (1, 39) = 0.88, p=0.3535	F (1, 39) = 0.01, p=0.9298	F (1, 39) = 0.18, p=0.6725
THC	F (1, 39) = 0.001, p=0.9685	F (1, 39) = 0.00, p=0.9984	F (1, 39) = 0.07, p=0.7896
Poly(I:C) x Sex	F (1, 39) = 0.74, p=0.3931	F (1, 39) = 0.06, p=0.8118	F (1, 39) = 0.33, p=0.5680
Poly(I:C) x THC	F (1, 39) = 0.31, p=0.5825	F (1, 39) = 2.29, p=0.1376	F (1, 39) = 3.78, p=0.0592
Sex x THC	F (1, 39) = 0.01, p=0.9081	F (1, 39) = 1.43, p=0.2385	F (1, 39) = 0.79, p=0.3804
Poly(I:C) x Sex x THC	F (1, 39) = 0.73, p=0.3973	F (1, 39) = 2.29, p=0.1387	F (1, 39) = 1.25, p=0.2698

In the case of total ERK 1/2 protein (Figure 53A) and the ratio of phospho(Tyr202/204)-ERK 1/2 / ERK 1/2 protein (Figure 53C), the statistical analysis did not reveal a statistically significant influence of Poly(I:C), THC, or sex. As for phospho(Tyr202/204)-ERK 1/2 protein (Figure 53B), a decrease (-47.13%, p=0.0008) in protein levels was observed compared to saline, driven by a significant effect of Poly(I:C) [$F_{Poly(I:C)}$ (1, 39) = 13.08, p=0.0008] (saline: 2.44 ± 0.26; Poly(I:C): 1.29 ± 0.19). No further significant effects were observed.

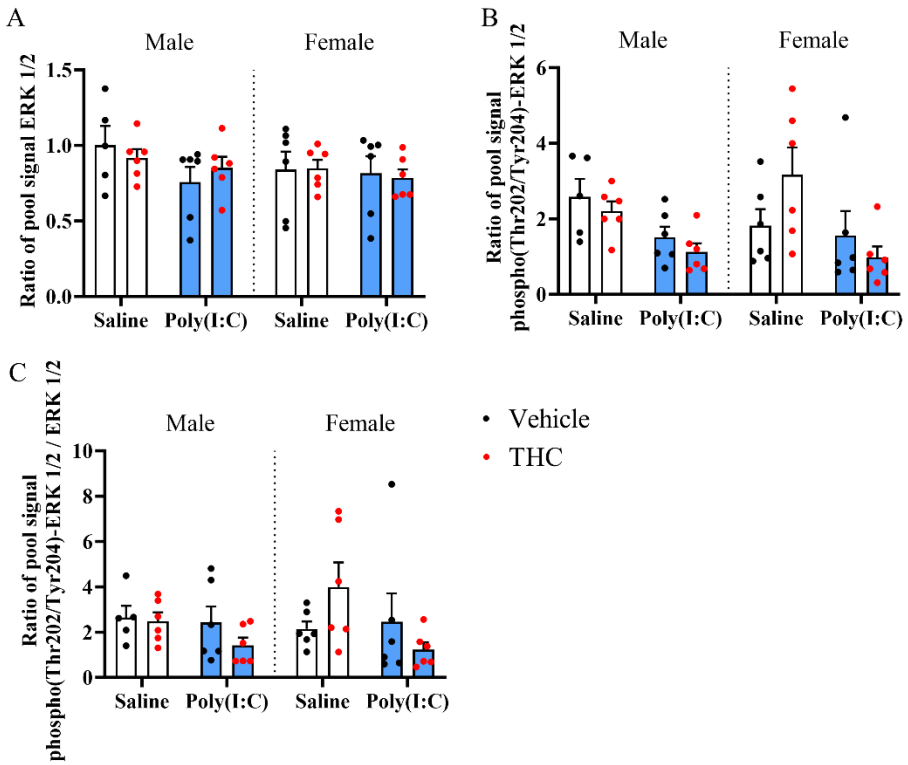

Figure 53: **Relative levels of (A) ERK 1/2 protein, (B) phospho(Tyr202/204)-ERK 1/2 and (C) ratio phospho(Tyr202/204)-ERK 1/2 / ERK 1/2 in males and females of the different experimental groups.** The values shown are the mean ± SEM (n=5-6 per group) of the relative levels of protein and phosphorylated form calculated from the "Alpha counts" signal values and normalized by the value obtained for the sample pool. The results were analyzed by three-way ANOVA analyzing the influence of Poly(I:C), THC administration and sex.

4.2.4.1.1.3. Total mTOR protein and phospho(Ser2448)-mTOR

The values obtained from the quantification of total mTOR protein, its phosphorylated form phospho(Ser2448)-mTOR, and the ratio of phospho(Ser2448)-mTOR / mTOR are depicted in Figure 54 (A, B, and C, respectively). Additionally, the results obtained through the three-way ANOVA analysis are presented in Table 15.

Table 15: **Results of three-way ANOVA analysis to study the effects of Poly(I:C), THC, sex and their interactions on the levels of total mTOR, phospho(Ser2448)-mTOR and the ratio between phospho(Ser2448)-mTOR / mTOR.**

Three-way ANOVA parameters for mTOR AlphaLISA® assays			
	mTOR	**Phospho(Ser2448)-mTOR**	**Phospho(Ser2448)-mTOR/mTOR**
Poly(I:C)	F (1, 39) = 3.87, p=0.0564	**F (1, 39) = 27.59, p<0.0001**	**F (1, 39) = 51.08, p<0.0001**
Sex	F (1, 39) = 0.01, p=0.9323	F (1, 39) = 0.64, p=0.4293	F (1, 39) = 0.75, p=0.3922
THC	F (1, 39) = 1.90, p=0.1763	F (1, 39) = 1.08, p=0.3044	F (1, 39) = 0.002, p=0.9630
Poly(I:C) x Sex	F (1, 39) = 0.27, p=0.6074	F (1, 39) = 0.43, p=0.5166	F (1, 39) = 0.11, p=0.7465
Poly(I:C) x THC	F (1, 39) = 0.36, p=0.5523	F (1, 39) = 0.003, p=0.9515	F (1, 39) = 0.68, p=0.4130
Sex x THC	F (1, 39) = 0.51, p=0.4789	F (1, 39) = 2.30, p=0.1371	F (1, 39) = 0.66, p=0.4207
Poly(I:C) x Sex x THC	F (1, 39) = 0.14, p=0.7112	F (1, 39) = 0.72, p=0.4010	F (1, 39) = 0.68, p=0.4149

In the case of total mTOR protein, the statistical analysis did not show a significant influence of Poly(I:C), THC, or sex (Figure 54A). As for phospho(Ser2448)-mTOR protein, levels were decreased (-56.98%, $p<0.0001$) compared to the saline group due to the significant effect of Poly(I:C) (saline: 1.59 ± 0.16; Poly(I:C): 0.68 ± 0.05) [$F_{Poly(I:C)}$ (1, 39) = 27.59, $p<0.0001$]. Regarding the ratio of phospho(Ser2448)-mTOR / mTOR protein, the statistical analysis revealed a significant decrease (-45.43%, $p<0.0001$) in the ratio in the Poly(I:C) group compared to the saline group due to the effect of Poly(I:C) (saline: 1.118 ± 0.06; Poly(I:C): 0.61 ± 0.03) [$F_{Poly(I:C)}$ (1,39) =51.08, $p<0.0001$]. There were no significant effects of THC or sex observed in either the phospho(Ser2448)-mTOR protein or the calculated ratio on total protein (Figure 54B and 54C).

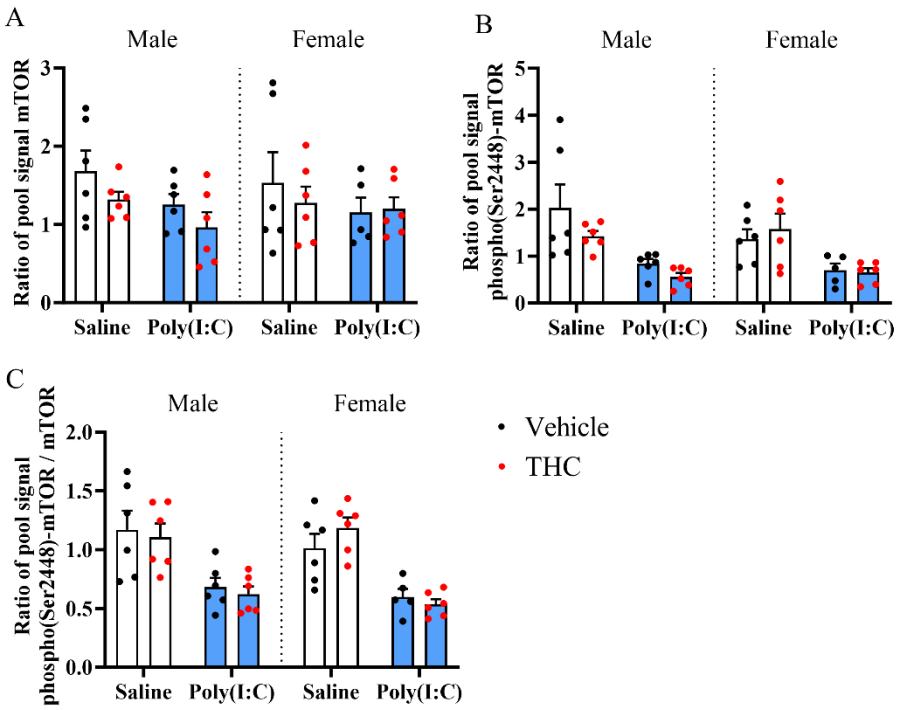

Figure 54: **Relative levels of (A) mTOR protein, (B) phospho(Ser2448)-mTOR and (C) ratio phospho(Ser2448)-mTOR / mTOR in males and females of the different experimental groups.** The values shown are the mean ± SEM (n=5-6 per group) of the relative levels of protein and phosphorylated form calculated from the "Alpha counts" signal values and normalized by the value obtained for the sample pool. The results were analyzed by three-way ANOVA analyzing the influence of Poly(I:C), THC administration and sex.

4.2.4.1.1.4. Total rpS6 protein, phospho(Ser235/236)-rpS6 and phospho(Ser240/244)-rpS6)

The values obtained from the quantification of total rpS6 protein, its phosphorylated form phospho(Ser235/236)-rpS6, and the ratio of phospho(Ser235/236)-rpS6 / rpS6 are displayed in Figure 55 (A, B, and C, respectively). Additionally, the results from the three-way ANOVA analysis are presented in Table 16.

Table 16: **Results of three-way ANOVA analysis to study the effects of Poly(I:C), THC, sex and their interactions on the levels of total rpS6, phospho(Ser235/236)-rpS6 and the ratio between phospho(Ser235/236)-rpS6 / rpS6.**

Three-way ANOVA parameters for rpS6 AlphaLISA® assays			
	rpS6	**Phospho(Ser235/236)-rpS6**	**Phospho(Ser235/236)-rpS6 / rpS6**
Poly(I:C)	F (1, 39) = 0.47, p=0.4958	**F (1, 39) = 17.85, p=0.0001**	**F (1, 39) = 14.09, p=0.0006**
Sex	F (1, 39) = 0.002, p=0.9606	F (1, 39) = 1.96, p=0.1696	F (1, 39) = 0.78, p=0.3817
THC	F (1, 39) = 0.32, p=0.5728	**F (1, 39) = 7.18, p=0.0108**	**F (1, 39) = 9.87, p=0.0032**
Poly(I:C) x Sex	F (1, 39) = 0.35, p=0.5556	F (1, 39) = 1.50, p=0.2282	F (1, 39) = 2.23, p=0.1436
Poly(I:C) x THC	F (1, 39) = 3.88, p=0.0561	F (1, 39) = 0.53, p=0.4700	**F (1, 39) = 5.18, p=0.0284**
Sex x THC	F (1, 39) = 0.77, p=0.3855	**F (1, 39) = 7.41, p=0.0096**	F (1, 39) = 3.66, p=0.0630
Poly(I:C) x Sex x THC	F (1, 39) = 0.48, p=0.4924	**F (1, 39) = 8.41, p=0.0061**	F (1, 39) = 3.66, p=0.0633

In the case of total rpS6 protein, the statistical analysis did not reveal a statistically significant influence of Poly(I:C), THC, or sex (Figure 55A). For phospho(Ser235/236)-rpS6 protein, the levels decreased (-26.51%, p=0.001) compared to saline due to a significant effect of Poly(I:C) (saline: 1.66 ± 0.11; Poly(I:C): 1.22 ± 0.08) [$F_{Poly(I:C)}$ (1, 39) = 17.85, p=0.001]. Phosphorylated rpS6 protein levels were also influenced by a significant effect of THC, decreasing levels compared to the vehicle group [F_{THC} (1, 39) = 7.176, p=0.0108]. Specifically, a decrease (-30.9%, p=0.0096) in the phosphorylated form of the protein compared to saline was observed in males but not in females (vehicle/male: 1.78 ± 0.2; THC/male: 1.23 ± 0.11), which was detected as a significant interaction between sex and THC [$F_{THCxsex}$ (1, 39) = 7.409, p=0.0096]. Finally, an interaction of all three factors (Poly(I:C) x sex x THC) was observed [$F_{Poly(I:C)xsexxTHC}$ (1, 39) = 8.410, p=0.0061] resulting after bonferroni´s post-hoc test in a significant decrease (-42.91%, p=0.0024) between saline/vehicle and Poly(I:C)/vehicle males (saline/vehicle/male: 2.33 ± 0.20; Poly(I:C)/vehicle/male: 1.33 ± 0.18), significant decrease (-42.65%, p=0.0026) between saline/vehicle and saline/THC males (saline/vehicle/male: 2.33 ± 0.20; saline/THC/male: 1.34 ± 0.12) and a significant decrease (-51.25%, p=0.0002) between saline/vehicle and Poly(I:C)/THC males (saline/vehicle/male: 2.33 ±

0.20; Poly(I:C)/THC/male: 1.14 ± 0.20). No further significant effects were observed (Figure 55B). In contrast, these differences were not observed in females.

Finally, in the case of the ratio of phospho(Ser235/236)-rpS6 / rpS6 protein (Figure 55C), a decrease (-25.74%, p=0.0006) in the ratio of Poly(I:C) group compared to saline was observed due to a significant effect of Poly(I:C) [$F_{Poly(I:C)}$ (1, 39) = 14.09, p=0.0006] (saline: 1.36 ± 0.11; Poly(I:C): 1.01 ± 0.05), and a decrease (-21.80%, p=0.0032) in the ratio of THC group compared to the vehicle was observed due to a significant effect of THC (vehicle: 1.33 ± 0.11; THC: 1.04 ± 0.05) [F_{THC} (1, 39) = 9.868, p=0.0032]. Additionally, a stronger effect of THC was also observed in the Poly(I:C) group but not in the saline group, detected as a significant interaction between Poly(I:C) x THC [$F_{Poly(I:C)xTHC}$ (1,39) = 5.180, p=0.0284]. After conducting Bonferroni's post-hoc test, a significant decrease (-35.54%, p=0.0009) in the ratio was observed in the Poly(I:C)/vehicle group when compared to the saline/vehicle group (saline/vehicle: 1.64 ± 0.18; Poly(I:C)/vehicle: 1.05 ± 0.07). Additionally, a decrease (-31.75%, p=0.0031) was noted in the saline/THC group in comparison to the saline/vehicle group (saline/vehicle: 1.64 ± 0.18; saline/THC: 1.12 ± 0.08). Furthermore, a decrease (-40.85%, p=0.0001) was observed in the Poly(I:C)/THC group when compared to the saline/vehicle group (saline/vehicle: 1.64 ± 0.18; Poly(I:C)/THC: 0.97 ± 0.07). All these differences were irrespective of sex.

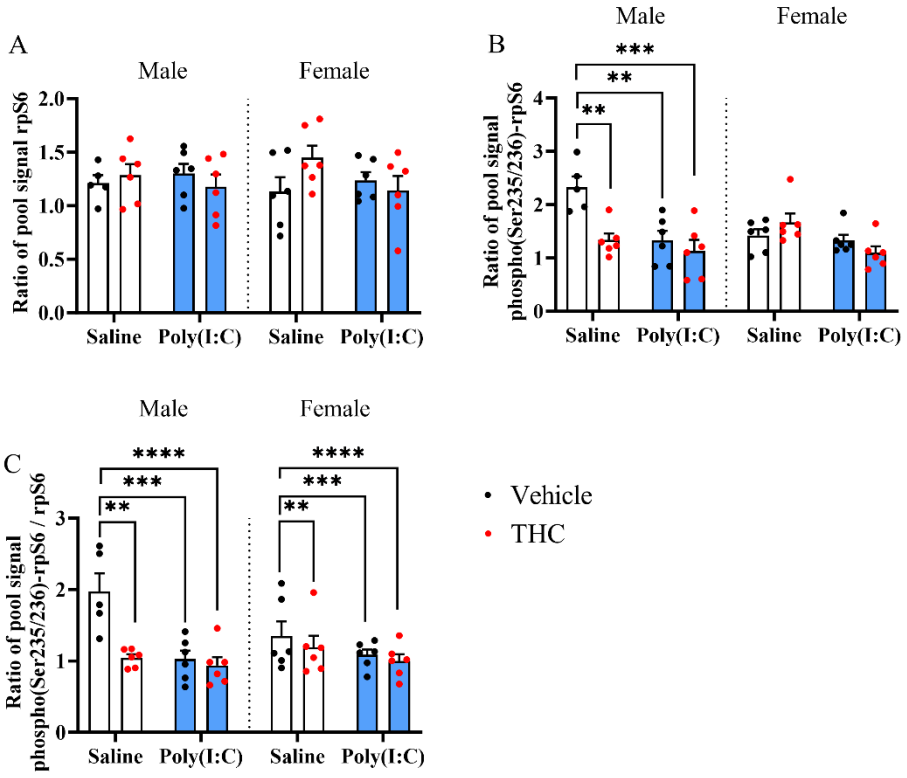

Figure 55: **Relative levels of (A) rpS6 protein, (B) phospho(Ser235/236)-rpS6 and (C) ratio phospho(Ser235/236)-rpS6 / rpS6 in males and females of the different experimental groups.** The values shown are the mean ± SEM (n=5-6 per group) of the relative levels of protein and phosphorylated form calculated from the "Alpha counts" signal values and normalized by the value obtained for the sample pool. The results were analyzed by three-way ANOVA analyzing the influence of Poly(I:C), THC administration and sex.

The values obtained for the quantification of the second phosphorylation of rpS6 (phospho(Ser240/244)-rpS6), and the ratio of phospho(Ser240/244)-rpS6 / rpS6, are depicted in Figure 56 (A and B, respectively). Additionally, the results from the three-way ANOVA analysis are presented in Table 17.

Table 17: **Results of three-way ANOVA analysis to study the effects of Poly(I:C), THC, sex and their interactions on the levels of phospho(Ser240/244)-rpS6 and the ratio between phospho(Ser240/244)-rpS6 / rpS6.**

Three-way ANOVA parameters for phospho(Ser240/244)-rpS6 AlphaLISA® assays		
	Phospho(Ser240/244)-rpS6	**Phospho(Ser240/244)-rpS6 / rpS6**
Poly(I:C)	**F (1, 23) = 7.23, p=0.0131**	F (1, 23) = 4.22, p=0.0514
Sex	F (1, 23) = 2.98, p=0.0978	F (1, 23) = 1.88, p=0.1837
THC	F (1, 23) = 0.27, p=0.6058	F (1, 23) = 0.22, p=0.6419
Poly(I:C) x Sex	F (1, 23) = 1.13, p=0.2983	F (1, 23) = 0.15, p=0.7036
Poly(I:C) x THC	F (1, 23) = 0.05, p=0.8338	F (1, 23) = 0.65, p=0.4271
Sex x THC	F (1, 23) = 0.27, p=0.6078	F (1, 23) = 0.02, p=0.8849
Poly(I:C) x Sex x THC	F (1, 23) = 0.46, p=0.5026	F (1, 23) = 0.01, p=0.9156

In the case of phospho(Ser240/244)-rpS6 protein, a decrease (-35.82%, p=0.0131) in phospho(Ser240/244)-rpS6 levels compared to saline was observed, driven by a significant effect of Poly(I:C) (saline: 1.34 ± 0.14; Poly(I:C): 0.86 ± 0.12) [$F_{Poly(I:C)}$ (1, 23) = 7.228, p=0.0131]. No significant effects of THC or sex were observed in this case (Figure 56A). Furthermore, no significant differences were observed in the ratio with respect to any variable (Figure 56B).

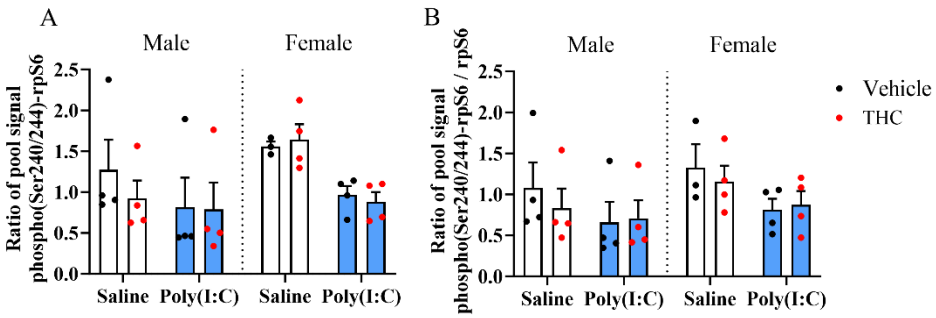

Figure 56: **Relative levels of (A) phospho(Ser240/244)-rpS6 and (B) ratio phospho(Ser240/244)-rpS6 / rpS6 in males and females of the different experimental groups.** The values shown are the mean ± SEM (n=3-4 per group) of the relative levels of protein and phosphorylated form calculated from the "Alpha counts" signal values and normalized by the value obtained for the sample pool. The results were analyzed by three-way ANOVA analyzing the influence of Poly(I:C), THC administration and sex.

4.2.4.1.2. Detection of total proteins and phosphorylated forms by Western Blotting

To validate the accuracy of results obtained through AlphaLISA® assays and to assess phosphorylation events not detectable via this technique, WB experiments were conducted using the same sample sets. This strategy aimed to provide a more comprehensive understanding of the biological processes under investigation.

4.2.4.1.2.1. Total Akt protein and phospho(Ser473)-Akt

The results of the three-way ANOVA (Table 18) for Akt, Phospho(Ser473)-Akt, and the Phospho(Ser473)-Akt / Akt ratio are represented in Figure 57. Representative image of bands obtained are shown in Figure 57D.

Table 18: **Results of three-way ANOVA evaluating the effect of Poly(I:C), THC, sex and their interaction in the immunodensity of total Akt, phospho(Ser473)-Akt and the ratio between phospho(Ser473)-Akt / Akt.**

Three-way ANOVA parameters for Akt WB experiments			
	Akt	**Phospho(Ser473)-Akt**	**Phospho(Ser473)-Akt / Akt**
Poly(I:C)	F (1, 37) = 0.34, p=0.5628	**F (1, 37) = 13.49, p=0.0008**	**F (1, 37) = 6.94, p=0.0122**
Sex	F (1, 37) = 0.16, p=0.6905	F (1, 37) = 0.66, p=0.4234	F (1, 37) = 0.23, p=0.6327
THC	F (1, 37) = 0.33, p=0.5698	F (1, 37) = 0.37, p=0.5459	F (1, 37) = 0.17, p=0.6859
Poly(I:C) x Sex	F (1, 37) = 0.38, p=0.5413	F (1, 37) = 0.11, p=0.7381	F (1, 37) = 0.30, p=0.5888
Poly(I:C) x THC	F (1, 37) = 0.25, p=0.6227	F (1, 37) = 0.29, p=0.5932	F (1, 37) = 0.47, p=0.4956
Sex x THC	F (1, 37) = 0.41, p=0.5240	F (1, 37) = 0.72, p=0.4002	F (1, 37) = 0.30, p=0.5877
Poly(I:C) x Sex x THC	F (1, 37) = 0.02, p=0.8983	F (1, 37) = 0.01, p=0.9418	F (1, 37) = 0.0008, p=0.9766

Firstly, with regard to Akt total protein (Figure 57A), any statistically significant effects was observed. However, when examining the level of phospho(Ser473)-Akt (Figure 57B), there was a significant effect of Poly(I:C) (F (1, 37) = 13.49, p=0.0008), indicating that Poly(I:C) treatment led to a decrease (-46.96%, p=0.0008) in the Akt phosphorylated form (saline: 131.0 ± 10.98; Poly(I:C): 69.48 ± 11.63). Similarly, the phospho(Ser473)-Akt / Akt ratio (Figure 57C) was significantly affected by Poly(I:C) treatment (F (1, 37) = 6.939, p=0.0122),

suggesting an altered balance between phosphorylated and total Akt levels resulting in a significant decrease (-47.27%, p=0.0122) of the ratio in the Poly(I:C) group comparing with saline mice (saline: 1.65 ± 2.11; Poly(I:C): 0.87 ± 0.18). Interestingly, no significant effects were observed for sex, THC exposure, or their interactions with Poly(I:C), indicating that these factors may not play a major role in the observed alterations in Akt activation associated with schizophrenia.

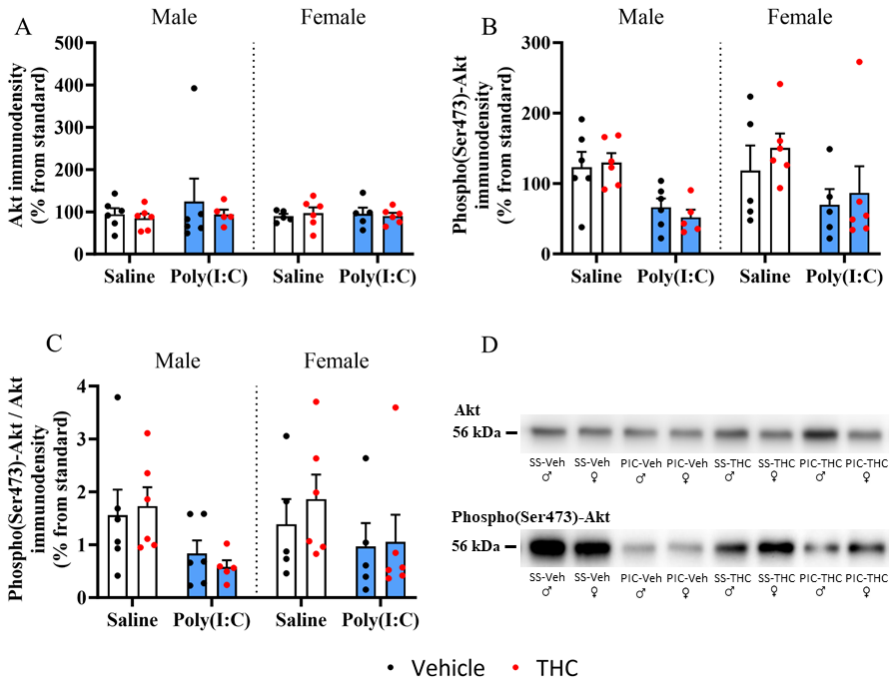

Figure 57: **Immunodensity values for (A) Akt, (B) phospho(Ser473)-Akt and (C) ratio phospho(Ser473)-Akt / Akt in males and females of the different experimental groups and (D) representative images of immunoblots.** Immunodensity values were normalized respect to a standard sample (STD) loaded by duplicate into each gel. Bars represent the mean ± SEM (n=5-6 per group) of the individual values depicted in points. The results were analyzed by three-way ANOVA analyzing the influence of Poly(I:C), THC administration and sex.

4.2.4.1.2.2. Total ERK 1/2 protein and phospho(Tyr 202/204)-ERK 1/2

The results of the three-way ANOVA (Table 19) for ERK 1/2, phospho(Tyr 202/204)-ERK 1/2, and the phospho(Tyr 202/204)-ERK 1/2 / ERK 1/2 ratio are represented in Figure 58. Representative image of bands obtained are shown in Figure 58D.

Statistical analysis revealed no significant effects or interactions when total ERK 1/2 protein measurement was performed (Figure 58A). Specifically, the treatment with Poly(I:C), sex, and THC exposure did not yield statistically significant effects on the levels of total ERK 1/2 protein. Additionally, the interactions between these factors, such as Poly(I:C) x sex, Poly(I:C) x THC, sex x THC, and the three-way interaction Poly(I:C) x sex x THC, also did not show statistically significant effects.

Table 19: **Results of three-way ANOVA evaluating the effect of Poly(I:C), THC, sex and their interaction in the immunodensity of total ERK 1/2, phospho(Tyr202/204)-ERK 1/2 and the ratio between phospho(Tyr202/204)-ERK 1/2 / ERK 1/2.**

Three-way ANOVA parameters for ERK 1/2 WB experiments			
	ERK 1/2	**Phospho(Tyr202/204)-ERK 1/2**	**Phospho(Tyr202/204)-ERK 1/2 / ERK 1/2**
Poly(I:C)	F (1. 38) = 0.46, p=0.5033	**F (1, 38) = 6.72, p=0.0135**	**F (1, 38) = 9.17, p=0.0044**
Sex	F (1, 38) = 0.12, p=0.7257	F (1, 38) = 1.20, p=0.2794	F (1, 38) = 0.35, p=0.5570
THC	F (1, 38) = 0.07, p=0.7946	F (1, 38) = 0.01, p=0.9070	F (1, 38) = 1.87, p=0.1796
Poly(I:C) x Sex	F (1, 38) = 1.95, p=0.1707	F (1, 38) = 0.90, p=0.3496	F (1, 38) = 0.48, p=0.4940
Poly(I:C) x THC	F (1, 38) = 0.05, p=0.8327	F (1, 38) = 0.84, p=0.3665	F (1, 38) = 0.34, p=0.5643
Sex x THC	F (1, 38) = 0.21, p=0.6504	F (1, 38) = 0.64, p=0.4285	F (1, 38) = 0.003, p=0.9561
Poly(I:C) x Sex x THC	F (1, 38) = 0.02, p=0.8857	F (1, 38) = 0.13, p=0.7178	F (1, 38) = 0.89, p=0.3503

However several significant findings were observed in the results for Phospho(Tyr202/204)-ERK 1/2 and the ratio of phospho(Tyr202/204)-ERK 1/2 / ERK 1/2. In terms of Phospho(Tyr202/204)-ERK 1/2 levels (Figure 58B), the treatment with Poly(I:C) showed a significant effect (F (1, 38) = 6.721, p=0.0135), indicating an impact on ERK 1/2 phosphorylation that produced a significant decrease (-35.39%, p=0.0135) in Phospho(Tyr202/204)-ERK 1/2

when comparing saline and Poly(I:C) mice (saline: 130.8 ± 14.19; Poly(I:C): 84.50 ± 9.21). However, sex, THC exposure, and their interactions did not yield significant effects on phospho(Tyr202/204)-ERK 1/2 levels. Similarly, when considering the ratio of phospho(Tyr202/204)-ERK 1/2 / ERK 1/2 (Figure 58C), Poly(I:C) had a significant effect (F (1, 38) = 9.172, p=0.0040), suggesting an altered balance in ERK 1/2 phosphorylation that produced a significant decrease (-40.58%, p=0.0040) in Phospho(Tyr202/204)-ERK 1/2 when comparing saline and Poly(I:C) mice (saline: 1.38 ± 0.15; Poly(I:C): 0.82 ± 0.10). Again, sex, THC exposure, and their interactions did not show significant effects on this ratio.

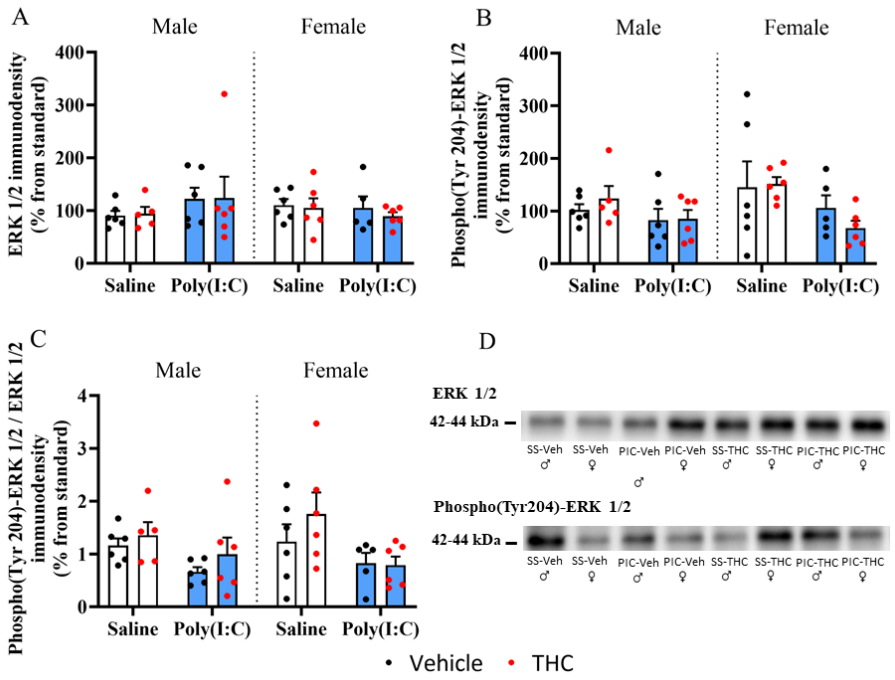

Figure 58: **Immunodensity values for (A) ERK 1/2, (B) phospho(Tyr202/204)-ERK 1/2 and (C) ratio phospho(Tyr202/204)-ERK 1/2 / ERK 1/2 in males and females of the different experimental groups and (D) representative images of immunoblots.** Immunodensity values were normalized respect to a standard sample (STD) loaded by duplicate into each gel. Bars represent the mean ± SEM (n=5-6 per group) of the individual values depicted in points. The results were analyzed by three-way ANOVA analyzing the influence of Poly(I:C), THC administration and sex.

4.2.4.1.2.3. Total rpS6 protein and phospho(Ser235/236)-rpS6

The results of the three-way ANOVA (Table 20) for rpS6, phospho(Ser235/236)-rpS6, and the phospho(Ser235/236)-rpS6/ rpS6 ratio are represented in Figure 59. Representative image of bands obtained are shown in Figure 59D.

When assessing the levels of total protein (Figure 59A) only the treatment with Poly(I:C) produced a significant effect. However, sex, nor THC exposure showed statistically significant effects.

Table 20: **Results of three-way ANOVA evaluating the effect of Poly(I:C), THC, sex and their interaction in the immunodensity of total rpS6, phospo(Ser235/236)-rpS6 and the ratio between phospo(Ser235/236)-rpS6 / rpS6.**

Three-way ANOVA parameters for rpS6 WB experiments

	rpS6	Phospho(Ser235/236)-rpS6	Phospho(Ser235/236)-rpS6 / rpS6
Poly(I:C)	**F (1, 39) = 7.57, p=0.0089**	**F (1, 39) = 11.38, p=0.0017**	F (1, 39) = 0.13, p=0.7199
Sex	F (1, 39) = 0.86, p=0.3605	F (1, 39) = 0.15, p=0.6973	F (1, 39) = 0.50, p=0.4822
THC	F (1, 39) = 0.14, p=0.7087	**F (1, 39) = 4.36, p=0.0433**	F (1, 39) = 3.49, p=0.0695
Poly(I:C) x Sex	F (1, 39) = 0.71, p=0.4045	F (1, 39) = 0.09, p=0.7611	F (1, 39) = 2.25, p=0.1413
Poly(I:C) x THC	F (1, 39) = 1.54, p=0.2225	**F (1, 39) = 7.36, p=0.0099**	F (1, 39) = 0.91, p=0.3449
Sex x THC	F (1, 39) = 1.06, p=0.3087	**F (1, 39) = 6.24, p=0.0168**	F (1, 39) = 2.43, p=0.1275
Poly(I:C) x Sex x THC	F (1, 39) = 2.90, p=0.0965	F (1, 39) = 0.13, p=0.7198	F (1, 39) = 0.77, p=0.3857

For phospho(Ser235/236)-rpS6 protein (Figure 59B), the levels decreased (-28.82%, p=0.0017) compared to saline due to a significant effect of Poly(I:C) (saline: 101.7 ± 6.75; Poly(I:C): 72.39 ± 6.86) [$F_{Poly(I:C)}$ (1, 39) = 11.38, p=0.0017]. Phosphorylated rpS6 protein levels were also influenced by a significant effect of THC, decreasing levels compared to the vehicle group [F_{THC} (1, 39) = 4.363, p=0.0433]. Specifically, after Bonferroni's post-hoc test a decrease (-37.19%, p=0.013) in the phosphorylated form of the protein compared to saline was observed in males but not in females (vehicle/male: 105.20 ± 10.67; THC/male: 66.08 ± 5.00), which was detected as a significant interaction between sex and THC [$F_{THCxsex}$ (1, 39) = 6.236, p=0.0168]. Finally, an interaction of Poly(I:C) x THC was observed [$F_{Poly(I:C)xTHC}$ (1, 39) =7.363, p=0.0099]. After

bonferroni´s post-hoc test a significant decrease (-42.91%, p=0.0024) between saline/vehicle and Poly(I:C)/vehicle (saline/vehicle: 2.33 ± 0.20; Poly(I:C)/vehicle: 1.33 ± 0.18). For phospho(Ser235/236)-rpS6 / rpS6 ratio, no further significant effects were observed (Figure 59C).

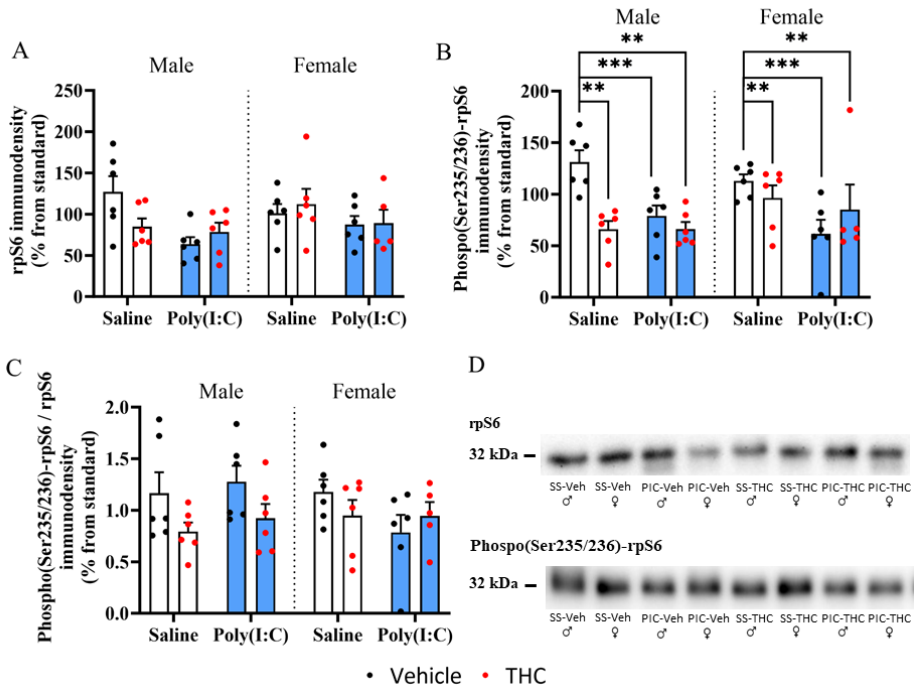

Figure 59: **Immunodensity values for (A) rpS6, (B) phospo(Ser235/236)-rpS6 and (C) ratio phospo(Ser235/236)-rpS6 / rpS6 in males and females of the different experimental groups and (D) representative images of immunoblots.** Immunodensity values were normalized respect to a standard sample (STD) loaded by duplicate into each gel. Bars represent the mean ± SEM (n=5-6 per group) of the individual values depicted in points. The results were analyzed by three-way ANOVA analyzing the influence of Poly(I:C), THC administration and sex.

Discussion

5. DISCUSSION

5.1. Study I: Cell cultures from olfactory neuroepithelium

Isolation and differentiation of neurospheres from olfactory neuroepithelium

Neural Stem Cells (NSCs) in the olfactory neuroepithelium play a pivotal role in continually replenishing sensory neurons throughout an individual's life, ensuring a sustained capacity for regeneration following injuries (Brann et al., 2015; Mackay-Sim & Kittel, 1991). Under appropriate *in vitro* conditions, these isolated progenitor neural cells, characterized by their robust mitotic activity, demonstrate the remarkable ability to form spherical aggregates known as neurospheres, a distinctive feature inherent to NSCs (Katz et al., 2010).

Originating from the olfactory mucosa, these structures have the potential to differentiate into both neurons and glial cells. Consequently, they represent a compelling avenue for establishing innovative human models to investigate diseases affecting the central nervous system.

What makes these neurospheres particularly valuable is their ability to serve as a platform for studying disease etiology without necessitating genetic reprogramming. This attribute makes them invaluable for gaining insights into various aspects of disease development, enhancing diagnostic approaches, monitoring treatment efficacy, and fostering the discovery of novel therapeutic drugs (Matigian et al., 2010). In this work, cells obtained from the olfactory neuroepithelium were able to form cell aggregates, called neurospheres, and demonstrated a capacity for unlimited division without differentiation over days, a remarkable characteristic of neurospheres (Begum et al., 2015; Gage et al., 1995; Galli et al., 2003; Othman et al., 2005; Rao, 1999).

On the other hand, once these neurospheres were formed, although no specific marker for neurospheres has been described to date, these structures transiently expressed the transcription factor SRY-box-2 (Sox2) or the mRNA-binding protein Musashi-1, which has been shown to play a critical role in promoting

stem cell self-renewal (Okano et al., 2005). In addition, neurospheres are formed by different cell types that also express the Nestin protein (Gil-Perotín et al., 2013). Nestin is a class VI intermediate filament protein found in nerve cells that has been widely used as a marker for neural stem/progenitor cells (Lendahl et al., 1990) that can differentiate into neurons and glial cells.

In conclusion, our findings unveil novel and significant insights into the nature of neurospheres originating from the olfactory neuroepithelium. The presence of distinct markers demonstrates that neurospheres are formed by a heterogeneous population of cells at different stages of differentiation, including stem cells or proliferating neural progenitors (da Silva Siqueira et al., 2021). Importantly, our results underscore that, under the specific conditions of our experiments, cells derived from the olfactory neuroepithelium are able to form neurospheres composed by neural progenitor cells, as previously demonstrated by other groups (Jiménez-Vaca et al., 2018; Krolewski et al., 2011; Murrell et al., 2005; Zelenova et al., 2021).

Under specific *in vitro* conditions, these neurospheres, demonstrated the remarkable capability to differentiate into both astrocytes and neurons (Flax et al., 1998; Svendsen et al., 1996; Unzueta-Larrinaga et al., 2023).

The resulting differentiated cells from these neurospheres exhibited an elongated morphology with projections that formed connections with neighboring cells, often displaying the development of synaptic terminals, characteristics similar to neurons. Additionally, observations revealed the presence of other cell types, such as astrocytes, characterized by a globular or stellate shape.

Immunofluorescence results validated the presence of these neural types, neurons, and astrocytes, through the detection of specific markers including βIII-Tubulin, Nestin, or GFAP. In the culture conditions used, neural precursors predominated as most cells were stained with the anti-βIII-Tubulin antibody. Tubulin is a major constituent protein of microtubules and consists of two 50-kDa subunits designated as α and β. Expression of Class III β-Tubulin, one of the

six isotypes of the β subunit expressed in mammals (Sullivan & Cleveland, 1986), is restricted almost entirely to neurons (Dráberová et al., 1998). Although it is expressed in the testis developmentally, its expression is exclusively neuronal in the nervous system of higher vertebrates (Havercroft & Cleveland, 1984; Lee, et al., 1990a; Lee, et al., 1990b). βIII-Tubulin marks developing neurons throughout the CNS and is also expressed by both immature and mature olfactory neurons (Jiang & Oblinger, 1992; Lee, et al., 1990b; Lee & Pixley, 1994). Moreover, cells recognized by the anti- βIII-Tubulin antibody displayed a microtubular network pattern. On the other hand, these differentiated cells from neurospheres, also expressed NeuN marker, a well-recognized marker, uniquely detectable in post-mitotic neurons. It was found in the nuclei of neurons, affirming their neuronal nature during specific developmental stages (Duan et al., 2016). Immunofluorescence studies established the expression of neuronal markers βIII-Tubulin and Nestin in the olfactory neuroepithelium cells of control subjects, in line with previous reports (Benítez-King et al., 2011; Ortiz-López et al., 2017).

While our data strongly aligned with the characterization of these cells as neuronal, the presence of glial cell markers (GFAP) has also been previously observed in neuronal cultures (Schubert et al., 1985). Coexistence of glial and neuronal markers has been documented in other developing systems, indicating incomplete differentiation. For example, neural stem cells can also express both glial and neuronal proteins (Omlin & Waldmeyer, 1989). This incomplete differentiation may be advantageous for facilitating cell proliferation, challenging the conventional notion that mature neurons are incapable of cell division. Immunofluorescence data strongly suggested a heterogeneous expression of differentiation states in these cultures, reinforcing the diverse neural lineage stages represented by these cells.

Adherent cultures obtained from olfactory neuroepithelium give rise to neuron- and glia-enriched cultures

In adulthood, the continuous transformation of precursor cells into neurons extends its influence across various cerebral structures and specific peripheral tissues, notably manifesting in the olfactory neuroepithelium. Within the olfactory neuroepithelium, an enduring revitalization of olfactory sensory neurons unfolds throughout an individual's lifespan, originating from stem or progenitor cells through the intricate process of neurogenesis. These cell populations find their residence at both the apical and basal membranes (Leung et al., 2007). Consequently, the olfactory neuroepithelium becomes a reservoir of multipotent cells endowed with the capacity for *in vitro* proliferation and differentiation into an array of cell types, including neurons and glia (Matigian et al., 2010). Our cell cultures, mostly composed of cells destined to become neurons, are in line with previous studies that have worked effectively with this type of culture, especially to study the complexities of neuropsychiatric disorders (Benítez-King et al., 2011; Borgmann-Winter et al., 2015; Guinart et al., 2020; Matigian et al., 2010; McCurdy et al., 2006).

Given the mix of cell types within this culture, encompassing both neuronal and non-neuronal entities, the morphology on display exhibits a remarkable diversity, defying any straightforward categorization into a singular cell type. Immunofluorescence experiments, harnessing markers such as βIII-Tubulin, MAP2, and GFAP, definitively corroborated the coexistence of both neuronal and non-neuronal cells in these adherent cultures. However, immunofluorescence assays revealed that primary antibodies to specific markers of neural lineage cells recognized the vast majority of cells present in these cultures, indicating their neural origin. Neurogenesis is a complex process that requires several stages such as cell proliferation, migration, cell cycle exit, survival and maturation. All of these are closely linked to the dynamic reorganization of the cytoskeleton (Benítez-King et al., 2011). That is why in this project antibodies recognizing the different components of the cytoskeleton were used in order to show

characteristic phenotypes of the cytoskeleton in progenitor cells obtained by nasal exfoliation of olfactory neuroepithelium. Thus, MAP2 emerges as a pivotal regulator of the cytoskeleton within neuronal dendrites, serving as a robust marker for somatodendritic regions due to its considerable abundance and specificity. It influences microtubule dynamics and microtubule/actin interactions to control neurite outgrowth and synaptic functions (DeGiosio et al., 2022).

However, as mentioned above, when the adherent cultures were characterized, it was observed that these cultures were mixed, containing neural progenitor cells and neural markers but also many other markers. Therefore, it was decided to purify these cultures to obtain cell cultures more specific to neuron and glia and to eliminate any other cell type. For that, we selected from these adherent cultures the cells that would give rise to neurons and astrocytes.

After cell separation by MACS, and after 5 days for culture stabilization (the cells that survive the magnetic separation begin to adhere to the flask and differentiate), it was observed that the cell separation had been carried out correctly, since the presence of the PSA-NCAM marker was found in the cells of the neuron-enriched cultures. PSA-NCAM is a highly polysialylated variant of NCAM, which is predominantly expressed in embryonic and neonatal neural tissue (Kiss & Muller, 2001), as well as in actively proliferating late intermediate neuronal progenitor cells (Seki, 2002). Indeed, PSA-NCAM is still present in the adult brain in a spatially restricted manner, contributing to functions such as synaptic plasticity, structural remodeling between neuronal and glial elements, cell migration and cell differentiation (Bonfanti & Nacher, 2012).

30 days after separation and seeding of the neuron-enriched cultures, these PSA-NCAM^{+} cells exhibited neuronal shape and long prolongations that connected to other cells via a button-like synaptic connection between two different cells. In addition, immunofluorescence assays confirmed the results obtained through the observation of these cultures in the brightfield microscopy. Thus, these cultures

showed positive labeling against neuronal antibodies such as MAP1B, Nestin, β-tubulin, NeuN and MAP2. MAP1B is a particular protein predominantly expressed during the initial phases of nervous system development, having functions like axonal guidance and elongation. Within the adult brain, MAP1B plays a role in the regulation of the structure and functioning of dendritic spines within glutamatergic synapses, and it is also identified in presynaptic synaptosomal preparations (Bodaleo et al., 2016).

These data suggest that the vast majority of cells in the neuron-enriched culture are neurons at different stages of development, with a scarce proportion of glial cells and null presence of epithelial cells. These findings are in line with other studies carried out in olfactory neuroepithelium where even without separating the cell cultures into neuron-enriched cultures, they are able to detect the presence of these neuronal markers (Delgado-Sequera et al., 2021; Galindo et al., 2018; Matigian et al., 2010).

In contrast to the neuron-enriched cultures, we did not find the presence of PSA-NCAM in glia-enriched cultures 5 days after MACS separation. Moreover, after 30 days of seeding, in glia-enriched cultures both brightfield and immunofluorescence characterization demonstrated a different growth pattern and the presence of specific glial proteins such as GFAP. Glia-enriched cultures presented a different growth pattern, with larger aggregates and less elongated cells. Furthermore, immunocytochemistry of the glia-enriched culture showed GFAP-positive cells confirming the presence of astrocytes in the glia-enriched cultures. These results are in line with previous studies, where the presence of astrocytes in olfactory neuroepithelium has also been observed (Delgado-Sequera et al., 2021; Hahn et al., 2005; Wolozin et al., 1992).

Finally, the immunofluorescence assay with the EpCAM marker showed the absence of EpCAM expression in both cultures. This observation leads to the conclusion that the presence of epithelial cells in these cultures can be discarded. This reaffirms the accuracy of the separation process and confirms the successful

enrichment of the desired cell types - neurons and glia - in the culture, demonstrating the efficacy of the experimental protocol.

FACS results showed that, as expected, in the neuron-enriched cultures, the majority of cells exhibited positivity for the neuronal marker NeuN. Conversely, there was minimal presence of cells positive for the astrocytic marker GFAP, and no detectable presence of cells positive for the epithelial cell marker EpCAM.

In the case of glia-enriched cells, just the opposite happened. In the glia-enriched cultures, the majority of cells exhibited positivity for the astrocytic marker GFAP, underscoring the successful enrichment of astrocytic populations. Conversely, there was minimal presence of cells positive for the neuronal marker NeuN. Similar to the findings in neuron-enriched cultures, there was no detectable presence of cells positive for the epithelial cell marker EpCAM in glia-enriched cultures.

These results further validate the successful enrichment of neuronal populations in the cultures after separation by MACS and differentiation with the selective culture medium for neurons, emphasizing the specificity of the experimental approach and the effective separation of neuronal cell types.

It is also important to mention that in both cultures there was a high percentage of cells, approximately 41-43%, that were not positive for any of the markers. The low percentages observed in the FACS data might be attributed to potential cell stress during sample processing, leading to cell damage or death. While a definitive assessment necessitates the incorporation of viability markers like propidium iodide (PI), it is conceivable that the subset of cells negative for both markers could be cells in a dead state due to processing protocols. This assumption aligns with their appearance in Forward Scatter (FSC) vs. Side Scatter (SSC), where all cells display a closely aggregated pattern with values approximating to 0.

Another interesting observation to comment is the percentage of cells that are positive for both the neuronal marker and the glia marker. As discussed above,

this may be due to the maturation state of the cells, since these cultures are not fully mature, and as they are in immature neuronal stages, the expression of certain antibodies persists (Omlin & Waldmeyer, 1989). Linked to this, we find that the limitation of the study is the use of magnetic beads with PSA-NCAM. As this protein is a marker for immature neuronal-committed progenitors, due to the immaturity of the cells, it can make the selection less effective. Nevertheless, to date, PSA-NCAM is the only neuron-specific protein expressed in the surface of the cell that can be used for the magnetic sorting in humans.

In this sense, to decrease cell death and improve the model for future applications, several strategies could be considered. First, optimizing cell culture conditions, such as adjusting nutrient levels or applying known anti-apoptotic agents or growth factors, could improve cell viability and result in less cell death. On the other hand, it would be useful to develop alternative markers that show greater specificity towards neuronal or glial cells. Moreover, improved isolation techniques or the use of advanced imaging technologies could help to distinguish and characterize cells more accurately, thus reducing the percentage of cells lacking definitive markers and improving the reliability of the model results.

Finally, it would be interesting to explore the possibility of extending the duration of cell culture in future experiments, allowing cells to mature for a longer period. This extended culture time could lead to the development of mature cells, potentially resulting in the loss of simultaneous expression of neural and glial markers. A secondary objective of the study was to detect in the neuron- and glia-enriched cultures any possible remaining cells after selection of PSA-NCAM-positive cells that were not of neural lineage. Therefore, EpCAM antibody was used for the detection of possible epithelial cells, as they are present in large quantities in the nasal cavity. EpCAM is a cell-cell adhesion molecule highly expressed in embryonic liver (De Boer et al., 1999; Schmelzer et al., 2006). It is a type I glycoprotein of 33–40 kDa with a long extracellular (EpEX) domain, a single transmembrane region and a 26 amino acid short intracellular tail (EpICD) (Imrich et al., 2012) located on the surface of epithelial cells. In both cultures, the

% of cells positive for EpCAM was less than 1%. Therefore, it can be said that the culture does not contain any cells that are not of neural lineage.

Given these experimental conditions, achieving a culture that is completely purified culture of either neurons or glia is extremely difficult.

As previously explained, the final objective of the work was to find a biological substrate from patients that allows the identification and quantification of trait, state, or prognostic biomarkers associated with the disease. To explore this, we aimed to investigate whether these enriched cultures could generate and release specific molecules detectable in the culture medium, potentially serving as biomarkers. To achieve this, we conducted measurements on established parameters used in psychiatric research, focusing on components associated with inflammation. These included IFNγ, PGE_2, IL-6, and Kyn/Trp (Leza et al., 2015).

Both types of cultures demonstrated the capability to produce and release these compounds. Notably, distinct variations were observed in the levels of PGE_2, Kyn/Trp, and IFNγ between neuron and glia enriched cultures. However, no significant alterations were detected in IL-6 levels.

Specifically, PGE_2 and Kyn levels exhibited significant increases in glia-enriched cultures in comparison to neuron-enriched cultures, while IFNγ levels were notably higher in neuronal cultures than in glia-enriched ones. These findings underscore that both culture types manifest varying levels of these molecules, suggesting that fluctuations in these mediators could serve as potential biomarkers.

Schizophrenia-associated neurodevelopmental fingerprint in human neural progenitor cells

Neurospheres, considered as three-dimensional aggregates of neural stem cells, play a key role in the maintenance and regeneration of the nervous system and in the repair of brain lesions, proving to be an effective and promising approach in the field of neuropsychiatry (Ahmed, 2009; Merkle & Alvarez-Buylla, 2006).

Our study has shown that, compared to healthy individuals, schizophrenia patients showed a reduction in the growth and proliferate rate of these cellular structures and, concomitantly, a significantly smaller size. These abnormalities suggest possible alterations in the processes of neuronal proliferation and differentiation in pathological contexts, which could have important implications for the functionality and balance of the nervous system.

Initially, the disparities may not be as pronounced, but over time, these differences gradually become more pronounced, eventually resulting in significant differences between the two groups. This progressive evolution suggests an intricate interaction between neuronal proliferation and the underlying pathophysiology of schizophrenia.

The observed differences in the proliferation and size of neurospheres derived from individuals with schizophrenia in comparison to controls can be explained by a multitude of factors. Firstly, the significant genetic component of schizophrenia is a key influencing factor. Alterations in specific genes associated with myelination, neurodevelopment and the AKT pathway have been studied in subjects with schizophrenia (Kumarasinghe et al., 2013). They may be significantly affecting neurosphere formation and expansion. In this sense, schizophrenia is a chronic neurodevelopmental disorder signified by an increase in the expression of apoptotic molecular signals. *Postmortem* studies have reported a reduced number of dendritic spines, especially on pyramidal neurons located in layer-III of the PFC, in the superior temporal gyrus, and in hippocampal subfields (CA3) (Li et al., 2015; Moyer et al., 2015). Moreover, impaired adult neurogenesis, has been associated with cognitive impairments that are often present in patients with psychiatric disorders such as major depression, schizophrenia, anxiety disorders, and addictive behaviors (Christian et al., 2014). Extensive research has revealed correlated alterations in adult hippocampal neurogenesis across various pathophysiological conditions, including aging, epilepsy, stroke, neurodegenerative disorders, and psychiatric diseases (Parent, 2003; Sahay & Hen, 2007; Winner et al., 2011). Interestingly, most psychiatric

disorders, such as major depression, schizophrenia, anxiety disorders, and addiction, exhibit diminished cell proliferation and decreased hippocampal volume. These changes are closely linked to compromised hippocampus dependent functions, encompassing specific memory, recognition memory, and spatial pattern separation (Lie et al., 2004; Mirescu & Gould, 2006; Morris et al., 2010; Nixon et al., 2010; Reif et al., 2007; Revest et al., 2009)

Moreover, alterations in neurotransmitter systems such as dopamine, glutamate, or serotonin, commonly associated to schizophrenia (Stahl, 2018), may disrupt the signaling pathways crucial for cell proliferation. The classical neuromodulatory effects of these monoamines exert a significant impact on neurogenesis, especially as levels of monoaminergic neurotransmitters fluctuate in the brain during psychiatric disorders, aging, or neurodegenerative conditions (Apple et al., 2017). Consequently, these alterations could directly influence the growth and dimensions of neurospheres.

Considering schizophrenia as a neurodevelopmental disorder clarifies these differences even more. In this sense, although the hypothesis of abnormal synaptic pruning in schizophrenia (Feinberg, 1982) has not been entirely corroborated, this hypothesis could explain the differences observed between the neurospheres of individuals with schizophrenia and control subjects. Several investigations indicate that a majority of excitatory synaptic inputs in the brain engage in asymmetrical synapses on dendritic spines. *Postmortem* examinations of the brain have disclosed a reduction in spine density on cortical pyramidal cells among schizophrenia patients in comparison to the control group (Broadbelt et al., 2002; Garey, 2010; Glantz & Lewis, 2000; Kalus et al., 2000). The axo-dendritic synapses onto spines, particularly of this nature, are predominantly eradicated during the process of developmental synaptic pruning. Conversely, at the molecular level, a multitude of studies have showcased declines in diverse presynaptic protein markers in the brains of individuals with schizophrenia (Faludi & Mirnics, 2011). While these studies are consistent with the conclusion that there are fewer synaptic connections in the *postmortem* brains of patients

with schizophrenia, it should be noted that these studies were conducted on adult brains and do not inform us about synaptic changes during the onset of symptoms in early adulthood.

Environmental factors, well-recognized for their impact on the development of schizophrenia (Stilo & Murray, 2019; Van Os et al., 2010), may also play a crucial role in contributing to differences in neurosphere formation. Factors such as prenatal infections, maternal stress, or exposure to toxins could significantly contribute to these observed disparities. Specifically, exposure to stress during early life (ELS) has been associated with a broad range of consequences later in life. Chronic ELS, a well-established inhibitor of neurogenesis in other neurogenic regions of the adult brain (Korosi et al., 2012; Mirescu et al., 2004; Naninck et al., 2015; Oomen et al., 2010), is accompanied by an overall reduction in proliferating cells and the number of putative adult neural stem cells in the adult hypothalamus (Bielefeld et al., 2021).

Finally, inflammation, particularly the dysregulation of the immune system and increased levels of inflammatory markers, has been observed in individuals with schizophrenia (Delaney et al., 2019; Kelly et al., 2018). Studies suggest that neuroinflammation induced by peripheral immune activation (e.g.,infections, injuries) causes diverse neuropsychiatric symptoms in individuals (Miller et al., 2011). Inflammation might affect the proliferation and survival of certain types of cells, including neural stem cells and progenitor cells, which are crucial for the generation of new neurons and maintaining brain health. Neuroinflammation and disorganization of synapses are common features in several developmental and neurodegenerative disorders, suggesting that factors that affect glia cells during development may also have long-term effects on synapse function. Some studies propose that neuroinflammation during perinatal life changes the ability of glia cells to sculpt neuronal synapses. Thus, either by increasing or decreasing elimination of synapses these changes may have important long-term effects on developmental psychiatric disorders (Mottahedin et al., 2017).

Schizophrenia-associated transcriptomic fingerprint

In our quest to unravel the molecular underpinnings of schizophrenia, we conducted a comprehensive transcriptomic analysis on neuron- and glia-enriched cultures. The results of this study shed light on significant gene alterations observed in neuroepithelium samples from subjects diagnosed with schizophrenia.

The results of **neuron-enriched cultures** indicated that patients with schizophrenia were discriminated from healthy controls by the gene expression levels in neurons. Furthermore, the genes differentially expressed have diverse connections to neuronal aspects. In this case, altered genes are associated with ontologies associated with cellular proliferation, developmental growth, synaptic transmission modulation, and cell morphogenesis involved in differentiation.

Glutamate is the most abundant fast excitatory neurotransmitter in the mammalian nervous system, with a critical role in synaptic plasticity. Several lines of evidence link the glutamate system to psychosis, in particular the observation that glutamate-receptor agonists can cause psychotic symptoms in unaffected individuals. In this context, several glutamatergic genes showed evidence of epigenetic dysregulation in psychosis (Mill et al., 2008). Subsequent investigations for related neurotransmitters revealed that the gene encoding Secretogranin II (*SCG2*), a secretory protein located in neuronal vesicles that is known to stimulate the release of glutamate, was hypomethylated in females suffering psychosis relative to unaffected controls (Mill et al., 2008). In addition, *SCG2* expression is known to be modulated by both chronic PCP exposure, which mimics symptoms of major psychosis (Marksteiner et al., 2001), and lithium treatment (McQuillin et al., 2007). This gene showed a large reduction of its expression in neuron-enriched cultures of subjects with schizophrenia. Unlike glutamate, which is a strong excitatory neurotransmitter, GABA acts as a potent inhibitory neurotransmitter. Hypofunctioning GABAergic interneurons appear to be important in the etiology of psychosis (Benes & Berretta, 2001). Finally, a number of physiological functions in the nervous system have been assigned to

this gene (Gasser et al., 2003; Li et al., 2008; Shyu et al., 2008; You et al., 1996) and *SCG2* has been postulate as a good candidate for the signal integrator required as activity-dependent plasticity, such as associative learning and memory (Iwase et al., 2014). These functions are altered in patients with schizophrenia, which may be associated with a downregulation of this gene.

L1CAM, the third most downregulated gene in our results, stands out as a crucial adhesion molecule integral to the nervous system's development. It's known for its role as a neuronal cell adhesion molecule, pivotal in fostering axonal growth (Chang et al., 1987; Rathjen & Schachner, 1984) and facilitating diverse processes at different developmental stages of the nervous system (Linneberg et al., 2019). In addition, more recent studies have linked *L1CAM* deletion in neurons to an earlier age-related decline in hippocampal neurogenesis. These data suggest that *L1CAM* is not only important for normal nervous system development, but also for maintaining certain neuronal processes in adulthood (Grońska-Pęski et al., 2020).

Remarkably, *L1CAM* has been observed to be in various cell types, including neurons (Beer et al., 1999). Notably, the presence of proteolytic fragments in brain lysates peaks postnatally (Mechtersheimer et al., 2001), hinting at a connection between developmental shifts and the shedding of *L1CAM*. The clinical manifestation of human *L1CAM* mutations, alongside observations from multiple mouse models, strongly suggests *L1CAM*'s involvement in pivotal neurological functions. This includes the facilitation of neuron migration, neurite outgrowth, axon guidance, and interactions between axons and glial cells. Moreover, it has been observed how in humans, loss of *L1CAM* expression in cultured ES-derived neurons leads to deficits in axonal and dendritic arborization (Patzke et al., 2016).

On the other hand, *NUF2*, the most upregulated gene in our results, gene participates in the regulation of cell apoptosis and proliferation by regulating the binding of centromere and spindle microtubules to achieve the correct separation

of chromosomes (Hu et al., 2015; Nabetani et al., 2001). The upregulation of the *NUF2* gene, a component of the NDC80 kinetochore complex, has sparked interest in its potential relationship with schizophrenia. While direct causation has not been firmly established, studies have stablished a plausible association. Dysregulation of *NUF2* expression levels have been observed in certain brain regions of individuals diagnosed with schizophrenia compared to healthy controls (Hertzler et al., 2020; Xia et al., 2019). This dysregulation might disrupt the delicate balance of cellular processes linked to cell division and neural function. However, the precise mechanisms underlying how increased *NUF2* expression might contribute to the manifestation or progression of schizophrenia remain an area of active investigation, warranting further exploration and experimentation.

Finally, Pleiotrophin (*PTN*), also highly overexpressed in our neuron-enriched cultures, emerges as a pivotal factor influencing neuronal development and function. This secreted cell cytokine, associated with the extracellular matrix, exerts a significant impact on neuron morphology, enhancing neurite length and the number of spiral ganglion neurons *in vitro* (Bertram et al., 2019). Its involvement in embryonic development is evident through predominant expression in neuroectodermal and mesodermal tissues, suggesting a role in neuron migration and epithelium-mesenchyme interactions (Rauvala, 1989; Wellstein et al., 1992).

Recent studies have underscored *PTN*'s growing prominence as a crucial neuromodulator, influencing multiple neuronal functions (González-Castillo et al., 2015). In this line, they have suggested *PTN* as a susceptibility gene for schizophrenia (Lv et al., 2020). This is particularly noteworthy considering the implications of aberrant neurogenesis in conditions like schizophrenia, which is associated with hippocampal volume reduction and cognitive impairment in affected individuals (Eisch et al., 2008; Reif et al., 2007). *PTN*'s influence on these neurological processes highlights its potential significance in understanding

and addressing conditions involving disrupted neurodevelopment, such as schizophrenia.

Understanding how these genes interact in the neuronal context is essential to advance our understanding of neural processes and potential implications in disorders such as schizophrenia.

The gene expression results of **glia-enriched cultures** indicate that patients with schizophrenia could also be differentiated from healthy controls by the gene expression levels in glial cells. In the context of schizophrenia, several genes have been studied for their potential relevance to the disorder. In this case, the alteration of genes appears to affect ontologies related to axonogenesis, extracellular matrix organization, synaptic transmission modulation, and cellular migration regulation.

Among all the downregulated genes, some of them are associated with various aspects of neural function, the central nervous system, neurodevelopment, and schizophrenia susceptibility. Notably, ubiquitin C-terminal hydrolase L1 (*UCH-L1*), a neuron and brain-specific protein accounting for 1% to 5% of total soluble brain protein (Kobayashi et al., 2004) emerges as one of the most significantly downregulated genes. The ubiquitin-proteasome system plays a crucial role as a master regulator in neural development, maintaining brain structure and function. Its influence extends to neurogenesis, synaptogenesis, and neurotransmission by orchestrating the localization, interaction, and turnover of scaffolding, presynaptic, and postsynaptic proteins. Additionally, this system transduces epigenetic changes in glial cells independently of protein degradation, contributing to a broad spectrum of brain conditions when its components and substrates malfunction (Luza et al., 2020).

UCH-L1 is vital for axonal function and potentially critical in the repair of damaged axons and neurons by eliminating abnormal proteins. Studies have consistently shown reduced expression of multiple proteins, including UCH-L1, in schizophrenia (Rubio et al., 2013). Recent investigations have further

evidenced notably lower gene expression and protein levels of UCH-L1 in the DLPFC and serum of individuals with schizophrenia compared to healthy controls (Andrews et al., 2017; Demirel et al., 2017; Novikova et al., 2006; Schubert et al., 2015; Vawter et al., 2001; Wang et al., 2017). These molecules serve diverse roles as neuromodulators, especially in influencing synaptic plasticity, myelination, and dopamine metabolism, all of which are key mechanisms discussed in the pathogenesis of schizophrenia.

Notably, the decrease in serum UCH-L1 levels was found to correlate with the Positive and Negative Syndrome Scale (PANSS) total and PANSS general psychopathology scores in individuals with schizophrenia (Demirel et al., 2017). This underscores the potential significance of *UCH-L1* in understanding and assessing the clinical manifestation of schizophrenia.

Neuronal pentraxins (*NPTX*s), another downregulated gene observed in patients with schizophrenia, have emerged as pivotal extracellular scaffolding proteins, showing promise as biomarkers for synaptic dysfunction in neurodegenerative conditions. Comprising three proteins – neuronal pentraxin 1 (NPTX1), neuronal pentraxin 2 (NPTX2) and NPTXR – this family actively participates in homeostatic synaptic plasticity by recruiting postsynaptic receptors to synapses. Recent research focuses on dynamic changes in NPTX levels within the CSF as indicative of synaptic damage, potentially associated with cognitive decline. In this sense, one study, has revealed simultaneous reductions of NPTX1/2/R in the CSF of individuals with schizophrenia in comparison to control subjects (Xiao et al., 2021). While limited studies exist for NPTXR, NPTX2 has been suggested as a plausible biomarker for schizophrenia. *NPTX2*, an immediate-early gene, assumes a critical role in regulating synaptic activity and neuroplasticity, crucial in neurodevelopmental processes (Tsui et al., 1996). Investigations exploring the link between *NPTX2* and schizophrenia have shown downregulation in *NPTX2* gene expression and mRNA levels (Manchia et al., 2017).

Lastly, Although *MAP1B* is one of the least downregulated genes, it remains a relevant gene due to its significant implications in neuronal microtubule-associated proteins (MAPs). *MAP1B* stands out as a major contributor, playing a crucial role in neuronal morphogenesis (Hirokawa, 1990, 1994). MAPs exhibit diverse expressions in both the CNS and peripheral nervous system (PNS), with *MAP1B* and *MAP2* being among the most abundant. *MAP1B* is notably expressed during the early stages of neuronal development (Tucker, 1990), pivotal for axonal development and regeneration, while *MAP2* spans both early and late stages (Sánchez et al., 2000).

Emerging genetic evidence emphasizes the central role of microtubules (MTs) in neuronal migration, a fundamental process in nervous system development. Perturbations in MT dynamics or organization due to MAP loss result in abnormal motility of migrating neurons. Studies in *MAP2*- and *MAP1B*-deficient mice have highlighted migration defects in cortical neurons (Rakic, 1988; Sheldon et al., 1997; Trommsdorff et al., 1999). This suggests a synergistic involvement of these proteins in neuronal cell migration (Teng et al., 2001).

Additionally, research has delineated three distinct stages in the organization of microtubules within neuronal growth cones. Significantly, increased occurrences of stages 1 and 2 were observed in *MAP2*- and *MAP1B*-deficient mouse neurons, indicating a selective impairment in the formation of compact structures (stage 3). This deficiency arises due to the proteins' inability to facilitate microtubule bundling, potentially reducing the motility of neuronal growth cones (Teng et al., 2001).

Among the upregulated genes, *FGF18* stands out as one of the most highly upregulated. Recent studies link genetic variations in fibroblast growth factor receptor (*FGFR*) to an increased risk of schizophrenia (O'Donovan et al., 2009). Fibroblast growth factors (*FGF*s), integral to glial growth factors, control brain structure growth, regulate neuronal tissue maintenance, and repair. The FGF system's involvement in schizophrenia-related processes has been highlighted in

multiple studies, demonstrating schizophrenia-related traits in rodents through *FGF* manipulation (Van Scheltinga et al., 2010). This system's aberrations might serve as a broader risk factor for psychiatric disorders, including mood disorders (Turner et al., 2006), given the observed overlap in symptomatology among the major psychiatric diagnoses (Murray et al., 2005). Disturbances in *FGF* signaling impact dopamine signaling, cortical functions, and neurodevelopmental processes, all implicated in schizophrenia (Thompson et al., 2004). Finally, genetic variations in growth factors may reduce plasticity and compromise neuroprotection, affecting responses to prenatal and lifelong environmental challenges, notably influencing adult neurogenesis in brain regions like the hippocampus (Kempermann et al., 2008). Disturbed adult neurogenesis may result in prolonged developmental problems and some of the symptoms of schizophrenia. These findings make *FGF*s plausible candidate genes for schizophrenia.

Another notable gene among the top 10 most upregulated genes was Semaphorin 6D (*SEMA6D*), belonging to a gene family responsible for encoding proteins that regulate axon guidance. Semaphorins play a multifaceted role, influencing various crucial processes in neural development, such as determining neuronal cell process identities, synapse formation, axon pruning, and dendrite regulation (Alto & Terman, 2017; Leslie et al., 2011). These genes have broader associations with neurodevelopmental conditions, extending beyond schizophrenia. They have been implicated in autism spectrum disorder (Mosca-Boidron et al., 2016), language disorders (Chen et al., 2017; Ercan-Sencicek et al., 2012), attention deficit hyperactivity disorder (Demontis et al., 2019; Hawi et al., 2018), and schizophrenia (Arion et al., 2010). All these conditions share underlying genetic and neural risk factors

Although these were genes that were not as upregulated among subjects with schizophrenia, it is also important to note the autism susceptibility candidate 2 (*AUTS2*) and *EPHB6.*

AUTS2 is primarily expressed in the developing brain (Bedogni et al., 2010), plays a crucial yet unclear role in neuronal development. Variations in this gene might impact transcriptional regulation and contribute to neurodevelopmental disorders (Amarillo et al., 2014; Bedogni et al., 2010; Pennacchio et al., 2006). Classically, *AUTS2* has been associated with autism (Bakkaloglu et al., 2008; Ben-David et al., 2011; Huang et al., 2010), alcohol consumption (Schumann et al., 2011), heroin dependence (Chen et al., 2013) and suicide (Chojnicka et al., 2013).

Although this gene has long been linked to Autism Spectrum Disorder (ASD), it is necessary to understand later discoveries to study the relationship between *AUST2* and schizophrenia. First, it has been observed that exists a genetic overlaps between autism and schizophrenia, with shared risk genes like *CNTNAP2* (Burbach & van der Zwaag, 2009). Additionally, schizophrenia presents a significant risk for suicide, particularly among younger individuals (Qin, 2011). Finally, some studies suggest that developmental neuropathologies in specific brain pathways contribute to both schizophrenia symptoms and vulnerability to addictive behavior. Thus, drug addiction and schizophrenia might have overlapping neurobiological substrates within the hippocampus and subcortical structures (Chambers et al., 2001; Green et al., 2002; Smith et al., 2011). Taken together, these findings indicate that it is vital to determine whether *AUTS2* is also associated with schizophrenia. In this sense, recent studies has associated *AUTS2* gene with schizophrenia and indicate that the *AUTS2* gene might play an important role in the etiology of schizophrenia (Zhang et al., 2014).

Finally, *EPHB6* is a member of the erythropoietin-producing human hepatocellular (Eph) receptors, a group of transmembrane receptor tyrosine kinases that interact with ephrin ligands and controls multiple aspects of neuronal development (Lisabeth et al., 2013; Nievergall et al., 2012; Wilkinson, 2014), including synapse formation and maturation, as well as synaptic structural and functional plasticity. Activation of EphB receptors by B-type ephrins in neurons

swiftly triggers dendritic spine formation and growth, along with accelerated synapse maturation.

Moreover, *EPHB6* plays a significant role in maintaining gut homeostasis. Emerging research in schizophrenia links the gut microbiome to the brain via the gut-brain axis, involving tryptophan metabolism (O'Mahony et al., 2015), neurotransmitter synthesis, and immune pathways (Kelly et al., 2021; Stilling et al., 2016). Changes in *EPHB6* expression might alter gut microbiota, associated with various conditions, from chronic gastrointestinal disorders to neurodevelopmental and neuropsychiatric disorders (Schroeder & Bäckhed, 2016). Some studies underscore the pivotal role of gut microbiota in diverse CNS pathologies, spanning mood disorders, Alzheimer's disease, addiction, and schizophrenia (Dinan et al., 2014; Patrono et al., 2017). More recent studies on correlations between gut dysbiosis and psychiatric diseases have observed a strong connection between schizophrenia and altered gut microbiota (Golofast & Vales, 2020; Lv et al., 2017; Zheng et al., 2019).

Once again, to the best of our knowledge, our study stands as the only research revealing transcriptomic differences in cells obtained from the olfactory neuroepithelium of individuals with schizophrenia compared to controls. This unique finding emphasizes the novelty and distinctiveness of our research in shedding light on previously unexplored aspects of gene expression in relation to schizophrenia although further studies are needed to better understand how these genes interact and how they are specifically involved in the etiology of schizophrenia. As the only study of its kind, our work provides valuable insights that may pave the way for a deeper understanding of the molecular mechanisms underpinning schizophrenia, utilizing the olfactory neuroepithelium as an easily accessible tool for the study of the disease.

Schizophrenia induces an aberrant functioning of the Akt/mTOR/S6 signaling pathway

Upon analyzing transcriptomic data, and identifying several genes associated with neurodevelopmental alterations, our focus shifted to the exploration of proteins within the Akt/mTOR/S6 pathway. This pathway plays a pivotal role in neurodevelopment and neuroplasticity and in the context of schizophrenia, there is an emerging notion of an altered activity of the pathway in the brain of subjects with schizophrenia (Chadha et al., 2021; Ibarra-Lecue et al., 2020).

The protein expression study carried out in neuron- and glia-enriched cultures both with AlphaLISA® and WB led us to conclude that in neuron-enriched cultures, rpS6 is hypofunctional in subjects with schizophrenia. P70S6K also seems to be altered, as there is a decrease in both its total and phosphorylated forms in subjects with schizophrenia compared to controls in neuron-enriched cultures, and an increase in ratio phospho(Thr389)-p70S6K / p70S6K in glia-enriched cultures in subjects with schizophrenia compared to controls. Finally, although through AlphaLISA® assays we were not able to detect any alterations in Akt protein, WB experiments conclude that Akt kinase is hyperactive in neuron-enriched cultures of subjects with schizophrenia.

Akt, being a multifunctional protein kinase, plays a crucial role in various functions such as cell growth, survival, and neuronal plasticity. Studies investigating genetic variations in AKT1 have revealed associations between certain polymorphisms and susceptibility to schizophrenia development in cannabis users (Di Forti et al., 2012). However, *postmortem* studies have reported contradictory findings regarding total Akt expression, with some indicating an increase (Hino et al., 2016) and others reporting a decrease (Chadha & Meador-Woodruff, 2020; Ibarra-Lecue et al., 2020). Moreover, while specific studies on phospho(Thr450)-Akt are limited, research on phospho(Ser473)-Akt has suggested a decrease in this phosphoprotein (Chadha & Meador-Woodruff, 2020) opposite to the results observed in our assays. However, contrasting findings

emerged from other studies, which showed no significant variation (Hino et al., 2016).

On the other hand, animal studies have linked cognitive impairment in mice exposed to fetal maternal infections to AKT1 deficiencies (Bitanihirwe et al., 2010). Additionally, research has shown an increased phospho(Ser473)-Akt/Akt ratio in mice treated with chronic THC (Ibarra-Lecue et al., 2018). These findings corroborate some studies on *postmortem* tissues of individuals with schizophrenia (Chadha & Meador-Woodruff, 2020).

mTOR, a crucial protein kinase in cell growth and survival processes, forms complexes (mTORC1) that modulate vital downstream functions, particularly in synaptic plasticity and neurodevelopment. *Postmortem* studies have noted negative dysregulation in the phospho(Ser2448) form of mTOR in both mTORC1 and mTORC2 complexes, impacting mTOR downstream functions (Chadha & Meador-Woodruff, 2020). Additionally, proteomic studies have highlighted mTOR dysregulation in schizophrenia patients, with mTORC2 dysregulation linked to neuronal impairment and synaptic plasticity (Huang et al., 2013). In our study, it appeared to be a decrease in mTOR total protein levels in neuron-enriched cultures of subjects with schizophrenia compared to controls, but it was not statistically significant. Furthermore, increasing evidence identifies mTOR pathway, which regulates downstream activity of p70S6K, as a crucial molecular substrate underlying schizophrenia related psychopathology and antipsychotic drugs efficacy (Gururajan & van den Buuse, 2014; Liu et al., 2015). A significant reduction in mTOR/p70S6K signaling was observed in the PFC of patients with major depressive disorder relative to controls (Jernigan et al., 2011). In line with our findings, it has been reported that antipsychotic drugs increase mTOR and p70S6K signaling in the mouse striatum (Park et al., 2018; Valjent et al., 2011). For example, olanzapine have been found to activate the mTORC1 signaling pathway (Park et al., 2018) and the typical antipsychotic haloperidol selectively increased phosphorylation levels of p70S6K in DRD2-expressing striatal medium spiny neurons (Valjent et al., 2011).

rpS6, a ribosomal protein implicated in protein synthesis and CNS regulation (Puighermanal et al., 2017), has shown decreased levels of its phosphorilated form in *postmortem* studies of subjects with schizophrenia (Chadha et al., 2021; Ibarra-Lecue et al., 2020) while no changes were found in the total form of rpS6 (Chadha et al., 2021). Our findings align with these results, demonstrating a decrease in the phospho(Ser235/236)-rpS6 / rpS6 ratio in individuals with schizophrenia both with AlphaLISA® and WB. Consistent with our results, previous research has shown a broad dysregulation of protein synthesis in olfactory neurosphere-derived cells from individuals with schizophrenia. This dysregulation involves not only rpS6 but also numerous other ribosomal proteins (English et al., 2015). Additionally, the deficiency in the phosphorylation of rpS6 has been shown to impact the translation efficiency of a subset of mRNAs in specific brain regions of mice (Puighermanal et al., 2017). The observed hypofunction of rpS6 in individuals with schizophrenia, coupled with results from *postmortem* studies indicating reduced spine density in the cortex of these individuals (Moyer et al., 2015), further supports the hypothesis that disruptions in protein synthesis and dendritic architecture may ultimately contribute to the dysfunction in synaptic connectivity underlying the clinical manifestations of schizophrenia.

Finally, regarding ERK protein, within the ERK/MAPK cascade, is fundamental in neurodevelopment, regulating cell proliferation and differentiation. Thus, its aberrant function has been implicated in the development of neurodevelopmental diseases, including schizophrenia. However, some *postmortem* studies have shown a positive regulation of the ERK/MAPK pathway in schizophrenia (Iroegbu et al., 2021) while others have not found changes in the amount of total and phosphorylated ERK protein leves (Hino et al., 2016).

Variations in results between AlphaLISA® and WB techniques when measuring the same protein and phosphorylation can stem from inherent differences in the principles and sensitivities of these methods. AlphaLISA® relies on a proximity-based assay, where signals are generated when donor and acceptor beads come

into close proximity due to specific interactions. In contrast, blotting techniques, such as WB, detect proteins based on their size and charge through electrophoretic separation and transfer to a membrane. Discrepancies may arise due to the diverse mechanisms underlying each technique, including potential interference in the AlphaLISA® assay from factors like assay conditions, sample matrix, or compound interference. Moreover, differences in detection sensitivity and dynamic range between the two methods can contribute to variations in measured protein levels.

5.2. Study II: Double-hit mouse model of MIA and THC chronic treatment

Developing an animal model that accurately replicates the intricate spectrum of schizophrenia symptoms is crucial for advancing treatment discovery and understanding the underlying mechanisms of this condition. While no existing animal model that fully mirrors the complexity of schizophrenia, double-hit models have proven to be among the most representative.

The second part of this Doctoral Thesis focused on creating a double-hit animal model by combining MIA with chronic THC treatment. MIA models, extensively used to simulate neuropsychiatric disorders like autism spectrum disorder and schizophrenia (Haddad et al., 2020), are rooted in human epidemiological studies. These studies identified prenatal viral infections as a risk factor for offspring, which grants the MIA model construct validity and translational relevance to human disease (Jones et al., 2011).

The initial hit or priming event involves inducing MIA by administering the antiviral immunity activator Poly(I:C) during pregnancy. This model has been thoroughly validated (Careaga et al., 2018; Meyer, 2014), and our laboratory has worked previously with it (MacDowell et al., 2021; Perez-Palomar et al., 2023; Prades et al., 2017).

Several authors have validated the Poly(I:C) elicited immune response to induce sickness behavior in pregnant dams, a hallmark of MIA (Ballendine et al., 2015; Song et al., 2011). However, multiple methods exist to induce MIA, including LPS (bacterial cell wall endotoxin) (Moreno-Fernández et al., 2023) or human influenza virus (Brown et al., 2004; Wischhof et al., 2015).

In this study, we validated the maternal immune response triggered by Poly(I:C) administration by monitoring body weight, temperature and offspring changes in pregnant dams treated with either saline or Poly(I:C).

Regarding temperature alterations, previous research indicates that Poly(I:C) administration commonly induces a decrease in rectal and surface temperature, resulting in a typical hypothermic response in mice (Careaga et al., 2018; Cunningham et al., 2007; Lins et al., 2018). In our study, pregnant dams treated with Poly(I:C) exhibited a more noticeable temperature reduction compared to those given saline, although this distinction did not reach statistical significance. This discrepancy might be attributed to the challenge of precisely controlling temperature, influenced by various experimental factors. Moreover, variations in administration timing and routes among different studies (Careaga et al., 2018; Lins et al., 2018; Mueller et al., 2019) or using diverse species (Careaga et al., 2018; Lins et al., 2018) could impact temperature measurements.

Regarding body weight, Poly(I:C) caused a significant reduction in the weight of pregnant dams at 6 and 8 hours post-administration, with a complete recovery observed 24 hours after Poly(I:C) administration. The decline in maternal body weight aligns with the sickness behavior induced by Poly(I:C) documented in prior studies (Careaga et al., 2018; Cunningham et al., 2007; Mueller et al., 2019). Conversely, saline treated pregnant dams also exhibited slight body weight reduction, likely associated with a stress response post-injection (Cunningham et al., 2007). However, these changes were minor and transient, fully restoring within 24 hours after the injection.

Finally, following immune response activation, cytokines are released, potentially influencing pregnancy outcomes by leading to abortion or reducing litter size (Arck et al., 1995; Joachim et al., 2001). In our investigation, administration of 5 mg/kg of Poly(I:C) resulted in a significantly reduced litter size but did not induce abortion.

Considering the notable impact on body weight, temperature, and litter size resulting from Poly(I:C) administration to pregnant mice, it is reasonable to assume that this immunogenic substance triggered an infection-like response in our mice, resembling the innate immune reaction to a viral infection.

The double-hit mouse model produces alterations in memory and sensory information processing

One of the most extended behavioral paradigm that evaluates cognitive impairment of schizophrenia rodent models is the NORT, a widely used behavioral test that assesses episodic-like declarative memory (da Cruz et al., 2020; Ennaceur, 2010).

In this case, we evaluated the long-term episodic-like memory by performing the NORT 24 hours after the training session. When assessing the NORT long-term memory, we observed that both male and female control mice showed a correct discrimination index between the presented objects, as they increased their exploration towards the novel object. In contrast, MIA-exposed, THC-exposed and double-hit mice showed a cognitive impairment in the NORT long-term memory, with decreased DI scores compared to the controls' DI scores. In addition, the object discrimination was influenced by sex, as females had higher DI scores than males. All these findings indicate that each single-hit exposure is able to produce, in both males and females, a cognitive impairment that diminish the animal's ability to distinguish between novel and familiar objects. Indeed, male and female MIA+THC mice, the double-hit groups, showed the lowest DI scores compared to the other groups of same sex. Altogether, these results suggest that, despite combination of both hits is not able to produce a synergistic impairment in cognitive performance (no "hit x hit" significant interaction was found); the expected additive effects of both hits are shown in both sexes.

Our findings are consistent with previous reports demonstrating impairments in the NORT long-term recognition memory in the offspring of Poly(I:C) challenged pregnant dams (Perez-Palomar et al., 2023; Prades et al., 2017; Wolff et al., 2011).

Furthermore THC is considered an amplifying component of genetic and neurodevelopmental models of schizophrenia, or in other words, as a secondary or complementary component of a double-hit model. Hence, some studies using

double-hit rodent models of schizophrenia with Poly(I:C) exposure during pregnancy and THC in the peripubertal period have been conducted (Dalton et al., 2012; Guma et al., 2023; Hollins et al., 2016; Lecca et al., 2019; Ľupták et al., 2021; Moreno-Fernández et al., 2023; Stollenwerk & Hillard, 2021). These authors reported that either of the single-hit manipulations caused deficits on novel object recognition with impaired DI scores, but the combination of the two hits did not further exacerbate the disabilities (Guma et al., 2023; Jalewa et al., 2023; Moreno-Fernández et al., 2023). This lack of synergies or unmasking effects has also been reported by Stollenwark and Hillard (Stollenwerk & Hillard, 2021) who, using Poly(I:C) induced MIA, and oral THC exposure, examined spatial learning and memory in the Morris water maze. Therefore, it seems that the lack of synergies so far reported generalizes across immunogens and ways of administration of THC.

Altogether, our results showed impaired long-term memory performance in the NORT in single-hit and double-hit groups, but combining the Poly(I:C) challenge with THC chronic administration, failed to exacerbate the cognitive deficit or to produce a synergistic effect between both hits (although NORT DI scores in male and female double-hit groups were the lowest). This lack of effects may be explained by potential compensatory mechanisms operating during development. However, combination of both prenatal and postnatal insults is able to amplify schizophrenia-related cognitive deficits, making our double-hit mouse model a valid tool to study this particular domain of the disease.

Notably, the majority of the discussed studies in this section are performed exclusively in males. Only some of them (Guma et al., 2023; Jalewa et al., 2023; Moreno-Fernández et al., 2023; Stollenwerk & Hillard, 2021) evaluated the sex influence in the cognitive performance. In the case of Moreno-Fernandez, working memory of the offspring did not reveal any main effect of MIA, THC or MIA x THC. However, they found a significant effect of sex and a MIA x sex interaction indicating a decrease in the working memory of Poly(I:C) exposed males (significant effect of MIA in the males). Finally, they found no synergistic

or cumulative effects of Poly(I:C) induced MIA and adolescent THC exposure relating to working memory performance in the Y-maze.

In this regard, our work provides novel information on the sex influence on cognitive assessment in the NORT, as we observe that sex-influence has different impact on the long-term memory in males and females on this task.

On the other hand, we evaluated sensorimotor gating of the double-hit mouse model trough PPI. Sensorimotor gating alterations are recognized as an endophenotype of schizophrenia (Braff & Geyer, 1990) and loss-of-normal PPI occurs in schizophrenia patients (Ludewig et al., 2003). PPI evaluation shows high translational validity, as it has traditionally been used as a proxy to evaluate positive symptoms in human patients and animal models of schizophrenia-like behaviors (Halberstadt & Geyer, 2018; Ioannidou et al., 2018; Powell et al., 2009; Sato, 2020; Schmidt-Hansen & Le Pelley, 2012; Swerdlow et al., 1994, 2016; Wynn et al., 2004).

In our study, we observed a significant impairment in the startle response in the 82 dB but, contrary to our expectations, we did not detect any interaction with THC. Similarly, in the 87 dB we found a significant effect of MIA causing a reduction in the startle response. Furthermore, in this decibel, a Poly(I:C) x THC interaction was observed, resulting in a decrease of the startle response of males Poly(I:C)/vehicle group compared with the control group (saline/vehicle). No additional significant results were detected in the rest of PPI conditions.

Our results showed PPI impairment in both male and female mice exposed to Poly(I:C) induced MIA, in accordance with previous studies (Hao et al., 2019; Li et al., 2021; Pacheco-López et al., 2013). However, in agreement with the literature, we found no detrimental effects of THC exposure on PPI (Moreno-Fernández et al., 2023; Stollenwerk & Hillard, 2021). Importantly, there was no interaction between Poly(I:C) induced MIA and THC exposure during adolescence, suggesting that there were no summative or synergistic actions between both hits in this model, as previously reported in other two-hit models

(Garcia-Mompo et al., 2020; Guma et al., 2023; Moreno-Fernández et al., 2023; Rodríguez et al., 2017; Santoni et al., 2023; Stollenwerk & Hillard, 2021).

The double-hit mouse model produces alterations in genes involved in memory, regulation of neurotransmitter transport and synaptic signaling

After differential expression analysis involving mice injected with THC born from dams injected with Poly(I:C), or exposed to a combination of both substances, a consistent observation emerged: a distinct set of genes associated with behavior, GPCR-mediated signaling, the neuronal system, regulation of neurotransmitter transport, synaptic signaling, and transmission showcased alterations in their expression levels across all the compared groups. The alterations in these gene families following exposure to THC or MIA can be attributed to the intricate mechanisms of action of these interactions within the brain.

THC, as the main psychoactive compound in cannabis, interacts with the endocannabinoid system, which modulates various physiological processes, including neuronal signaling and neurotransmitter release. The modulation of gene expression is likely a consequence of its influence on cannabinoid receptors in the brain, particularly its predominant action on presynaptic CB1 receptors, leading to inhibitory effects on synaptic transmission (Felder et al., 1995). Furthermore, these compounds can trigger different CB1 receptor-mediated intracellular signaling pathways, which may contribute to functional specificity (Laprairie et al., 2015).

Furthermore, THC's impact on the endocannabinoid system may disrupt the processes that can also be involved in memory formation and learning. After prolonged exposure to THC, there is a shift from cortical regions involved in cognitive processes to subcortical regions, which are involved in memory and emotional processes to promote drug seeking and dependence (Hwang & Lupica, 2020; Lafferty & Britt, 2020). Additionally, the modulation of cannabinoid

receptors in the brain may produce a dysregulation in synaptic transmission that contributes to the cannabinoid-induced deficits associated with memory formation (Augustin & Lovinger, 2022). Similar impairments in hippocampal CA1 LTP are observed *in vivo* with repeated exposure to HU-210, a CB1 receptor full agonist (Hill et al., 2004). Moreover, these impairments are associated with deficits in working memory. Thus, it will be of interest to determine how cannabis use and THC exposure alter striatal synaptic plasticity and associated forms of learning and memory (Augustin & Lovinger, 2018).

Poly(I:C), on the other hand, mimics viral infection resulting in the dysregulation of the neuronal system. This immune activation can lead to the release of pro-inflammatory cytokines and subsequent alterations in gene expression due to the developing brain's susceptibility to environmental insults. Poly(I:C) MIA exposure induces expression of several inflammation-related genes, and the induction of these molecules plays a pivotal role in Poly(I:C) induced neuronal impairment (Yamada et al., 2018) given that cytokines are small signaling molecules of the innate immune system that also have defined roles in neurodevelopment (Garay & McAllister, 2010).

Moreover, Poly(I:C) induced immune responses may alter the delicate balance of neurotransmitter systems and synaptic signaling, contributing to alterations in gene families associated with neuronal function and behavior. Poly(I:C) produces structural and functional changes in the neurons in the offspring (Coiro et al., 2015; Fernández de Cossío et al., 2017). In this regard, the density of dendritic spines in pyramidal neurons of the cortex was found to be reduced in Poly(I:C) offspring (Baharnoori et al., 2009; Coiro et al., 2015; Li et al., 2014). This reduction in the structural integrity of synapses is accompanied by decreased expression of both presynaptic proteins and postsynaptic proteins in the cerebellum and hippocampus of Poly(I:C) offspring (Giovanoli et al., 2015, 2016; Pendyala et al., 2017). Finally, Poly(I:C) impairs synaptic transmission, primarily resulting in a reduced signal (Canetta et al., 2016; Coiro et al., 2015; Ito et al., 2010; Patrich et al., 2016; Shin Yim et al., 2017) observed in both cortex

and hippocampus. Alongside these synaptic impairments, neurons in the hippocampus exhibit altered membrane properties, leading to reduced excitability.

The genetic alterations induced by THC and Poly(I:C) in the mouse models reflect some of the alterations observed in the molecular pathways associated with schizophrenia. This similarity in gene expression changes points to potential mechanisms through which these substances might contribute to alterations in neuronal function and behavior, linked to the processes observed in schizophrenia. Many studies have implicated alterations in neuronal signaling, synaptic transmission and neurotransmitter systems in individuals with schizophrenia (Keshavan et al., 1994; Ľupták et al., 2021; Luvsannyam et al., 2022; Woolley & Shaw, 1954). In addition, several studies suggest an involvement of immune dysfunction and inflammatory processes in the development of schizophrenia (Brown et al., 2010; Karlsson & Dalman, 2020; Khandaker et al., 2015; Menninger, 1919).

Furthermore, when studying the Poly(I:C)/THC group of mice, intriguing findings have emerged beyond the previously discussed gene families. Notably, genes related to memory and learning, neuronal projection development, and the regulation of nervous system development exhibited alterations in their expression levels.

The disruption of these gene families in the Poly(I:C)/THC group hints at potential mechanisms through which these substances might contribute to cognitive impairments and aberrant brain development reminiscent of features observed in schizophrenia. The impact on memory-related genes might contribute to the cognitive deficits seen in schizophrenia, while alterations in genes governing neuronal projection and nervous system development could contribute to the structural and functional abnormalities observed in the brains of individuals with schizophrenia.

This study provides a new insight into possible mechanisms linking substance exposure to alterations in gene families associated with schizophrenia-like traits, and highlights the complex interaction between genes and administered substances that affect behavior and neural functions.

The double-hit mouse model produces disruptions in the Akt/mTOR/S6 signaling pathway

As previously discussed, it is known that Akt/mTOR/S6 pathway is altered in schizophrenia patients and can be influenced by both Poly(I:C) and THC. THC acts via CB_1, altering the properties of the serotonergic 5-HT2AR (Ibarra-Lecue et al., 2018). Therefore, one of the key aims of this Doctoral Thesis was to assess the protein levels within these pathways in the cerebral cortex of mice from the double-hit model. In addition to these two variables, the influence of sex on the pathway was studied.

The results from both AlphaLISA® assays and WB experiments, concluded that Poly(I:C) had a strong effect on the deregulation of this pathway as it caused a decrease in the expression of all the phosphorylated forms of all measured proteins. This reduction was primarily driven by the effect of Poly(I:C), with a secondary influence from THC and sex, with the effect being greater in the male mice. This highlights an altered Akt/mTOR/S6 pathway in the double-hit model, primarily due to Poly(I:C), and to a lesser extent, THC and sex.

Implication of the Akt/mTOR/S6 pathway and some of its proteins in schizophrenia has been demonstrated in *postmortem* studies (Ibarra-Lecue et al., 2020; Zheng et al., 2012). Specifically, negative dysregulation of the Akt/mTOR/S6 pathway has been observed in *postmortem* tissues from individuals with schizophrenia (Chadha & Meador-Woodruff, 2020; Ibarra-Lecue et al., 2020).

Regarding Akt kinase, in the present study, no changes were observed in total protein, but a decrease was observed in phospho(Ser473)-Akt and phospho(Thr450)-Akt being only significant the phospho(Thr450)-Akt measured

with AlphaLISA®. In this case, an interaction between Poly(I:C) and sex (male) was observed, leading to decreased levels of phospho(Thr450)-Akt in Poly(I:C) males compared to the saline group. This aligns with previous studies (Bitanihirwe et al., 2010). In this sense, although different phosphorilated forms of Akt were assessed by AlphaLISA® and WB, they exhibited a similar trend, suggesting that MIA diminishes both phospho(Thr450)-Akt and phospho(Ser473)-Akt, affecting their functionality.

Regarding mTOR protein, animal studies have shown contradictory results. Studies in mice have shown both an increase in mTOR expression and activity in the cortex of double-hit mice by MIA and isolation (Goh et al., 2020) and a negative downregulation of mTOR due to Poly(I:C) (Amodeo et al., 2019). In this sense, in the present study, a decrease in phospho(Ser2448)-mTOR was observed in the Poly(I:C) group compared to saline (as well as a decrease in the phospho(Ser2448)-mTOR / mTOR ratio), in agreement with what has been previously found in human brain *postmortem*, as well as in animal studies of MIA.

As for the rpS6, previous studies have demonstrated that THC is able to modify the phosphor(Ser235/236)-rpS6 / rpS6 ratio in mice (Ibarra-Lecue et al., 2018). In the present study, although the results obtained by WB and AlphaLISA® are very similar and go in the same direction, there are small differences between them. In neither technique were changes in total rpS6 observed. However in AlphaLISA® assays a decrease of phospho(Ser235/236)-rpS6 was observed in males but not in females and in the WB experiments this decrease was observed in both males and females. As discussed above, these differences may be due to the methodology of each of the techniques. Furthermore, in AlphaLISA® assays a decrease in phospho(Ser235/236)-rpS6 / rpS6 ratio levels was detected as previously described (Ibarra-Lecue et al., 2020) but not in the WB experiments. Even so, all these results are mostly in agreement with what has been previously described in humans (Ibarra-Lecue et al., 2020), showing the apparent validity of the model used. These results are in agreement with those previously reported,

although they had not detected differences between sexes. This could be explained because in our study such variations have been observed in the THC group, which was not studied in previous studies (Haddad et al., 2020). These observations highlights a potential combined impact of THC and Poly(I:C) on the regulation of rpS6, indicating a noteworthy interaction between both conditions in affecting this specific cellular pathway.

Finally, studies in rats have shown that chronic administration of THC and cannabidiol (CBD), increases ERK phosphorylation, proposing a pathway of action of THC as a risk factor in schizophrenia (Hudson et al., 2019). On the other hand, studies in MIA in rats have shown decreased activation (phosphorylation) of ERK (Li et al., 2020). In this study, a decrease in phospho(Thr202/Tyr204)-ERK1/2 was observed in Poly(I:C) group relative to saline, in agreement with what was observed in the MIA animal model (Li et al., 2020), but not in *postmortem* studies (Hino et al., 2016; Iroegbu et al., 2021). The present results are in the same direction as other MIA animal models, but not with human studies, suggesting that the regulation of this protein in schizophrenia would be subject to other factors and showing a lack of apparent validity of MIA models in terms of ERK pathway alterations.

The results, both in human olfactory neuroepithelium and in mice, point to a decrease in the phosphorylated forms of the proteins of the Akt/mTOR/S6 pathway, in agreement with most of the *postmortem* studies. For this reason, it could be suggested that a decrease in the functionality of this pathway could be associated with the development and/or pathophysiology of schizophrenia.

In summary, regarding the implications of MIA and THC in the development of schizophrenia, it has been observed that MIA is the main factor causing hypofunction of the Akt/mTOR/S6 pathway, so this pathway could be implicated in the mechanism of MIA as a risk factor for schizophrenia (Amodeo et al., 2019; Goh et al., 2020). THC alone also induces changes in rpS6 protein, suggesting the possible involvement of the pathway in the effects of THC on the increased

risk of developing schizophrenia (Ibarra-Lecue et al., 2018), although further studies would be desirable.

5.3. Strengths and limitations on the present study

The results of the present Doctoral Thesis show several strengths that should be contextualized in the context of their own limitations.

The study has some limitations that obviously can not be ignored. First, what we have obtained after selecting the cells based on the presence or absence of PSA-NCAM, are cultures enriched in neurons or glia, but not pure cultures. Another limitation is the fact that these neuron and glial cells have developed in vitro, without the natural inputs that they would have had if they had developed physiologically. It must be further studied whether the manipulation of neural progenitors has interfered in their development in terms of the ability to reproduce some alterations inherent to psychiatric conditions.

Moreover, these cultures may be considered with an "olfactory-specific" origin, which should be kept in consideration when comparing with other models.

Furthermore, the results have been constrained by technical aspects. On one hand, regarding AlphaLISA® assays, despite the advantages offered by Multiplex kits (greater speed and a simpler procedure) when using a single kit to measure total and phosphorylated forms of a protein, the simultaneous use of terbium and europium limited measurements of both forms. This limitation arose due to the lower intensity of terbium compared to europium, resulting in a lower signal-to-noise (S/N) ratio for the total form (measured with terbium). Another significant limitation was the withdrawal of several kits due to an inadequate S/N ratio despite using europium, preventing the quantification of proteins of great importance in the Akt/mTOR/S6 pathway. On the other hand, regarding WB experiments, one challenge is the potential for nonspecific binding, where the antibodies may interact with unintended proteins, leading to inaccurate results. Additionally, variations in antibody specificity and sensitivity can affect the reliability of the method. Another limitation lies in the semi-quantitative nature

of Western blotting, making precise quantification challenging. The technique's dependency on protein size and the need for suitable housekeeping proteins for normalization further contribute to its limitations.

Another limitation of regarding study II, is that THC administration typically involves injection (i.p.), which does not mimic the natural consumption method of cannabis in humans, where it is predominantly smoked. This disparity in administration routes may introduce variations in pharmacokinetics and pharmacodynamics, potentially impacting the interpretation of results and the translatability of findings to human cannabis consumption patterns. Each system has its own limitation and it has been useful in addressing distinct objectives of this study. Whereas inherent difference regarding species and tissues should not be overlooked, common observations among the experimental systems, understood as reproducible in more than one system, strength the reliability of the conclusions that can be extracted.

However, it is important to note the strengths present in this Doctoral Thesis.

As for the animal model, modelling human neuropsychiatric disorders in animals is extremely difficult given the subjective nature of many key symptoms, the lack of biomarkers and objective diagnostic tests, and the early state of relevant neurobiology and genetics. Nevertheless, advances in the understanding of pathophysiology and the development of treatments would benefit greatly from improved animal models. In our specific case, double-hit mouse model has successfully emulated the symptomatology observed in patients and has demonstrated substantial congruence with *postmortem* findings, especially for mTOR and rpS6 proteins. Moreover, in vitro outcomes have closely paralleled those obtained in olfactory neuroepithelium, affirming the apparent validity of the model. Given its apparent validity, further exploration into the model's predictive validity becomes crucial, enabling its utilization in drug studies and enhancing its potential as a valuable tool in the field.

This model can be used to facilitate the identification of potential therapeutic targets and interventions. Furthermore, it provides a valuable platform to explore the intricate interplay between genetic susceptibility and environmental factors, contributing to a more complete understanding of the disorder and paving the way for innovative research in the field of schizophrenia.

Finally, to our knowledge, this study marks the first attempt to evaluate the expression of Akt/mTOR/S6 proteins in the double-hit mouse model involving Poly(I:C) and THC.

Regarding the use of cell cultures from olfactory neuroepithelium, to our knowledge, this is the first study describing a method for the generation of sufficient amount of human neurons or glial cells subpopulations in living subjects in an easy and non-invasively form. Other studies had developed similar methods but obtaining the sample invasively in biopsies after nasal surgery and with anesthesia, or even *postmortem* in autopsies. On the other hand, other groups have developed and characterized non-invasively obtained adherent cultures of the olfactory neuroepithelium in patients, but none of them has reached the step of selecting and culturing neurons and glia.

Regarding neurospheres, to our knowledge, this is the first study exploring the distinctions in neurosphere proliferation and size between individuals with schizophrenia and controls. This exploration provides crucial insights into the underlying cellular and molecular mechanisms linked with the disorder. Understanding these differences could potentially lead to the development of targeted therapeutic interventions, shedding light on the pathological processes involved in schizophrenia.

These samples represent a readily obtainable sample that facilitates a longitudinal study of patients at various stages of the disease. This approach enables an in-depth exploration of the ongoing changes within the diseased brain of each patient, providing valuable insights into the progression of the illness. Such an understanding serves as a crucial foundation for tailoring more individualized

treatments, allowing clinicians to discern the unique characteristics of each patient's condition. With these samples, researchers can unravel the complexities of the diseased brain and pave the way for more personalized and effective interventions to optimize patient outcomes.

Despite the aforementioned limitations, we believe that this work has an important translational impact since it will allow the characterization of new biomarkers and disease fingerprints through the study of neurons and glial cells from patients. Furthermore, the possibility of measuring these and other putative biomarkers with this methodology in samples from patients opens the possibility to predict the response to the treatment and presumably, improve the quality-of-life of subjects with a psychiatric disease.

Conclusions

6. CONCLUSIONS

The main conclusions derived from this Doctoral Thesis are:

1. Olfactory neuroepithelium provides a non-invasive, easy, reproducible and reliable method for the isolation of neurospheres, neurons and glial cells from living subjects.
2. Neurospheres from subjects with schizophrenia show altered growth compared to neurospheres from their matched controls.
3. Neuron- and glia-enriched cultures from schizophrenia patients and healthy controls show differences in gene expression levels. Among the most relevant altered genes found are *L1CAM, NUF2, PTN*, and *NPTX*, which have already been described as potentially implicated in schizophrenia.
4. Neuron- and glia-enriched cultures provide a substrate for the study of mental illnesses. Furthermore, these cultures are a source for the search of useful predictive, diagnostic or prognostic biomarkers.
5. The double-hit animal model of MIA and THC chronic administration is able to reproduce, in the behavioral tests, some of the symptoms observed in patients with schizophrenia by producing alterations in memory and sensory information processing.
6. The double-hit animal model induces a transcriptomic profile that differs significantly from the gene expression profile in control rodents. Among the most relevant altered genes discovered are those related to neurodevelopment, memory, regulation of neurotransmitter transport, and synaptic signaling.
7. Functioning of the Akt/mTOR/S6 pathway is decreased in the double-hit animal model and in the neuron-enriched cultures from schizophrenia patients, suggesting a downregulation of the pathway and a reduced functionality in schizophrenia.

References

7. REFERENCES

Ahmed, S. (2009). The culture of neural stem cells. In *Journal of Cellular Biochemistry, 106*(1). https://doi.org/10.1002/jcb.21972

Al-Asmari, A. K., & Khan, M. W. (2014). Inflammation and schizophrenia: Alterations in cytokine levels and perturbation in antioxidative defense systems. *Human and Experimental Toxicology*, *33*(2). https://doi.org/10.1177/0960327113493305

al-Haddad, B. J. S., Oler, E., Armistead, B., Elsayed, N. A., Weinberger, D. R., Bernier, R., Burd, I., Kapur, R., Jacobsson, B., Wang, C., Mysorekar, I., Rajagopal, L., & Adams Waldorf, K. M. (2019). The fetal origins of mental illness. *American Journal of Obstetrics and Gynecology*, *221*(6), 549–562. https://doi.org/10.1016/j.ajog.2019.06.013

Allardyce, J., & Boydell, J. (2006). Environment and Schizophrenia: Review: The Wider Social Environment and Schizophrenia. *Schizophrenia Bulletin*, *32*(4), 592–598. https://doi.org/https://doi.org/10.1093/schbul/sbl008

Alto, L. T., & Terman, J. R. (2017). Semaphorins and their signaling mechanisms. *Methods in Molecular Biology*, *1493*. https://doi.org/10.1007/978-1-4939-6448-2_1

Álvarez, P., Bellosillo, B., Colom, F., Longarón, R., Barrera-Conde, M., Fernández-Ibarrondo, L., Toll, A., Ginés, J. M., de la Torre, R., Pérez-Solá, V., & Robledo, P. (2023). Y-chromosome in the olfactory neuroepithelium as a potential biomarker of depression in women with male offspring: an exploratory study. *Molecular and Cellular Biochemistry*. https://doi.org/10.1007/s11010-023-04807-y

Amarillo, I. E., Li, W. L., Li, X., Vilain, E., & Kantarci, S. (2014). De novo single exon deletion of AUTS2 in a patient with speech and language disorder: A review of disrupted AUTS2 and further evidence for its role in neurodevelopmental disorders. *American Journal of Medical Genetics, Part A*, *164*(4). https://doi.org/10.1002/ajmg.a.36393

Amodeo, D. A., Lai, C. Y., Hassan, O., Mukamel, E. A., Behrens, M. M., & Powell, S. B. (2019). Maternal immune activation impairs cognitive flexibility and alters transcription in frontal cortex. *Neurobiology of Disease*, *125*. https://doi.org/10.1016/j.nbd.2019.01.025

Anderson, K. K., Cheng, J., Susser, E., McKenzie, K. J., & Kurdyak, P. (2015). Incidence of psychotic disorders among first-generation immigrants and refugees in Ontario. *CMAJ*, *187*(9). https://doi.org/10.1503/cmaj.141420

Andrews, J. L., Goodfellow, F. J., Matosin, N., Snelling, M. K., Newell, K. A., Huang, X. F., & Fernandez-Enright, F. (2017). Alterations of ubiquitin related proteins in the pathology and development of schizophrenia: Evidence from human and animal studies. *Journal of Psychiatric Research*, *90*. https://doi.org/10.1016/j.jpsychires.2017.01.009

Apple, D. M., Fonseca, R. S., & Kokovay, E. (2017). The role of adult neurogenesis in psychiatric and cognitive disorders. In *Brain Research, 1655*. https://doi.org/10.1016/j.brainres.2016.01.023

Arck, P. C., Merali, F. S., Stanisz, A. M., Stead, R. H., Chaouat, G., Manuel, J., & Clark, D. A. (1995). Stress-induced murine abortion associated with substance P-dependent alteration in cytokines in maternal uterine decidua. *Biology of Reproduction*, *53*(4). https://doi.org/10.1095/biolreprod53.4.814

Arion, D., Horváth, S., Lewis, D. A., & Mirnics, K. (2010). Infragranular gene expression disturbances in the prefrontal cortex in schizophrenia: Signature of altered neural development? *Neurobiology of Disease*, *37*(3). https://doi.org/10.1016/j.nbd.2009.12.013

Arseneault, L., Cannon, M., Poulton, R., Murray, R., Caspi, A., & Moffitt, T. E. (2002). Cannabis use in adolescence and risk for adult psychosis: Longitudinal prospective study. *British Medical Journal*, *325*(7374), 1212–1213. https://doi.org/10.1136/bmj.325.7374.1212

Augustin, S. M., & Lovinger, D. M. (2018). Functional Relevance of Endocannabinoid-Dependent Synaptic Plasticity in the Central Nervous System. In *ACS Chemical Neuroscience, 9*(9). https://doi.org/10.1021/acschemneuro.7b00508

Augustin, S. M., & Lovinger, D. M. (2022). Synaptic changes induced by cannabinoid drugs and cannabis use disorder. In *Neurobiology of Disease, 167*. https://doi.org/10.1016/j.nbd.2022.105670

Avguštin, B., Wraber, B., & Tavčar, R. (2005). Increased Th1 and Th2 immune reactivity with relative Th2 dominance in patients with acute exacerbation of schizophrenia. *Croatian Medical Journal*, *46*(2).

Baharnoori, M., Brake, W. G., & Srivastava, L. K. (2009). Prenatal immune challenge induces developmental changes in the morphology of pyramidal neurons of the prefrontal cortex and hippocampus in rats. *Schizophrenia Research*, *107*(1). https://doi.org/10.1016/j.schres.2008.10.003

Bakkaloglu, B., O'Roak, B. J., Louvi, A., Gupta, A. R., Abelson, J. F., Morgan, T. M., Chawarska, K., Klin, A., Ercan-Sencicek, A. G., Stillman, A. A., Tanriover, G., Abrahams, B. S., Duvall, J. A., Robbins, E. M., Geschwind, D. H., Biederer, T., Gunel, M., Lifton, R. P., & State, M. W. (2008). Molecular Cytogenetic Analysis and Resequencing of Contactin Associated Protein-Like 2 in Autism Spectrum Disorders. *American Journal of Human Genetics*, *82*(1). https://doi.org/10.1016/j.ajhg.2007.09.017

Ballendine, S. A., Greba, Q., Dawicki, W., Zhang, X., Gordon, J. R., & Howland, J. G. (2015). Behavioral alterations in rat offspring following maternal immune activation and ELR-CXC chemokine receptor antagonism during pregnancy: Implications for neurodevelopmental psychiatric disorders. *Progress in Neuro-Psychopharmacology and Biological Psychiatry*, *57*. https://doi.org/10.1016/j.pnpbp.2014.11.002

Barrera-Conde, M., Ausin, K., Lachén-Montes, M., Fernández-Irigoyen, J., Galindo, L., Cuenca-Royo, A., Fernández-Avilés, C., Pérez, V., de la Torre, R., Santamaría, E., & Robledo, P. (2021). Cannabis use induces distinctive proteomic alterations in olfactory neuroepithelial cells of schizophrenia patients. *Journal of Personalized Medicine*, *11*(3). https://doi.org/10.3390/jpm11030160

Baumeister, A. A., & Hawkins, M. F. (2004). The serotonin hypothesis of schizophrenia: A historical case study on the heuristic value of theory in clinical neuroscience. In *Journal of the History of the Neurosciences, 13*(3). https://doi.org/10.1080/09647040490510560

Bayer, T. A., Falkai, P., & Maier, W. (1999). Genetic and non-genetic vulnerability factors in schizophrenia: The basis of the "two hit hypothesis." *Journal of Psychiatric Research*, *33*(6), 543–548. https://doi.org/https://doi.org/10.1016/s0022-3956(99)00039-4

Bedogni, F., Hodge, R. D., Nelson, B. R., Frederick, E. A., Shiba, N., Daza, R. A., & Hevner, R. F. (2010). Autism susceptibility candidate 2 (Auts2) encodes a nuclear protein expressed in developing brain regions implicated in autism neuropathology. *Gene Expression Patterns*, *10*(1). https://doi.org/10.1016/j.gep.2009.11.005

Beer, S., Oleszewski, M., Gutwein, P., Geiger, C., & Altevogt, P. (1999). Metalloproteinase-mediated release of the ectodomain of L1 adhesion molecule. *Journal of Cell Science*, *112*(16). https://doi.org/10.1242/jcs.112.16.2667

Begum, A. N., Guoynes, C., Cho, J., Hao, J., Lutfy, K., & Hong, Y. (2015). Rapid generation of sub-type, region-specific neurons and neural networks from human pluripotent stem cell-derived neurospheres. *Stem Cell Research*, *15*(3). https://doi.org/10.1016/j.scr.2015.10.014

Ben-David, E., Granot-Hershkovitz, E., Monderer-Rothkoff, G., Lerer, E., Levi, S., Yaari, M., Ebstein, R. P., Yirmiya, N., & Shifman, S. (2011). Identification of a functional rare variant in autism using genome-wide screen for monoallelic expression. *Human Molecular Genetics*, *20*(18). https://doi.org/10.1093/hmg/ddr283

Benes, F. M., & Berretta, S. (2001). GABAergic interneurons: Implications for understanding schizophrenia and bipolar disorder. *Neuropsychopharmacology*, *25*(1). https://doi.org/10.1016/S0893-133X(01)00225-1

Benítez-King, G., Riquelme, A., Ortíz-López, L., Berlanga, C., Rodríguez-Verdugo, M. S., Romo, F., Calixto, E., Solís-Chagoyán, H., Jímenez, M., Montaño, L. M., Ramírez-Rodríguez, G., Morales-Mulia, S., & Domínguez-Alonso, A. (2011). A non-invasive method to isolate the neuronal linage from the nasal epithelium from schizophrenic and bipolar diseases. *Journal of Neuroscience Methods*, *201*(1). https://doi.org/10.1016/j.jneumeth.2011.07.009

Bentall, R. P., De Sousa, P., Varese, F., Wickham, S., Sitko, K., Haarmans, M., & Read, J. (2014). From adversity to psychosis: Pathways and mechanisms from specific adversities to specific symptoms. *Social Psychiatry and Psychiatric Epidemiology*, *49*(7), 1011–1022. https://doi.org/10.1007/s00127-014-0914-0

Bertram, S., Roll, L., Reinhard, J., Groß, K., Dazert, S., Faissner, A., & Volkenstein, S. (2019). Pleiotrophin increases neurite length and number of spiral ganglion neurons in vitro. *Experimental Brain Research*, *237*(11). https://doi.org/10.1007/s00221-019-05644-6

Bhattacharyya, S., Atakan, Z., Martin-Santos, R., Crippa, J. A., Kambeitz, J., Prata, D., Williams, S., Brammer, M., Collier, D. A., & McGuire, P. K. (2012). Preliminary report of biological basis of sensitivity to the effects of cannabis on psychosis: AKT1 and DAT1 genotype modulates the effects of δ-9-tetrahydrocannabinol on midbrain and striatal function. In *Molecular Psychiatry, 17*(12). https://doi.org/10.1038/mp.2011.187

Bielefeld, P., Abbink, M. R., Davidson, A. R., Reijner, N., Abiega, O., Lucassen, P. J., Korosi, A., & Fitzsimons, C. P. (2021). Early life stress decreases cell proliferation and the number of putative adult neural stem cells in the adult hypothalamus. *Stress*, *24*(2). https://doi.org/10.1080/10253890.2021.1879787

Birnbaum, R., & Weinberger, D. R. (2017). Genetic insights into the neurodevelopmental origins of schizophrenia. *Nature Reviews Neuroscience*, *18*(12), 727–740. https://doi.org/10.1038/nrn.2017.125

Bitanihirwe, B. K. Y., Weber, L., Feldon, J., & Meyer, U. (2010). Cognitive impairment following prenatal immune challenge in mice correlates with prefrontal cortical AKT1 deficiency. *International Journal of Neuropsychopharmacology*, *13*(8). https://doi.org/10.1017/S1461145710000192

Blomström, Å., Karlsson, H., Wicks, S., Yang, S., Yolken, R. H., & Dalman, C. (2012). Maternal antibodies to infectious agents and risk for non-affective psychoses in the offspring-a matched case-control study. *Schizophrenia Research*, *140*(1–3), 25–30. https://doi.org/10.1016/j.schres.2012.06.035

Bodaleo, F. J., Montenegro-Venegas, C., Henríquez, D. R., Court, F. A., & Gonzalez-Billault, C. (2016). Microtubule-associated protein 1B (MAP1B)-deficient neurons show structural presynaptic deficiencies in vitro and altered presynaptic physiology. *Scientific Reports*, *6*. https://doi.org/10.1038/srep30069

Bonfanti, L., & Nacher, J. (2012). New scenarios for neuronal structural plasticity in non-neurogenic brain parenchyma: The case of cortical layer II immature neurons. In *Progress in Neurobiology, 98*(1). https://doi.org/10.1016/j.pneurobio.2012.05.002

Borgmann-Winter, K. E., Rawson, N. E., Wang, H. Y., Wang, H., MacDonald, M. L., Ozdener, M. H., Yee, K. K., Gomez, G., Xu, J., Bryant, B., Adamek, G., Mirza, N., Pribitkin, E., & Hahn, C. G. (2009). Human olfactory epithelial cells generated in vitro express diverse neuronal characteristics. *Neuroscience*, *158*(2). https://doi.org/10.1016/j.neuroscience.2008.09.059

Borgmann-Winter, K., Willard, S. L., Sinclair, D., Mirza, N., Turetsky, B., Berretta, S., & Hahn, C. G. (2015). Translational potential of olfactory mucosa for the study of neuropsychiatric illness. In *Translational Psychiatry, 5*(3). https://doi.org/10.1038/tp.2014.141

Borovcanin, M., Jovanovic, I., Radosavljevic, G., Djukic Dejanovic, S., Bankovic, D., Arsenijevic, N., & Lukic, M. L. (2012). Elevated serum level of type-2 cytokine and low IL-17 in first episode psychosis and schizophrenia in relapse. *Journal of Psychiatric Research*, *46*(11). https://doi.org/10.1016/j.jpsychires.2012.08.016

Bourque, F., van der Ven, E., & Malla, A. (2011). A meta-analysis of the risk for psychotic disorders among first- and second-generation immigrants. *Psychological Medicine*, *41*(5), 897–910.

Braff, D. L., & Geyer, M. A. (1990). Sensorimotor gating and schizophrenia human and animal model studies. *Archives of General Psychiatry*, *47*(2). https://doi.org/10.1001/archpsyc.1990.01810140081011

Brann, J. H., Ellis, D. P., Ku, B. S., Spinazzi, E. F., & Firestein, S. (2015). Injury in aged animals robustly activates quiescent olfactory neural stem cells. *Frontiers in Neuroscience*, *9*(OCT). https://doi.org/10.3389/fnins.2015.00367

Broadbelt, K., Byne, W., & Jones, L. B. (2002). Evidence for a decrease in basilar dendrites of pyramidal cells in schizophrenic medial prefrontal cortex. *Schizophrenia Research*, *58*(1). https://doi.org/10.1016/S0920-9964(02)00201-3

Brown, A. S., Begg, M. D., Gravenstein, S., Schaefer, C. A., Wyatt, R. J., Bresnahan, M., Babulas, V. P., & Susser, E. S. (2004). Serologic evidence of prenatal influenza in the etiology of schizophrenia. *Archives of General Psychiatry*, *61*(8), 774–780. https://doi.org/https://doi.org/10.1001/archpsyc.61.8.774

Brown, A. S., Cohen, P., Harkavy-friedman, J., Babulas, V., Malaspina, D., Gorman, J. M., & Susser, E. S. (2001). Prenatal Rubella, Premorbid Abnormalities, and Adult Schizophrenia. *Biological Psychiatry*, *49*(6), 473–486. https://doi.org/doi: 10.1016/s0006-3223(01)01068-x.

Brown, A. S., M.D., M.P.H., Derkits, E. J., & B.A. (2010). Prenatal Infection and Schizophrenia: A Review of Epidemiologic and Translational Studies. *Am J Psychiatry*, *167*(3), 261–280. https://doi.org/10.1176/appi.ajp.2009.09030361.

Brown, A. S., Schaefer, C. A., Quesenberry, C. P., Liu, L., Babulas, V. P., & Susser, E. S. (2005). Maternal exposure to toxoplasmosis and risk of schizophrenia in adult offspring. *American Journal of Psychiatry*, *162*(4), 767–773. https://doi.org/10.1176/appi.ajp.162.4.767

Buka, S. L., Tsuang, M. T., Torrey, E. F., Klebanoff, M. A., Bernstein, D., & Yolken, R. H. (2001). Maternal Infections and Subsequent PsychosisAmong Offspring. *Archives of General Psychiatry*, *58*(11), 1032–1037. https://doi.org/https://doi.org/10.1001/archpsyc.58.11.1032

Burbach, J. P. H., & van der Zwaag, B. (2009). Contact in the genetics of autism and schizophrenia. In *Trends in Neurosciences, 32*(2). https://doi.org/10.1016/j.tins.2008.11.002

Byrne, M., Agerbo, E., Eaton, W. W., & Mortensen, P. B. (2004). Parental socio-economic status and risk of first admission with schizophrenia- a Danish national register based study. *Social Psychiatry and Psychiatric Epidemiology*, *39*(2), 87–96. https://doi.org/https://doi.org/10.1007/s00127-004-0715-y

Caldeira, G. L., Peça, J., & Carvalho, A. L. (2019). New insights on synaptic dysfunction in neuropsychiatric disorders. *Current Opinion in Neurobiology*, *57*(Id), 62–70. https://doi.org/10.1016/j.conb.2019.01.004

Campbell, B. M., Charych, E., Lee, A. W., & Möller, T. (2014). Kynurenines in CNS disease: Regulation by inflammatory cytokines. In *Frontiers in Neuroscience* (Issue 8 FEB). https://doi.org/10.3389/fnins.2014.00012

Canetta, S., Bolkan, S., Padilla-Coreano, N., Song, L. J., Sahn, R., Harrison, N. L., Gordon, J. A., Brown, A., & Kellendonk, C. (2016). Maternal immune activation leads to selective functional deficits in offspring parvalbumin interneurons. *Molecular Psychiatry*, *21*(7). https://doi.org/10.1038/mp.2015.222

Cannon, M., Jones, P. B., & Murray, R. M. (2002). Obstetric complications andCannon, M., Jones, P.B. & Murray, R.M., 2002. Obstetric complications and schizophrenia: Historical and meta-analytic review. American Journal of Psychiatry, 159(7), pp.1080–1092. schizophrenia: Historical and meta-analytic revi. *American Journal of Psychiatry*, *159*(7), 1080–1092.

Cantor-Graae, E., & Pedersen, C. B. (2013). Full spectrum of psychiatric disorders related to foreign migration: A danish population-based cohort study. *JAMA Psychiatry*, *70*(4), 427–435. https://doi.org/10.1001/jamapsychiatry.2013.441

Cantor-Graae, E., & Selten, J. P. (2005). Schizophrenia and migration: A meta-analysis and review. *American Journal of Psychiatry*, *162*(1), 12–24. https://doi.org/10.1176/appi.ajp.162.1.12

Careaga, M., Taylor, S. L., Chang, C., Chiang, A., Ku, K. M., Berman, R. F., Van de Water, J. A., & Bauman, M. D. (2018). Variability in PolyIC induced immune response: Implications for preclinical maternal immune activation models. *Journal of Neuroimmunology*, *323*. https://doi.org/10.1016/j.jneuroim.2018.06.014

Cattane, N., Richetto, J., & Cattaneo, A. (2020). Prenatal exposure to environmental insults and enhanced risk of developing Schizophrenia and Autism Spectrum Disorder: focus on biological pathways and epigenetic mechanisms. *Neuroscience and Biobehavioral Reviews*, *117*(June 2018), 253–278. https://doi.org/10.1016/j.neubiorev.2018.07.001

Chadha, R., Alganem, K., Mccullumsmith, R. E., & Meador-Woodruff, J. H. (2021). mTOR kinase activity disrupts a phosphorylation signaling network in schizophrenia brain. *Molecular Psychiatry*, *26*(11). https://doi.org/10.1038/s41380-021-01135-9

Chadha, R., & Meador-Woodruff, J. H. (2020). Downregulated AKT-mTOR signaling pathway proteins in dorsolateral prefrontal cortex in Schizophrenia. *Neuropsychopharmacology*, *45*(6). https://doi.org/10.1038/s41386-020-0614-2

Chambers, R. A., Krystal, J. H., & Self, D. W. (2001). A neurobiological basis for substance abuse comorbidity in schizophrenia. In *Biological Psychiatry, 50*(2). https://doi.org/10.1016/S0006-3223(01)01134-9

Chang, S., Rathjen, F. G., & Raper, J. A. (1987). Extension of neurites on axons is impaired by antibodies against specific neural cell surface glycoproteins. *The Journal of Cell Biology*, *104*(2). https://doi.org/10.1083/jcb.104.2.355

Chen, X. S., Reader, R. H., Hoischen, A., Veltman, J. A., Simpson, N. H., Francks, C., Newbury, D. F., & Fisher, S. E. (2017). Next-generation DNA sequencing identifies novel gene variants and pathways involved in specific language impairment. *Scientific Reports*, *7*. https://doi.org/10.1038/srep46105

Chen, Y. H., Liao, D. L., Lai, C. H., & Chen, C. H. (2013). Genetic analysis of AUTS2 as a susceptibility gene of heroin dependence. *Drug and Alcohol Dependence*, *128*(3). https://doi.org/10.1016/j.drugalcdep.2012.08.029

Chiang, S. S. W., Riedel, M., Schwarz, M., & Mueller, N. (2013). Is T-helper type 2 shift schizophrenia-specific? Primary results from a comparison of related psychiatric disorders and healthy controls. *Psychiatry and Clinical Neurosciences*, *67*(4). https://doi.org/10.1111/pcn.12040

Chiappelli, J., Postolache, T. T., Kochunov, P., Rowland, L. M., Wijtenburg, S. A., Shukla, D. K., Tagamets, M., Du, X., Savransky, A., Lowry, C. A., Can, A., Fuchs, D., & Hong, L. E. (2016). Tryptophan Metabolism and White Matter Integrity in Schizophrenia. *Neuropsychopharmacology*, *41*(10). https://doi.org/10.1038/npp.2016.66

Chojnicka, I., Gajos, K., Strawa, K., Broda, G., Fudalej, S., Fudalej, M., Stawiński, P., Pawlak, A., Krajewski, P., Wojnar, M., & Płoski, R. (2013). Possible Association between Suicide Committed under Influence of Ethanol and a Variant in the AUTS2 Gene. *PLoS ONE*, *8*(2). https://doi.org/10.1371/journal.pone.0057199

Chong, H. Y., Teoh, S. L., Wu, D. B. C., Kotirum, S., Chiou, C. F., & Chaiyakunapruk, N. (2016). Global economic burden of schizophrenia: A systematic review. In *Neuropsychiatric Disease and Treatment, 12*. https://doi.org/10.2147/NDT.S96649

Choudhury, Z., & Lennox, B. (2021). Maternal Immune Activation and Schizophrenia–Evidence for an Immune Priming Disorder. *Frontiers in Psychiatry*, *12*(February), 1–8. https://doi.org/10.3389/fpsyt.2021.585742

Christian, K. M., Song, H., & Ming, G. L. (2014). Functions and dysfunctions of adult hippocampal neurogenesis. In *Annual Review of Neuroscience, 37*. https://doi.org/10.1146/annurev-neuro-071013-014134

Close, C., Kouvonen, A., Bosqui, T., Patel, K., O'Reilly, D., & Donnelly, M. (2016). The mental health and wellbeing of first generation migrants: A systematic-narrative review of reviews. *Globalization and Health*, *12*(1), 1–13. https://doi.org/10.1186/s12992-016-0187-3

Coiro, P., Padmashri, R., Suresh, A., Spartz, E., Pendyala, G., Chou, S., Jung, Y., Meays, B., Roy, S., Gautam, N., Alnouti, Y., Li, M., & Dunaevsky, A. (2015). Impaired synaptic development in a maternal immune activation mouse model of neurodevelopmental disorders. *Brain, Behavior, and Immunity*, *50*. https://doi.org/10.1016/j.bbi.2015.07.022

Cunningham, C., Campion, S., Teeling, J., Felton, L., & Perry, V. H. (2007). The sickness behaviour and CNS inflammatory mediator profile induced by systemic challenge of mice with synthetic double-stranded RNA (poly I:C). *Brain, Behavior, and Immunity*, *21*(4). https://doi.org/10.1016/j.bbi.2006.12.007

da Cruz, J. F. O., Gomis-Gonzalez, M., Maldonado, R., Marsicano, G., Ozaita, A., & Busquets-Garcia, A. (2020). An Alternative Maze to Assess Novel Object Recognition in Mice. *Bio-Protocol*, *10*(12). https://doi.org/10.21769/BioProtoc.3651

da Silva Siqueira, L., Majolo, F., da Silva, A. P. B., da Costa, J. C., & Marinowic, D. R. (2021). Neurospheres: a potential in vitro model for the study of central nervous system disorders. In *Molecular Biology Reports, 48*(4). https://doi.org/10.1007/s11033-021-06301-4

da Silva, T. L., & Ravindran, A. V. (2015). Contribution of sex hormones to gender differences in schizophrenia: A review. *Asian Journal of Psychiatry*, *18*(2015), 2–14. https://doi.org/10.1016/j.ajp.2015.07.016

Dalton, V. S., Verdurand, M., Walker, A., Hodgson, D. M., & Zavitsanou, K. (2012). Synergistic Effect between Maternal Infection and Adolescent Cannabinoid Exposure on Serotonin 5HT 1A Receptor Binding in the Hippocampus: Testing the "Two Hit" Hypothesis for the Development of Schizophrenia . *ISRN Psychiatry*, *2012*. https://doi.org/10.5402/2012/451865

Das, I., & Khan, N. S. (1998). Increased arachidonic acid induced platelet chemiluminescence indicates cyclooxygenase overactivity in schizophrenic subjects. *Prostaglandins Leukotrienes and Essential Fatty Acids*, *58*(3). https://doi.org/10.1016/S0952-3278(98)90109-0

Davies, G., Welham, J., Chant, D., Torrey, E. F., & McGrath, J. (2003). A systematic review and meta-analysis of Northern Hemisphere season of birth studies in schizophrenia. *Schizophrenia Bulletin*, *29*(3), 587–593. https://doi.org/https://doi.org/10.1093/oxfordjournals.schbul.a007030

Davis, K. L., Kahn, R. S., Ko, G., & Davidson, M. (1991). Dopamine in schizophrenia: A review and reconceptualization. *American Journal of Psychiatry*, *148*(11). https://doi.org/10.1176/ajp.148.11.1474

De Bartolomeis, A., Buonaguro, E. F., & Iasevoli, F. (2013). Serotonin-glutamate and serotonin-dopamine reciprocal interactions as putative molecular targets for novel antipsychotic treatments: From receptor heterodimers to postsynaptic scaffolding and effector proteins. In *Psychopharmacology, 225*(1). https://doi.org/10.1007/s00213-012-2921-8

De Boer, C. J., Van Krieken, J. H. J. M., Rhijn, C. M. J. Van, & Litvinov, S. V. (1999). Expression of Ep-CAM in normal, regenerating, metaplastic, and neoplastic liver. *Journal of Pathology*, *188*(2). https://doi.org/10.1002/(SICI)1096-9896(199906)188:2<201::AID-PATH339>3.0.CO;2-8

De Witte, L., Tomasik, J., Schwarz, E., Guest, P. C., Rahmoune, H., Kahn, R. S., & Bahn, S. (2014). Cytokine alterations in first-episode schizophrenia patients before and after antipsychotic treatment. *Schizophrenia Research*, *154*(1–3). https://doi.org/10.1016/j.schres.2014.02.005

DeGiosio, R. A., Grubisha, M. J., MacDonald, M. L., McKinney, B. C., Camacho, C. J., & Sweet, R. A. (2022). More than a marker: potential pathogenic functions of MAP2. *Frontiers in Molecular Neuroscience*, *15*. https://doi.org/10.3389/fnmol.2022.974890

Delaney, S., Fallon, B., Alaedini, A., Yolken, R., Indart, A., Feng, T., Wang, Y., & Javitt, D. (2019). Inflammatory biomarkers in psychosis and clinical high risk populations. *Schizophrenia Research*, *206*. https://doi.org/10.1016/j.schres.2018.10.017

Delgado-Sequera, A., Hidalgo-Figueroa, M., Barrera-Conde, M., Duran-Ruiz, M. [a]C, Castro, C., Fernández-Avilés, C., de la Torre, R., Sánchez-Gomar, I., Pérez, V., Geribaldi-Doldán, N., Robledo, P., & Berrocoso, E. (2021). Olfactory Neuroepithelium Cells from Cannabis Users Display Alterations to the Cytoskeleton and to Markers of Adhesion, Proliferation and Apoptosis. *Molecular Neurobiology*, *58*(4). https://doi.org/10.1007/s12035-020-02205-9

Demirel, Ö. F., Cetin, İ., Turan, Ş., Sağlam, T., Yıldız, N., & Duran, A. (2017). Decreased expression of α-synuclein, Nogo-A and UCH-L1 in patients with schizophrenia: A preliminary serum study. *Psychiatry Investigation*, *14*(3). https://doi.org/10.4306/pi.2017.14.3.344

Demontis, D., Walters, R. K., Martin, J., Mattheisen, M., Als, T. D., Agerbo, E., Baldursson, G., Belliveau, R., Bybjerg-Grauholm, J., Bækvad-Hansen, M., Cerrato, F., Chambert, K., Churchhouse, C., Dumont, A., Eriksson, N., Gandal, M., Goldstein, J. I., Grasby, K. L., Grove, J., … Neale, B. M. (2019). Discovery of the first genome-wide significant risk loci for attention deficit/hyperactivity disorder. *Nature Genetics*, *51*(1). https://doi.org/10.1038/s41588-018-0269-7

Di Forti, M., Iyegbe, C., Sallis, H., Kolliakou, A., Falcone, M. A., Paparelli, A., Sirianni, M., La Cascia, C., Stilo, S. A., Marques, T. R., Handley, R., Mondelli, V., Dazzan, P., Pariante, C., David, A. S., Morgan, C., Powell, J., & Murray, R. M. (2012). Confirmation that the AKT1 (rs2494732) genotype influences the risk of psychosis in cannabis users. *Biological Psychiatry*, *72*(10), 811–816. https://doi.org/10.1016/j.biopsych.2012.06.020

Di Forti, M., Marconi, A., Carra, E., Fraietta, S., Trotta, A., Bonomo, M., Bianconi, F., Gardner-Sood, P., O'Connor, J., Russo, M., Stilo, S. A., Marques, T. R., Mondelli, V., Dazzan, P., Pariante, C., David, A. S., Gaughran, F., Atakan, Z., Iyegbe, C., … Murray, R. M. (2015). Proportion of patients in south London with first-episode psychosis attributable to use of high potency cannabis: A case-control study. *The Lancet Psychiatry*, *2*(3), 233–238. https://doi.org/10.1016/S2215-0366(14)00117-5

Di Forti, M., Sallis, H., Allegri, F., Trotta, A., Ferraro, L., Stilo, S. A., Marconi, A., La Cascia, C., Marques, T. R., Pariante, C., Dazzan, P., Mondelli, V., Paparelli, A., Kolliakou, A., Prata, D., Gaughran, F., David, A. S., Morgan, C., Stahl, D., … Murray, R. M. (2014). Daily use, especially of high-potency cannabis, drives the earlier onset of psychosis in cannabis users. *Schizophrenia Bulletin*, *40*(6), 1509–1517. https://doi.org/10.1093/schbul/sbt181

Di Nicola, M., Cattaneo, A., Hepgul, N., Di Forti, M., Aitchison, K. J., Janiri, L., Murray, R. M., Dazzan, P., Pariante, C. M., & Mondelli, V. (2013). Serum and gene expression profile of cytokines in first-episode psychosis. *Brain, Behavior, and Immunity*, *31*. https://doi.org/10.1016/j.bbi.2012.06.010

Dinan, T. G., Borre, Y. E., & Cryan, J. F. (2014). Genomics of schizophrenia: Time to consider the gut microbiome? In *Molecular Psychiatry, 19*(12). https://doi.org/10.1038/mp.2014.93

Ding, M., Song, X., Zhao, J., Gao, J., Li, X., Yang, G., Wang, X., Harrington, A., Fan, X., & Lv, L. (2014). Activation of Th17 cells in drug naïve, first episode schizophrenia. *Progress in Neuro-Psychopharmacology and Biological Psychiatry*, *51*. https://doi.org/10.1016/j.pnpbp.2014.01.001

Divac, N., Prostran, M., Jakovcevski, I., & Cerovac, N. (2014). Second-generation antipsychotics and extrapyramidal adverse effects. In *BioMed Research International, 2014*. https://doi.org/10.1155/2014/656370

Dráberová, E., Lukáš, Z., Ivanyi, D., Viklický, V., & Dráber, P. (1998). Expression class III β-tubulin in normal and neoplastic human tissues. *Histochemistry and Cell Biology*, *109*(3). https://doi.org/10.1007/s004180050222

Duan, W., Zhang, Y. P., Hou, Z., Huang, C., Zhu, H., Zhang, C. Q., & Yin, Q. (2016). Novel Insights into NeuN: from Neuronal Marker to Splicing Regulator. In *Molecular Neurobiology, 53(*3). https://doi.org/10.1007/s12035-015-9122-5

Eisch, A. J., Cameron, H. A., Encinas, J. M., Meltzer, L. A., Ming, G. L., & Overstreet-Wadiche, L. S. (2008). Adult neurogenesis, mental health, and mental illness: Hope or hype? *Journal of Neuroscience*, *28*(46). https://doi.org/10.1523/JNEUROSCI.3798-08.2008

Elkis, H., & Buckley, P. F. (2016). Treatment-Resistant Schizophrenia. In *Psychiatric Clinics of North America, 39*(2). https://doi.org/10.1016/j.psc.2016.01.006

Emamian, E. S., Hall, D., Birnbaum, M. J., Karayiorgou, M., & Gogos, J. A. (2004). Convergent evidence for impaired AKT1-GSK3beta signaling in schizophrenia. *Nature Genetics*, *36*(2), 131–137. https://doi.org/https://doi.org/10.1038/ng1296

English, J. A., Fan, Y., Föcking, M., Lopez, L. M., Hryniewiecka, M., Wynne, K., Dicker, P., Matigian, N., Cagney, G., Mackay-Sim, A., & Cotter, D. R. (2015). Reduced protein synthesis in schizophrenia patient-derived olfactory cells. *Translational Psychiatry*, *5*(10). https://doi.org/10.1038/TP.2015.119

Ennaceur, A. (2010). One-trial object recognition in rats and mice: Methodological and theoretical issues. In *Behavioural Brain Research, 215*(2). https://doi.org/10.1016/j.bbr.2009.12.036

Ercan-Sencicek, A. G., Davis Wright, N. R., Sanders, S. J., Oakman, N., Valdes, L., Bakkaloglu, B., Doyle, N., Yrigollen, C. M., Morgan, T. M., & Grigorenko, E. L. (2012). A balanced t(10;15) translocation in a male patient with developmental language disorder. *European Journal of Medical Genetics*, *55*(2). https://doi.org/10.1016/j.ejmg.2011.12.005

Falcone, T., Carlton, E., Lee, C., Janigro, M., Fazio, V., Forcen, F. E., Franco, K., & Janigro, D. (2015). Does systemic inflammation play a role in pediatric psychosis? *Clinical Schizophrenia and Related Psychoses*, *9*(2). https://doi.org/10.3371/CSRP.FACA.030813

Faludi, G., & Mirnics, K. (2011). Synaptic changes in the brain of subjects with schizophrenia. *International Journal of Developmental Neuroscience*, *29*(3). https://doi.org/10.1016/j.ijdevneu.2011.02.013

Fegert, J. M., Diehl, C., Leyendecker, B., Hahlweg, K., Prayon-Blum, V., Schuler-Harms, M., Werding, M., Andresen, S., Beblo, M., Diewald, M., Fangerau, H., Gerlach, I., Kreyenfeld, M., Nebe, K., Ott, N., Rauschenbach, T., Spieb, C. K., & Walper, S. (2018). Psychosocial problems in traumatized refugee families: Overview of risks and some recommendations for support services. *Child and Adolescent Psychiatry and Mental Health*, *12*(1). https://doi.org/10.1186/s13034-017-0210-3

Feinberg, I. (1982). Schizophrenia: Caused by a fault in programmed synaptic elimination during adolescence? *Journal of Psychiatric Research*, *17*(4). https://doi.org/10.1016/0022-3956(82)90038-3

Felder, C. C., Joyce, K. E., Briley, E. M., Mansouri, J., Mackie, K., Blond, O., Lai, Y., Ma, A. L., & Mitchell, R. L. (1995). Comparison of the pharmacology and signal transduction of the human cannabinoid CB1 and CB2 receptors. *Molecular Pharmacology*, *48*(3).

Fernández de Cossío, L., Guzmán, A., van der Veldt, S., & Luheshi, G. N. (2017). Prenatal infection leads to ASD-like behavior and altered synaptic pruning in the mouse offspring. *Brain, Behavior, and Immunity*, *63*. https://doi.org/10.1016/j.bbi.2016.09.028

Féron, F., Perry, C., McGrath, J. J., & Mackay-Sim, A. (1998). New techniques for biopsy and culture of human olfactory epithelial neurons. *Archives of Otolaryngology - Head and Neck Surgery*, *124*(8). https://doi.org/10.1001/archotol.124.8.861

Filbey, F. M., Aslan, S., Calhoun, V. D., Spence, J. S., Damaraju, E., Caprihan, A., & Segall, J. (2014). Long-term effects of marijuana use on the brain. *Proceedings of the National Academy of Sciences of the United States of America*, *111*(47). https://doi.org/10.1073/pnas.1415297111

Flax, J. D., Aurora, S., Yang, C., Simonin, C., Wills, A. M., Billinghurst, L. L., Jendoubi, M., Sidman, R. L., Wolfe, J. H., Kim, S. U., & Snyder, E. Y. (1998). Engraftable human neural stem cells respond to developmental cues, replace neurons, and express foreign genes. *Nature Biotechnology*, *16*(11). https://doi.org/10.1038/3473

Fleige, S., & Pfaffl, M. W. (2006). RNA integrity and the effect on the real-time qRT-PCR performance. In *Molecular Aspects of Medicine, 27(*2–3). https://doi.org/10.1016/j.mam.2005.12.003

Foti, D. J., Kotov, R., Guey, L. T., & Bromet, E. J. (2010). Cannabis use and the course of schizophrenia: 10-year follow-up after first hospitalization. *American Journal of Psychiatry*, *167*(8). https://doi.org/10.1176/appi.ajp.2010.09020189

Frydecka, D., Krzystek-Korpacka, M., Lubeiro, A., Stramecki, F., Stańczykiewicz, B., Beszłej, J. A., Piotrowski, P., Kotowicz, K., Szewczuk-Bogusławska, M., Pawlak-Adamska, E., & Misiak, B. (2018). Profiling inflammatory signatures of schizophrenia: A cross-sectional and meta-analysis study. *Brain, Behavior, and Immunity*, *71*. https://doi.org/10.1016/j.bbi.2018.05.002

Gage, F. H., Ray, J., & Fisher, L. J. (1995). Isolation, characterization, and use of stem cells from the CNS. In *Annual Review of Neuroscience, 18*. https://doi.org/10.1146/annurev.ne.18.030195.001111

Gage, S. H. (2019). Cannabis and psychosis : triangulating the evidence Engaging families to advance global mental health intervention research. *The Lancet Psychiatry*, *6*(5), 364–365. https://doi.org/10.1007/s00406-019-00983-5.Verweij

Galindo, L., Moreno, E., López-Armenta, F., Guinart, D., Cuenca-Royo, A., Izquierdo-Serra, M., Xicota, L., Fernandez, C., Menoyo, E., Fernández-Fernández, J. M., Benítez-King, G., Canela, E. I., Casadó, V., Pérez, V., de la Torre, R., & Robledo, P. (2018). Cannabis Users Show Enhanced Expression of CB1-5HT2A Receptor Heteromers in Olfactory Neuroepithelium Cells. *Molecular Neurobiology*, *55*(8). https://doi.org/10.1007/s12035-017-0833-7

Galli, R., Gritti, A., Bonfanti, L., & Vescovi, A. L. (2003). Neural stem cells: An overview. In *Circulation Research, 92*(6). https://doi.org/10.1161/01.RES.0000065580.02404.F4

Ganguli, R., Yang, Z., Shurin, G., Chengappa, K. N. R., Brar, J. S., Gubbi, A. V., & Rabin, B. S. (1994). Serum interleukin-6 concentration in schizophrenia: Elevation associated with duration of illness. *Psychiatry Research*, *51*(1). https://doi.org/10.1016/0165-1781(94)90042-6

Garay, P. A., & McAllister, A. K. (2010). Novel roles for immune molecules in neural development: Implications for neurodevelopmental disorders. In *Frontiers in Synaptic Neuroscience* (Issue SEP). https://doi.org/10.3389/fnsyn.2010.00136

García-Bea, A., Miranda-Azpiazu, P., Muguruza, C., Marmolejo-Martinez-Artesero, S., Diez-Alarcia, R., Gabilondo, A. M., Callado, L. F., Morentin, B., González-Maeso, J., & Meana, J. J. (2019). Serotonin 5-HT2A receptor expression and functionality in postmortem frontal cortex of subjects with schizophrenia: Selective biased agonism via Gαi1-proteins. *European Neuropsychopharmacology*, *29*(12). https://doi.org/10.1016/j.euroneuro.2019.10.013

Garcia-Mompo, C., Curto, Y., Carceller, H., Gilabert-Juan, J., Rodriguez-Flores, E., Guirado, R., & Nacher, J. (2020). Δ-9-Tetrahydrocannabinol treatment during adolescence and alterations in the inhibitory networks of the adult prefrontal cortex in mice subjected to perinatal NMDA receptor antagonist injection and to postweaning social isolation. *Translational Psychiatry*, *10*(1). https://doi.org/10.1038/s41398-020-0853-3

Garey, L. (2010). When cortical development goes wrong: Schizophrenia as a neurodevelopmental disease of microcircuits. *Journal of Anatomy*, *217*(4). https://doi.org/10.1111/j.1469-7580.2010.01231.x

Garver, D. L., Tamas, R. L., & Holcomb, J. A. (2003). Elevated interleukin-6 in the cerebrospinal fluid of a previously delineated schizophrenia subtype. *Neuropsychopharmacology*, *28*(8). https://doi.org/10.1038/sj.npp.1300217

Gasser, M. C., Berti, I., Hauser, K. F., Fischer-Colbrie, R., & Saria, A. (2003). Secretoneurin promotes pertussis toxin-sensitive neurite outgrowth in cerebellar granule cells. *Journal of Neurochemistry*, *85*(3). https://doi.org/10.1046/j.1471-4159.2003.01677.x

GBD 2017 Disease and Injury Incidence and Prevalence Collaborators, S. L., Abate, D., Abate, K. H., Abay, S. M., Abbafati, C., Abbasi, N., Abbastabar, H., Abd-Allah, F., Abdela, J., Abdelalim, A., Abdollahpour, I., Abdulkader, R. S., Abebe, Z., Abera, S. F., Abil, O. Z., Abraha, H. N., Abu-Raddad, L. J., Abu-Rmeileh, N. M. E., Accrombessi, M. M. K., … Murray, C. J. L. (2018). Global, regional, and national incidence, prevalence, and years lived with disability for 354 diseases and injuries for 195 countries and territories, 1990-2017: a systematic analysis for the Global Burden of Disease Study 2017. *Lancet (London, England)*, *392*(10159), 1789–1858. https://doi.org/10.1016/S0140-6736(18)32279-7

Gil-Perotín, S., Duran-Moreno, M., Cebrián-Silla, A., Ramírez, M., García-Belda, P., & García-Verdugo, J. M. (2013). Adult neural stem cells from the subventricular zone: A review of the neurosphere assay. *Anatomical Record*, *296*(9). https://doi.org/10.1002/ar.22746

Gilmore, J. H., & Jarskog, L. F. (1997). Exposure to infection and brain development: cytokines in the pathogenesis of schizophrenia. *Schizophrenia Research*, *24*(3), 365–367. https://doi.org/https://doi.org/10.1016/s0920-9964(96)00123-5

Giovanoli, S., Notter, T., Richetto, J., Labouesse, M. A., Vuillermot, S., Riva, M. A., & Meyer, U. (2015). Late prenatal immune activation causes hippocampal deficits in the absence of persistent inflammation across aging. *Journal of Neuroinflammation*, *12*(1). https://doi.org/10.1186/s12974-015-0437-y

Giovanoli, S., Weber-Stadlbauer, U., Schedlowski, M., Meyer, U., & Engler, H. (2016). Prenatal immune activation causes hippocampal synaptic deficits in the absence of overt microglia anomalies. *Brain, Behavior, and Immunity*, *55*. https://doi.org/10.1016/j.bbi.2015.09.015

Glantz, L. A., & Lewis, D. A. (2000). Decreased dendritic spine density on prefrontal cortical pyramidal neurons in schizophrenia. *Archives of General Psychiatry*, *57*(1). https://doi.org/10.1001/archpsyc.57.1.65

Gogos, A., Ney, L. J., Seymour, N., & Van Rheenen, T. E., Felmingham, K. L. (2019). Sex differences in schizophrenia, bipolar disorder, and post-traumatic stress disorder: Are gonadal hormones the link? *British Journal of Pharmacology*, *176*(21), 4119–4135. https://doi.org/10.1111/bph.14584

Goh, J. Y., O'Sullivan, S. E., Shortall, S. E., Zordan, N., Piccinini, A. M., Potter, H. G., Fone, K. C. F., & King, M. V. (2020). Gestational poly(I:C) attenuates, not exacerbates, the behavioral, cytokine and mTOR changes caused by isolation rearing in a rat 'dual-hit' model for neurodevelopmental disorders. *Brain, Behavior, and Immunity*, *89*. https://doi.org/10.1016/j.bbi.2020.05.076

Goldsmith, D. R., Rapaport, M. H., & Miller, B. J. (2016). A meta-analysis of blood cytokine network alterations in psychiatric patients: Comparisons between schizophrenia, bipolar disorder and depression. *Molecular Psychiatry*, *21*(12). https://doi.org/10.1038/mp.2016.3

Golofast, B., & Vales, K. (2020). The connection between microbiome and schizophrenia. In *Neuroscience and Biobehavioral Reviews, 108*. https://doi.org/10.1016/j.neubiorev.2019.12.011

González-Castillo, C., Ortuño-Sahagún, D., Guzmán-Brambila, C., Pallàs, M., & Rojas-Mayorquín, A. E. (2015). Pleiotrophin as a central nervous system neuromodulator, evidences from the hippocampus. *Frontiers in Cellular Neuroscience*, *8*(JAN). https://doi.org/10.3389/fncel.2014.00443

Green, A. I., Salomon, M. S., Brenner, M. J., & Rawlins, K. (2002). Treatment of schizophrenia and comorbid substance use disorder. In *Current drug targets. CNS and neurological disorders, 1*(2). https://doi.org/10.2174/1568007024606230

Grohmann, U., Fallarino, F., & Puccetti, P. (2003). Tolerance, DCs and tryptophan: Much ado about IDO. In *Trends in Immunology, 24*(5). https://doi.org/10.1016/S1471-4906(03)00072-3

Grońska-Pęski, M., Schachner, M., & Hébert, J. M. (2020). L1cam curbs the differentiation of adult-born hippocampal neurons. *Stem Cell Research*, *48*. https://doi.org/10.1016/j.scr.2020.101999

Guerrin, C. G. J., Doorduin, J., Sommer, I. E., & de Vries, E. F. J. (2021). The dual hit hypothesis of schizophrenia: Evidence from animal models. *Neuroscience and Biobehavioral Reviews*, *131*(October), 1150–1168. https://doi.org/10.1016/j.neubiorev.2021.10.025

Guinart, D., Moreno, E., Galindo, L., Cuenca-Royo, A., Barrera-Conde, M., Pérez, E. J., Fernández-Avilés, C., Correll, C. U., Canela, E. I., Casadó, V., Cordomi, A., Pardo, L., De La Torre, R., Pérez, V., & Robledo, P. (2020). Altered Signaling in CB1R-5-HT2AR Heteromers in Olfactory Neuroepithelium Cells of Schizophrenia Patients is Modulated by Cannabis Use. *Schizophrenia Bulletin*, *46*(6). https://doi.org/10.1093/schbul/sbaa038

Guloksuz, S., Pries, L. K., Delespaul, P., Kenis, G., Luykx, J. J., Lin, B. D., Richards, A. L., Akdede, B., Binbay, T., Altınyazar, V., Yalınçetin, B., Gümüş-Akay, G., Cihan, B., Soygür, H., Ulaş, H., Cankurtaran, E., Kaymak, S. U., Mihaljevic, M. M., Petrovic, S. A., … van Os, J. (2019). Examining the independent and joint effects of molecular genetic liability and environmental exposures in schizophrenia: results from the EUGEI study. *World Journal of Psychiatry*, *18*(2), 173–182. https://doi.org/doi: 10.1002/wps.20629

Gulsuner, S., Stein, D. J., Susser, E. S., Sibeko, G., Pretorius, A., Walsh, T., Majara, L., Mndini, M. M., Mqulwana, S. G., Ntola, O. A., Casadei, S., Ngqengelele, L. L., Korchina, V., Van Der Merwe, C., Malan, M., Fader, K. M., Feng, M., Willoughby, E., Muzny, D., … McClellan, J. M. (2020). Genetics of schizophrenia in the South African Xhosa. *Science*, *367*(6477), 569–573. https://doi.org/10.1126/science.aay8833

Guma, E., Bordignon, P. do C., Devenyi, G. A., Gallino, D., Anastassiadis, C., Cvetkovska, V., Barry, A. D., Snook, E., Germann, J., Greenwood, C. M. T., Misic, B., Bagot, R. C., & Chakravarty, M. M. (2021). Early or Late Gestational Exposure to Maternal Immune Activation Alters Neurodevelopmental Trajectories in Mice: An Integrated Neuroimaging, Behavioral, and Transcriptional Study. *Biological Psychiatry*, *90*(5). https://doi.org/10.1016/j.biopsych.2021.03.017

Guma, E., Cupo, L., Ma, W., Gallino, D., Moquin, L., Gratton, A., Devenyi, G. A., & Chakravarty, M. M. (2023). Investigating the "two-hit hypothesis": Effects of prenatal maternal immune activation and adolescent cannabis use on neurodevelopment in mice. *Progress in Neuro-Psychopharmacology and Biological Psychiatry*, *120*. https://doi.org/10.1016/j.pnpbp.2022.110642

Gururajan, A., & van den Buuse, M. (2014). Is the mTOR-signalling cascade disrupted in Schizophrenia? *Journal of Neurochemistry*, *129*, 377.387. https://doi.org/10.1111/jnc.12622

Haddad, F. L., Patel, S. V., & Schmid, S. (2020). Maternal Immune Activation by Poly I:C as a preclinical Model for Neurodevelopmental Disorders: A focus on Autism and Schizophrenia. *Neuroscience and Biobehavioral Reviews*, *113*(April), 546–567. https://doi.org/10.1016/j.neubiorev.2020.04.012

Haddad, P. M., & Correll, C. U. (2018). The acute efficacy of antipsychotics in schizophrenia: a review of recent meta-analyses. *Therapeutic Advances in Psychopharmacology*, *8*(11). https://doi.org/10.1177/2045125318781475

Häfner, H. (2003). Gender differences in schizophrenia. *Psychoneuroendocrinology*, *28*(SUPPL. 2), 17–54. https://doi.org/10.1016/S0306-4530(02)00125-7

Hahn, C. G., Han, L. Y., Rawson, N. E., Mirza, N., Borgmann-Winter, K., Lenox, R. H., & Arnolb, S. E. (2005). In vivo and in vitro neurogenesis in human olfactory epithelium. *Journal of Comparative Neurology*, *483*(2). https://doi.org/10.1002/cne.20424

Halberstadt, A. L., & Geyer, M. A. (2018). Effect of hallucinogens on unconditioned behavior. In *Current Topics in Behavioral Neurosciences, 36*. https://doi.org/10.1007/7854_2016_466

Hall, W., & Degenhardt, L. (2009). Adverse health effects of non-medical cannabis use. In *The Lancet, 374*(9698). https://doi.org/10.1016/S0140-6736(09)61037-0

Hampe, C. S., Mitoma, H., & Manto, M. (2018). GABA and Glutamate: Their Transmitter Role in the CNS and Pancreatic Islets. In *GABA And Glutamate - New Developments In Neurotransmission Research*. https://doi.org/10.5772/intechopen.70958

Hamshere, M. L., Walters, J. T. R., Richards, A. L., Green, E., Grozeva, D., Jones, I., Forty, L., Gordon-Smith, K., Riley, B. P., O'Neill, F. A., Kendler, K. S., Sklar, P., Purcell, S., & Kranz, J. (2013). Genome-wide significant associations in schizophrenia to ITIH3/4, CACNA1C and SDCCAG8, and extensive replication of associations reported by the Schizophrenia PGC. *Molecular Psychiatry*, *18*(6), 708–712. https://doi.org/doi: 10.1038/mp.2012.67.

Handunnetthi, L., Saatci, D., Hamley, J. C., & Knight, J. C. (2021). Maternal immune activation downregulates schizophrenia genes in the foetal mouse brain. *Brain Communications*, *3*(4), 1–9. https://doi.org/10.1093/braincomms/fcab275

Hao, K., Su, X., Luo, B., Cai, Y., Chen, T., Yang, Y., Shao, M., Song, M., Zhang, L., Zhong, Z., Li, W., & Lv, L. (2019). Prenatal immune activation induces age-related alterations in rat offspring: Effects upon NMDA receptors and behaviors. *Behavioural Brain Research*, *370*. https://doi.org/10.1016/j.bbr.2019.111946

Hasan, A., Falkai, P., Lehmann, I., & Gaebel, W. (2020). Clinical practice guideline: Schizophrenia. *Deutsches Arzteblatt International*, *117*(24), 412–419. https://doi.org/10.3238/arztebl.2020.0412

Havercroft, J. C., & Cleveland, D. W. (1984). Programmed expression of β-tubulin genes during development and differentiation of the chicken. *Journal of Cell Biology*, *99*(6). https://doi.org/10.1083/jcb.99.6.1927

Hawi, Z., Yates, H., Pinar, A., Arnatkeviciute, A., Johnson, B., Tong, J., Pugsley, K., Dark, C., Pauper, M., Klein, M., Heussler, H. S., Hiscock, H., Fornito, A., Tiego, J., Finlay, A., Vance, A., Gill, M., Kent, L., & Bellgrove, M. A. (2018). A case-control genome-wide association study of ADHD discovers a novel association with the tenascin R (TNR) gene. *Translational Psychiatry*, *8*, 284. https://doi.org/10.1038/s41398-018-0329-x

Hertzler, J. I., Simonovitch, S. I., Albertson, R. M., Weiner, A. T., Nye, D. M. R., & Rolls, M. M. (2020). Kinetochore proteins suppress neuronal microtubule dynamics and promote dendrite regeneration. *Molecular Biology of the Cell*, *31*(19). https://doi.org/10.1091/mbc.E20-04-0237-T

Hilker, R., Helenius, D., Fagerlund, B., Skytthe, A., Christensen, K., Werge, T. M., Nordentoft, M., & Glenthøj, B. (2018). Heritability of Schizophrenia and Schizophrenia Spectrum Based on the Nationwide Danish Twin Register. *Biological Psychiatry*, *83*(6), 492–498. https://doi.org/10.1016/j.biopsych.2017.08.017

Hill, M. N., Froc, D. J., Fox, C. J., Gorzalka, B. B., & Christie, B. R. (2004). Prolonged cannabinoid treatment results in spatial working memory deficits and impaired long-term potentiation in the CA1 region of the hippocampus in vivo. *European Journal of Neuroscience*, *20*(3). https://doi.org/10.1111/j.1460-9568.2004.03522.x

Hino, M., Kunii, Y., Matsumoto, J., Wada, A., Nagaoka, A., Niwa, S. ichi, Takahashi, H., Kakita, A., Akatsu, H., Hashizume, Y., Yamamoto, S., & Yabe, H. (2016). Decreased VEGFR2 expression and increased phosphorylated Akt1 in the prefrontal cortex of individuals with schizophrenia. *Journal of Psychiatric Research*, *82*. https://doi.org/10.1016/j.jpsychires.2016.07.018

Hirokawa, N. (1990). Neuronal cytoskeleton: molecular architecture, function and dynamics. *Tanpakushitsu Kakusan Koso. Protein, Nucleic Acid, Enzyme*, *35*(4 Suppl).

Hirokawa, N. (1994). Microtubule organization and dynamics dependent on microtubule-associated proteins. *Current Opinion in Cell Biology*, *6*(1). https://doi.org/10.1016/0955-0674(94)90119-8

Hjorthøj, C., Stürup, A. E., McGrath, J. J., & Nordentoft, M. (2017). Years of potential life lost and life expectancy in schizophrenia: a systematic review and meta-analysis. *The Lancet Psychiatry*, *4*(4), 295–301. https://doi.org/10.1016/S2215-0366(17)30078-0

Hollins, S. L., Zavitsanou, K., Walker, F. R., & Cairns, M. J. (2016). Alteration of transcriptional networks in the entorhinal cortex after maternal immune activation and adolescent cannabinoid exposure. *Brain, Behavior, and Immunity*, *56*. https://doi.org/10.1016/j.bbi.2016.02.021

Howard, R., Rabins, P. V., Seeman, M. V., & Jeste, D. V. (2000). Late-onset schizophrenia and very-late-onset schizophrenia-like psychosis: An international consensus. *American Journal of Psychiatry*, *157*(2). https://doi.org/10.1176/appi.ajp.157.2.172

Hu, P., Chen, X., Sun, J., Bie, P., & Zhang, L. Da. (2015). SiRNA-mediated knockdown against NUF2 suppresses pancreatic cancer proliferation in vitro and in vivo. *Bioscience Reports*, *35*. https://doi.org/10.1042/BSR20140124

Huang, H. S., & Akbarian, S. (2007). GAD1 mRNA expression and DNA methylation in prefrontal cortex of subjects with schizophrenia. *PLoS ONE*, *2*(8). https://doi.org/10.1371/journal.pone.0000809

Huang, W., Zhu, P. J., Zhang, S., Zhou, H., Stoica, L., Galiano, M., Krnjević, K., Roman, G., & Costa-Mattioli, M. (2013). MTORC2 controls actin polymerization required for consolidation of long-term memory. *Nature Neuroscience*, *16*(4). https://doi.org/10.1038/nn.3351

Huang, X. L., Zou, Y. S., Maher, T. A., Newton, S., & Milunsky, J. M. (2010). A de novo balanced translocation breakpoint truncating the autism susceptibility candidate 2 (AUTS2) gene in a patient with autism. In *American Journal of Medical Genetics, Part A, 152*(8). https://doi.org/10.1002/ajmg.a.33497

Hudson, R., Renard, J., Norris, C., Rushlow, W. J., & Laviolette, S. R. (2019). Cannabidiol counteracts the psychotropic side-effects of Δ-9-tetrahydrocannabinol in the ventral hippocampus through bidirectional control of erk1-2 phosphorylation. *Journal of Neuroscience*, *39*(44). https://doi.org/10.1523/JNEUROSCI.0708-19.2019

Huhn, M., Nikolakopoulou, A., Schneider-Thoma, J., Krause, M., Samara, M., Peter, N., Arndt, T., Bäckers, L., Rothe, P., Cipriani, A., Davis, J., Salanti, G., & Leucht, S. (2019). Comparative efficacy and tolerability of 32 oral antipsychotics for the acute treatment of adults with multi-episode schizophrenia: a systematic review and network meta-analysis. *The Lancet*, *394*(10202). https://doi.org/10.1016/S0140-6736(19)31135-3

Hwang, E. K., & Lupica, C. R. (2020). Altered Corticolimbic Control of the Nucleus Accumbens by Long-term Δ9-Tetrahydrocannabinol Exposure. *Biological Psychiatry*, *87*(7). https://doi.org/10.1016/j.biopsych.2019.07.024

Ibarra-Lecue, I., Diez-Alarcia, R., Morentin, B., Meana, J. J., Callado, L. F., & Urigüen, L. (2020). Ribosomal Protein S6 Hypofunction in Postmortem Human Brain Links mTORC1-Dependent Signaling and Schizophrenia. *Frontiers in Pharmacology*, *11*. https://doi.org/10.3389/fphar.2020.00344

Ibarra-Lecue, I., Diez-Alarcia, R., & Urigüen, L. (2021). Serotonin 2A receptors and cannabinoids. In *Progress in Brain Research, 259*. https://doi.org/10.1016/bs.pbr.2021.01.004

Ibarra-Lecue, I., Mollinedo-Gajate, I., Meana, J. J., Callado, L. F., Diez-Alarcia, R., & Urigüen, L. (2018). Chronic cannabis promotes pro-hallucinogenic signaling of 5-HT2A receptors through Akt/mTOR pathway. *Neuropsychopharmacology*, *43*(10), 2028–2035. https://doi.org/10.1038/s41386-018-0076-y

Idotta, C., Tibaldi, E., Brunati, A. M., Pagano, M. A., Cadamuro, M., Miola, A., Martini, A., Favaretto, N., Cazzador, D., Favaro, A., Pavan, C., Pigato, G., Tenconi, E., Gentili, F., Cremonese, C., Bertocci, I., Solmi, M., & Toffanin, T. (2019). Olfactory neuroepithelium alterations and cognitive correlates in schizophrenia. *European Psychiatry*, *61*. https://doi.org/10.1016/j.eurpsy.2019.06.004

Imrich, S., Hachmeister, M., & Gires, O. (2012). EpCAM and its potential role in tumor-initiating cells. In *Cell Adhesion and Migration, 6*(1). https://doi.org/10.4161/cam.18953

Institute for Health Metrics and Evaluation (IHME). (2020). *GBD 2019*. *October*. www.ghdx.healthdata.org

Ioannidou, C., Marsicano, G., & Busquets-Garcia, A. (2018). Assessing Prepulse Inhibition of Startle in Mice. *BIO-PROTOCOL*, *8*(7). https://doi.org/10.21769/bioprotoc.2789

Iroegbu, J. D., Ijomone, O. K., Femi-Akinlosotu, O. M., & Ijomone, O. M. (2021). ERK/MAPK signalling in the developing brain: Perturbations and consequences. In *Neuroscience and Biobehavioral Reviews, 131*. https://doi.org/10.1016/j.neubiorev.2021.10.009

Ito, H. T., Smith, S. E. P., Hsiao, E., & Patterson, P. H. (2010). Maternal immune activation alters nonspatial information processing in the hippocampus of the adult offspring. *Brain, Behavior, and Immunity*, *24*(6). https://doi.org/10.1016/j.bbi.2010.03.004

Iwase, K., Ishihara, A., Yoshimura, S., Andoh, Y., Kato, M., Seki, N., Matsumoto, E., Hiwasa, T., Muller, D., Fukunaga, K., & Takiguchi, M. (2014). The secretogranin II gene is a signal integrator of glutamate and dopamine inputs. *Journal of Neurochemistry*, *128*(2). https://doi.org/10.1111/jnc.12467

Jacobus, J., Squeglia, L. M., Sorg, S. F., Nguyen-Louie, T. T., & Tapert, S. F. (2014). Cortical thickness and neurocognition in adolescent marijuana and alcohol users following 28 days of monitored abstinence. *Journal of Studies on Alcohol and Drugs*, *75*(5). https://doi.org/10.15288/jsad.2014.75.729

Jalewa, J., Todd, J., Michie, P. T., Hodgson, D. M., & Harms, L. (2023). The effect of schizophrenia risk factors on mismatch responses in a rat model. *Psychophysiology*, *60*(2). https://doi.org/10.1111/psyp.14175

Jarskog, L. F., Miyamoto, S., & Lieberman, J. A. (2007). Schizophrenia: New pathological insights and therapies. In *Annual Review of Medicine, 58*. https://doi.org/10.1146/annurev.med.58.060904.084114

Jauhar, S., Johnstone, M., & McKenna, P. J. (2022). Schizophrenia. *Lancet*, *399*(10323), 473–486. https://doi.org/10.1016/S0140-6736(21)01730-X

Javitt, D. C. (2007). Glutamate and Schizophrenia: Phencyclidine, N-Methyl-d-Aspartate Receptors, and Dopamine-Glutamate Interactions. In *International Review of Neurobiology, 78*. https://doi.org/10.1016/S0074-7742(06)78003-5

Jernigan, C. S., Goswami, D. B., Austin, M. C., Iyo, A. H., Chandran, A., Stockmeier, C. A., & Karolewicz, B. (2011). The mTOR signaling pathway in the prefrontal cortex is compromised in major depressive disorder. *Progress in Neuro-Psychopharmacology and Biological Psychiatry*, *35*(7). https://doi.org/10.1016/j.pnpbp.2011.05.010

Jiang, Y. Q., & Oblinger, M. M. (1992). Differential regulation of βiii and other tubulin genes during peripheral and central neuron development. *Journal of Cell Science*, *103*(3), 643–651. https://doi.org/10.1242/jcs.103.3.643

Jiménez-Vaca, A. L., Benitez-King, G., Ruiz, V., Ramírez-Rodríguez, G. B., Hernández-de la Cruz, B., Salamanca-Gómez, F. A., González-Márquez, H., Ramírez-Sánchez, I., Ortíz-López, L., Vélez-del Valle, C., & Ordoñez-Razo, R. M. (2018). Exfoliated Human Olfactory Neuroepithelium: A Source of Neural Progenitor Cells. *Molecular Neurobiology*, *55*(3). https://doi.org/10.1007/s12035-017-0500-z

Joachim, R. A., Hildebrandt, M., Oder, J., Klapp, B. F., & Arck, P. C. (2001). Murine stress-triggered abortion is mediated by increase of CD8+ TNF-α+ decidual cells via substance P. *American Journal of Reproductive Immunology*, *45*(5). https://doi.org/10.1111/j.8755-8920.2001.450506.x

Jones, C., Watson, D., Fone, K., & Fone, K. (2011). *Themed Issue: Translational Neuropharmacology-Using Appropriate Animal Models to Guide Clinical Drug Development Animal models of schizophrenia Correspondence LINKED ARTICLES*. https://doi.org/10.1111/bph.2011.164.issue-4

Jones, P. B., Barnes, T. R. E., Davies, L., Dunn, G., Lloyd, H., Hayhurst, K. P., Murray, R. M., Markwick, A., & Lewis, S. W. (2006). Randomized controlled trial of the effect on quality of life of second- vs first-generation antipsychotic drugs in schizophrenia: Cost Utility of the Latest Antipsychotic Drugs in Schizophrenia Study (CUtLASS 1). *Archives of General Psychiatry*, *63*(10). https://doi.org/10.1001/archpsyc.63.10.1079

Jongsma, H. E., Turner, C., Kirkbride, J. B., & Jones, P. B. (2019). International incidence of psychotic disorders, 2002-17: a systematic review and meta-analysis. *The Lancet. Public Health*, *4*(5), e229–e244. https://doi.org/10.1016/S2468-2667(19)30056-8

Kaiya, H., Uematsu, M., Ofuji, M., Nishida, A., Takeuchi, K., Nozaki, M., & Idaka, E. (1989). Elevated plasma prostaglandin E2 levels in schizophrenia. *Journal of Neural Transmission*, *77*(1). https://doi.org/10.1007/BF01255817

Kalus, P., Muller, T. J., Zuschratter, W., & Senitz, D. (2000). The dendritic architecture of prefrontal pyramidal neurons in schizophrenic patients. *NeuroReport*, *11*(16). https://doi.org/10.1097/00001756-200011090-00044

Karlsson, H., & Dalman, C. (2020). Epidemiological Studies of Prenatal and Childhood Infection and Schizophrenia. In *Current topics in behavioral neurosciences, 44*. https://doi.org/10.1007/7854_2018_87

Katz, J., Keenan, B., & Snyder, E. Y. (2010). Culture and manipulation of neural stem cells. *Advances in Experimental Medicine and Biology*, *671*. https://doi.org/10.1007/978-1-4419-5819-8_2

Keenan, T. M., Nelson, A. D., Grinager, J. R., Thelen, J. C., & Svendsen, C. N. (2010). Real time imaging of human progenitor neurogenesis. *PLoS ONE*, *5*(10). https://doi.org/10.1371/journal.pone.0013187

Kelly, D. L., Li, X., Kilday, C., Feldman, S., Clark, S., Liu, F., Buchanan, R. W., & Tonelli, L. H. (2018). Increased circulating regulatory T cells in medicated people with schizophrenia. *Psychiatry Research*, *269*. https://doi.org/10.1016/j.psychres.2018.09.006

Kelly, J. R., Minuto, C., Cryan, J. F., Clarke, G., & Dinan, T. G. (2021). The role of the gut microbiome in the development of schizophrenia. *Schizophrenia Research*, *234*. https://doi.org/10.1016/j.schres.2020.02.010

Kempermann, G., Krebs, J., & Fabel, K. (2008). The contribution of failing adult hippocampal neurogenesis to psychiatric disorders. In *Current Opinion in Psychiatry, 21*(3). https://doi.org/10.1097/YCO.0b013e3282fad375

Kentner, A. C., Bilbo, S. D., Brown, A. S., Hsiao, E. Y., McAllister, A. K., Meyer, U., Pearce, B. D., Pletnikov, M. V., Yolken, R. H., & Bauman, M. D. (2019). Maternal immune activation: reporting guidelines to improve the rigor, reproducibility, and transparency of the model. In *Neuropsychopharmacology, 44*(2). https://doi.org/10.1038/s41386-018-0185-7

Keshavan, M. S., Anderson, S., & Pettergrew, J. W. (1994). Is Schizophrenia due to excessive synaptic pruning in the prefrontal cortex? The Feinberg hypothesis revisited. *Journal of Psychiatric Research*, *28*(3). https://doi.org/10.1016/0022-3956(94)90009-4

Khandaker, G. M., Cousins, L., Deakin, J., Lennox, B. R., Yolken, P. R., & Jones, P. P. B. (2015). Inflammation and immunity in schizophrenia: implications for pathophysiology and treatment. *Lancet Psychiatry*, *2*(3), 258–270. https://doi.org/10.1016/S2215-0366(14)00122-9.

Khandaker, G. M., Pearson, R. M., Zammit, S., Lewis, G., & Jones, P. B. (2014). Association of serum interleukin 6 and C-reactive protein in childhood with depression and psychosis in young adult life a population-based longitudinal study. *JAMA Psychiatry*, *71*(10). https://doi.org/10.1001/jamapsychiatry.2014.1332

Kim, Y. K., Myint, A. M., Verkerk, R., Scharpe, S., Steinbusch, H., & Leonard, B. (2009). Cytokine changes and tryptophan metabolites in medication-naïve and medication-free schizophrenic patients. *Neuropsychobiology*, *59*(2). https://doi.org/10.1159/000213565

Kindler, J., Lim, C. K., Weickert, C. S., Boerrigter, D., Galletly, C., Liu, D., Jacobs, K. R., Balzan, R., Bruggemann, J., O'Donnell, M., Lenroot, R., Guillemin, G. J., & Weickert, T. W. (2020). Dysregulation of kynurenine metabolism is related to proinflammatory cytokines, attention, and prefrontal cortex volume in schizophrenia. *Molecular Psychiatry*, *25*(11). https://doi.org/10.1038/s41380-019-0401-9

King, S., St-Hilaire, A., & Heidkamp, D. (2010). Prenatal factors in schizophrenia. *Current Directions in Psychological Science*, *19*(4), 209–213. https://doi.org/10.1177/0963721410378360

Kirkbride, J. B., Errazuriz, A., Croudace, T. J., Morgan, C., Jackson, D., Boydell, J., Murray, R. M., & Jones, P. B. (2012). Incidence of schizophrenia and other psychoses in England, 1950-2009: A systematic review and meta-analyses. *PLoS ONE*, *7*(3). https://doi.org/10.1371/journal.pone.0031660

Kiss, J. Z., & Muller, D. (2001). Contribution of the neural cell adhesion molecule to neuronal and synaptic plasticity. In *Reviews in the Neurosciences, 12*(4). https://doi.org/10.1515/REVNEURO.2001.12.4.297

Kline, E. R., Ferrara, M., Li, F., D'Souza, D. C., Keshavan, M., & Srihari, V. H. (2022). Timing of cannabis exposure relative to prodrome and psychosis onset in a community-based first episode psychosis sample. *Journal of Psychiatric Research*, *147*. https://doi.org/10.1016/j.jpsychires.2022.01.039

Knight, Z. A., Tan, K., Birsoy, K., Schmidt, S., Garrison, J. L., Wysocki, R. W., Emiliano, A., Ekstrand, M. I., & Friedman, J. M. (2012). Molecular Profiling of Activated Neurons by Phosphorylated Ribosome Capture. *Cell*, *151*(5). https://doi.org/10.1016/j.cell.2012.10.039.

Kobayashi, H., Ide, S., Hasegawa, J., Ujike, H., Sekine, Y., Ozaki, N., Inada, T., Harano, M., Komiyama, T., Yamada, M., Iyo, M., Shen, H. W., Ikeda, K., & Sora, I. (2004). Study of association between α-synuclein gene polymorphism and methamphetamine psychosis/dependence. *Annals of the New York Academy of Sciences*, *1025*. https://doi.org/10.1196/annals.1316.040

Korosi, A., Naninck, E. F. G., Oomen, C. A., Schouten, M., Krugers, H., Fitzsimons, C., & Lucassen, P. J. (2012). Early-life stress mediated modulation of adult neurogenesis and behavior. In *Behavioural Brain Research, 227*(2). https://doi.org/10.1016/j.bbr.2011.07.037

Krause, D., Weidinger, E., Dippel, C., Riedel, M., Schwarz, M. J., Müller, N., & Myint, A. M. (2013). Impact of different antipsychotics on cytokines and tryptophan metabolites in stimulated cultures from patients with schizophrenia. *Psychiatria Danubina*, *25*(4).

Krolewski, R. C., Jang, W., & Schwob, J. E. (2011). The generation of olfactory epithelial neurospheres in vitro predicts engraftment capacity following transplantation in vivo. *Experimental Neurology*, *229*(2). https://doi.org/10.1016/j.expneurol.2011.02.014

Kumar, V., Rao, N. P., Narasimha, V., Sathyanarayanan, G., Muralidharan, K., Varambally, S., Venkatasubramanian, G., & Gangadhar, B. N. (2016). Antipsychotic dose in maintenance treatment of schizophrenia: A retrospective study. *Psychiatry Research*, *245*. https://doi.org/10.1016/j.psychres.2016.08.042

Kumarasinghe, N., Beveridge, N. J., Gardiner, E., Scott, R. J., Yasawardene, S., Perera, A., Mendis, J., Suriyakumara, K., Schall, U., & Tooney, P. A. (2013). Gene expression profiling in treatment-naive schizophrenia patients identifies abnormalities in biological pathways involving AKT1 that are corrected by antipsychotic medication. *International Journal of Neuropsychopharmacology*, *16*(7). https://doi.org/10.1017/S1461145713000035

Labouesse, M. A., Dong, E., Grayson, D. R., Guidotti, A., & Meyer, U. (2015). Maternal immune activation induces GAD1 and GAD2 promoter remodeling in the offspring prefrontal cortex. *Epigenetics*, *10*(12), 1143–1155. https://doi.org/10.1080/15592294.2015.1114202

Lafferty, C. K., & Britt, J. P. (2020). Cannabis Exposure Enhances Subcortical Control of Nucleus Accumbens Activity. In *Biological Psychiatry, 87*(7). https://doi.org/10.1016/j.biopsych.2019.12.017

Lally, J., & MacCabe, J. H. (2015). Antipsychotic medication in schizophrenia: A review. *British Medical Bulletin*, *114*(1). https://doi.org/10.1093/bmb/ldv017

Laplante, M., & Sabatini, D. M. (2012). MTOR signaling in growth control and disease. In *Cell, 149*(2). https://doi.org/10.1016/j.cell.2012.03.017

Laprairie, R. B., Bagher, A. M., Kelly, M. E. M., & Denovan-Wright, E. M. (2015). Cannabidiol is a negative allosteric modulator of the cannabinoid CB1 receptor. *British Journal of Pharmacology*, *172*(20). https://doi.org/10.1111/bph.13250

Lecca, S., Luchicchi, A., Scherma, M., Fadda, P., Muntoni, A. L., & Pistis, M. (2019). Δ9-Tetrahydrocannabinol During Adolescence Attenuates Disruption of Dopamine Function Induced in Rats by Maternal Immune Activation. *Frontiers in Behavioral Neuroscience*, *13*. https://doi.org/10.3389/fnbeh.2019.00202

Lee, M. K., Rebhun, L. I., & Frankfurter, A. (1990). Posttranslational modification of class III β-tubulin. *Proceedings of the National Academy of Sciences of the United States of America*, *87*(18). https://doi.org/10.1073/pnas.87.18.7195

Lee, M. K., Tuttle, J. B., Rebhun, L. I., Cleveland, D. W., & Frankfurter, A. (1990). The expression and posttranslational modification of a neuron-specific β-tubulin isotype during chick embryogenesis. *Cell Motility and the Cytoskeleton*, *17*(2). https://doi.org/10.1002/cm.970170207

Lee, V. M., & Pixley, S. K. (1994). Age and differentiation-related differences in neuron-specific tubulin immunostaining of olfactory sensory neurons. *Developmental Brain Research*, *83*(2). https://doi.org/10.1016/0165-3806(94)00139-1

Lendahl, U., Zimmerman, L. B., & McKay, R. D. G. (1990). CNS stem cells express a new class of intermediate filament protein. *Cell*, *60*(4). https://doi.org/10.1016/0092-8674(90)90662-X

Lesh, T. A., Careaga, M., Rose, D. R., McAllister, A. K., Van de Water, J., Carter, C. S., & Ashwood, P. (2018). Cytokine alterations in first-episode schizophrenia and bipolar disorder: Relationships to brain structure and symptoms. *Journal of Neuroinflammation*, *15*(1). https://doi.org/10.1186/s12974-018-1197-2

Leslie, J. R., Imai, F., Fukuhara, K., Takegahara, N., Rizvi, T. A., Friedel, R. H., Wang, F., Kumanogoh, A., & Yoshida, Y. (2011). Ectopic myelinating oligodendrocytes in the dorsal spinal cord as a consequence of altered semaphorin 6D signaling inhibit synapse formation. *Development*, *138*(18). https://doi.org/10.1242/dev.066076

Lester, S. N., & Li, K. (2014). Toll-like receptors in antiviral innate immunity. In *Journal of Molecular Biology, 426*(6). https://doi.org/10.1016/j.jmb.2013.11.024

Leucht, S., Cipriani, A., Spineli, L., Mavridis, D., Örey, D., Richter, F., Samara, M., Barbui, C., Engel, R. R., Geddes, J. R., Kissling, W., Stapf, M. P., Lässig, B., Salanti, G., & Davis, J. M. (2013). Comparative efficacy and tolerability of 15 antipsychotic drugs in schizophrenia: A multiple-treatments meta-analysis. *The Lancet*, *382*(9896). https://doi.org/10.1016/S0140-6736(13)60733-3

Leung, C. T., Coulombe, P. A., & Reed, R. R. (2007). Contribution of olfactory neural stem cells to tissue maintenance and regeneration. *Nature Neuroscience*, *10*(6). https://doi.org/10.1038/nn1882

Lewis, D. A., Hashimoto, T., & Morris, H. M. (2008). Cell and receptor type-specific alterations in markers of GABA neurotransmission in the prefrontal cortex of subjects with schizophrenia. In *Neurotoxicity Research, 14*(2–3). https://doi.org/10.1007/BF03033813

Lewis, D. A., Hashimoto, T., & Volk, D. W. (2005). Cortical inhibitory neurons and schizophrenia. In *Nature Reviews Neuroscience, 6*(4). https://doi.org/10.1038/nrn1648

Leza, J. C., Bueno, B., Bioque, M., Arango, C., Parellada, M., Do, K., O'Donnell, P., & Bernardo, M. (2015). Inflammation in schizophrenia: A question of balance. In *Neuroscience and Biobehavioral Reviews, 55*. https://doi.org/10.1016/j.neubiorev.2015.05.014

Li, R., Ma, X., Wang, G., Yang, J., & Wang, C. (2016). Why sex differences in schizophrenia? *Journal of Translational Neuroscience (Beijing)*, *1*(1), 37–42.

Li, L., Hung, A. C., & Porter, A. G. (2008). Secretogranin II: A key AP-1-regulated protein that mediates neuronal differentiation and protection from nitric oxide-induced apoptosis of neuroblastoma cells. *Cell Death and Differentiation*, *15*(5). https://doi.org/10.1038/cdd.2008.8

Li, W., Chen, M., Feng, X., Song, M., Shao, M., Yang, Y., Zhang, L., Liu, Q., Lv, L., & Su, X. (2021). Maternal immune activation alters adult behavior, intestinal integrity, gut microbiota and the gut inflammation. *Brain and Behavior*, *11*(5). https://doi.org/10.1002/brb3.2133

Li, W., Ghose, S., Gleason, K., Begovic, A., Perez, J., Bartko, J., Russo, S., Wagner, A. D., Selemon, L., & Tamminga, C. A. (2015). Synaptic proteins in the hippocampus indicative of increased neuronal activity in CA3 in schizophrenia. *American Journal of Psychiatry*, *172*(4). https://doi.org/10.1176/appi.ajp.2014.14010123

Li, W., Sun, F., Guo, X., Hu, Y., Ding, S., Ding, M., Song, M., Shao, M., Yang, Y., Guo, W., Zhang, L., Zhang, Y., Wang, X., Su, X., & Lv, L. (2020). Behavioral abnormalities and phosphorylation deficits of extracellular signal-regulated kinases 1 and 2 in rat offspring of the maternal immune activation model. *Physiology and Behavior*, *217*. https://doi.org/10.1016/j.physbeh.2020.112805

Li, W. Y., Chang, Y. C., Lee, L. J. H., & Lee, L. J. (2014). Prenatal infection affects the neuronal architecture and cognitive function in adult mice. *Developmental Neuroscience*, *36*(5). https://doi.org/10.1159/000362383

Lie, D. C., Song, H., Colamarino, S. A., Ming, G. L., & Gage, F. H. (2004). Neurogenesis in the Adult Brain: New Strategies for Central Nervous System Diseases. In *Annual Review of Pharmacology and Toxicology, 44*. https://doi.org/10.1146/annurev.pharmtox.44.101802.121631

Lieberman, J. A., Stroup, T. S., McEvoy, J. P., Swartz, M. S., Rosenheck, R. A., Perkins, D. O., Keefe, R. S. E., Davis, S. M., Davis, C. E., Lebowitz, B. D., Severe, J., & Hsiao, J. K. (2005). Effectiveness of Antipsychotic Drugs in Patients with Chronic Schizophrenia. *New England Journal of Medicine*, *353*(12). https://doi.org/10.1056/nejmoa051688

Lin, A., Kenis, G., Bignotti, S., Tura, G. J. B., De Jong, R., Bosmans, E., Pioli, R., Altamura, C., Scharpé, S., & Maes, M. (1998). The inflammatory response system in treatment-resistant schizophrenia: Increased serum interleukin-6. *Schizophrenia Research*, *32*(1). https://doi.org/10.1016/S0920-9964(98)00034-6

Lin, Y., Peng, Y., He, S., Xu, J., Shi, Y., Su, Y., Zhu, C., Zhang, X., Zhou, R., & Cui, D. (2018). Serum IL-1ra, a novel biomarker predicting olanzapine-induced hypercholesterolemia and hyperleptinemia in schizophrenia. *Progress in Neuro-Psychopharmacology and Biological Psychiatry*, *84*. https://doi.org/10.1016/j.pnpbp.2018.01.020

Linneberg, C., Toft, C. L. F., Kjaer-Sorensen, K., & Laursen, L. S. (2019). L1cam-mediated developmental processes of the nervous system are differentially regulated by proteolytic processing. *Scientific Reports*, *9*(1). https://doi.org/10.1038/s41598-019-39884-x

Lins, B. R., Hurtubise, J. L., Roebuck, A. J., Marks, W. N., Zabder, N. K., Scott, G. A., Greba, Q., Dawicki, W., Zhang, X., Rudulier, C. D., Gordon, J. R., & Howland, J. G. (2018). Prospective analysis of the effects of maternal immune activation on rat cytokines during pregnancy and behavior of the male offspring relevant to Schizophrenia. *ENeuro*, *5*(4). https://doi.org/10.1523/ENEURO.0249-18.2018

Lisabeth, E. M., Falivelli, G., & Pasquale, E. B. (2013). Eph receptor signaling and ephrins. *Cold Spring Harbor Perspectives in Biology*, *5*(9). https://doi.org/10.1101/cshperspect.a009159

Liu, X., Wu, Z., Lian, J., Hu, C. H., Huang, X. F., & Deng, C. (2017). Time-dependent changes and potential mechanisms of glucose-lipid metabolic disorders associated with chronic clozapine or olanzapine treatment in rats. *Scientific Reports*, *7*(1). https://doi.org/10.1038/s41598-017-02884-w

Liu, Y., Pham, X., Zhang, L., Chen, P. lung, Burzynski, G., McGaughey, D. M., He, S., McGrath, J. A., Wolyniec, P., Fallin, M. D., Pierce, M. S., McCallion, A. S., Pulver, A. E., Avramopoulos, D., & Valle, D. (2015). Functional variants in DPYSL2 sequence increase risk of schizophrenia and suggest a link to mTOR signaling. *G3: Genes, Genomes, Genetics*, *5*(1). https://doi.org/10.1534/g3.114.015636

Ludewig, K., Geyer, M. A., & Vollenweider, F. X. (2003). Deficits in prepulse inhibition and habituation in never-medicated, first-episode schizophrenia. *Biological Psychiatry*, *54*(2). https://doi.org/10.1016/S0006-3223(02)01925-X

Ľupták, M., Michaličková, D., Fišar, Z., Kitzlerová, E., & Hroudová, J. (2021). Novel approaches in schizophrenia-from risk factors and hypotheses to novel drug targets. *World Journal of Psychiatry*, *11*(7), 277–296. https://doi.org/10.5498/wjp.v11.i7.277

Luvsannyam, E., Jain, M. S., Pormento, M. K. L., Siddiqui, H., Balagtas, A. R. A., Emuze, B. O., & Poprawski, T. (2022). Neurobiology of Schizophrenia: A Comprehensive Review. *Cureus*, *14*(4). https://doi.org/10.7759/cureus.23959

Luza, S., Opazo, C. M., Bousman, C. A., Pantelis, C., Bush, A. I., & Everall, I. P. (2020). The ubiquitin proteasome system and schizophrenia. In *The Lancet Psychiatry, 7*(6). https://doi.org/10.1016/S2215-0366(19)30520-6

Lv, F., Chen, S., Wang, L., Jiang, R., Tian, H., Li, J., Yao, Y., & Zhuo, C. (2017). The role of microbiota in the pathogenesis of schizophrenia and major depressive disorder and the possibility of targeting microbiota as a treatment option. In *Oncotarget, 8*(59). https://doi.org/10.18632/oncotarget.21284

Lv, Y., Sun, Y., Dai, D., Luan, Z. L., Lu, H. Y., Li, C. J., & Luo, Y. Y. (2020). Positive association between PTN polymorphisms and schizophrenia in Northeast Chinese Han population. *Psychiatric Genetics*, *30*(5). https://doi.org/10.1097/YPG.0000000000000262

MacDowell, K. S., Munarriz-Cuezva, E., Meana, J. J., Leza, J. C., & Ortega, J. E. (2021). Paliperidone Reversion of Maternal Immune Activation-Induced Changes on Brain Serotonin and Kynurenine Pathways. *Frontiers in Pharmacology*, *12*. https://doi.org/10.3389/fphar.2021.682602

Mackay-Sim, A., & Kittel, P. W. (1991). On the Life Span of Olfactory Receptor Neurons. *European Journal of Neuroscience*, *3*(3). https://doi.org/10.1111/j.1460-9568.1991.tb00081.x

Macleod, J., Oakes, R., Copello, A., Crome, P. I., Egger, P. M., Hickman, M., Oppenkowski, T., Stokes-Lampard, H., & Smith, G. D. (2004). Psychological and social sequelae of cannabis and other illicit drug use by young people: A systematic review of longitudinal, general population studies. *Lancet*, *363*(9421). https://doi.org/10.1016/S0140-6736(04)16200-4

Magdalon, J., Sánchez-Sánchez, S. M., Griesi-Oliveira, K., & Sertié, A. L. (2017). Dysfunctional mTORC1 signaling: A convergent mechanism between syndromic and nonsyndromic forms of autism spectrum disorder? In *International Journal of Molecular Sciences, 18*(3). https://doi.org/10.3390/ijms18030659

Malone, D. T., Hill, M. N., & Rubino, T. (2010). Adolescent cannabis use and psychosis: Epidemiology and neurodevelopmental models. In *British Journal of Pharmacology, 160*(3). https://doi.org/10.1111/j.1476-5381.2010.00721.x

Manchia, M., Piras, I. S., Huentelman, M. J., Pinna, F., Zai, C. C., Kennedy, J. L., & Carpiniello, B. (2017). Pattern of gene expression in different stages of schizophrenia: Down-regulation of NPTX2 gene revealed by a meta-analysis of microarray datasets. *European Neuropsychopharmacology*, *27*(10). https://doi.org/10.1016/j.euroneuro.2017.07.002

Manning, B. D., & Cantley, L. C. (2007). AKT/PKB Signaling: Navigating Downstream. In *Cell, 129*(7). https://doi.org/10.1016/j.cell.2007.06.009

March, D., Hatch, S. L., Morgan, C., Kirkbride, J. B., Bresnahan, M., Fearon, P., & Susser, E. (2008). Psychosis and place. *Epidemiologic Reviews*, *30*, 84–100. https://doi.org/doi: 10.1093/epirev/mxn006

Marconi, A., Di Forti, M., Lewis, C., Murray, R. M., & Vassos, E. (2016). Meta-analysis of the Association Between the Level of Cannabis Use and Risk of Psychosis. *Schizophrenia Bulletin*, *42*(5), 1262–1269. https://doi.org/https://doi.org/10.1093/schbul/sbw003

Marder, S. R., & Cannon, T. D. (2019). Schizophrenia. *The New England Journal of Medicine*, *381*, 1753–1761. https://doi.org/10.1056/NEJMra1808803

Maric, N. P., Jovicic, M. J., Mihaljevic, M., & Miljevic, C. (2016). Improving Current Treatments for Schizophrenia. *Drug Development Research*, *77*(7). https://doi.org/10.1002/ddr.21337

Marksteiner, J., Weiss, U., Weis, C., Laslop, A., Fischer-Colbrie, R., Humpel, C., Feldon, J., & Fleischhacker, W. W. (2001). Differential regulation of chromogranin A, chromogranin B and secretogranin II in rat brain by phencyclidine treatment. *Neuroscience*, *104*(2). https://doi.org/10.1016/S0306-4522(01)00081-1

Martinez-Gras, I., Perez-Nievas, B. G., Garcia-Bueno, B., Madrigal, J. L. M., Andres-Esteban, E., Rodriguez-Jimenez, R., Hoenicka, J., Palomo, T., Rubio, G., Martinez-Gras, I., Perez-Nievas, B. G., Garcia-Bueno, B., Madrigal, J. L. M., Andres-Esteban, E., Rodriguez-Jimenez, R., Hoenicka, J., Palomo, T., Rubio, G., & Leza, J. C. (2011). The anti-inflammatory prostaglandin 15d-PGJ2 and its nuclear receptor PPARgamma are decreased in schizophrenia. *Schizophrenia Research*, *128*(1–3).

Marx, W., McGuinness, A. J., Rocks, T., Ruusunen, A., Cleminson, J., Walker, A. J., Gomes-da-Costa, S., Lane, M., Sanches, M., Diaz, A. P., Tseng, P. T., Lin, P. Y., Berk, M., Clarke, G., O'Neil, A., Jacka, F., Stubbs, B., Carvalho, A. F., Quevedo, J., … Fernandes, B. S. (2021). The kynurenine pathway in major depressive disorder, bipolar disorder, and schizophrenia: a meta-analysis of 101 studies. *Molecular Psychiatry*, *26*(8). https://doi.org/10.1038/s41380-020-00951-9

Matheson, S. L., Shepherd, A. M., Pinchbeck, R. M., Laurens, K. R., & Carr, V. J. (2013). Childhood adversity in schizophrenia: a systematicmeta-analysis. *Psychological Medicine*, *43*(2), 225–238. https://doi.org/https://doi.org/10.1017/S0033291712000785

Mathur, A., Law, M. H., Megson, I. L., Shaw, D. J., & Wei, J. (2010). Genetic association of the AKT1 gene with schizophrenia in a British population. *Psychiatric Genetics*, *20*(3). https://doi.org/10.1097/YPG.0b013e32833a2234

Matigian, N. A., McCurdy, R. D., Féron, F., Perry, C., Smith, H., Filippich, C., McLean, D., McGrath, J., Mackay-Sim, A., Mowry, B., & Hayward, N. K. (2008). Fibroblast and lymphoblast gene expression profiles in schizophrenia: Are non-neural cells informative? *PLoS ONE*, *3*(6). https://doi.org/10.1371/journal.pone.0002412

Matigian, N., Abrahamsen, G., Sutharsan, R., Cook, A. L., Vitale, A. M., Nouwens, A., Bellette, B., An, J., Anderson, M., Beckhouse, A. G., Bennebroek, M., Cecil, R., Chalk, A. M., Cochrane, J., Fan, Y., Féron, F., McCurdy, R., McGrath, J. J., Murrell, W., Perry, C., & Mackay-Sim, A. (2010). Disease-specific, neurosphere-derived cells as models for brain disorders. *DMM Disease Models and Mechanisms*, *3*(11–12). https://doi.org/10.1242/dmm.005447

Maynard, T. M., Sikich, L., Lieberman, J. A., & LaMantia, A. S. (2001). Neural development, cell-cell signaling, and the "two-hit" hypothesis of schizophrenia. *Schizophrenia Bulletin*, *27*(3), 457–476. https://doi.org/https://doi.org/10.1093/oxfordjournals.schbul.a006887

McCurdy, R. D., Féron, F., Perry, C., Chant, D. C., McLean, D., Matigian, N., Hayward, N. K., McGrath, J. J., & Mackay-Sim, A. (2006). Cell cycle alterations in biopsied olfactory neuroepithelium in schizophrenia and bipolar I disorder using cell culture and gene expression analyses. *Schizophrenia Research*, *82*(2–3). https://doi.org/10.1016/j.schres.2005.10.012

McGuire, J. L., Depasquale, E. A., Funk, A. J., O'Donnovan, S. M., Hasselfeld, K., Marwaha, S., Hammond, J. H., Hartounian, V., Meador-Woodruff, J. H., Meller, J., & McCullumsmith, R. E. (2017). Abnormalities of signal transduction networks in chronic schizophrenia. *Npj Schizophrenia*, *3*(1). https://doi.org/10.1038/s41537-017-0032-6

McQuillin, A., Rizig, M., & Gurling, H. M. D. (2007). A microarray gene expression study of the molecular pharmacology of lithium carbonate on mouse brain mRNA to understand the neurobiology of mood stabilization and treatment of bipolar affective disorder. *Pharmacogenetics and Genomics*, *17*(8). https://doi.org/10.1097/FPC.0b013e328011b5b2

Meana, J. J., Callado, L. F., & Morentin, B. (2014). Do post-mortem brain studies provide useful information for Psychiatry? *Revista de Psiquiatria y Salud Mental*, *7*(3). https://doi.org/10.1016/j.rpsm.2014.05.001

Mechtersheimer, S., Gutwein, P., Agmon-Levin, N., Stoeck, A., Oleszewski, M., Riedle, S., Postina, R., Fahrenholz, F., Fogel, M., Lemmon, V., & Altevogt, P. (2001). Ectodomain shedding of L1 adhesion molecule promotes cell migration by autocrine binding to integrins. *Journal of Cell Biology*, *155*(4). https://doi.org/10.1083/jcb.200101099

Meltzer, H. Y., & Massey, B. W. (2011). The role of serotonin receptors in the action of atypical antipsychotic drugs. In *Current Opinion in Pharmacology, 11*(1). https://doi.org/10.1016/j.coph.2011.02.007

Menninger, K. A. (1919). Psychoses associated with influenza: I. general data: Statistical analysis. *Journal of the American Medical Association*, *72*(4). https://doi.org/10.1001/jama.1919.02610040001001

Merkle, F. T., & Alvarez-Buylla, A. (2006). Neural stem cells in mammalian development. In *Current Opinion in Cell Biology, 18*(6). https://doi.org/10.1016/j.ceb.2006.09.008

Meyer, U. (2013). Developmental neuroinflammation and schizophrenia. *Progress in Neuro-Psychopharmacology and Biological Psychiatry*, *42*, 20–34. https://doi.org/10.1016/j.pnpbp.2011.11.003

Meyer, U. (2014). Prenatal Poly(I:C) exposure and other developmental immune activation models in rodent systems. In *Biological Psychiatry, 75*(4). https://doi.org/10.1016/j.biopsych.2013.07.011

Meyer, U., Feldon, J., & Fatemi, S. H. (2009). In-vivo rodent models for the experimental investigation of prenatal immune activation effects in neurodevelopmental brain disorders. In *Neuroscience and Biobehavioral Reviews, 33*(7). https://doi.org/10.1016/j.neubiorev.2009.05.001

Meyer, U., Nyffeler, M., Schwendener, S., Knuesel, I., Yee, B. K., & Feldon, J. (2008). Relative prenatal and postnatal maternal contributions to schizophrenia-related neurochemical dysfunction after in utero immune challenge. *Neuropsychopharmacology*, *33*(2). https://doi.org/10.1038/sj.npp.1301413

Mill, J., Tang, T., Kaminsky, Z., Khare, T., Yazdanpanah, S., Bouchard, L., Jia, P., Assadzadeh, A., Flanagan, J., Schumacher, A., Wang, S. C., & Petronis, A. (2008). Epigenomic Profiling Reveals DNA-Methylation Changes Associated with Major Psychosis. *American Journal of Human Genetics*, *82*(3). https://doi.org/10.1016/j.ajhg.2008.01.008

Miller, B. J., Buckley, P., Seabolt, W., Mellor, A., & Kirkpatrick, B. (2011). Meta-analysis of cytokine alterations in schizophrenia: Clinical status and antipsychotic effects. *Biological Psychiatry*, *70*(7). https://doi.org/10.1016/j.biopsych.2011.04.013

Miller, B. J., Culpepper, N., Rapaport, M. H., & Buckley, P. (2013). Prenatal inflammation and neurodevelopment in schizophrenia: A review of human studies. *Progress in Neuro-Psychopharmacology and Biological Psychiatry*, *42*, 92–100. https://doi.org/10.1016/j.pnpbp.2012.03.010

Ministerio de Sanidad. (2022). *Prestación Farmacéutica en el Sistema Nacional de Salud, 2022. Informe monográfico*.

Mirescu, C., & Gould, E. (2006). Stress and adult neurogenesis. In *Hippocampus, 16*(3). https://doi.org/10.1002/hipo.20155

Mirescu, C., Peters, J. D., & Gould, E. (2004). Early life experience alters response of adult neurogenesis to stress. *Nature Neuroscience*, *7*(8). https://doi.org/10.1038/nn1290

Momtazmanesh, S., Zare-Shahabadi, A., & Rezaei, N. (2019). Cytokine Alterations in Schizophrenia: An Updated Review. In *Frontiers in Psychiatry, 10*. https://doi.org/10.3389/fpsyt.2019.00892

Moran, L. V., Tsang, E. S., Ongur, D., Hsu, J., & Choi, M. Y. (2022). Geographical variation in hospitalization for psychosis associated with cannabis use and cannabis legalization in the United States: Submit to: Psychiatry Research. *Psychiatry Research*, *308*. https://doi.org/10.1016/j.psychres.2022.114387

Moreno-Fernández, M., Ucha, M., Reis-de-Paiva, R., Marcos, A., Ambrosio, E., & Higuera-Matas, A. (2023). Lack of interactions between prenatal immune activation and Δ9-tetrahydrocannabinol exposure during adolescence in behaviours relevant to symptom dimensions of schizophrenia in rats. *Progress in Neuro-Psychopharmacology & Biological Psychiatry*, *31*, 110889. https://doi.org/10.1016/j.pnpbp.2023.110889

Morgan, C., Charalambides, M., Hutchinson, G., & Murray, R. M. (2010). Migration, ethnicity, and psychosis: Toward a sociodevelopmental model. *Schizophrenia Bulletin*, *36*(4), 655–664. https://doi.org/10.1093/schbul/sbq051

Morgan, C., Kirkbride, J., Leff, J., Craig, T., Hutchinson, G., McKenzie, K., Morgan, K., Dazzan, P., Doody, G. A., Jones, P., Murray, R., & Fearon, P. (2007). Parental separation, loss and psychosis in different ethnic groups: a case-control study. *Psychological Medicine*, *37*(4), 495.503. https://doi.org/https://doi.org/10.1017/S0033291706009330

Morris, S. A., Eaves, D. W., Smith, A. R., & Nixon, K. (2010). Alcohol inhibition of neurogenesis: A mechanism of hippocampal neurodegeneration in an adolescent alcohol abuse model. *Hippocampus*, *20*(5). https://doi.org/10.1002/hipo.20665

Mosca-Boidron, A. L., Gueneau, L., Huguet, G., Goldenberg, A., Henry, C., Gigot, N., Pallesi-Pocachard, E., Falace, A., Duplomb, L., Thevenon, J., Duffourd, Y., ST-Onge, J., Chambon, P., Rivire, J. B., Thauvin-Robinet, C., Callier, P., Marle, N., Payet, M., Ragon, C., … Bourgeron, T. (2016). A de novo microdeletion of SEMA5A in a boy with autism spectrum disorder and intellectual disability. *European Journal of Human Genetics*, *24*(6). https://doi.org/10.1038/ejhg.2015.211

Mottahedin, A., Ardalan, M., Chumak, T., Riebe, I., Ek, J., & Mallard, C. (2017). Effect of neuroinflammation on synaptic organization and function in the developing brain: Implications for neurodevelopmental and neurodegenerative disorders. In *Frontiers in Cellular Neuroscience, 11*. https://doi.org/10.3389/fncel.2017.00190

Moyer, C. E., Shelton, M. A., & Sweet, R. A. (2015). Dendritic spine alterations in schizophrenia. In *Neuroscience Letters, 601*. https://doi.org/10.1016/j.neulet.2014.11.042

Mueller, F. S., Polesel, M., Richetto, J., Meyer, U., & Weber-Stadlbauer, U. (2018). Mouse models of maternal immune activation: Mind your caging system! *Brain, Behavior, and Immunity*, *73*. https://doi.org/10.1016/j.bbi.2018.07.014

Mueller, F. S., Richetto, J., Hayes, L. N., Zambon, A., Pollak, D. D., Sawa, A., Meyer, U., & Weber-Stadlbauer, U. (2019). Influence of poly(I:C) variability on thermoregulation, immune responses and pregnancy outcomes in mouse models of maternal immune activation. *Brain, Behavior, and Immunity*, *80*. https://doi.org/10.1016/j.bbi.2019.04.019

Muguruza, C., Meana, J. J., & Callado, L. F. (2016). Group II Metabotropic Glutamate Receptors as Targets for Novel Antipsychotic Drugs. *Frontiers in Pharmacology*, *7*(130). https://doi.org/https://doi.org/10.3389/fphar.2016.00130

Muguruza, C., Moreno, J. L., Umali, A., Callado, L. F., Meana, J. J., & González-Maeso, J. (2013). Dysregulated 5-HT2A receptor binding in postmortem frontal cortex of schizophrenic subjects. *European Neuropsychopharmacology*, *23*(8). https://doi.org/10.1016/j.euroneuro.2012.10.006

Murga, C., Laguinge, L., Wetzker, R., Cuadrado, A., & Gutkind, J. S. (1998). Activation of Akt/Protein Kinase B by G Protein-coupled Receptors. *Journal of Biological Chemistry*, *273*(30). https://doi.org/10.1074/jbc.273.30.19080

Murray, V., McKee, I., Miller, P. M., Young, D., Muir, W. J., Pelosi, A. J., & Blackwood, D. H. R. (2005). Dimensions and classes of psychosis in a population cohort: A four-class, four-dimension model of schizophrenia and affective psychoses. *Psychological Medicine*, *35*(4). https://doi.org/10.1017/S0033291704003745

Murrell, W., Féron, F., Wetzig, A., Cameron, N., Splatt, K., Bellette, B., Bianco, J., Perry, C., Lee, G., & Mackay-Sim, A. (2005). Multipotent stem cells from adult olfactory mucosa. *Developmental Dynamics*, *233*(2). https://doi.org/10.1002/dvdy.20360

Myint, A. M., Kim, Y. K., Verkerk, R., Scharpé, S., Steinbusch, H., & Leonard, B. (2007). Kynurenine pathway in major depression: Evidence of impaired neuroprotection. *Journal of Affective Disorders*, *98*(1–2). https://doi.org/10.1016/j.jad.2006.07.013

Na, K. S., & Kim, Y. K. (2008). Monocytic, Th1 and Th2 cytokine alterations in the pathophysiology of schizophrenia. *Neuropsychobiology*, *56*(2–3). https://doi.org/10.1159/000111535

Nabetani, A., Koujin, T., Tsutsumi, C., Haraguchi, T., & Hiraoka, Y. (2001). A conserved protein, Nuf2, is implicated in connecting the centromere to the spindle during chromosome segregation: A link between the kinetochore function and the spindle checkpoint. *Chromosoma*, *110*(5). https://doi.org/10.1007/s004120100153

Nakazawa, K., Zsiros, V., Jiang, Z., Nakao, K., Kolata, S., Zhang, S., & Belforte, J. E. (2012). GABAergic interneuron origin of schizophrenia pathophysiology. In *Neuropharmacology, 62*(3). https://doi.org/10.1016/j.neuropharm.2011.01.022

Naninck, E. F. G., Hoeijmakers, L., Kakava-Georgiadou, N., Meesters, A., Lazic, S. E., Lucassen, P. J., & Korosi, A. (2015). Chronic early life stress alters developmental and adult neurogenesis and impairs cognitive function in mice. *Hippocampus*, *25*(3). https://doi.org/10.1002/hipo.22374

Nestler, E. J., & Hyman, S. E. (2010). Animal models of neuropsychiatric disorders. In *Nature Neuroscience, 13*(10). https://doi.org/10.1038/nn.2647

Nielsen, R. E., Levander, S., Kjaersdam Telléus, G., Jensen, S. O. W., Østergaard Christensen, T., & Leucht, S. (2015). Second-generation antipsychotic effect on cognition in patients with schizophrenia-a meta-analysis of randomized clinical trials. *Acta Psychiatrica Scandinavica*, *131*(3). https://doi.org/10.1111/acps.12374

Nievergall, E., Lackmann, M., & Janes, P. W. (2012). Eph-dependent cell-cell adhesion and segregation in development and cancer. In *Cellular and Molecular Life Sciences, 69*(11). https://doi.org/10.1007/s00018-011-0900-6

Nishimura, M., & Naito, S. (2005). Tissue-specific mRNA expression profiles of human toll-like receptors and related genes. *Biological and Pharmaceutical Bulletin*, *28*(5). https://doi.org/10.1248/bpb.28.886

Nixon, K., Morris, S. A., Liput, D. J., & Kelso, M. L. (2010). Roles of neural stem cells and adult neurogenesis in adolescent alcohol use disorders. In *Alcohol, 44*(1). https://doi.org/10.1016/j.alcohol.2009.11.001

Noto, C., Ota, V. K., Santoro, M. L., Ortiz, B. B., Rizzo, L. B., Higuchi, C. H., Cordeiro, Q., Belangero, S. I., Bressan, R. A., Gadelha, A., Maes, M., & Brietzke, E. (2015). Effects of depression on the cytokine profile in drug naïve first-episode psychosis. *Schizophrenia Research*, *164*(1–3). https://doi.org/10.1016/j.schres.2015.01.026

Novikova, S. I., He, F., Cutrufello, N. J., & Lidow, M. S. (2006). Identification of protein biomarkers for schizophrenia and bipolar disorder in the postmortem prefrontal cortex using SELDI-TOF-MS ProteinChip profiling combined with MALDI-TOF-PSD-MS analysis. *Neurobiology of Disease*, *23*(1). https://doi.org/10.1016/j.nbd.2006.02.002

Nunes, S. O. V., Matsuo, T., Kaminami, M. S., Watanabe, M. A. E., Reiche, E. M. V., & Itano, E. N. (2006). An autoimmune or an inflammatory process in patients with schizophrenia, schizoaffective disorder, and in their biological relatives. In *Schizophrenia Research, 84*(1). https://doi.org/10.1016/j.schres.2006.02.003

O'Donovan, M. C., Norton, N., Williams, H., Peirce, T., Moskvina, V., Nikolov, I., Hamshere, M., Carroll, L., Georgieva, L., Dwyer, S., Holmans, P., Marchini, J. L., Spencer, C. C. A., Howie, B., Leung, H. T., Giegling, I., Hartmann, A. M., Möller, H. J., Morris, D. W., … Cloninger, C. R. (2009). Analysis of 10 independent samples provides evidence for association between schizophrenia and a SNP flanking fibroblast growth factor receptor 2. *Molecular Psychiatry*, *14*(1). https://doi.org/10.1038/mp.2008.108

O'Mahony, S. M., Clarke, G., Borre, Y. E., Dinan, T. G., & Cryan, J. F. (2015). Serotonin, tryptophan metabolism and the brain-gut-microbiome axis. In *Behavioural Brain Research, 277*. https://doi.org/10.1016/j.bbr.2014.07.027

Ochoa, S., Usall, J., Cobo, J., Labad, X., & Kulkarni, J. (2012). Gender Differences in Schizophrenia and First-Episode Psychosis: A Comprehensive Literature Review. *Schizophrenia Research and Treatment*, *2012*, 1–9. https://doi.org/10.1155/2012/916198

Okano, H., Kawahara, H., Toriya, M., Nakao, K., Shibata, S., & Imai, T. (2005). Function of RNA-binding protein Musashi-1 in stem cells. In *Experimental Cell Research, 306*(2). https://doi.org/10.1016/j.yexcr.2005.02.021

Okusaga, O., Fuchs, D., Reeves, G., Giegling, I., Hartmann, A. M., Konte, B., Friedl, M., Groer, M., Cook, T. B., Stearns-Yoder, K. A., Pandey, J. P., Kelly, D. L., Hoisington, A. J., Lowry, C. A., Eaton, W. W., Brenner, L. A., Rujescu, D., & Postolache, T. T. (2016). Kynurenine and Tryptophan Levels in Patients with Schizophrenia and Elevated Antigliadin Immunoglobulin G Antibodies. *Psychosomatic Medicine*, *78*(8). https://doi.org/10.1097/PSY.0000000000000352

Omlin, F. X., & Waldmeyer, J. (1989). Differentiation of neuron-like cells in cultured rat optic nerves: A neuron or common neuron-glia progenitor? *Developmental Biology*, *133*(1). https://doi.org/10.1016/0012-1606(89)90315-1

Oomen, C. A., Soeters, H., Audureau, N., Vermunt, L., Van Hasselt, F. N., Manders, E. M. M., Joëls, M., Lucassen, P. J., & Krugers, H. (2010). Severe early life stress hampers spatial learning and neurogenesis, but improves hippocampal synaptic plasticity and emotional learning under high-stress conditions in adulthood. *Journal of Neuroscience*, *30*(19). https://doi.org/10.1523/JNEUROSCI.0247-10.2010

Ortiz-López, L., González-Olvera, J. J., Vega-Rivera, N. M., García-Anaya, M., Carapia-Hernández, A. K., Velázquez-Escobar, J. C., & Ramírez-Rodríguez, G. B. (2017). Human neural stem/progenitor cells derived from the olfactory epithelium express the TrkB receptor and migrate in response to BDNF. *Neuroscience*, *355*. https://doi.org/10.1016/j.neuroscience.2017.04.047

Othman, M., Lu, C., Klueber, K., Winstead, W., & Roisen, F. J. (2005). Clonal analysis of adult human olfactory neurosphere forming cells. *Biotechnic and Histochemistry*, *80*(5–6). https://doi.org/10.1080/10520290500469777

Pacheco-López, G., Giovanoli, S., Langhans, W., & Meyer, U. (2013). Priming of metabolic dysfunctions by prenatal immune activation in mice: Relevance to schizophrenia. *Schizophrenia Bulletin*, *39*(2). https://doi.org/10.1093/schbul/sbr178

Paksarian, D., Eaton, W. W., Mortensen, P. B., & Pedersen, C. B. (2015). Childhood Residential Mobility, Schizophrenia, and Bipolar Disorder: A Population-based Study in Denmark. *Schizophrenia Bulletin*, *41*(2), 346–354. https://doi.org/10.1093/schbul/sbu074

Pardiñas, A. F., Holmans, P., Pocklington, A. J., Escott-Price, V., Ripke, S., Carrera, N., Legge, S. E., Bishop, S., Cameron, D., Hamshere, M. L., Han, J., Hubbard, L., Lynham, A., Mantripragada, K., Rees, E., MacCabe, J. H., McCarroll, S. A., Baune, B. T., Breen, G., … Walters, J. T. R. (2018). Common schizophrenia alleles are enriched in mutation-intolerant genes and in regions under strong background selection. *Nature Genetics*, *50*(3), 381–389. https://doi.org/10.1038/s41588-018-0059-2

Parent, J. M. (2003). Injury-induced neurogenesis in the adult mammalian brain. In *Neuroscientist, 9*(4). https://doi.org/10.1177/1073858403252680

Park, S. W., Seo, M. K., McIntyre, R. S., Mansur, R. B., Lee, Y., Lee, J. H., Park, S. C., Huh, L., & Lee, J. G. (2018). Effects of olanzapine and haloperidol on mTORC1 signaling, dendritic outgrowth, and synaptic proteins in rat primary hippocampal neurons under toxic conditions. *Neuroscience Letters*, *686*. https://doi.org/10.1016/j.neulet.2018.08.031

Patrich, E., Piontkewitz, Y., Peretz, A., Weiner, I., & Attali, B. (2016). Maternal immune activation produces neonatal excitability defects in offspring hippocampal neurons from pregnant rats treated with poly I:C. *Scientific Reports*, *6*. https://doi.org/10.1038/srep19106

Patrono, E., Matsumoto, J., Nishimaru, H., Takamura, Y., Chinzorig, I. C., Ono, T., & Nishijo, H. (2017). Rewarding effects of operant dry-licking behavior on neuronal firing in the nucleus accumbens core. *Frontiers in Pharmacology*, *8*(AUG). https://doi.org/10.3389/fphar.2017.00536

Patzke, C., Acuna, C., Giam, L. R., Wernig, M., & Südhof, T. C. (2016). Conditional deletion of L1CAM in human neurons impairs both axonal and dendritic arborization and action potential generation. *Journal of Experimental Medicine*, *213*(4). https://doi.org/10.1084/jem.20150951

Pedersen, C. B., & Mortensen, P. B. (2001). Evidence of a dose-response relationship between urbanicity during upbringing and schizophrenia risk. *Archives of General Psychiatry*, *58*(11), 1039–1046. https://doi.org/10.1001/archpsyc.58.11.1039

Pedraz-Petrozzi, B., Elyamany, O., Rummel, C., & Mulert, C. (2020). Effects of inflammation on the kynurenine pathway in schizophrenia - A systematic review. In *Journal of Neuroinflammation, 17*(1). https://doi.org/10.1186/s12974-020-1721-z

Pendyala, G., Chou, S., Jung, Y., Coiro, P., Spartz, E., Padmashri, R., Li, M., & Dunaevsky, A. (2017). Maternal Immune Activation Causes Behavioral Impairments and Altered Cerebellar Cytokine and Synaptic Protein Expression. *Neuropsychopharmacology*, *42*(7). https://doi.org/10.1038/npp.2017.7

Pennacchio, L. A., Ahituv, N., Moses, A. M., Prabhakar, S., Nobrega, M. A., Shoukry, M., Minovitsky, S., Dubchak, I., Holt, A., Lewis, K. D., Plajzer-Frick, I., Akiyama, J., De Val, S., Afzal, V., Black, B. L., Couronne, O., Eisen, M. B., Visel, A., & Rubin, E. M. (2006). In vivo enhancer analysis of human conserved non-coding sequences. *Nature*, *444*(7118). https://doi.org/10.1038/nature05295

Penzel, N., Sanfelici, R., Antonucci, L. A., Betz, L. T., Dwyer, D., Ruef, A., Cho, K. I. K., Cumming, P., Pogarell, O., Howes, O., Falkai, P., Upthegrove, R., Borgwardt, S., Brambilla, P., Lencer, R., Meisenzahl, E., Schultze-Lutter, F., Rosen, M., Lichtenstein, T., & Kambeitz-Ilankovic, L. (2022). Pattern of predictive features of continued cannabis use inpatients with recent-onset psychosis and clinical high-risk forpsychosis. *Schizophrenia (Heidelberg, Germany)*, *8*(1), 19. https://doi.org/https://doi.org/10.1038/s41537-022-00218-y

Perez-Palomar, B., Erdozain, A. M., Erkizia-Santamaría, I., Ortega, J. E., & Meana, J. J. (2023). Maternal Immune Activation Induces Cortical Catecholaminergic Hypofunction and Cognitive Impairments in Offspring. *Journal of Neuroimmune Pharmacology*. https://doi.org/10.1007/s11481-023-10070-1

Perry, B. I., Zammit, S., Jones, P. B., & Khandaker, G. M. (2021). Childhood inflammatory markers and risks for psychosis and depression at age 24: Examination of temporality and specificity of association in a population-based prospective birth cohort. *Schizophrenia Research*, *230*. https://doi.org/10.1016/j.schres.2021.02.008

Pietiläinen, O. P. H., Paunio, T., Loukola, A., Tuulio-Henriksson, A., Kieseppä, T., Thompson, P., Toga, A. W., Van Erp, T. G. M., Silventoinen, K., Soronen, P., Hennah, W., Turunen, J. A., Wedenoja, J., Palo, O. M., Silander, K., Lönnqvist, J., Kaprio, J., Cannon, T. D., & Peltonen, L. (2009). Association of AKT1 with verbal learning, verbal memory, and regional cortical gray matter density in twins. *American Journal of Medical Genetics, Part B: Neuropsychiatric Genetics*, *150*(5). https://doi.org/10.1002/ajmg.b.30890

Potvin, S., Stip, E., Sepehry, A. A., Gendron, A., Bah, R., & Kouassi, E. (2008). Inflammatory Cytokine Alterations in Schizophrenia: A Systematic Quantitative Review. *Biological Psychiatry*, *63*(8). https://doi.org/10.1016/j.biopsych.2007.09.024

Powell, S. B., Zhou, X., & Geyer, M. A. (2009). Prepulse inhibition and genetic mouse models of schizophrenia. *Behavioural Brain Research*, *204*(2). https://doi.org/10.1016/j.bbr.2009.04.021

Prades, R., Munarriz-Cuezva, E., Urigüen, L., Gil-Pisa, I., Gómez, L., Mendieta, L., Royo, S., Giralt, E., Tarragó, T., & Meana, J. J. (2017). The prolyl oligopeptidase inhibitor IPR19 ameliorates cognitive deficits in mouse models of schizophrenia. *European Neuropsychopharmacology*, *27*(2). https://doi.org/10.1016/j.euroneuro.2016.11.016

Puighermanal, E., Biever, A., Pascoli, V., Melser, S., Pratlong, M., Cutando, L., Rialle, S., Severac, D., Boubaker-Vitre, J., Meyuhas, O., Marsicano, G., Lüscher, C., & Valjent, E. (2017). Ribosomal protein s6 phosphorylation is involved in novelty-induced locomotion, synaptic plasticity and mRNA translation. *Frontiers in Molecular Neuroscience*, *10*(December), 1–16. https://doi.org/10.3389/fnmol.2017.00419

Puighermanal, E., Busquets-Garcia, A., Gomis-González, M., Marsicano, G., Maldonado, R., & Ozaita, A. (2013). Dissociation of the pharmacological effects of THC by mTOR blockade. *Neuropsychopharmacology*, *38*(7), 1334–1343. https://doi.org/10.1038/npp.2013.31

Purcell, S. M., Wray, N. R., Stone, J. L., Visscher, P. M., O'Donovan, M. C., Sullivan, P. F., Ruderfer, D. M., McQuillin, A., Morris, D. W., Oĝdushlaine, C. T., Corvin, A., Holmans, P. A., Oĝdonovan, M. C., MacGregor, S., Gurling, H., Blackwood, D. H. R., Craddock, N. J., Gill, M., Hultman, C. M., … Sklar, P. (2009). Common polygenic variation contributes to risk of schizophrenia and bipolar disorder. *Nature*, *460*(7256). https://doi.org/10.1038/nature08185

Qin, P. (2011). The impact of psychiatric illness on suicide: Differences by diagnosis of disorders and by sex and age of subjects. *Journal of Psychiatric Research*, *45*(11). https://doi.org/10.1016/j.jpsychires.2011.06.002

Rakic, P. (1988). Specification of cerebral cortical areas. *Science*, *241*(4862). https://doi.org/10.1126/science.3291116

Rao, M. S. (1999). Multipotent and restricted precursors in the central nervous system. In *Anatomical Record, 257*(4). https://doi.org/10.1002/(SICI)1097-0185(19990815)257:4<137::AID-AR7>3.0.CO;2-Q

Rathjen, F. G., & Schachner, M. (1984). Immunocytological and biochemical characterization of a new neuronal cell surface component (L1 antigen) which is involved in cell adhesion. *The EMBO Journal*, *3*(1). https://doi.org/10.1002/j.1460-2075.1984.tb01753.x

Rauvala, H. (1989). An 18-kd heparin-binding protein of developing brain that is distinct from fibroblast growth factors. *EMBO Journal*, *8*(10). https://doi.org/10.1002/j.1460-2075.1989.tb08443.x

Read, J., van Os, J., Morrison, A. P., & Ross, C. (2005). Childhood trauma, psychosis and schizophrenia: a literature review with theoretical and clinical implications. *Acta Psychiatrica Scandinavica*, *112*(5), 330–350. https://doi.org/https://doi.org/10.1111/j.1600-0447.2005.00634.x

Redfern, W. S., Tse, K., Grant, C., Keerie, A., Simpson, D. J., Pedersen, J. C., Rimmer, V., Leslie, L., Klein, S. K., Karp, N. A., Sillito, R., Chartsias, A., Lukins, T., Heward, J., Vickers, C., Chapman, K., & Armstrong, J. D. (2017). Automated recording of home cage activity and temperature of individual rats housed in social groups: The Rodent Big Brother project. *PLoS ONE*, *12*(9). https://doi.org/10.1371/journal.pone.0181068

Reif, A., Schmitt, A., Fritzen, S., & Lesch, K. P. (2007). Neurogenesis and schizophrenia: Dividing neurons in a divided mind? In *European Archives of Psychiatry and Clinical Neuroscience, 257*(5). https://doi.org/10.1007/s00406-007-0733-3

Reisinger, S., Khan, D., Kong, E., Berger, A., Pollak, A., & Pollak, D. D. (2015). The Poly(I:C)-induced maternal immune activation model in preclinical neuropsychiatric drug discovery. In *Pharmacology and Therapeutics, 149*. https://doi.org/10.1016/j.pharmthera.2015.01.001

Revest, J. M., Dupret, D., Koehl, M., Funk-Reiter, C., Grosjean, N., Piazza, P. V., & Abrous, D. N. (2009). Adult hippocampal neurogenesis is involved in anxiety-related behaviors. *Molecular Psychiatry*, *14*(10). https://doi.org/10.1038/mp.2009.15

Riecher-Rössler, A., Butler, S., & Kulkarni, J. (2018). Sex and gender differences in schizophrenic psychoses-a critical review. *Archives of Women's Mental Health*, *21*, 627–648. https://doi.org/https://doi.org/10.1007/s00737-018-0847-9

Ripke, S., O'Dushlaine, C., Chambert, K., Moran, J. L., Kähler, A. K., Akterin, S., Bergen, S. E., Collins, A. L., Crowley, J. J., Fromer, M., Kim, Y., Lee, S. H., Magnusson, P. K., Sanchez, N., Stahl, E. A., Williams, S., Wray, N. R., Xia, K., & Bettella, P. F. (2013). Genome-wide association analysis identifies 13 new risk loci for schizophrenia. *Nature Genetics*, *45*(10), 1150–1159. https://doi.org/https://doi.org/10.1038/ng.2742

Rodríguez, G., Neugebauer, N. M., Yao, K. L., Meltzer, H. Y., Csernansky, J. G., & Dong, H. (2017). Δ9-tetrahydrocannabinol (Δ9-THC) administration after neonatal exposure to phencyclidine potentiates schizophrenia-related behavioral phenotypes in mice. *Pharmacology Biochemistry and Behavior*, *159*. https://doi.org/10.1016/j.pbb.2017.06.010

Ronnett, G. V., Leopold, D., Cai, X., Hoffbuhr, K. C., Moses, L., Hoffman, E. P., & Naidu, S. B. (2003). Olfactory biopsies demonstrate a defect in neuronal development in Rett's syndrome. *Annals of Neurology*, *54*(2). https://doi.org/10.1002/ana.10633

Rougon, G., & Marshak, D. R. (1986). Structural and immunological characterization of the amino-terminal domain of mammalian neural cell adhesion molecules. *Journal of Biological Chemistry*, *261*(7). https://doi.org/10.1016/s0021-9258(17)35796-4

Rubio, M. D., Wood, K., Haroutunian, V., & Meador-Woodruff, J. H. (2013). Dysfunction of the ubiquitin proteasome and ubiquitin-like systems in schizophrenia. *Neuropsychopharmacology*, *38*(10). https://doi.org/10.1038/npp.2013.84

Ruvinsky, I., & Meyuhas, O. (2006). Ribosomal protein S6 phosphorylation: from protein synthesis to cell size. *Trends in Biochemical Sciences*, *31*(6), 342–348. https://doi.org/10.1016/j.tibs.2006.04.003

Sahay, A., & Hen, R. (2007). Adult hippocampal neurogenesis in depression. In *Nature Neuroscience, 10*(9). https://doi.org/10.1038/nn1969

Samara, M. T., Klupp, E., Helfer, B., Rothe, P. H., Schneider-Thoma, J., & Leucht, S. (2018). Increasing antipsychotic dose for non response in schizophrenia. In *Cochrane Database of Systematic Reviews, 2018*(5). https://doi.org/10.1002/14651858.CD011883.pub2

Sánchez, C., Díaz-Nido, J., & Avila, J. (2000). Phosphorylation of microtubule-associated protein 2 (MAP2) and its relevance for the regulation of the neuronal cytoskeleton function. In *Progress in Neurobiology, 61*(2). https://doi.org/10.1016/S0301-0082(99)00046-5

Santoni, M., Sagheddu, C., Serra, V., Mostallino, R., Castelli, M. P., Pisano, F., Scherma, M., Fadda, P., Muntoni, A. L., Zamberletti, E., Rubino, T., Melis, M., & Pistis, M. (2023). Maternal immune activation impairs endocannabinoid signaling in the mesolimbic system of adolescent male offspring. *Brain, Behavior, and Immunity*, *109*. https://doi.org/10.1016/j.bbi.2023.02.002

Sato, K. (2020). Why is prepulse inhibition disrupted in schizophrenia? *Medical Hypotheses*, *143*. https://doi.org/10.1016/j.mehy.2020.109901

Schizophrenia Working Group of the Psychiatric Genomics Consortium, 2014. (2014). *Biological Insights From 108 Schizophrenia-Associated Genetic Loci*. *511*(7510), 421–427. https://doi.org/doi:10.1038/nature13595.

Schmelzer, E., Wauthier, E., & Reid, L. M. (2006). The Phenotypes of Pluripotent Human Hepatic Progenitors. *STEM CELLS*, *24*(8). https://doi.org/10.1634/stemcells.2006-0036

Schmidt-Hansen, M., & Le Pelley, M. (2012). The positive symptoms of acute schizophrenia and latent inhibition in humans and animals: Underpinned by the same process(es)? *Cognitive Neuropsychiatry*, *17*(6). https://doi.org/10.1080/13546805.2012.667202

Schoeler, T., Petros, N., Di Forti, M., Klamerus, E., Foglia, E., Ajnakina, O., Gayer-Anderson, C., Colizzi, M., Quattrone, D., Behlke, I., Shetty, S., McGuire, P., David, A. S., Murray, R., & Bhattacharyya, S. (2016). Effects of continuation, frequency, and type of cannabis use on relapse in the first 2 years after onset of psychosis: an observational study. *The Lancet Psychiatry*, *3*(10). https://doi.org/10.1016/S2215-0366(16)30188-2

Schroeder, B. O., & Bäckhed, F. (2016). Signals from the gut microbiota to distant organs in physiology and disease. In *Nature Medicine, 22*(10). https://doi.org/10.1038/nm.4185

Schubert, D., Stallcup, W., LaCorbiere, M., Kidokoro, Y., & Orgel, L. (1985). Ontogeny of electrically excitable cells in cultured olfactory epithelium. *Proceedings of the National Academy of Sciences of the United States of America*, *82*(22). https://doi.org/10.1073/pnas.82.22.7782

Schubert, K. O., Föcking, M., & Cotter, D. R. (2015). Proteomic pathway analysis of the hippocampus in schizophrenia and bipolar affective disorder implicates 14-3-3 signaling, aryl hydrocarbon receptor signaling, and glucose metabolism: Potential roles in GABAergic interneuron pathology. *Schizophrenia Research*, *167*(1–3). https://doi.org/10.1016/j.schres.2015.02.002

Schumann, G., Coin, L. J., Lourdusamy, A., Charoen, P., Berger, K. H., Stacey, D., Desrivières, S., Aliev, F. A., Khan, A. A., Amin, N., Aulchenko, Y. S., Bakalkin, G., Bakker, S. J., Balkau, B., Beulens, J. W., Bilbao, A., De Boer, R. A., Beury, D., Bots, M. L., … Elliott, P. (2011). Genome-wide association and genetic functional studies identify autism susceptibility candidate 2 gene (AUTS2) in the regulation of alcohol consumption. *Proceedings of the National Academy of Sciences of the United States of America*, *108*(17). https://doi.org/10.1073/pnas.1017288108

Schwab, S. G., Hoefgen, B., Hanses, C., Hassenbach, M. B., Albus, M., Lerer, B., Trixler, M., Maier, W., & Wildenauer, D. B. (2005). Further evidence for association of variants in the AKT1 gene with schizophrenia in a sample of european sib-pair families. *Biological Psychiatry*, *58*(6). https://doi.org/10.1016/j.biopsych.2005.05.005

Seki, T. (2002). Expression patterns of immature neuronal markers PSA-NCAM, CRMP-4 and NeuroD in the hippocampus of young adult and aged rodents. *Journal of Neuroscience Research*, *70*(3). https://doi.org/10.1002/jnr.10387

Sheldon, M., Rice, D. S., D'Arcangelo, G., Yoneshima, H., Nakajima, K., Mikoshiba, K., Howell, B. W., Cooper, J. A., Goldowitz, D., & Curran, T. (1997). Scrambler and yotari disrupt the disabled gene and produce a reeler- like phenotype in mice. *Nature*, *389*(6652). https://doi.org/10.1038/39601

Shi, J., Levinson, D. F., Duan, J., Sanders, A. R., Zheng, Y., Péer, I., Dudbridge, F., Holmans, P. A., Whittemore, A. S., Mowry, B. J., Olincy, A., Amin, F., Cloninger, C. R., Silverman, J. M., Buccola, N. G., Byerley, W. F., Black, D. W., Crowe, R. R., Oksenberg, J. R., … Gejman, P. V. (2009). Common variants on chromosome 6p22.1 are associated with schizophrenia. *Nature*, *460*(7256). https://doi.org/10.1038/nature08192

Shin Yim, Y., Park, A., Berrios, J., Lafourcade, M., Pascual, L. M., Soares, N., Yeon Kim, J., Kim, S., Kim, H., Waisman, A., Littman, D. R., Wickersham, I. R., Harnett, M. T., Huh, J. R., & Choi, G. B. (2017). Reversing behavioural abnormalities in mice exposed to maternal inflammation. *Nature*, *549*(7673). https://doi.org/10.1038/nature23909

Shirzadi, A. A., & Ghaemi, S. N. (2006). Side effects of atypical antipsychotics: Extrapyramidal symptoms and the metabolic syndrome. In *Harvard Review of Psychiatry, 14*(3). https://doi.org/10.1080/10673220600748486

Shyu, W. C., Lin, S. Z., Chiang, M. F., Chen, D. C., Su, C. Y., Wang, H. J., Liu, R. S., Tsai, C. H., & Li, H. (2008). Secretoneurin promotes neuroprotection and neuronal plasticity via the Jak2/Stat3 pathway in murine models of stroke. *Journal of Clinical Investigation*, *118*(1). https://doi.org/10.1172/JCI32723

Singh, T., Poterba, T., Curtis, D., Akil, H., Al Eissa, M., Barchas, J. D., Bass, N., Bigdeli, T. B., Breen, G., Bromet, E. J., Buckley, P. F., Bunney, W. E., Bybjerg-Grauholm, J., Byerley, W. F., Chapman, S. B., Chen, W. J., Churchhouse, C., Craddock, N., Cusick, C. M., … Daly, M. J. (2022). Rare coding variants in ten genes confer substantial risk for schizophrenia. *Nature*, *604*, 509–516. https://doi.org/https://doi.org/10.1038/s41586-022-04556-w

Smith, M. J., Wang, L., Cronenwett, W., Goldman, M. B., Mamah, D., Barch, D. M., & Csernansky, J. G. (2011). Alcohol use disorders contribute to hippocampal and subcortical shape differences in schizophrenia. *Schizophrenia Research*, *131*(1–3). https://doi.org/10.1016/j.schres.2011.05.014

Solek, C. M., Farooqi, N., Verly, M., Lim, T. K., & Ruthazer, E. S. (2018). Maternal immune activation in neurodevelopmental disorders. In *Developmental Dynamics, 247*(4). https://doi.org/10.1002/dvdy.24612

Song, X., Li, W., Yang, Y., Zhao, J., Jiang, C., Li, W., & Lv, L. (2011). The nuclear factor-κB inhibitor pyrrolidine dithiocarbamate reduces polyinosinic-polycytidilic acid-induced immune response in pregnant rats and the behavioral defects of their adult offspring. *Behavioral and Brain Functions*, *7*. https://doi.org/10.1186/1744-9081-7-50

Stahl, S. M. (2018). Beyond the dopamine hypothesis of schizophrenia to three neural networks of psychosis: Dopamine, serotonin, and glutamate. *CNS Spectrums*, *23*(3). https://doi.org/10.1017/S1092852918001013

Stefansson, H., Ophoff, R. A., Steinberg, S., Andreassen, O. A., Cichon, S., Rujescu, D., Werge, T., ́inen, O. P. H. P., Mors, O., B.Mortensen, P., Sigurdsson, E., Gustafsson, O., Nyegaard, M., Tuulio-Henriksson, A., & Ingason, A. (2009). Common variants conferring risk of schizophrenia. *Nature*, *460*, 744–747. https://doi.org/https://doi.org/10.1038/nature08186

Stefansson, H., Rujescu, D., Cichon, S., Pietiläinen, O. P. H., Steinberg, S., Fossdal, R., Sigurdsson, E., Muglia, P., Francks, C., Matthews, P. M., Gylfason, A., & Bjarni, V. (2008). Large recurrent microdeletions associated with schizophrenia. *Nature*, *455*(7210), 232–236. https://doi.org/doi:10.1038/nature07229

Steiner, J., Brisch, R., Schiltz, K., Dobrowolny, H., Mawrin, C., Krzyżanowska, M., Bernstein, H. G., Jankowski, Z., Braun, K., Schmitt, A., Bogerts, B., & Gos, T. (2016). GABAergic system impairment in the hippocampus and superior temporal gyrus of patients with paranoid schizophrenia: A post-mortem study. *Schizophrenia Research*, *177*(1–3). https://doi.org/10.1016/j.schres.2016.02.018

Stilling, R. M., van de Wouw, M., Clarke, G., Stanton, C., Dinan, T. G., & Cryan, J. F. (2016). The neuropharmacology of butyrate: The bread and butter of the microbiota-gut-brain axis? In *Neurochemistry International, 99*. https://doi.org/10.1016/j.neuint.2016.06.011

Stilo, S. A., & Murray, R. M. (2010). The epidemology of schizophrenia: replacing dogma with knowledge. *Dialogues in Clinical Neuroscience*, *12*(3), 305–315. https://doi.org/https://doi.org/10.31887/DCNS.2010.12.3/sstilo

Stilo, S. A., & Murray, R. M. (2019). Non-Genetic Factors in Schizophrenia. *Current Psychiatry Reports*, *21*(10), 100. https://doi.org/10.1007/s11920-019-1091-3

Stollenwerk, T. M., & Hillard, C. J. (2021). Adolescent thc treatment does not potentiate the behavioral effects in adulthood of maternal immune activation. *Cells*, *10*(12). https://doi.org/10.3390/cells10123503

Stone, J. M., Erlandsson, K., Arstad, E., Squassante, L., Teneggi, V., Bressan, R. A., Krystal, J. H., Ell, P. J., & Pilowsky, L. S. (2008). Relationship between ketamine-induced psychotic symptoms and NMDA receptor occupancy - A [123I]CNS-1261 SPET study. *Psychopharmacology*, *197*(3). https://doi.org/10.1007/s00213-007-1047-x

Stowkowy, J., & Addington, J. (2012). Maladaptive Schemas as a Mediator between Social Defeat and Positive Symptoms in Young People at Clinical High Risk for Psychosis. *Early Intervention in Psychiatry*, *6*(1), 87–90. https://doi.org/https://doi.org/10.1111/j.1751-7893.2011.00297.x

Strachan, R. T., Sciaky, N., Cronan, M. R., Kroeze, W. K., & Roth, B. L. (2010). Genetic deletion of p90 ribosomal S6 kinase 2 alters patterns of 5-hydroxytryptamine2A serotonin receptor functional selectivity. *Molecular Pharmacology*, *77*(3), 327–338. https://doi.org/10.1124/mol.109.061440

Sullivan, K. F., & Cleveland, D. W. (1986). Identification of conserved isotype-defining variable region sequences for four vertebrate β tubulin polypeptide classes. *Proceedings of the National Academy of Sciences of the United States of America*, *83*(12). https://doi.org/10.1073/pnas.83.12.4327

Sullivan, P. F., Agrawal, A., Bulik, C. M., Andreassen, O. A., Børglum, A. D., Breen, G., Cichon, S., Edenberg, H. J., Faraone, S. V., Gelernter, J., Mathews, C. A., Nievergelt, C. M., Smoller, J. W., & O'Donovan, M. C. (2018). Psychiatric Genomics: An Update and an Agenda. *The American Journal of Psychiatry*, *175*(1), 15–27. https://doi.org/https://doi.org/10.1176/appi.ajp.2017.17030283

Sun, J., Walker, A. J., Dean, B., van den Buuse, M., & Gogos, A. (2016). Progesterone: The neglected hormone in schizophrenia? A focus on progesterone-dopamine interactions. *Psychoneuroendocrinology*, *74*, 126–140. https://doi.org/10.1016/j.psyneuen.2016.08.019

Svendsen, C. N., Clarke, D. J., Rosser, A. E., & Dunnett, S. B. (1996). Survival and differentiation of rat and human epidermal growth factor-responsive precursor cells following grafting into the lesioned adult central nervous system. *Experimental Neurology*, *137*(2). https://doi.org/10.1006/exnr.1996.0039

Swerdlow, N. R., Braff, D. L., & Geyer, M. A. (2016). Sensorimotor gating of the startle reflex: What we said 25 years ago, what has happened since then, and what comes next. In *Journal of Psychopharmacology, 30*(11). https://doi.org/10.1177/0269881116661075

Swerdlow, N. R., Braff, D. L., Taaid, N., & Geyer, M. A. (1994). Assessing the validity of an animal model of deficient sensorimotor gating in schizophrenic patients. In *Archives of General Psychiatry, 51*(2). https://doi.org/10.1001/archpsyc.1994.03950020063007

Teng, J., Takei, Y., Harada, A., Nakata, T., Chen, J., & Hirokawa, N. (2001). Synergistic effects of MAP2 and MAP1B knockout in neuronal migration, dendritic outgrowth, and microtubule organization. *Journal of Cell Biology*, *155*(1). https://doi.org/10.1083/jcb.200106025

Thiselton, D. L., Vladimirov, V. I., Kuo, P. H., McClay, J., Wormley, B., Fanous, A., O'Neill, F. A., Walsh, D., Van den Oord, E. J. C. G., Kendler, K. S., & Riley, B. P. (2008). AKT1 Is Associated with Schizophrenia Across Multiple Symptom Dimensions in the Irish Study of High Density Schizophrenia Families. *Biological Psychiatry*, *63*(5). https://doi.org/10.1016/j.biopsych.2007.06.005

Thompson, J. L., Pogue-Geile, M. F., & Grace, A. A. (2004). Developmental pathology, dopamine, and stress: A model for the age of onset of schizophrenia symptoms. In *Schizophrenia Bulletin, 30*(4). https://doi.org/10.1093/oxfordjournals.schbul.a007139

Thomson, P., & Jaque, S. V. (2018). Childhood Adversity and the Creative Experience in Adult Professional Performing Artists. *Frontiers in Psychology*, *9*, 111. https://doi.org/doi: 10.3389/fpsyg.2018.00111. eCollection 2018.

Tochigi, M., Okazaki, Y., Kato, N., & Sasaki, T. (2004). What causes seasonality of birth in schizophrenia? *Neuroscience Research*, *48*(1), 1–11. https://doi.org/10.1016/j.neures.2003.09.002

Toto, S., Grohmann, R., Bleich, S., Frieling, H., Maier, H. B., Greil, W., Cordes, J., Schmidt-Kraepelin, C., Kasper, S., Stübner, S., Degner, D., Druschky, K., Zindler, T., & Neyazi, A. (2019). Psychopharmacological Treatment of Schizophrenia Over Time in 30 908 Inpatients: Data From the AMSP Study. *International Journal of Neuropsychopharmacology*, *22*(9). https://doi.org/10.1093/IJNP/PYZ037

Trabzuni, D., Ryten, M., Walker, R., Smith, C., Imran, S., Ramasamy, A., Weale, M. E., & Hardy, J. (2011). Quality control parameters on a large dataset of regionally dissected human control brains for whole genome expression studies. *Journal of Neurochemistry*, *119*(2). https://doi.org/10.1111/j.1471-4159.2011.07432.x

Trommsdorff, M., Gotthardt, M., Hiesberger, T., Shelton, J., Stockinger, W., Nimpf, J., Hammer, R. E., Richardson, J. A., & Herz, J. (1999). Reeler/disabled-like disruption of neuronal migration in knockout mice lacking the VLDL receptor and ApoE receptor 2. *Cell*, *97*(6). https://doi.org/10.1016/S0092-8674(00)80782-5

Trubetskoy, V., Pardiñas, A. F., Qi, T., Panagiotaropoulou, G., Awasthi, S., Bigdeli, T. B., Bryois, J., Chen, C. Y., Dennison, C. A., Hall, L. S., Lam, M., Watanabe, K., Frei, O., Ge, T., Harwood, J. C., Koopmans, F., Magnusson, S., Richards, A. L., Sidorenko, J., … van Os, J. (2022). Mapping genomic loci implicates genes and synaptic biology in schizophrenia. *Nature*, *604*(7906), 502–508. https://doi.org/10.1038/s41586-022-04434-5

Tsui, C. C., Copeland, N. G., Gilbert, D. J., Jenkins, N. A., Barnes, C., & Worley, P. F. (1996). Narp, a novel member of the pentraxin family, promotes neurite outgrowth and is dynamically regulated by neuronal activity. *Journal of Neuroscience*, *16*(8). https://doi.org/10.1523/jneurosci.16-08-02463.1996

Tucker, R. P. (1990). The roles of microtubule-associated proteins in brain morphogenesis: a review. In *Brain Research Reviews, 15*(2). https://doi.org/10.1016/0165-0173(90)90013-E

Turner, C. A., Akil, H., Watson, S. J., & Evans, S. J. (2006). The Fibroblast Growth Factor System and Mood Disorders. In *Biological Psychiatry, 59*(12). https://doi.org/10.1016/j.biopsych.2006.02.026

Unzueta-Larrinaga, P., Barrena-Barbadillo, R., Callado, L. F., & Urigüen, L. (2023). Obtaining neurons and glia from the olfactory neuroepithelium of living subjects for the study of psychiatric diseases. *Neuroscience Applied*, *2*. https://doi.org/10.1016/j.nsa.2023.101026

Unzueta-Larrinaga, P., & Urigüen, L. (2023). Evaluation of Sensorimotor Gating Deficits in Mice Through Prepulse Inhibition (PPI) of the Startle Response. In *Methods in Molecular Biology, 2687*. https://doi.org/10.1007/978-1-0716-3307-6_5

Urigüen, L., García-Fuster, M. J., Callado, L. F., Morentin, B., La Harpe, R., Casadó, V., Lluis, C., Franco, R., García-Sevilla, J. A., & Meana, J. J. (2009). Immunodensity and mRNA expression of A2A adenosine, D 2 dopamine, and CB1 cannabinoid receptors in postmortem frontal cortex of subjects with schizophrenia: Effect of antipsychotic treatment. *Psychopharmacology*, *206*(2). https://doi.org/10.1007/s00213-009-1608-2

Vaissiere, J., Thorp, J. G., Ong, J. S., Ortega-Alonzo, A., & Derks, E. M. (2020). Exploring Phenotypic and Genetic Overlap between Cannabis Use and Schizotypy. *Twin Research and Human Genetics*, *23*(4). https://doi.org/10.1017/thg.2020.68

Valjent, E., Bertran-Gonzalez, J., Bowling, H., Lopez, S., Santini, E., Matamales, M., Bonito-Oliva, A., Hervé, D., Hoeffer, C., Klann, E., Girault, J. A., & Fisone, G. (2011). Haloperidol regulates the state of phosphorylation of ribosomal protein S6 via activation of PKA and phosphorylation of DARPP-32. *Neuropsychopharmacology*, *36*(12). https://doi.org/10.1038/npp.2011.144

Van Os, J., Kenis, G., & Rutten, B. P. F. (2010). The environment and schizophrenia. *Nature*, *468*(7321), 203–212. https://doi.org/10.1038/nature09563

Van Os, J., Pedersen, C. B., & Mortensen, P. B. (2004). Confirmation of synergy between urbanicity and familial liability in the causation of psychosis. *American Journal of Psychiatry*, *161*(12), 2312–2314. https://doi.org/10.1176/appi.ajp.161.12.2312

Van Scheltinga, A. F. T., Bakker, S. C., & Kahn, R. S. (2010). Fibroblast growth factors in schizophrenia. *Schizophrenia Bulletin*, *36*(6). https://doi.org/10.1093/schbul/sbp033

Van Winkel, R., Kahn, R. S., Linszen, D. H., Van Os, J., Wiersma, D., Bruggeman, R., Cahn, W., De Haan, L., Krabbendam, L., & Myin-Germeys, I. (2011). Family-based analysis of genetic variation underlying psychosis-inducing effects of cannabis: Sibling analysis and proband follow-up. *Archives of General Psychiatry*, *68*(2). https://doi.org/10.1001/archgenpsychiatry.2010.152

Varese, F., Smeets, F., Drukker, M., Lieverse, R., Lataster, T., Viechtbauer, W., Read, J., van Os, J., & Bentall, R. P. (2012). Childhood adversities increase the risk of psychosis: A meta-analysis of patient-control, prospective-and cross-sectional cohort studies. *Schizophrenia Bulletin*, *38*(4), 661–671. https://doi.org/10.1093/schbul/sbs050

Vawter, M. P., Barrett, T., Cheadle, C., Sokolov, B. P., Wood, W. H., Donovan, D. M., Webster, M., Freed, W. J., & Becker, K. G. (2001). Application of cDNA microarrays to examine gene expression differences in schizophrenia. *Brain Research Bulletin*, *55*(5). https://doi.org/10.1016/S0361-9230(01)00522-6

Vlahov, D., & Galea, S. (2002). Urbanization , Urbanicity , and Health. *Journal of Urban Health : Bulletin of the New York Academy of Medicine*, *79*(4), 1–12. https://doi.org/https://doi.org/10.1093/jurban/79.suppl_1.s1

Walsh, T., McClellan, J. M., McCarthy, S. E., Addington, A. M., Pierce, S. B., Cooper, G. M., Nord, A. S., Kusenda, M., Malhotra, D., Bhandari, A., Stray, S. M., Rippey, C. F., Roccanova, P., Makarov, V., Lakshmi, B., Findling, R. L.,

Sikich, L., Stromberg, T., Merriman, B., … Sebat, J. (2008). Rare Structural Variants DisruptMultiple Genes in NeurodevelopmentalPathways in Schizophrenia. *Science*, *320*(5875), 539–543. https://doi.org/10.1126/science.1155174

Wang, K. K., Yang, Z., Sarkis, G., Torres, I., & Raghavan, V. (2017). Ubiquitin C-terminal hydrolase-L1 (UCH-L1) as a therapeutic and diagnostic target in neurodegeneration, neurotrauma and neuro-injuries. In *Expert Opinion on Therapeutic Targets, 21*(6). https://doi.org/10.1080/14728222.2017.1321635

Wellstein, A., Fang, W., Khatri, A., Lu, Y., Swain, S. S., Dickson, R. B., Sasse, J., Riegel, A. T., & Lippman, M. E. (1992). A heparin-binding growth factor secreted from breast cancer cells homologous to a developmentally regulated cytokine. *Journal of Biological Chemistry*, *267*(4). https://doi.org/10.1016/s0021-9258(18)45920-0

Wilkinson, D. G. (2014). Regulation of cell differentiation by Eph receptor and ephrin signaling. In *Cell Adhesion and Migration, 8*(4). https://doi.org/10.4161/19336918.2014.970007

Winner, B., Kohl, Z., & Gage, F. H. (2011). Neurodegenerative disease and adult neurogenesis. *European Journal of Neuroscience*, *33*(6). https://doi.org/10.1111/j.1460-9568.2011.07613.x

Winship, I. R., Dursun, S. M., Baker, G. B., Balista, P. A., Kandratavicius, L., Maia-de-Oliveira, J. P., Hallak, J., & Howland, J. G. (2019). An Overview of Animal Models Related to Schizophrenia. *Canadian Journal of Psychiatry*, *64*(1), 5–17. https://doi.org/10.1177/0706743718773728

Wischhof, L., Irrsack, E., Dietz, F., & Koch, M. (2015). Maternal lipopolysaccharide treatment differentially affects 5-HT2A and mGlu2/3 receptor function in the adult male and female rat offspring. *Neuropharmacology*, *97*. https://doi.org/10.1016/j.neuropharm.2015.05.029

Wolff, A. R., Cheyne, K. R., & Bilkey, D. K. (2011). Behavioural deficits associated with maternal immune activation in the rat model of schizophrenia. *Behavioural Brain Research*, *225*(1). https://doi.org/10.1016/j.bbr.2011.07.033

Wolozin, B., Sunderland, T., Zheng, B. bin, Resau, J., Dufy, B., Barker, J., Swerdlow, R., & Coon, H. (1992). Continuous culture of neuronal cells from adult human olfactory epithelium. *Journal of Molecular Neuroscience*, *3*(3). https://doi.org/10.1007/BF02919405

Woolley, D. W., & Shaw, E. (1954). A BIOCHEMICAL AND PHARMACOLOGICAL SUGGESTION ABOUT CERTAIN MENTAL DISORDERS. *Proceedings of the National Academy of Sciences*, *40*(4). https://doi.org/10.1073/pnas.40.4.228

Wullschleger, S., Loewith, R., & Hall, M. N. (2006). TOR signaling in growth and metabolism. *Cell*, *124*(3), 471–484. https://doi.org/10.1016/j.cell.2006.01.016

Wynn, J. K., Dawson, M. E., Schell, A. M., McGee, M., Salveson, D., & Green, M. F. (2004). Prepulse facilitation and prepulse inhibition in schizophrenia patients and their unaffected siblings. *Biological Psychiatry*, *55*(5). https://doi.org/10.1016/j.biopsych.2003.10.018

Xia, L., Xia, K., Weinberger, D., & Zhang, F. (2019). Common genetic variants shared among five major psychiatric disorders: a large-scale genome-wide combined analysis. *Global Clinical and Translational Research*. https://doi.org/10.36316/gcatr.01.0003

Xiao, M. F., Roh, S. E., Zhou, J., Chien, C. C., Lucey, B. P., Craig, M. T., Hayes, L. N., Coughlin, J. M., Markus Leweke, F., Jia, M., Xu, D., Zhou, W., Conover Talbot, J., Arnold, D. B., Staley, M., Jiang, C., Reti, I. M., Sawa, A., Pelkey, K. A., … Worley, P. F. (2021). A biomarker-authenticated model of schizophrenia implicating NPTX2 loss of function. *Science Advances*, *7*(48). https://doi.org/10.1126/sciadv.abf6935

Xiong, P., Zeng, Y., Wu, Q., Huang, D. X. H., Zainal, H., Xu, X., Wan, J., Xu, F., & Lu, J. (2014). Combining serum protein concentrations to diagnose schizophrenia: A preliminary exploration. *Journal of Clinical Psychiatry*, *75*(8). https://doi.org/10.4088/JCP.13m08772

Yamada, S., Itoh, N., Nagai, T., Nakai, T., Ibi, D., Nakajima, A., Nabeshima, T., & Yamada, K. (2018). Innate immune activation of astrocytes impairs neurodevelopment via upregulation of follistatin-like 1 and interferon-induced transmembrane protein 3. *Journal of Neuroinflammation*, *15*(1). https://doi.org/10.1186/s12974-018-1332-0

Yamaguchi, Y., Lee, Y. A., & Goto, Y. (2015). Dopamine in socioecological and evolutionary perspectives: Implications for psychiatric disorders. *Frontiers in Neuroscience*, *9*(JUN). https://doi.org/10.3389/fnins.2015.00219

You, Z. B., Saria, A., Fischer-Colbrie, R., Terenius, L., Goiny, M., & Herrera-Marschitz, M. (1996). Effects of secretogranin II-derived peptides on the release of neurotransmitters monitored in the basal ganglia of the rat with in vivo microdialysis. *Naunyn-Schmiedeberg's Archives of Pharmacology*, *354*(6). https://doi.org/10.1007/BF00166897

Zelenova, E. A., Kondratyev, N. V., Lezheiko, T. V., Tsarapkin, G. Y., Kryukov, A. I., Kishinevsky, A. E., Tovmasyan, A. S., Momotyuk, E. D., Dashinimaev, E. B., & Golimbet, V. E. (2021). Characterisation of neurospheres-derived cells from human olfactory epithelium. *Cells*, *10*(7). https://doi.org/10.3390/cells10071690

Zhang, B., Xu, Y. H., Wei, S. G., Zhang, H. B., Fu, D. K., Feng, Z. F., Guan, F. L., Zhu, Y. S., & Li, S. Bin. (2014). Association study identifying a new susceptibility gene (AUTS2) for Schizophrenia. *International Journal of Molecular Sciences*, *15*(11). https://doi.org/10.3390/ijms151119406

Zheng, P., Zeng, B., Liu, M., Chen, J., Pan, J., Han, Y., Liu, Y., Cheng, K., Zhou, C., Wang, H., Zhou, X., Gui, S., Perry, S. W., Wong, M. L., Licinio, J., Wei, H., & Xie, P. (2019). The gut microbiome from patients with schizophrenia modulates the glutamate-glutamine-GABA cycle and schizophrenia-relevant behaviors in mice. *Science Advances*, *5*(2). https://doi.org/10.1126/sciadv.aau8317

Zheng, W., Wang, H., Zeng, Z., Lin, J., Little, P. J., Srivastava, L. K., & Quirion, R. (2012). The possible role of the Akt signaling pathway in schizophrenia. In *Brain Research, 1470*. https://doi.org/10.1016/j.brainres.2012.06.032

Zhu, Y., Krause, M., Huhn, M., Rothe, P., Schneider-Thoma, J., Chaimani, A., Li, C., Davis, J. M., & Leucht, S. (2017). Antipsychotic drugs for the acute treatment of patients with a first episode of schizophrenia: a systematic review with pairwise and network meta-analyses. *The Lancet Psychiatry*, *4*(9). https://doi.org/10.1016/S2215-0366(17)30270-5

Annex

ARTICLE 1

Isolation and Differentiation of Neurons and Glial Cells from Olfactory Epithelium in Living Subjects

Paula Unzueta-Larrinaga, Rocío Barrena-Barbadillo, Inés Ibarra-Lecue, Igor Horrillo, Aitor Villate, María Recio, José Javier Meana, Rebeca Diez-Alarcia, Oihane Mentxaka, Rafael Segarra, Nestor Etxebarria, Luis Felipe Callado, Leyre Urigüen

Molecular neurobiology (2023), 60(8), 4472–4487

DOI: 10.1007/s12035-023-03363-2

Impact factor 2022: 5.1

Relative position: 69/272, Q2 Neurosciences

Molecular Neurobiology (2023) 60:4472–4487
https://doi.org/10.1007/s12035-023-03363-2

ORIGINAL ARTICLE

Isolation and Differentiation of Neurons and Glial Cells from Olfactory Epithelium in Living Subjects

Paula Unzueta-Larrinaga[1,2] · Rocío Barrena-Barbadillo[2,3] · Inés Ibarra-Lecue[1] · Igor Horrillo[1,2,4] · Aitor Villate[5,6] · Maria Recio[2,7] · J. Javier Meana[1,2,4] · Rebeca Diez-Alarcia[1,2,4] · Oihane Mentxaka[2,7,8] · Rafael Segarra[2,4,7,8] · Nestor Etxebarria[5,6] · Luis F. Callado[1,2,4] · Leyre Urigüen[1,2,4]

Received: 17 January 2023 / Accepted: 19 April 2023 / Published online: 28 April 2023

Abstract

The study of psychiatric and neurological diseases requires the substrate in which the disorders occur, that is, the nervous tissue. Currently, several types of human bio-specimens are being used for research, including postmortem brains, cerebrospinal fluid, induced pluripotent stem (iPS) cells, and induced neuronal (iN) cells. However, these samples are far from providing a useful predictive, diagnostic, or prognostic biomarker. The olfactory epithelium is a region close to the brain that has received increased interest as a research tool for the study of brain mechanisms in complex neuropsychiatric and neurological diseases. The olfactory sensory neurons are replaced by neurogenesis throughout adult life from stem cells on the basement membrane. These stem cells are multipotent and can be propagated in neurospheres, proliferated in vitro and differentiated into multiple cell types including neurons and glia. For all these reasons, olfactory epithelium provides a unique resource for investigating neuronal molecular markers of neuropsychiatric and neurological diseases. Here, we describe the isolation and culture of human differentiated neurons and glial cells from olfactory epithelium of living subjects by an easy and non-invasive exfoliation method that may serve as a useful tool for the research in brain diseases.

Keywords Olfactory epithelium · Neurospheres · Neurons · Glia · Neuropsychiatric diseases · PSA-NCAM

Introduction

Modeling neuropsychiatric disorders is extremely challenging given the subjective nature of many of the symptoms and the lack of biomarkers and objective diagnostic tests [1]. Currently, several types of human bio-specimens are being used for research, including postmortem tissue, cerebrospinal fluid, induced pluripotent stem (iPS) cells, or induced neuronal (iN) cells [2–4].

The human olfactory epithelium supplies information to the olfactory bulbs of the brain and displays a continuous and powerful neurogenesis in humans, by which olfactory sensory neurons are replaced [5]. Neuronal progenitor cells present in the olfactory epithelium are defined as undifferentiated clonogenic cells that possess the capacity for self-renewal, to generate neuronal or astrocytic cells, as well as to remain as neurospheres in cell culture [6–8]. In this context, the olfactory epithelium has received increased interest as a window to brain mechanisms in complex psychiatric diseases [4, 9–13]. To date, other studies have developed different methods for obtaining the olfactory neuroepithelium (ON) sample, invasively in biopsies after nasal surgery [14], postmortem

✉ Leyre Urigüen
leyre.uriguen@ehu.eus

1 Department of Pharmacology, University of the Basque Country, UPV/EHU, Leioa, Spain

2 Biocruces Bizkaia Health Research Institute, Barakaldo, Spain

3 Department of Nursery, University of the Basque Country UPV/EHU, Leioa, Spain

4 Centro de Investigación Biomédica en Red de Salud Mental, CIBERSAM, Madrid, Spain

5 Department of Analytical Chemistry, University of the Basque Country UPV/EHU, Leioa, Spain

6 PiE-UPV/EHU, Plentzia, ItsasEstazioa, Areatza Pasealekua, 48620 Plentzia, Spain

7 Department of Psychiatry, Cruces University Hospital, Barakaldo, Spain

8 Department of Neurosciences, University of the Basque Country, UPV/EHU, Leioa, Spain

at autopsies [15], or even by a recent non-invasive method [16]. However, all these studies have mainly focused on the evaluation of the olfactory epithelium cells, without further differentiation, that could provide more information on the disease-specific alterations in neurons and/or glial cells.

We aimed to obtain and grow the neural progenitor cells (NPCs) from the olfactory epithelium and differentiate into neurons or glial cells for obtaining specific cell-type cultures in sufficient quantity for the study of neuropsychiatric disorders.

The final objective of this work is the development of a non-invasive, easy, reproducible, and reliable method for the isolation, culture, and characterization of neurons and glial cells from human olfactory epithelium. In this way, a unique resource can be obtained for the investigation of the neuronal and glia-related molecular mechanisms underlying psychiatric and neurological disorders.

Material and Methods

A complete workflow of the method is described in Fig. 1.

Nasal Exfoliation

The olfactory epithelium was obtained by nasal exfoliation from eight healthy donors as previously described [16]. Briefly, the nasal area was exfoliated by circular movements with a sterile swab (brush 2.4 cm long and 3 mm in diameter) introduced into the nasal cavity. Four different swabs were used for each donor for exfoliating the middle and upper regions of the two nasal cavities. After exfoliation, each brush was placed in tubes with 250 µl conventional culture medium (Dulbecco's Modified Eagle Medium/Ham F-12 (DMEM/F12) supplemented with 10% fetal bovine serum (FBS), 2% glutamine, and 1% streptomycin-penicillin (supplemented DMEM medium) (Gibco BRL, USA), keeping the samples on ice. Four samples were obtained for each subject, two (middle and upper regions) for each nostril. The sample from the upper part of the right nostril was mixed with the sample from the middle part of the left nostril and put together in the same tube; the same was done with the other two samples. One of these mixed samples was used for the culture of adherent cells and the other for the culture of neurospheres.

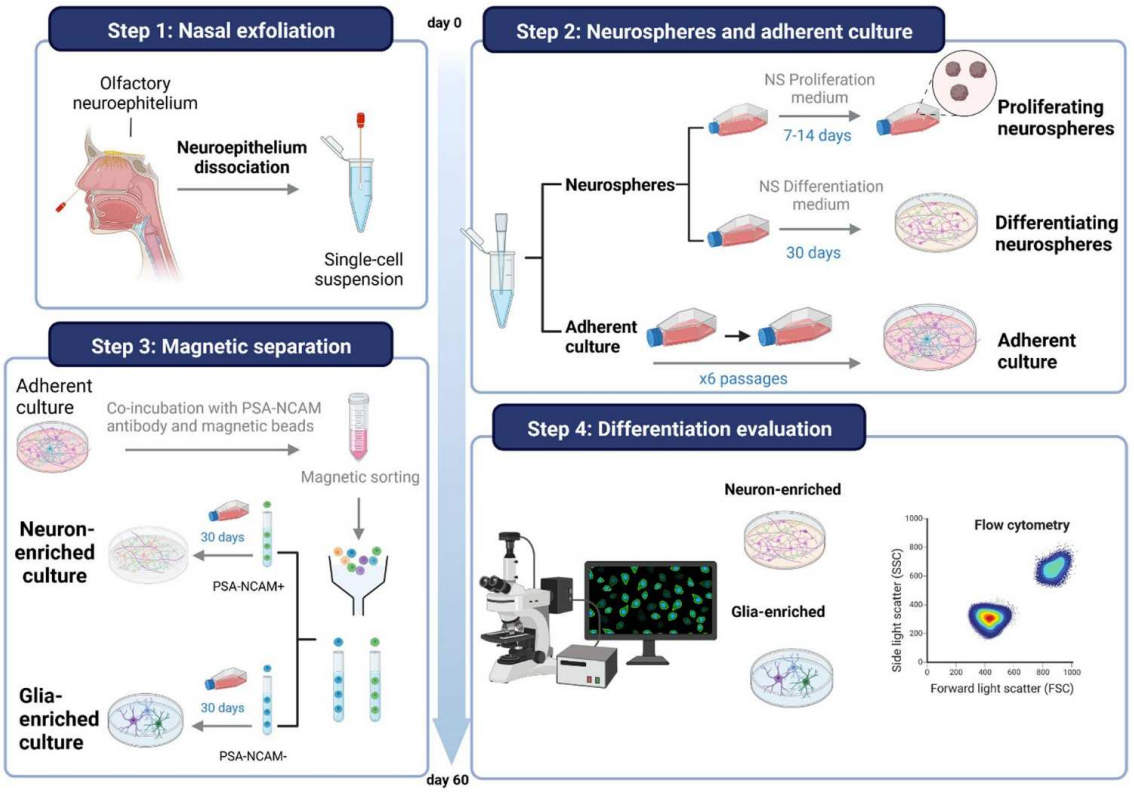

Fig. 1 Workflow of the complete step-by-step protocol for differentiating neurons and glial cells from olfactory epithelium

Neurospheres were cultured and characterized for the demonstration of the presence of stem cells in the olfactory epithelium. Obtaining differentiated cells from neurospheres is extremely complicated, and the number of cells obtained is very low. For this reason, the generation of neuron- or glia-enriched cultures was performed from adherent cultures.

Culture of Neurospheres from Olfactory Epithelium

For the culture of these neurospheres, the samples previously obtained by nasal exfoliation were undergone to a manual disintegration followed by centrifugation (500 g for 5 min, room temperature (RT)). The supernatant was removed and the pellet was resuspended in 500 µl of NeuroCult™ NS-A Proliferation Medium (StemCell Technologies, France) supplemented with 20 ng/ml human recombinant EGF, 10 ng/ml human recombinant bFGF, and 2 µg/ml heparin solution (supplemented NeuroCult™ NS-A Proliferation Medium) and seeded in a 25 cm^2 flask with 4 ml of this supplemented medium. Cells were grown at 37 °C with 5% CO_2 and observed under a direct bright-light microscope (Primovert KMAT, Zeiss, Germany). Neurospheres were then submitted to passages to test their regeneration and multiplication capacity. In this case, the passage was done when neurospheres reach approximately 100–150 µm in diameter, usually 7–14 days after seeding, although in some cases, it may take up to 21 days. If the medium became acidic before the neurospheres reached 100–150 µm in diameter, 500/1000 µl of supplemented proliferation medium was added to renew nutrients and prevent cell death. On passage 5, neurospheres were isolated by centrifugation and fixed for immunocytochemistry characterization.

On the other hand, another flask of neurospheres was maintained without making any passes. Only additions of supplemented proliferation medium were made for renewing of nutrients every 2 days until adhesion to the flask spontaneously occurred. When neurospheres were adhered to the flask, the neurosphere culture medium was changed to NeuroCult™ NS-A Differentiation medium (StemCell Technologies, France) to promote the differentiation of the cells. This would result in a pure culture of cells of neuronal lineage. After 30 days in differentiation medium, the mix of cells was fixed for immunocytochemistry.

Adherent Culture of Cells from Olfactory Epithelium

For the culture of adherent cells, the samples were manually disaggregated and seeded in a 25 cm^2 flask and cells were grown at 37 °C and with 5% CO_2 in supplemented DMEM medium. When the culture reached confluence, cells were washed twice with sterile and tempered phosphate-buffered saline (PBS 1X), detached with 0.5% trypsin–EDTA (GibcoBRL, USA), neutralized with supplemented DMEM medium, and centrifuged at 1000 g RT for 5 min and the pellet was resuspended in supplemented DMEM medium. Finally, cells were seeded on a larger surface to obtain a stock of cells. In this way, cells at different stages of maturation were obtained. Characterization of cells with immunocytochemistry was carried out on cells cultured to passage 5.

Neuron and Glia Culture Enrichment Using Magnetic Activated Cell Sorting

For the isolation and purification of neuron- or glia-enriched cultures, anti-PSA-NCAM micro beads (Miltenyi Biotec, Germany) were used for the positive selection of PSA-NCAM$^+$ cells from the adherent cell cultures. Anti-PSA-NCAM micro beads recognize polysialic acid (PSA), which is linked to the extracellular domain of the neural cell adhesion molecule (NCAM, CD56) [17]. Once culture reached confluence at passage 5 (approximately 4/5 days after seeding, although it depends on the cells in the culture), cells were washed twice with sterile and tempered PBS 1X, detached with 0.5% trypsin–EDTA, neutralized with differentiation medium, and centrifuged at 300 g for 10 min. The supernatant was removed and the pellet was resuspended in 60 µl of buffer (0.5% bovine serum albumin (BSA) in PBS 1X) per 10^7 total cells (Fluidlab R-300, Anvajo, Germany) well mixed and incubated for 10 min RT at 4 °C. The cells were then incubated with 20 µl of anti-PSA-NCAM MicroBeads/10^7 cells for 15 min RT at 4 °C. Finally, cells were washed by adding 1 ml of buffer/10^7 cells and centrifuged at 300 g RT for 10 min, and the pellet was resuspended in 500 µl of buffer/10^8 cells.

After magnetic labeling, cells were passed through a magnetic activated cell sorting (MACS) column (Miltenyi Biotec, Germany) placed in a strong permanent magnet. The ferromagnetic spheres in the column amplify the magnetic field by 10,000-fold, thus inducing a high gradient. Unlabeled cells (PSA-NCAM$^-$) pass through the column while magnetically labeled cells (PSA-NCAM$^+$) are retained within it. After removal of the column from the magnetic field, the retained fraction was eluted. Both fractions, labeled (PSA-NCAM$^+$, neuron-enriched fraction) and non-labeled (PSA-NCAM$^-$, glia-enriched fraction), were completely recovered. The glia-enriched culture was then seeded in NeuroCult™ NS-A Differentiation medium with medium changes every 2 days for approximately 30 days. The neuron-enriched culture, however, was first seeded in supplemented DMEM/F12 + medium to allow cell growth, and after 7 days, the medium was changed to NeuroCult™ NS-A Differentiation with medium changes every 2 days until 30 days, when cells were characterized by immunocytochemistry and flow cytometry.

Characterization of Cultures by Immunocytochemistry

After the MACS, approximately 5 days are needed for the culture to stabilize; the cells that survive the magnetic separation begin to adhere to the flask and to differentiate. At this time, we performed the PSA-NCAM immunocytochemistry in both types of cultures, to ensure the quality of the separation. Afterwards, we let the cultures grow for approximately 30 days, and the immunocytochemical characterization of the neuron-enriched and glia-enriched cultures was carried out. Cells were washed twice with sterile and tempered PBS 1X and fixed with 4% paraformaldehyde (PFA; Sigma-Aldrich Chemicals, Spain) in PBS for 20 min at 4 °C and shaking. Cells were washed again with PBS 1X, then 2 times with A solution (PBS 1% BSA + 0.02% azide) at RT for 5 min and with agitation at 90 rpm, continued by a quick wash with B solution (PBS 0.5% Triton X100) at RT for 5 min and with agitation at 90 rpm and two final washes with A solution again (RT for 5 min and with agitation at 90 rpm). After washing, cells were incubated for 1 h RT and agitation at 90 rpm with blocking solution (PBS 2% BSA + 0.02% azide). Finally, cells were then incubated overnight at 4 °C with the primary antibodies diluted in a solution with PBS 0.5% BSA and 0.1% azide.

Antibodies against Nestin, Sox2, and Musashi-1 were used for staining the neurospheres; PSA-NCAM, βIII-Tubulin, Neuronal-Nuclei (NeuN), Nestin, Microtubule-associated protein 2 (MAP2) and Microtubule-associated protein 1B (MAP1B) for neural cells; glial fibrillary acidic protein (GFAP) for astrocytes; and epithelial cell adhesion molecule (EpCAM) for epithelial cells. A detailed description of primary antibodies and dilutions can be found in Supplemental Table 1.

In the next day, the primary antibodies were removed and washed three times with solution A (RT, 5 min; agitation, 90 rpm). Finally, cells were incubated with the secondary antibodies (90 min, RT; agitation, 90 rpm; and darkness) (Supplemental Table 2). Secondary antibodies were removed, and cells were washed again three times with solution A (RT, 5 min; agitation, 90 rpm). The nuclei were stained with 4′, 6′-diamidino-2-phenylindole dihydrochloride (DAPI 1/5000; Panreac Applichem (A4099), Spain). The immunocytochemistry of the neurospheres was carried out in the same way but with a previous centrifugation for the precipitation of the neurospheres on a slide. Images were acquired with a Nikon Eclipse 80I and processed with ImageJ software.

Characterization of Neuron- and Glia-Enriched Cultures with Flow Cytometry

Sample Preparation

The flow cytometry assays were performed 30 days after the MACS. During this 30-day period, cells are allowed to grow and differentiate with the final objective of having a sufficient amount of differentiated cells.

Cells were washed twice with sterile and tempered PBS 1X, 0.5% trypsin–EDTA was added, and cells were placed in the incubator (37℃) for 2 min. When cells were completely detached, the trypsin was neutralized by pipetting with differentiation medium up and down over the surface of the flask to detach as many cells as possible. Once it was verified that the cells were correctly detached, the cell suspension was collected in a falcon. Cells were then centrifuged at 500 g for 10 min, the supernatant was discarded, and the pellet was resuspended in 600 µl of blocking solution (1 h, with agitation at 4℃). Primary antibodies were added over the blocking solution overnight with agitation at 4℃. In the following day, the cell suspension was centrifuged at 500 g for 10 min, the supernatant was discarded, and the pellet was resuspended in 600 µl of sterile (cold) PBS 1X. Another centrifugation was made at 500 g for 10 min, the supernatant was discarded, and the pellet was resuspended in 600 µl secondary antibody dilution in blocking solution. After incubating 90 min with agitation at 4℃, cells were washed and centrifuged twice at 500 g for 10 min. The resulting pellet was then resuspended in 600 µl of PBS 1X the first time and the second time in 600 µl of HBSS solution (Hank's balanced salt solution) which is the solution needed to analyze the sample in the cytometer.

Fluorescence-Activated Cell Sorting (FACS)

The samples were analyzed and sorted in a BD FACSJazz Cell sorter equipped with two independently aligned B488 and Y/G561 lasers. System pressure is 27 psi. Prior to analysis, the sample was filtered through a sterile sieve with a pore diameter of 50 µm (BD Filcon, sterile, cup-type, ref: 340,629) to avoid clumps in the sample line.

Quantification of Prostaglandin E2, Interleukin-6, Ratio of Kynunerine/Tryptophan, and Interferon Gamma in Culture Medium

Prostaglandin E2 (PGE2), interleukin-6 (IL6), ratio of kynunerine (Kyn)/tryptophan (Trp), and interferon gamma (IFNγ) were quantified with commercial enzyme-linked immunosorbent assay (ELISA) kits (human IFNγ ELISA Kit, cat. no. BMS228, Invitrogen, Thermo Fisher Scientific, Inc.; human IL-6 ELISA kit, cat. no. BMS213-2, Invitrogen, Thermo Fisher Scientific, Inc.; and Prostaglandin E 2 ELISA Kit—monoclonal, cat. no. 514010, Cayman Chemical, Ann Arbor, MI, USA) in culture medium samples, according to the manufacturer's instructions. No dilution was performed, and the absorption peak was at 450 nm. Protein content in culture medium was measured by Bradfords' method [18], and results are shown as pg/mg protein of culture medium.

HPLC with electrochemical detection was used to quantify Trp and Kyn in culture medium samples. Each sample was first diluted 1:5 in 0.1 M $HClO_4$ and 100 µl EDTA and filtered by centrifugation at 18,000 g × 15 min using Costar® Spin-X® Centrifuge Tubes (0.22 µm Pore CA Membrane, Corning). The concentration of Trp and Kyn was estimated with reference to standards prepared and injected on the same day. The mobile phase composition was 150 mM H_2NaPO_4, 0.2 mM EDTA, 4.3 mM octyl sodium sulfate (pH 6.3), and 8% (vol/vol) methanol. The mobile phase was filtered and delivered at a flow rate of 0.2 ml/min by a Hewlett-Packard model 1200 pump. Separation was carried out at 30 °C on a Zorbax Eclipse Plus column (3.5 µm C18, 2.1 × 150 mm, Agilent Technologies, Spain). Amperometric detection of Trp and Kyn was done by a Hewlett-Packard model 1049 A detector at an oxidizing potential of + 950 mV. Results are expressed as Kyn/Trp concentration ratio.

Ethical Aspects

All subjects ($n = 8$) were volunteers without a psychiatric condition and gave their written consent before sample extraction. The entire procedure was approved by the corresponding ethics committee (CEI E22/27).

Results and Discussion

Olfactory Epithelium Cells from Living Subjects Are Able to Form Growing and Proliferating Neurospheres

NPCs in the olfactory epithelium are responsible for renewing the population of sensory neurons throughout life, maintaining a lifelong capacity of regeneration after injuries [19, 20]. When the in vitro culture conditions are adequate, the isolated progenitor neural cells, with high mitotic capacity, are capable of growing in the form of spherical aggregates, called neurospheres. This is an inherent capacity of NPCs [21]. These structures derived from the olfactory mucosa might give rise to neurons and glia. So, they are very interesting for establishing new human models for the study of diseases that affect the central nervous system. As they do not require genetic reprogramming, they are very useful for understanding aspects of the etiology of the disease, improving diagnosis, monitoring treatment, or promoting the development of new therapeutic drugs [6].

To demonstrate the presence and functionality of NPCs after nasal exfoliation in our control subjects, we set out to obtain and multiply cultured neurospheres (Fig. 2a). As seen in Fig. 2, when NPCs were cultured in a specific proliferation medium, cells formed rounded aggregates (Fig. 2b). These neurospheres, being formed by multipotent stem cells, have the ability to divide without differentiation (Fig. 2c). When the neurospheres were disaggregated by centrifugation and afterwards with manual pipetting disaggregation and cultured again in a new flask, these independent cells reassembled, giving rise to the formation of new neurospheres for unlimited proliferation, a remarkable characteristic of neurospheres [22–26]. When neurospheres were adhered to the flask, after 10/12 days of culture in differentiation medium, cells begin to appear in different stages of differentiation. As can be seen in Fig. 2d, e, and f, some of these cells have neuronal profile, with extensions that connect with other cells, and some have even developed synaptic buttons.

The ability to obtain growing and dividing neurospheres and that these neurospheres were able to differentiate to neural-like cells demonstrates that NPCs can be isolated from nasal exfoliation in living subjects.

Olfactory Epithelium-Derived Neurospheres Express NPC-Specific Markers

Although, to date, no specific marker for neurospheres has been described, these formations transiently express the protein Nestin [27]. Nestin is an intermediate filament found in nerve cells that has become widely used as a marker for neural precursors. Additionally, neurospheres are formed by different type of cells expressing also the SRY-box transcription factor-2 (Sox2) or the mRNA-binding protein Musashi-1 that has been demonstrated to play a critical role in promoting stem cell self-renewal [28]. The presence of these markers demonstrates that neurospheres from olfactory epithelium are formed by a heterogeneous population of cells in different stages of differentiation such as stem cells or proliferating neural progenitors [29].

Characterization by immunocytochemistry (Fig. 3) using neural markers Sox2 (Fig. 3b, e, f, i), Musashi-1 (Fig. 3c, e), and Nestin (Fig. 3g, i) showed the co-expression of all these markers in the neurosphere culture. These results demonstrate that under our experimental conditions, cells from the olfactory epithelium are able to form neurospheres composed by neural progenitor cells, as previously demonstrated by other groups [7, 30–32].

Olfactory Epithelium-Derived Neurospheres Give Rise to Differentiated Neural Progenitors

As described above, neurospheres are capable of giving rise to neurons and glial cells under the right conditions. When neurosphere culture medium was changed to differentiation medium (Fig. 4a), NPCs from the neurospheres begin to differentiate. Figure 4 shows cells expressing βIII-Tubulin (Fig. 4b, d), Nestin (Fig. 4b), GFAP (Fig. 4c), and MAP2 (Fig. 4d).

Despite being able to differentiate to cells expressing neuronal or glial markers, the number of cells obtained from neurospheres is extremely low. Moreover, when these culture of

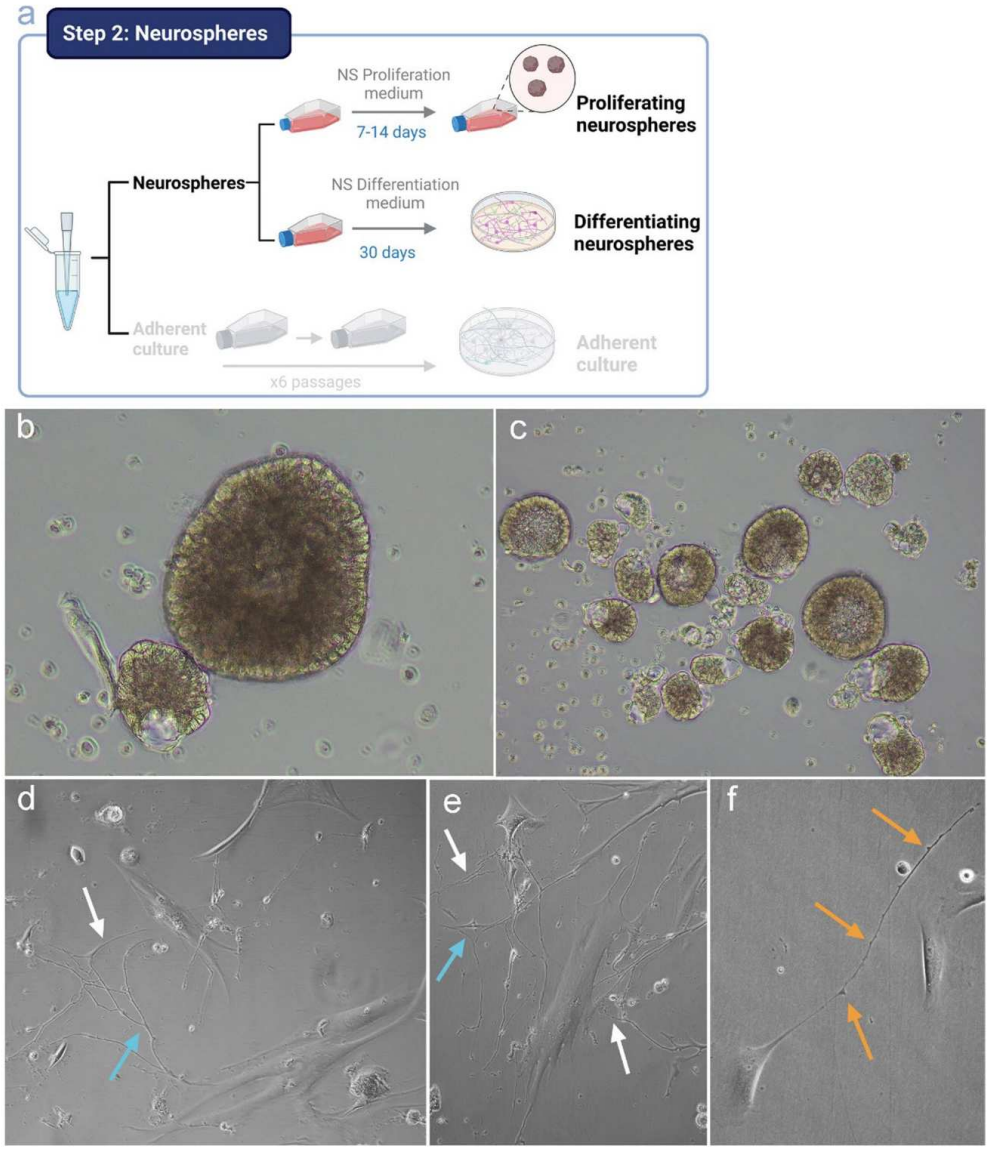

Fig. 2 Neurosphere cultures. Schematic representation of the workflow for the culture of neurospheres (**a**). Bright-field visual characterization (10X) of growing neurospheres (**b**) and proliferating neurospheres (**c**). Cell with neuronal shape and long prolongation (white arrow) connecting with another similar cell (blue arrow) including dendritic spines (orange arrow) (**d**, **e**, **f**)

neurosphere-derived differentiated cells reaches confluence, we are not able to re-seed the culture and the cells die because mature neurons do not undergo cell division. As previously stated, the objective of the study was to obtain neuronal and glial cells for studying the cellular and molecular hallmarks of neuropsychiatric diseases. If the number of cells obtained is low, it would be difficult to use these cultures as a useful research tool. For this reason, we decided to grow adherent cultures from olfactory epithelium and then differentiate this culture to neurons and glia.

Differentiation to Neuronal and Glial Cells from Adherent Cell Cultures

As it has been previously explained, the number of differentiated cells obtained from neurospheres is extremely low for

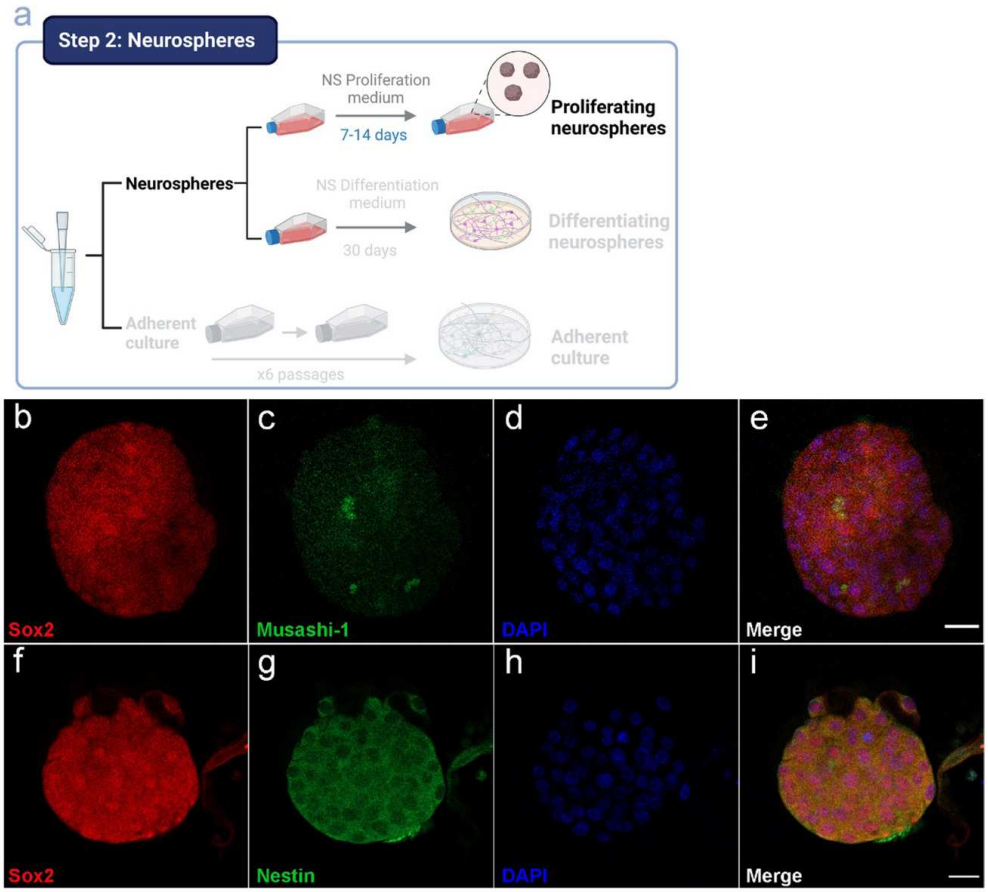

Fig. 3 Characterization of proliferating neurospheres by immunocytochemistry. Schematic representation of the workflow for the culture of neurospheres (**a**). Immunostaining of neural markers Nestin, Sox2, and Musashi-1. Double labeling of Sox2 (**b**) and Musashi-1 (**c**) and merge image for Sox2 and Musashi-1 (**e**). Double labeling of Sox2 (**f**) and Nestin (**g**) and merge image for Sox2 and Nestin (**i**). DAPI was used to stain the nuclei (**d**, **h**). Bar = 20 μm

potentially being used in neuropsychiatric research. For this reason, the generation of neuron- or glia-enriched cultures was carried out from adherent cultures (Fig. 5a). As shown in Fig. 5, cells begin to grow after seeding (Fig. 5b, c, d). On passage 5, culture was mainly formed by a mix of cells at different stages of differentiation expressing neural markers such as βIII-Tubulin (Fig. 5e), GFAP (Fig. 5f), or MAP2 (Fig. 5g). These results indicate that under our specific conditions, cells from olfactory epithelium can be carried to a mix culture formed mainly by neural-fate cells and are in accordance with other previous studies that have reached this stage of culture for the study of neuropsychiatric disorders [6, 13, 16, 33, 34].

To this point, we aimed to separate this mix of cells in the adherent culture so that we could obtain neuronal- or glia-enriched different cultures. For this purpose, we tried to pick up from the adherent culture only the cells differentiating to neurons and seed these cells again in a new plate with a specific neuronal growth medium. For that, we carried out a magnetic labeling of the cells expressing PSA-NCAM in the surface. PSA-NCAM, the highly polysialated form of NCAM, is predominantly expressed in embryonic and neonatal neural tissue [35] and in proliferating late intermediate neuronal progenitor cells [36]. Indeed, PSA-NCAM persists in the adult brain in a spatially restricted way, contributing to synaptic plasticity, neuronal-glial structural remodeling, cell migration, and cell differentiation [37].

After magnetic labeling, cells were separated by magnetic activated cell sorting, and both fractions, labeled (PSA-NCAM$^+$, neuronal-enriched fraction) and non-labeled (PSA-NCAM$^-$, glia-enriched fraction), were completely recovered and cultured in differentiation medium. Figure 6 shows the

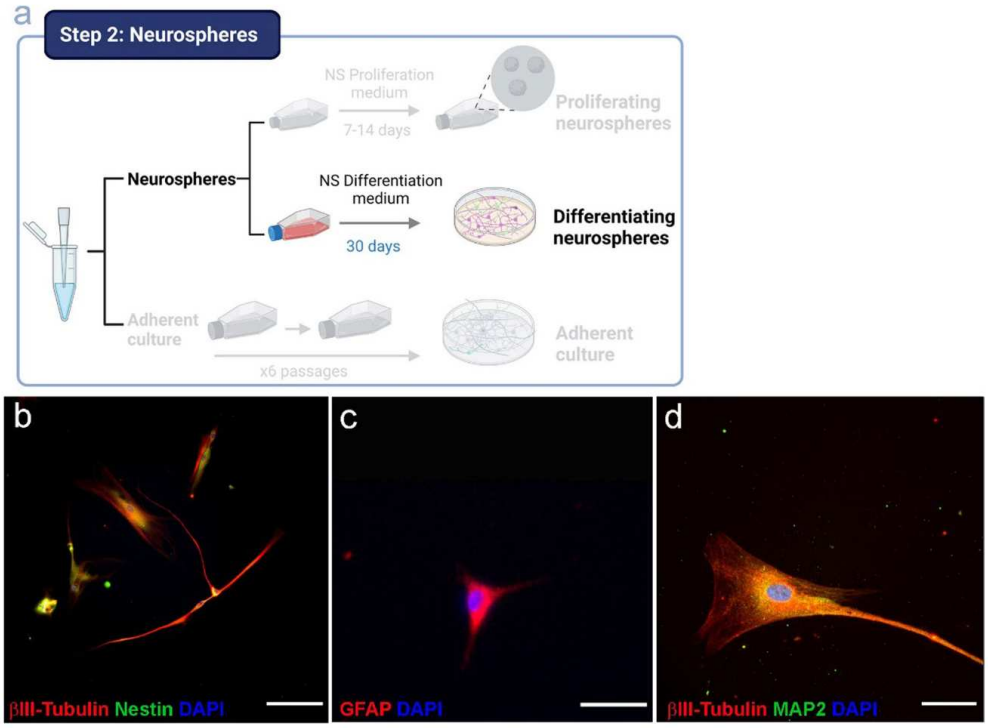

Fig. 4 Characterization of differentiating cells from neurospheres. Schematic representation of the workflow for the culture of differentiating neurospheres (**a**). Immunostaining of βIII-Tubulin/Nestin (**b**), GFAP (**c**), and βIII-Tubulin/MAP2 (**d**). Nuclei were stained with DAPI. Bar = 200 µm (**b**, **c**) and 50 µm (**d**)

morphological shape of both types of cultures after 30 days of culture. PSA-NCAM$^+$ cells, with a higher proportion of neurons, show a more neuronal morphology, with more elongated shapes (Fig. 6b, c). Moreover, we found differentiated cells with a characteristic neuron shape (Fig. 6d, e, f). In contrast, cultures with a higher proportion of glial cells or lower proportion of neuronal cells (PSA-NCAM$^-$ cultures), show a completely different growth, with larger cell aggregates and less elongated cells (Fig. 6g, h).

Neuron-Enriched or Glia-Enriched Cultures Express-Specific Markers of Their Cellular Fate

After the magnetic separation, approximately 5 days are needed for the culture to stabilize; the cells that survive the magnetic separation begin to adhere to the flask and to differentiate. At this time, we perform the PSA-NCAM immunocytochemistry to ensure the quality of the separation (Fig. 7a, b, c). Afterwards, we let the cultures grow for approximately 30 days. Upon reaching 30 days, the cultures have a sufficient number of cells in each flask (F75) in both types of cultures. These 30-day F75s are the ones that we will use to carry out the different experiments in the patients. For the characterization of both types of cultures, the expression of specific neural and glial markers was evaluated by immunocytochemistry. As seen in Fig. 7, neuron-enriched cultures abundantly express neuronal proteins, such as MAP1B (Fig. 7d). This protein is expressed predominantly during the early stages of development of the nervous system, where it regulates processes such as axonal guidance and elongation. In the adult brain, it participates in the regulation of the structure and physiology of dendritic spines in glutamatergic synapses and is also found in presynaptic synaptosomal preparations [38]. Nestin (Fig. 7e) is a class VI intermediate filament protein and a specific marker of neural stem/progenitor cells [39] that can differentiate into neurons and glial cells. Co-expression of both proteins was found in the neuronal-enriched cultures (Fig. 7f). These cultures also express βIII-Tubulin (Fig. 7g, j) together with NeuN (Fig. 7h) and with MAP2 (Fig. 7k) as demonstrated the immunocytochemistry assays. Moreover, co-expression of these proteins was found in the neuronal-enriched cultures (Fig. 7i, l).

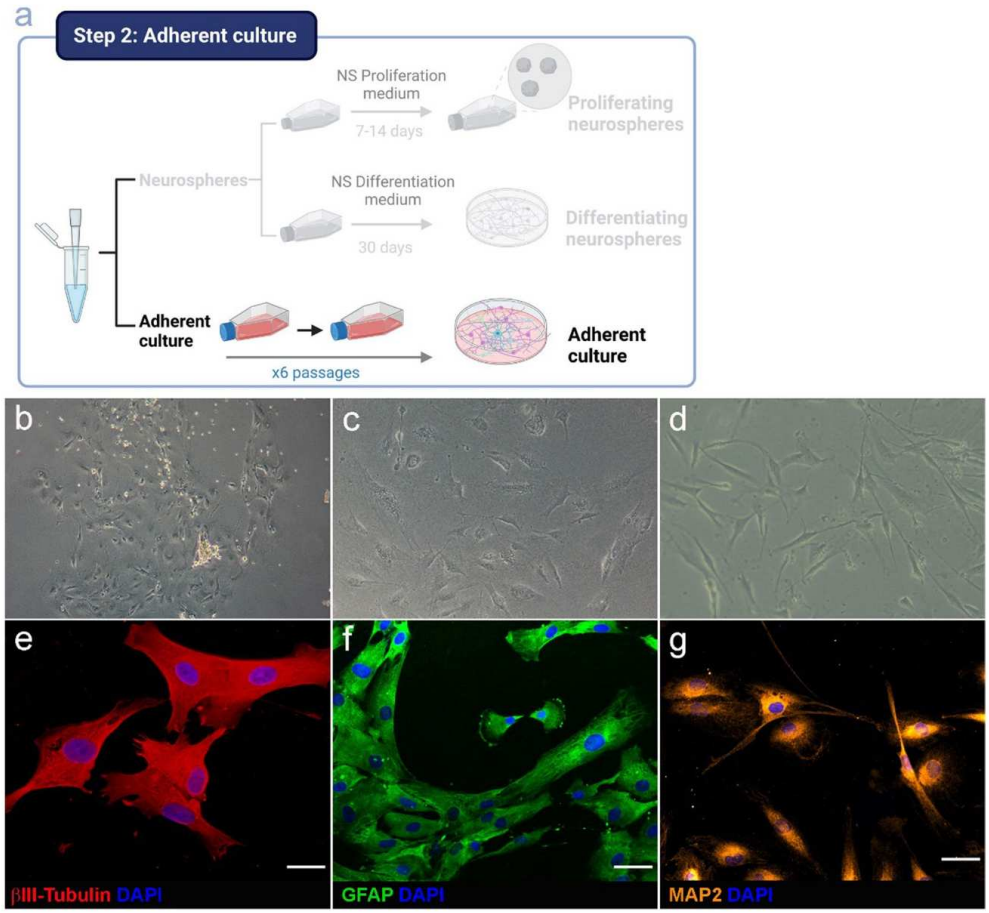

Fig. 5 Characterization of adherent cells from olfactory epithelium. Upper panel shows the schematic representation of the workflow for the adherent cultures (**a**). Cells growing at different days after seeding (10X), at passage 0 (**b**), at passage 2 (**c**), and at passage 4 (**d**). Lower panel shows the immunocytochemistry of adherent cells on passage 5. Immunostaining of βIII-Tubulin (**e**), GFAP (**f**), and MAP2 (**g**). DAPI was used to stain the nuclei. Bar = 50 µm

Tubulin is a major constituent protein of microtubules and consists of two 50-kDa subunits designated as α and β. Expression of class III β-Tubulin, one of the six isotypes of the β subunit expressed in mammals [40], is restricted almost entirely to neurons [41]. In addition, NeuN is a well-recognized marker that is detected in post-mitotic neurons being distributed in the nuclei of neurons in almost all parts of the nervous system and is stably expressing during specific stages of development [42]. The co-expression of these two neuronal markers has been reported in differentiating and mature neuronal cells from diverse sources [43–45]. For this reason, the co-expression of NeuN and βIII-Tubulin in the neuron-enriched cultures suggests that these cultures are formed by a mix of neurons at different stages of differentiation.

On the other hand, MAP2 is the predominant cytoskeletal regulator within neuronal dendrites, and a robust somatodendritic marker due to its abundance and specificity. It influences microtubule dynamics and microtubule/actin interactions to control neurite outgrowth and synaptic functions [46].

A limitation of the study is the use of magnetic beads with PSA-NCAM since this protein is a marker for immature neuronal-committed progenitors, which again, due to the immaturity of the cells, can make the selection less effective. Nevertheless, to date, PSA-NCAM is the only neuron-specific protein expressed in the surface of the cell that can be used for the magnetic sorting in humans. In addition, for discarding the presence of epithelial cells in this culture of ON-derived cells, we carried out an immunocytochemistry assay for the labeling of EpCAM, which was not found in the culture (Fig. 7m, o).

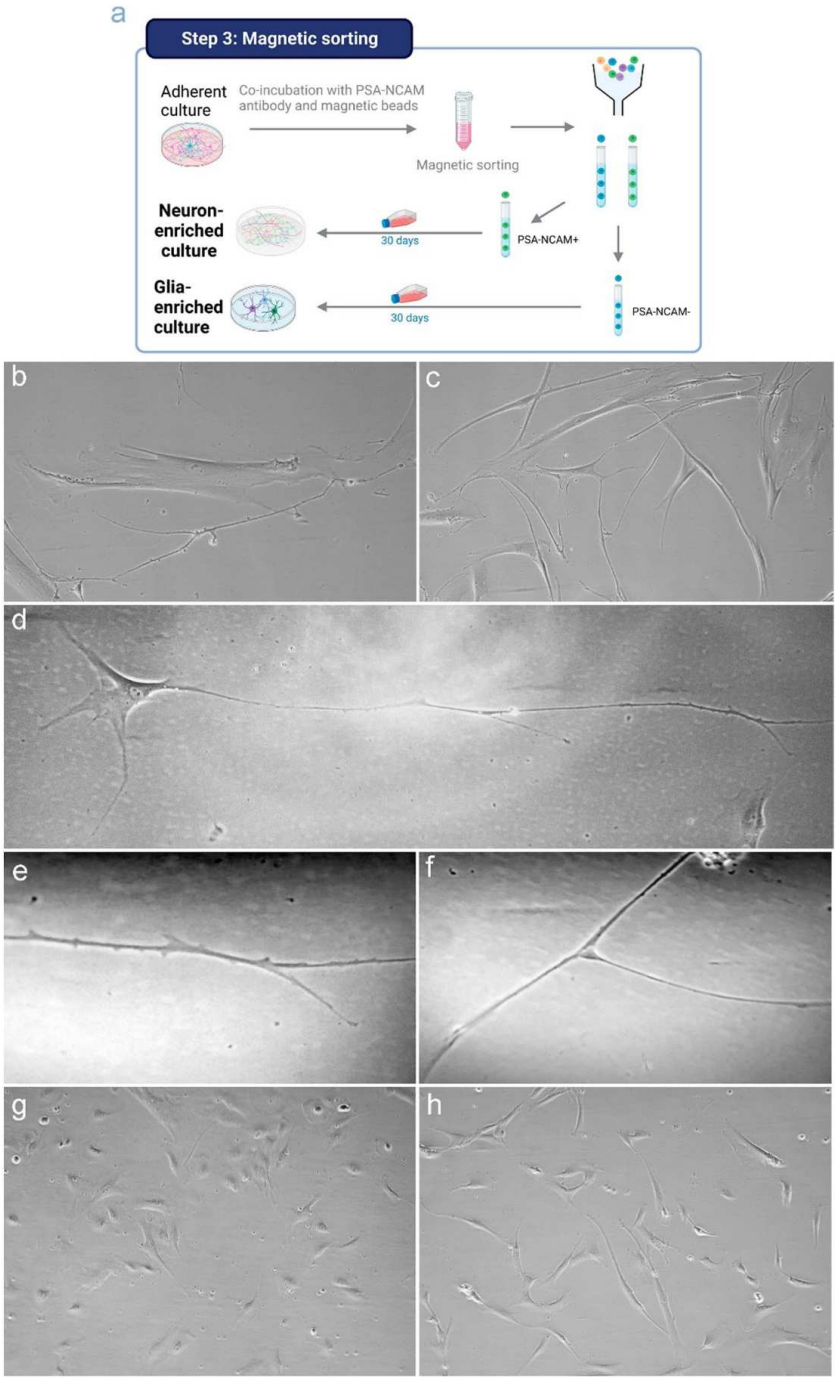

Fig. 6 Bright-field visual characterization of the neuron- or glia-enriched cultures. Schematic representation of the workflow for the magnetic selection of cells (**a**). Bright-field image of PSA-NCAM-positive cells (neuron-enriched fraction) (10X) showing neuronal shape and long prolongations connecting with other cells (**b**, **c**). Differentiated cell with characteristic neuron shape (10X) (**d**). Prolongation of a neuron (20X) (**e**) and end of prolongation of a neuron in a synaptic button-like connection between two different cells (20X) (**f**). Bright-field image of PSA-NCAM-negative cells (glia-enriched fraction) (10X) showing a different growth pattern, with larger aggregates and less elongated cells (**g**, **h**)

These results suggest that the vast majority of cells in the neuron-enriched culture are neurons at different stages of development, with null presence of epithelial cells.

In addition, we did not find the presence of PSA-NCAM (Fig. 8a, b, c) in the glia-enriched cultures immediately after the magnetic separation. Moreover, in glia-enriched

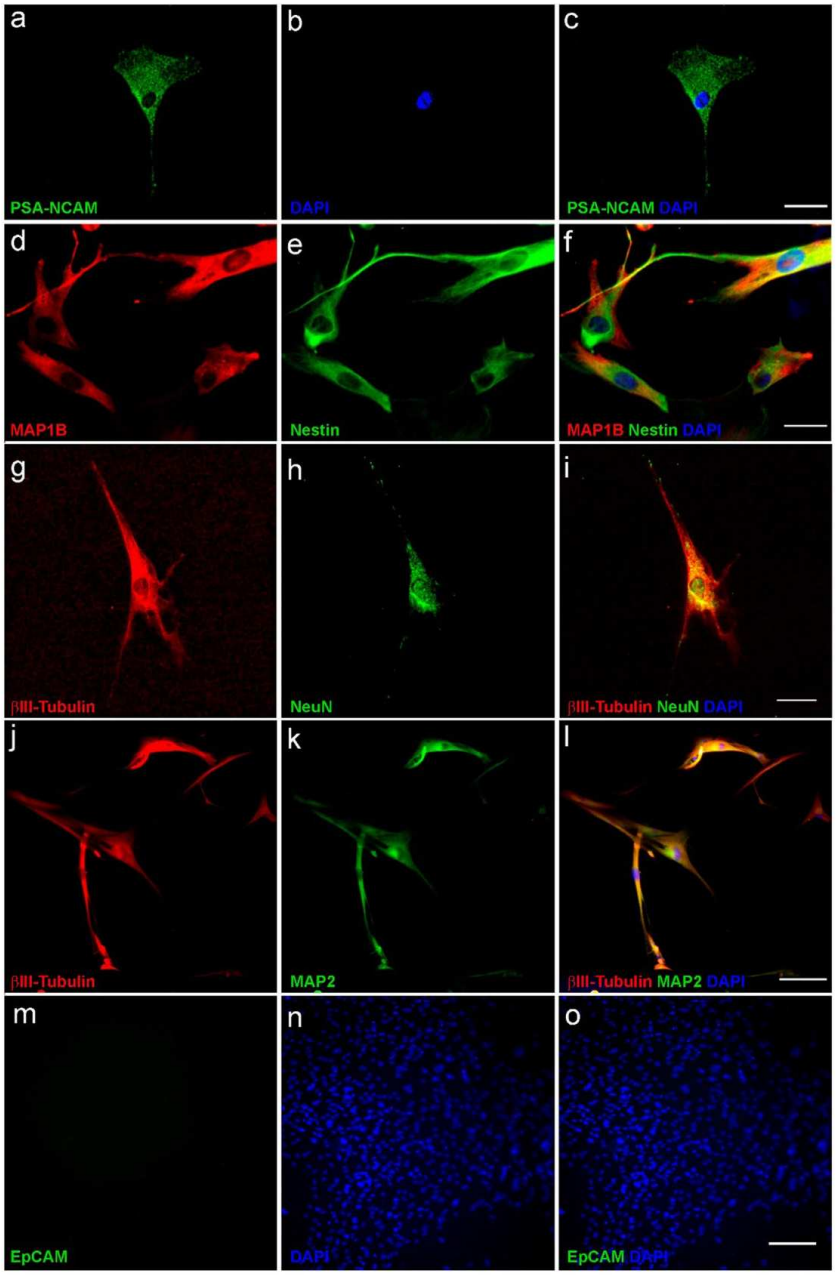

Fig. 7 Neuron-enriched cultures express specific neuronal markers. Immunocytochemistry of neuron-enriched culture derived from the olfactory epithelium. Immunostaining of PSA-NCAM (**a**, **c**). Double labeling of MAP1B (**d**) and Nestin (**e**) and merge image for MAP1B and Nestin (**f**). Double labeling of βIII-Tubulin (**g**) and NeuN (**h**) and merge image for βIII-Tubulin and NeuN (**i**). Double labeling of βIII-Tubulin (**j**) and MAP2 (**k**) and merge image for βIII-Tubulin and MAP2 (**l**). Labeling of EpCAM (**m**, **o**). DAPI was used to stain the nuclei (**b**, **n**). Bar = 200 µm

cultures, as seen in Fig. 8, immunocytochemistry assays demonstrated the presence of specific glial proteins such as GFAP (Fig. 8d, e, f), but not the epithelial EpCAM (Fig. 8g, h, i).

To confirm these results and further characterize the two cell-type populations, we performed a flow cytometry analysis by labeling the cells either with NeuN or GFAP. We use the NeuN marker to demonstrate that in these cultures, 30 days after the magnetic separation, there is a sufficient amount of mature neurons in the culture, although the culture may potentially present neurons at different stages of differentiation, which demonstrates the presence of markers

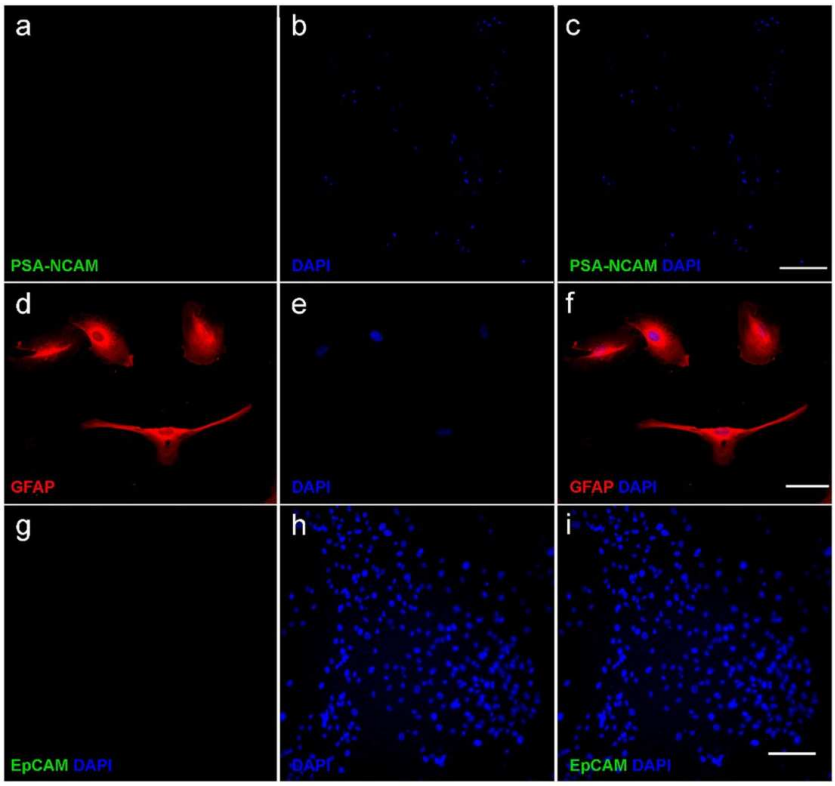

Fig. 8 Glia-enriched cultures express specific glial markers. Immunocytochemistry of glia-enriched culture derived from the olfactory epithelium. Immunostaining of PSA-NCAM (**a**, **c**). Labeling of GFAP (**d**, **f**) and EpCAM (**g**, **i**). DAPI was used to stain the nuclei (**b**, **e**, **h**). Bar = 200 µm

of immature neurons in the immunocytochemical characterization as previously explained.

Besides, we also labeled the cultures with EpCAM to discard the presence of epithelial cells. As seen in Fig. 9, we detected an increase of up to 46% of NeuN-positive cell population in the culture of cells positively selected with PSA-NCAM (Fig. 9a). In contrast, the flow cytometry analysis only gave a residual value of 1.90% of GFAP-positive cells in this neuronal-enriched culture.

The percentages obtained on FACS may be so low because the cells suffer during sample processing and may be dying. Although it is difficult to be sure without a propidium iodide (PI) or other viability marker analysis, this population negative to both markers may correspond to cells that are dying due to sample processing since looking at their appearance in forward scatter (FSC) vs. side scatter (SSC), all cells are very stuck together and in values close to 0.

In the glia-enriched fraction, an increase of up to 48% of GFAP-positive cell population was found in the culture of cells negatively selected with PSA-NCAM (Fig. 9b). In contrast, the flow cytometry analysis only gave a residual value of 0.095% of NeuN-positive cells. Moreover, the flow cytometry analysis gave a residual value of 0.093% of EpCAM-positive cells in neuronal-enriched cultures (Fig. 9c) and 0.73% in glia-enriched cultures (Fig. 9d).

These results demonstrate that our methodology has improved the purity of the cultures, obtaining subpopulations of neurons or glia at different stages of development.

Different Pattern of Measurable Molecules in Neuron-Enriched and Glia-Enriched cultures

As previously explained, the final objective of the work is to obtain a biological substrate of the patient in which we will be able to find and measure trait, state, or prognostic biomarkers of the disease. For this reason, we wanted to know if these enriched cultures may produce and release molecules that we could measure in the culture medium and that could serve as potential biomarkers. To do this, we decided to measure some biomarkers already established in psychiatric research, which are related to the inflammatory component of the disease, such as IFNγ, PGE2, IL-6, or the Kyn/Trp ratio [47].

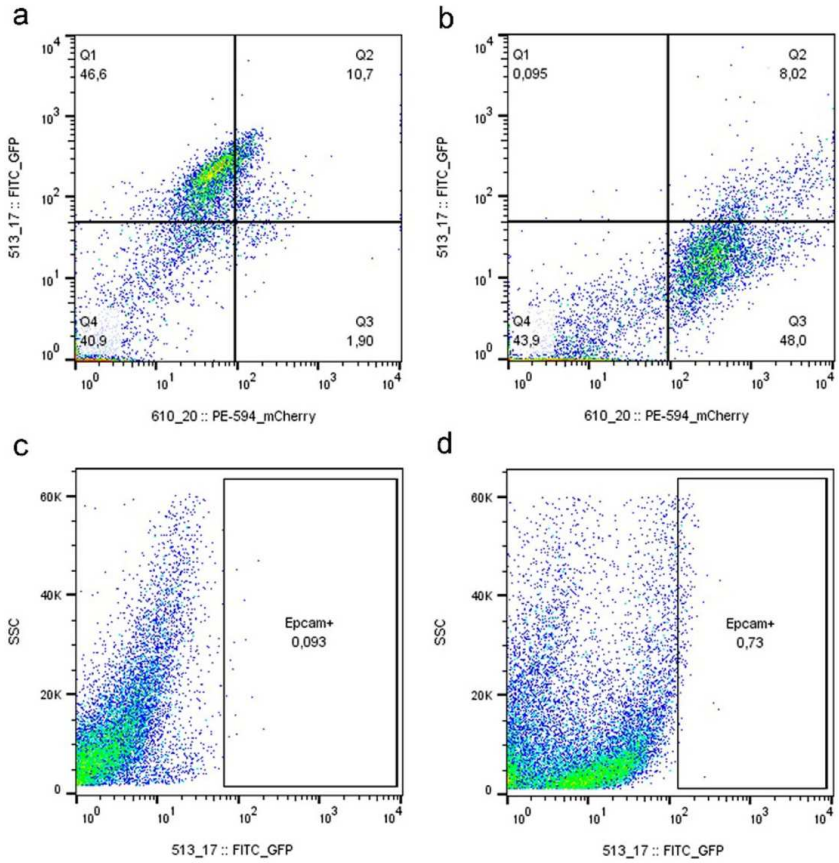

Fig. 9 Fluorescence-activated cell sorting (FACS) of neuron-enriched or glia-enriched cultures. The purity of enriched cultures was determined by performing post-sort FACS analysis on samples of neuron or glia cell subpopulations and assessing the percentages of cells in each gate. Sorting cells under the described conditions yielded over > 46% NeuN- and FITC-positive cell populations in neuron-enriched cultures (**a**) and 48% GFAP- and mCherry-positive cell populations in glia-enriched cultures (**b**). FACS plots of negative control for EpCAM in neuron-enriched cultures (**c**) and in glia-enriched cultures (**d**) are displayed in the lower panel

As seen in Fig. 10, both types of cultures are capable to produce and release these compounds. Moreover, significant differences were found in the levels of PGE2 (Fig. 10a), Kyn/Trp ratio (Fig. 10c), and IFNγ (Fig. 10d) between neuron- and glia-enriched cultures, while no significant changes were found in the IL6 levels (Fig. 10b). Specifically, levels of PGE2 and kynunerine were significantly increased in glia-enriched cultures compared to neuron-enriched cultures, while IFNγ levels were higher in neuronal than in glia-enriched cultures. These results demonstrate that both types of cultures exhibit different levels of these measurable molecules in the culture medium.

Limitations and Concluding Remarks

To our knowledge, this is the first study describing a method for the generation of sufficient amount of human neurons or glial cells subpopulations in living subjects in an easy and non-invasively form. Other studies had developed similar methods but obtaining the sample invasively in biopsies after nasal surgery and with anesthesia, or even postmortem in autopsies. On the other hand, other groups have developed and characterized non-invasively obtained adherent cultures of the olfactory epithelium in patients, but none of them has reached the step of selecting and culturing neurons and glia.

The study has some limitations that obviously cannot be ignored. First, what we have obtained after selecting the cells based on the presence or absence of PSA-NCAM are cultures enriched in neurons or glia, but not pure cultures. Another limitation is the fact that these neuron and glial cells have developed in vitro, without the natural inputs that they would have had if they had developed physiologically. It must be further studied whether the manipulation of neural progenitors has interfered in their development in terms of the ability to reproduce some alterations inherent to psychiatric or neurological conditions. Moreover, these cultures may be considered with an "olfactory-specific"

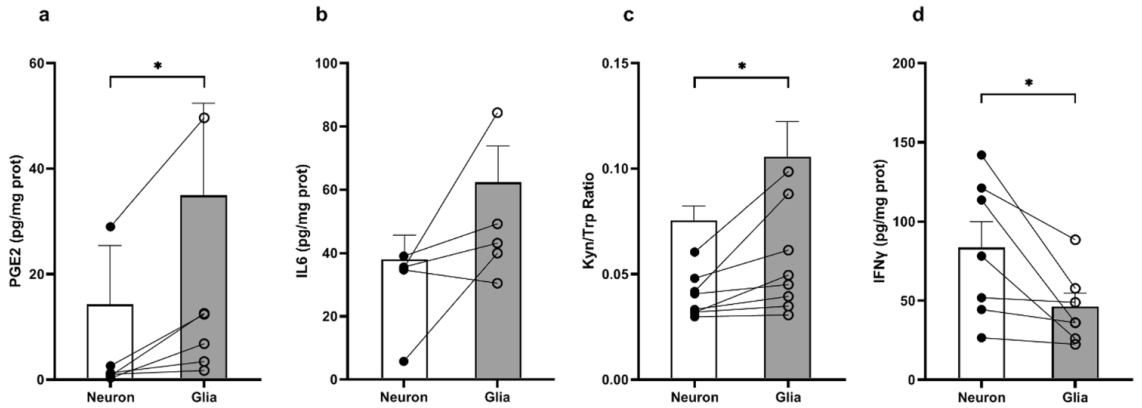

Fig. 10 Levels of PGE2, IL6, Kyn/Trp, and IFNγ in the medium of neuron-enriched or glia-enriched cultures. Levels of PGE2 (**a**), IL6 (**b**), ratio of Kyn/Trp (**c**), and IFNγ (**d**) measured by ELISA assay in both neuron-enriched and glia-enriched culture medium and expressed in pg/mg protein. Bars represent the mean, and circles represent individual values ($n = 5–8$ subjects). Statistical analyses consisted on a paired *T*-test for each subject comparing the levels of the different molecules in neuron or glial cultures. Significance was set at. $^{*}p < 0.05$

origin which should be kept in consideration when comparing with other models.

Despite these limitations, we believe that this work has an important clinical impact since it will allow the characterization of disease fingerprints through the study of neurons and glial cells from patients.

Supplementary Information The online version contains supplementary material available at https://doi.org/10.1007/s12035-023-03363-2.

Acknowledgements The authors thank the donors for their kind participation in the study and Maria Dolores Boyano and Patricia Robledo for the scientific and technical support. The authors also thank technical and human support provided by the nursing staff of the Department of Psychiatry, Cruces University Hospital, Central Service of Microscopy–SGIker-UPV/EHU and Achucarro Basque Center for Neuroscience-Cell Analytics Facility.

Author Contribution Leyre Urigüen, Luis F Callado, and Paula Unzueta-Larrinaga designed the experiments. María Recio, Oihane Mentxaka, and Rafael Segarra recruited the donors and collected the samples. Paula Unzueta-Larrinaga, Rocío Barrena-Barbadillo, Ines Ibarra-Lecue, Igor Horrillo, Aitor Villate, and Nestor Etxebarria performed the experiments. Leyre Urigüen, Luis F Callado, Rebeca Diez-Alarcia, Javier Meana, and Paula Unzueta-Larrinaga analyzed the data, and Leyre Urigüen and Paula Unzueta-Larrinaga wrote the manuscript. All the co-authors gave their final approval of this manuscript.

Funding Open Access funding provided thanks to the CRUE-CSIC agreement with Springer Nature. This study was funded by the Spanish Ministry of Science and Innovation (PID2019-106404RB-I00), Spanish Ministry of Health (PNSD 2019I021), and Basque Government (2019111082, IT1211/19 and IT1512/22).

Data Availability The datasets generated during and/or analyzed during the current study are available from the corresponding author on reasonable request.

Declarations

Ethics Approval All subjects gave their written consent before sample extraction. The entire procedure was approved by the corresponding ethics committee (CEI E22/27).

Consent to Participate Informed consent was obtained from all individual participants included in the study.

Consent for Publication The authors affirm that human research participants provided informed consent for publication of the images in Figs. 2, 3, 4, 5, 6, 7, 8, 9, and 10.

Competing Interests The authors declare no competing interests.

References

1. Nestler EJ, Hyman SE (2010) Animal models of neuropsychiatric disorders. Nat Neurosci 13(10):1161–1169. https://doi.org/10.1038/nn.2647

2. McCullumsmith RE, Hammond JH, Shan D, Meador-Woodruff JH (2014) Postmortem brain: an underutilized substrate for studying severe mental illness. Neuropsychopharmacology 39(1):65–87. https://doi.org/10.1038/npp.2013.239
3. Alciati A, Reggiani A, Caldirola D, Perna G (2022) Human-induced pluripotent stem cell technology: toward the future of personalized psychiatry. J Personalized Med 12 (8). https://doi.org/10.3390/jpm12081340
4. Unterholzner J, Millischer V, Wotawa C, Sawa A, Lanzenberger R (2021) Making sense of patient-derived iPSCs, transdifferentiated neurons, olfactory neuronal cells, and cerebral organoids as models for psychiatric disorders. Int J Neuropsychopharmacol 24(10):759–775. https://doi.org/10.1093/ijnp/pyab037
5. Durante MA, Kurtenbach S, Sargi ZB, Harbour JW, Choi R, Kurtenbach S, Goss GM, Matsunami H et al (2020) Single-cell analysis of olfactory neurogenesis and differentiation in adult humans. Nat Neurosci 23(3):323–326. https://doi.org/10.1038/s41593-020-0587-9
6. Matigian N, Abrahamsen G, Sutharsan R, Cook AL, Vitale AM, Nouwens A, Bellette B, An J et al (2010) Disease-specific, neurosphere-derived cells as models for brain disorders. Dis Model Mech 3(11–12):785–798. https://doi.org/10.1242/dmm.005447
7. Jimenez-Vaca AL, Benitez-King G, Ruiz V, Ramirez-Rodriguez GB, Hernandez-de la Cruz B, Salamanca-Gomez FA, Gonzalez-Marquez H, Ramirez-Sanchez I et al (2018) Exfoliated human olfactory neuroepithelium: a source of neural progenitor cells. Mol Neurobiol 55(3):2516–2523. https://doi.org/10.1007/s12035-017-0500-z
8. Idotta C, Tibaldi E, Brunati AM, Pagano MA, Cadamuro M, Miola A, Martini A, Favaretto N et al (2019) Olfactory neuroepithelium alterations and cognitive correlates in schizophrenia. Eur Psychiatry 61:23–32. https://doi.org/10.1016/j.eurpsy.2019.06.004
9. Borgmann-Winter K, Willard SL, Sinclair D, Mirza N, Turetsky B, Berretta S, Hahn CG (2015) Translational potential of olfactory mucosa for the study of neuropsychiatric illness. Transl Psychiatry 5(3):527. https://doi.org/10.1038/tp.2014.141
10. Lavoie J, Sawa A, Ishizuka K (2017) Application of olfactory tissue and its neural progenitors to schizophrenia and psychiatric research. Curr Opin Psychiatry 30(3):176–183. https://doi.org/10.1097/yco.0000000000000327
11. Delgado-Sequera A, Hidalgo-Figueroa M, Barrera-Conde M, Duran-Ruiz MC, Castro C, Fernández-Avilés C, de la Torre R, Sánchez-Gomar I et al (2021) Olfactory neuroepithelium cells from Cannabis users display alterations to the cytoskeleton and to markers of adhesion, proliferation and apoptosis. Mol Neurobiol 58(4):1695–1710. https://doi.org/10.1007/s12035-020-02205-9
12. McLean CK, Narayan S, Lin SY, Rai N, Chung Y, Hipolito MS, Cascella NG, Nurnberger JI Jr et al (2018) Lithium-associated transcriptional regulation of CRMP1 in patient-derived olfactory neurons and symptom changes in bipolar disorder. Transl Psychiatry 8(1):81. https://doi.org/10.1038/s41398-018-0126-6
13. Guinart D, Moreno E, Galindo L, Cuenca-Royo A, Barrera-Conde M, Pérez EJ, Fernández-Avilés C, Correll CU et al (2020) Altered signaling in CB1R-5-HT2AR heteromers in olfactory neuroepithelium cells of schizophrenia patients is modulated by Cannabis use. Schizophr Bull 46(6):1547–1557. https://doi.org/10.1093/schbul/sbaa038
14. Féron F, Perry C, Girard SD, Mackay-Sim A (2013) Isolation of adult stem cells from the human olfactory mucosa. Methods Mol Biol 1059:107–114. https://doi.org/10.1007/978-1-62703-574-3_10
15. English JA, Fan Y, Focking M, Lopez LM, Hryniewiecka M, Wynne K, Dicker P, Matigian N et al (2015) Reduced protein synthesis in schizophrenia patient-derived olfactory cells. Transl Psychiatry 5:663. https://doi.org/10.1038/tp.2015.119
16. Benitez-King G, Riquelme A, Ortiz-Lopez L, Berlanga C, Rodriguez-Verdugo MS, Romo F, Calixto E, Solis-Chagoyan H et al (2011) A non-invasive method to isolate the neuronal linage from the nasal epithelium from schizophrenic and bipolar diseases. J Neurosci Methods 201(1):35–45. https://doi.org/10.1016/j.jneumeth.2011.07.009
17. Rougon G, Marshak DR (1986) Structural and immunological characterization of the amino-terminal domain of mammalian neural cell adhesion molecules. J Biol Chem 261(7):3396–3401
18. Bradford MM (1976) A rapid and sensitive method for the quantitation of microgram quantities of protein utilizing the principle of protein-dye binding. Anal Biochem 72:248–254. https://doi.org/10.1006/abio.1976.9999
19. Brann JH, Ellis DP, Ku BS, Spinazzi EF, Firestein S (2015) Injury in aged animals robustly activates quiescent olfactory neural stem cells. Front Neurosci 9:367. https://doi.org/10.3389/fnins.2015.00367
20. Mackay-Sim A, Kittel PW (1991) On the life span of olfactory receptor neurons. Eur J Neurosci 3(3):209–215. https://doi.org/10.1111/j.1460-9568.1991.tb00081.x
21. Katz J, Keenan B, Snyder EY (2010) Culture and manipulation of neural stem cells. Adv Exp Med Biol 671:13–22. https://doi.org/10.1007/978-1-4419-5819-8_2
22. Othman M, Lu C, Klueber K, Winstead W, Roisen F (2005) Clonal analysis of adult human olfactory neurosphere forming cells. Biotech Histochem 80(5–6):189–200. https://doi.org/10.1080/10520290500469777
23. Gage FH, Ray J, Fisher LJ (1995) Isolation, characterization, and use of stem cells from the CNS. Annu Rev Neurosci 18:159–192. https://doi.org/10.1146/annurev.ne.18.030195.001111
24. Galli R, Gritti A, Bonfanti L, Vescovi AL (2003) Neural stem cells: an overview. Circ Res 92(6):598–608. https://doi.org/10.1161/01.RES.0000065580.02404.F4
25. Rao MS (1999) Multipotent and restricted precursors in the central nervous system. Anat Rec 257(4):137–148. https://doi.org/10.1002/(SICI)1097-0185(19990815)257:4%3c137::AID-AR7%3e3.0.CO;2-Q
26. Begum AN, Guoynes C, Cho J, Hao J, Lutfy K, Hong Y (2015) Rapid generation of sub-type, region-specific neurons and neural networks from human pluripotent stem cell-derived neurospheres. Stem Cell Res 15(3):731–741. https://doi.org/10.1016/j.scr.2015.10.014
27. Gil-Perotin S, Duran-Moreno M, Cebrian-Silla A, Ramirez M, Garcia-Belda P, Garcia-Verdugo JM (2013) Adult neural stem cells from the subventricular zone: a review of the neurosphere assay. Anat Rec (Hoboken) 296(9):1435–1452. https://doi.org/10.1002/ar.22746
28. Okano H, Kawahara H, Toriya M, Nakao K, Shibata S, Imai T (2005) Function of RNA-binding protein Musashi-1 in stem cells. Exp Cell Res 306(2):349–356. https://doi.org/10.1016/j.yexcr.2005.02.021
29. da Silva SL, Majolo F, da Silva APB, da Costa JC, Marinowic DR (2021) Neurospheres: a potential in vitro model for the study of central nervous system disorders. Mol Biol Rep 48(4):3649–3663. https://doi.org/10.1007/s11033-021-06301-4
30. Murrell W, Feron F, Wetzig A, Cameron N, Splatt K, Bellette B, Bianco J, Perry C, Lee G, Mackay-Sim A (2005) Multipotent stem cells from adult olfactory mucosa. Dev Dyn 233(2):496–515. https://doi.org/10.1002/dvdy.20360
31. Krolewski RC, Jang W, Schwob JE (2011) The generation of olfactory epithelial neurospheres in vitro predicts engraftment capacity following transplantation in vivo. Exp Neurol 229(2):308–323. https://doi.org/10.1016/j.expneurol.2011.02.014
32. Zelenova EA, Kondratyev NV, Lezheiko TV, Tsarapkin GY, Kryukov AI, Kishinevsky AE, Tovmasyan AS, Momotyuk ED, Dashinimaev EB, Golimbet VE (2021) Characterisation of

neurospheres-derived cells from human olfactory epithelium. Cells 10 (7). https://doi.org/10.3390/cells10071690
33. McCurdy RD, Feron F, Perry C, Chant DC, McLean D, Matigian N, Hayward NK, McGrath JJ et al (2006) Cell cycle alterations in biopsied olfactory neuroepithelium in schizophrenia and bipolar I disorder using cell culture and gene expression analyses. Schizophr Res 82(2–3):163–173. https://doi.org/10.1016/j.schres.2005.10.012
34. Borgmann-Winter K, Willard SL, Sinclair D, Mirza N, Turetsky B, Berretta S, Hahn CG (2015) Translational potential of olfactory mucosa for the study of neuropsychiatric illness. Transl Psychiatry 5:527. https://doi.org/10.1038/tp.2014.141
35. Kiss JZ, Muller D (2001) Contribution of the neural cell adhesion molecule to neuronal and synaptic plasticity. Rev Neurosci 12(4):297–310. https://doi.org/10.1515/revneuro.2001.12.4.297
36. Seki T (2002) Expression patterns of immature neuronal markers PSA-NCAM, CRMP-4 and NeuroD in the hippocampus of young adult and aged rodents. J Neurosci Res 70(3):327–334. https://doi.org/10.1002/jnr.10387
37. Bonfanti L, Nacher J (2012) New scenarios for neuronal structural plasticity in non-neurogenic brain parenchyma: the case of cortical layer II immature neurons. Prog Neurobiol 98(1):1–15. https://doi.org/10.1016/j.pneurobio.2012.05.002
38. Bodaleo FJ, Montenegro-Venegas C, Henríquez DR, Court FA, Gonzalez-Billault C (2016) Microtubule-associated protein 1B (MAP1B)-deficient neurons show structural presynaptic deficiencies in vitro and altered presynaptic physiology. Sci Rep 6(1):30069. https://doi.org/10.1038/srep30069
39. Lendahl U, Zimmerman LB, McKay RDG (1990) CNS stem cells express a new class of intermediate filament protein. Cell 60(4):585–595. https://doi.org/10.1016/0092-8674(90)90662-X
40. Sullivan KF, Cleveland DW (1986) Identification of conserved isotype-defining variable region sequences for four vertebrate beta tubulin polypeptide classes. Proc Natl Acad Sci U S A 83(12):4327–4331. https://doi.org/10.1073/pnas.83.12.4327
41. Dráberová E, Lukás Z, Ivanyi D, Viklický V, Dráber P (1998) Expression of class III beta-tubulin in normal and neoplastic human tissues. Histochem Cell Biol 109(3):231–239. https://doi.org/10.1007/s004180050222
42. Duan W, Zhang YP, Hou Z, Huang C, Zhu H, Zhang CQ, Yin Q (2016) Novel insights into NeuN: from neuronal marker to splicing regulator. Mol Neurobiol 53(3):1637–1647. https://doi.org/10.1007/s12035-015-9122-5
43. Delgado D, Bilbao AM, Beitia M, Garate A, Sánchez P, González-Burguera I, Isasti A, López De Jesús M, Zuazo-Ibarra J, Montilla A, Domercq M, Capetillo-Zarate E, García Del Caño G, Sallés J, Matute C, Sánchez M (2021) Effects of platelet-rich plasma on cellular populations of the central nervous system: the influence of donor age. Int J Mol Sci 22 (4). https://doi.org/10.3390/ijms22041725
44. Mendivil-Perez M, Velez-Pardo C, Jimenez-Del-Rio M (2019) Direct transdifferentiation of human Wharton's jelly mesenchymal stromal cells into cholinergic-like neurons. J Neurosci Methods 312:126–138. https://doi.org/10.1016/j.jneumeth.2018.11.019
45. Sultan N, Amin LE, Zaher AR, Grawish ME, Scheven BA (2020) Neurotrophic effects of dental pulp stem cells on trigeminal neuronal cells. Sci Rep 10(1):19694. https://doi.org/10.1038/s41598-020-76684-0
46. DeGiosio RA, Grubisha MJ, MacDonald ML, McKinney BC, Camacho CJ, Sweet RA (2022) More than a marker: potential pathogenic functions of MAP2. Frontiers in molecular neuroscience 15:974890. https://doi.org/10.3389/fnmol.2022.974890
47. Leza JC, Garcia-Bueno B, Bioque M, Arango C, Parellada M, Do K, O'Donnell P, Bernardo M (2015) Inflammation in schizophrenia: a question of balance. Neurosci Biobehav Rev 55:612–626. https://doi.org/10.1016/j.neubiorev.2015.05.014